

A new method in determination of electrical parameters for failure diagnostic applicable to power transformers

Von der Fakultät für Elektrotechnik und Informatik
der Gottfried Wilhelm Leibniz Universität Hannover

zur Erlangung des akademischen Grades

**Doktor-Ingenieur
(Dr.-Ing.)**

genehmigte Dissertation

von

M. Sc. Dinh Anh Khoi Pham

geboren am 23.10.1979 in Ninh-Thuan, Vietnam

2013

1. Referent:	Prof. Dr.-Ing. Ernst Gockenbach
2. Referent:	Prof. Dr.-Ing. Albert Claudi
3. Referent:	Prof. Dr.-Ing. habil. Hossein Borsi
Vorsitzender der Prüfungskommission:	Prof. Dr.-Ing. habil. Lutz Hofmann
Tag der Promotion:	22.11.2013

Acknowledgement

The PhD work had been motivated and conducted during my stay as scientific guest and employee at the Schering-Institute of High Voltage Technology, Gottfried Wilhelm Leibniz Universität Hannover, Germany from 2008 to 2013.

First of all, I would like to express my deepest appreciation to my supervisor and examiner, Prof. Dr.-Ing. Ernst Gockenbach for his professional guidance, understanding, enthusiasm and encouragement for the PhD work, publications, the dissertation and partial financial support.

Then I would like to show my special gratitude to Prof. Dr.-Ing. habil. Hossein Borsi for his professional and enthusiastic supervision with stressful but fruitful discussions on the PhD work in the direction of practical aspect, which is always required for any research activity.

I am grateful to Prof. Dr.-Ing. Albert Claudi from the university of Kassel as external examiner with his comments. I am also indebted to Prof. Dr.-Ing. habil. Lutz Hofmann from the department of Electrical Power Supply (elektrische Energieversorgung) as the president of the committee of doctoral examination which is one of great events in my life.

Many thanks are given to my colleagues who had helped me during my stay in conducting industrial projects and scientific activities, Dr.-Ing. Claus-Dieter Ritschel, Dr.-Ing. Mohsen Farahani, Dr.-Ing. Xiang Zhang, Dipl.-Ing. Christian Eichler, Dipl.-Ing. Lars Hoppe, Dipl.-Ing. Markus Fischer, M.Sc. Mohammad Mahdi Saei Shirazi and all other colleagues for their friendship.

I would like to sincerely thank Mrs. Vera Vortmann as secretary for her time and enthusiastic help for a lot of time-consuming paper-related work. In addition, time and effort of Dipl.-Ing. Christian Eichler and Dipl.-Ing. Ishwar-Singh Sarpal in translation of the dissertation abstract are appreciated.

I would like also to thank the dedicated help from the workshop staffs of Schering-Institute: Mr. Karl-Heinz Maske, Mr. Claus-Dieter Hasselberg and Mr. Erich Semke in supporting my practical work for the research activities.

Special thanks from me are given to Dr. Juan Lorenzo Velásquez Contreras (former employee of Omicron electronics), Dr. Stephanie Rätzke and Mr. Michael Rädler (Omicron electronics), for their technical support and fruitful discussions concerning the cooperation between the Schering-Institute and Omicron with regard to transformer diagnostic. The permission of Omicron for the presentation of measurement results of a test transformer in the dissertation is highly appreciated.

Finally, the financial support from the Vietnamese Ministry of Education and Training for my PhD in Germany in 2008 – 2012 is really appreciated. The PhD could not be successful without any of above-mentioned supports and helps, which will be with me in all my rest life time.

Hannover, November 2013

Dinh Anh Khoi Pham

Abstract

A new method in determination of electrical parameters for failure diagnostic applicable to power transformers

Key words: electrical transformer parameter – Frequency Response Analysis (FRA) – failure diagnostic – measurement methods – power transformers – transformer active part – electrical and mechanical failure – transformer model

The dissertation introduces a new measurement-based method that combines two adapted and three *new* approaches in determining electrical parameters of power transformers for purposes of a parameter-based FRA interpretation as well as a comprehensive diagnostic of electrical and mechanical failures in the transformer active part, i.e. mainly the core and windings. The method is proposed due to the fact that the electrical parameters of power transformers cannot be fully determined so far through conventional methods for both FRA and diagnostic purpose, especially one of key parameters associated with the mechanical failures, the winding series capacitance.

In the first step of the proposed method, an appropriate lumped “physical” transformer model valid in low and mid frequency range is required. The term “physical” means the required model must be developed based on dual electric-magnetic phenomena appearing inside the transformers under specific excitation and terminal conditions. Of the equivalent transformer circuits which have been developed so far for different purposes, the duality principle based equivalent circuit for the purpose of transient analysis is selected and then adapted. The adaptation of the circuit is then for another goal: analysis of frequency responses based on electrical parameters to support the current FRA interpretation which is not fully efficient in detection of mechanical failures in transformer windings at the moment.

Once the transformer circuit is derived, the measurement-based approaches in next steps are developed to determine the circuit’s components, i.e. the transformer’s electrical parameters. To enable the FRA interpretation as well as the diagnostic of the electrical and mechanical failures in the transformer active part, following electrical parameters should be determined according to the approaches:

- Impedance of sections of the core (legs and yokes)
- Winding resistances and capacitances
- Leakage and zero-sequence inductances

The above electrical parameters are only required to be available in low frequency range for the diagnostic purpose and therefore are determined directly through analysis of *non-destructive* measurements of different input impedances measured by means of a scattering-parameter vector network analyzer (VNA). On the other hand, the parameters should be frequency dependent in broad frequency range for the simulation-based FRA interpretation; thus, the frequency dependency of electrical parameters is developed by combination of measurement-based values at low frequencies and formula-based values at high frequencies.

The new method is then applied to determine electrical parameters for FRA purpose on three test transformers having different rated powers, voltages and vector groups and verified by comparison with other conventional diagnostic methods carried out by means of the commercial testing device “CPC 100” of Omicron. In addition, since one transformer was opened, several electrical and mechanical failures were performed in its active part so that the new method could be ap-

plied to find the change of electrical parameters for diagnostic purpose. Results confirm a clear contribution of the proposed method in detection of the failures, indicating the fact that the method should be combined with other conventional methods for a better diagnostic.

Kurzfassung

Ein neues Verfahren zur Bestimmung der elektrischen Parameter von Leistungstransformatoren zwecks Fehlerdiagnose

Schlagworte: elektrische Transformator-Parameter – Frequenz Response Analyse (FRA) – Fehlerdiagnose – Messmethoden – Leistungstransformatoren – Transformatoraktivteil – elektrische und mechanische Fehler – Transformatorenmodell

Diese Dissertation beschreibt eine neue Diagnosemethode, die zwei bereits erprobte und drei neue Ansätze zur Bestimmung elektrischer Parameter von Leistungstransformatoren mit dem Zweck der Diagnose von elektrischen und mechanischen Defekten im Aktivteil, d.h. im Wesentlichen den Kern und den Wicklungen, verbindet. Die Vorstellung dieser Methode erfolgt aufgrund der Tatsache, dass mit konventionellen Verfahren die elektrischen Parameter der Leistungstransformatoren, wie z.B. die Wicklungsreihenkapazität, nicht vollständig für die FRA-Interpretation und Diagnosen ermittelt werden können.

Für die Diagnosemethode ist zunächst ein entsprechendes physikalisches Transformatorersatzmodell notwendig, um die elektrischen Parameter aus Messungen richtig interpretieren zu können. Das verwendete Ersatzmodell muss auf den gleichen elektro-magnetischen Phänomenen basieren wie bei realen Transformatoren und bei spezifischen Eingangsimpulsen sowie Betriebszuständen möglichst ähnlich reagieren. Als gewählte äquivalente Transformatornachbildung wurde der auf dem Dualitätsprinzip basierende Wandlerkreis zum Zwecke der Analyse transients Vorgänge ausgewählt und adaptiert, welche ursprünglich bereits für andere Zwecke entwickelt und eingesetzt wurde. Die Anpassung dieses Modells an die realen physikalischen und elektrischen Parameter wurde durchgeführt, um die Interpretation / Beurteilung der standardisierten FRA-Technik zu unterstützen, welche eine der am meisten verwendeten diagnostischen Methoden darstellt, die jedoch nicht immer zufriedenstellende Ergebnisse liefert.

Zunächst wird die Transformatorschaltung nachgebildet. Danach werden neue Messansätze entwickelt, um die elektrischen Transformatorparameter zu bestimmen. Um die FRA zu interpretieren und eine komplette Diagnose der elektrischen und mechanischen Störungen im Aktivteil eines Transformators zu bestimmen, müssen folgende elektrische Parameter bestimmt werden:

- Die Impedanz der Kernabschnitte (Schenkel und Joch)
- Der Wicklungswiderstand und die Wicklungskapazitäten
- Die Streu- und Null-Induktivität

Die oben genannten elektrischen Parameter werden für diese diagnostischen Zwecke nur im niedrigen Frequenzbereich benötigt und können daher mit Hilfe der Streuparameter eines Netzwerkanalysators (VNA) ermittelt werden. Durch diesen neuen Messansatz wird eine zerstörungsfreie, bequemere und einfachere Messung der Größen als die derzeit als Stand der Technik verwendeten Methoden möglich. Auf der anderen Seite sollte eine Frequenzabhängigkeit der elektrischen Parameter für die FRA-Interpretation auch über einen breiten Frequenzbereich gegeben sein, weshalb die Parameter für niedrige Frequenzen mit Werten von frequenzabhängigen Funktionen für hohe Frequenzbereiche kombiniert werden.

Auf der anderen Seite werden die Parameter auch in breitem Frequenzbereich, mit Hilfe frequenzabhängiger Funktionen berechnet, damit die ermittelten Kurvenzüge mit bekannten Methoden der FRA interpretiert werden können.

Die neu entwickelte Methode wird anschließend auf drei Transformatoren in einwandfreiem Zustand mit verschiedenen Nennleistungen, Spannungen und Schaltgruppen angewendet und überprüft sowie mit anderen konventionellen diagnostischen Verfahren für praktische Anwendungen verglichen. Darüber hinaus wird das Verfahren auch an einem Prüftransformator zur Diagnose mehrerer nachgebildeter elektrischer und mechanischer Fehler im Aktivteil getestet. Die Ergebnisse zeigen einen eindeutigen Beitrag der vorgeschlagenen Methode zur Fehlerdiagnose, weshalb das neu entwickelte Verfahren, in Kombination mit anderen konventionellen Messmethoden, für eine bessere Fehlerdiagnose angewendet werden sollte.

Table of contents

Abbreviation and frequently used symbols.....	X
Overview.....	1
Introduction.....	2
1 State-of-the-art of electrical measurement methods in diagnostics of electrical and mechanical failures in the active part of power transformers	7
1.1 Traditional measurement methods.....	7
1.1.1 Measurement methods to detect core problems.....	7
1.1.2 Measurement methods to identify winding electrical parameters	9
1.2 Advanced measurement methods	12
1.2.1 What is FRA and applications of the FRA method	12
1.2.2 How the FRA measurement is conducted.....	13
1.2.3 Assessment of FRA results according to current standards.....	15
1.2.4 Assessment of FRA results according to worldwide researches	18
2 Physical electrical transformer models	21
2.1 Classification of physical electrical models for power transformers.....	21
2.1.1 Single phase transformer circuit at power frequency.....	21
2.1.2 Single phase transformer circuits in different frequency ranges.....	22
2.1.3 Three-phase transformer circuits for purpose of transient analysis	23
2.1.4 Three-phase transformer circuits for purpose of FRA	26
2.2 Summary of state-of-the-art transformer circuits for diagnostic and FRA purpose	27
2.3 Adapted duality based equivalent circuits for FRA purpose	28
3 A new method for FRA interpretation and failure diagnostics	31
3.1 Equivalent transformer circuit	32
3.2 Per-phase short-circuit input impedance tests and relevant electrical parameters.....	34
3.2.1 Per-phase short-circuit input impedance tests and measurement based parameters (winding resistance, leakage inductance) at low frequencies	34
3.2.2 Winding resistances and leakage inductance at high frequencies.....	38
3.2.3 Frequency dependencies of winding resistances and leakage inductances in broad frequency range (20 Hz to 2 MHz)	39
3.3 Zero-sequence input impedance test on star winding and zero-sequence impedances ..	40
3.3.1 Overview of zero-sequence impedance in power transformers	40
3.3.2 Determination of zero-sequence impedance	43
3.4 Open-circuit input impedance tests and core section impedances.....	45
3.4.1 Measurement-based approach to calculate core impedances at low frequencies	46
3.4.2 Formula-based approach to determine core impedances at high frequencies.....	58
3.5 Capacitive input impedance tests and winding capacitances.....	62
3.6 Circuit simulation for determining winding series capacitance and FRA interpretation	65
4 Case study I: A 200 kA 10.4/0.462 kV YNyn6 transformer (T_1)	67
4.1 Adaptation of the transformer T_1 for research compatibility.....	67
4.2 Application of the new method in determination of electrical parameters referred into the HV star winding.....	69
4.2.1 Per-phase winding resistances and leakage inductances.....	70
4.2.2 Zero-sequence inductance and resistance of the HV star winding	71

4.2.3	Core section inductances and resistances.....	72
4.2.4	Ground and inter-winding HV-LV capacitance.....	77
4.3	Parameter-based FRA interpretation and failure diagnostic.....	78
4.3.1	Parameter-based FRA interpretation in broad frequency range.....	78
4.3.2	Parameter-based failure diagnostic.....	80
4.4	Application of the proposed method in diagnosis of electrical failures performed on the active part of the test transformer T_1	81
4.4.1	Overview of the electrical failures.....	81
4.4.2	Failure detection based on electrical parameters.....	81
4.5	Application of the proposed method in diagnosis of mechanical failures performed on the active part of the test transformer T_1	83
4.5.1	Overview of the mechanical failures.....	83
4.5.2	Failure detection based on FRA assessments and electrical parameters.....	85
4.5.3	Discussion.....	87
4.6	Summary.....	88
5	Case study II: A 2.5 MVA 22/0.4 kV Dyn5 transformer (T_2).....	89
5.1	Application of the new method in determination of electrical parameters referred into the HV delta winding.....	89
5.1.1	Per-phase winding resistances and leakage inductances.....	90
5.1.2	Core section inductances and resistances.....	92
5.1.3	Ground and inter-winding HV-LV capacitance.....	94
5.2	Parameter-based FRA interpretation and failure diagnostic.....	94
5.2.1	Parameter-based FRA interpretation in broad frequency range.....	95
5.2.2	Parameter-based failure diagnostic.....	97
5.3	Summary.....	98
6	Case study III: A 6.5 MVA 47/27.2 kV YNd5 transformer (T_3).....	99
6.1	Application of the new method in determination of electrical parameters referred into the HV star winding.....	99
6.1.1	Per-phase winding resistances and leakage inductances.....	100
6.1.2	Zero-sequence inductance and resistance of the HV star winding.....	101
6.1.3	Core section inductances and resistances.....	103
6.1.4	Ground and inter-winding HV-LV capacitance.....	104
6.1.5	Contribution of winding series capacitances.....	105
6.2	Application of the proposed method in determination of electrical parameters referred into the LV delta winding.....	105
6.2.1	Per-phase winding resistances and leakage inductances.....	106
6.2.2	Core section inductances and resistances.....	107
6.3	Determination of series capacitance of the HV and LV windings.....	109
6.4	Parameter-based FRA interpretation and failure diagnostic.....	110
6.4.1	Parameter-based FRA interpretation in broad frequency range.....	110
6.4.2	Parameter-based failure diagnostic.....	111
6.5	Summary.....	112
	Conclusions.....	113
	References.....	118
	Curriculum vitae.....	130

Abbreviations and frequently used symbols

Abbreviations

2D	Two dimensional
CAP	Capacitive inter-winding
CBC	Phase-based comparison
CON	Conventional measurement method
D or d	Delta connection
DSO	Digital storage oscilloscope
EEOC	End-to-end open-circuit
EESC	End-to-end short-circuit
FEM	Finite Element Method
FRA	Frequency Response Analysis
GST	Grounded specimen test mode
GSTg	Grounded specimen test mode with guard
HV	High-voltage
Im{}	Imaginary part of a complex quantity
IMP	Proposed impedance method
IND	Inductive inter-winding
LV	Low-voltage
PBC	Construction-based comparison
Re{}	Real part of a complex quantity
T ₁ , T ₂ , T ₃	Test transformers
TBC	Time-based comparison
UST	Ungrounded specimen test
VNA	Vector Network Analyzer
Y or y	Star connection

Variables and Symbols

A	Magnetic vector potential
A _{cr}	Cross-sectional area
A, B, C, N	HV terminals
a, b, c, n	LV terminals
b _o	Half of a lamination thickness
B _{rms}	Effective flux density
C ₁ , C ₂ , C ₃ , C ₄	Equivalent capacitances calculated from the impedance tests
C _{gH}	Ground capacitance of a HV phase winding
C _{gH0}	Ground capacitance of a section of the HV winding
C _{gL}	Ground capacitance of a LV phase winding
C _{gL0}	Ground capacitance of a section of the LV winding
C _{HG}	Total ground capacitance of the HV windings
C _{HL}	Total inter-winding capacitance between HV-LV windings
C _{iw}	Inter-winding capacitance between HV-LV phase winding
C _{iw0}	Inter-winding capacitance between HV-LV phase winding

C_{LG}	Total ground capacitance of the LV windings
C_{sH}	Series capacitance of the HV windings
C_{sH0}	Series capacitance of a section of the HV windings
C_{sL}	Series capacitance of the LV windings
C_{sL0}	Series capacitance of a section of the LV windings
f	Frequency
F	Magnetomotive force
H	Magnetic field
I	Current
I_r	Reference current
\mathbf{J}	Current density vector
k_1	Constant depending on material
k_{fe}	Stacking factor representing fraction of core steel in the total cross section
k_L	Multiple factor to convert the inductance reference curve at high frequencies
k_R	Multiple factor to convert the resistance reference curve at high frequencies
L	Inductance
L_1	Core leg inductance
L_3 or $L_{leakage}$	Leakage inductance
L_4	Zero-sequence inductance
L_i, L_j	Self inductance of a winding section
L_m	Equivalent magnetizing inductance of the core
L_p	Core inductance in parallel model
L_s	Core inductance in series model
L_y	Core yoke inductance
M_{ij}	Mutual inductance between two winding sections
M_s	Domain magnetization
N	Number of turn
N_H	Number of turns of the HV winding
N_L	Number of turns of the LV winding
P_e	Eddy current loss
R_W or $R_{W AC}$	AC winding resistance
R_1	Core leg resistance
R_4	Zero-sequence resistance
R_{DC} or $R_{W DC}$	DC winding resistance
R_H	Resistance of HV winding
R_{HF}	Correlation coefficients calculated in high frequency range according to the standard DL/T911-04
R_L	Resistance of LV winding
R_{LF}	Correlation coefficients calculated in low frequency range according to the standard DL/T911-04
R_m	Equivalent magnetizing resistance of the core
R_{MF}	Correlation coefficients calculated in mid frequency range according to the standard DL/T911-04
R_p	Core resistance in parallel model
R_s	Core resistance in series model
R_{stray_losses}	Equivalent resistance from stray losses
R_y	Core yoke resistance

t_0	Thickness of a lamination
t	Time
V	Voltage
V_m	Measured voltage
V_r	Reference voltage
V_s	Source voltage
W_j	j^{th} winding
W_m	Magnetic energy
Z_{in}	Input impedance
Z_{mea}	Measured impedance
Δh	Axial displacement
Δx	Radial displacement
$\ x\ $	Norm
X	Reactance
δ	Skin depth
ℓ	Magnetic flux path length
μ_r	Local relative permeability in the rolling direction
μ'_{eff}	Real part of the complex permeability
μ''_{eff}	Imaginary part of the complex permeability
$\underline{\mu}_{\text{eff}}$	Complex permeability in the rolling direction
μ_0	Permeability of free space
Φ	Flux
φ	Phase angle of a complex quantity
ω	Angular frequency
\mathfrak{R}	Magnetic reluctance
σ	Electrical conductivity

Overview

The work is promoted to deal with two state-of-the-art problems in diagnostic of electrical and mechanical failures in the active part of power transformers: a new way to support the standardized Frequency Response Analysis (FRA) assessment which is currently based on kind of non-physical analysis, e.g. via correlation coefficients and waveform identification, and the determination of several important electrical parameters of transformers, e.g. core section impedances and winding series capacitances, for the failure diagnostic purpose. Result derived from the work is a new practical method consisting of two adapted and three new approaches that can be applied on power transformers to improve the diagnostic quality:

- Two adapted approach to calculate leakage/zero-sequence inductances from measurements and develop their frequency dependency in broad frequency range for simulation feasibility
- A new approach to calculate core section impedances from measurements and develop the frequency dependency of the parameters for simulation in wide frequency range
- A new approach to determine ground and inter-winding capacitances from measurements
- A feasible approach to identify winding series capacitance in transformer bulk

In appearance, after introduction the state-of-the-art of diagnostics of electrical and mechanical failure on the active part of power transformers with regard to relevant standards and measurement methods is summarized in chapter 1. To present the background of adapted and new approaches, chapter 2 introduces physical transformer models from which an adapted transformer model is proposed. Based on the model, the complete method combining the approaches in determination of transformer's (physical) electrical parameters for purposes of diagnostic and FRA interpretation are explained in chapter 3.

Chapters 4, 5 and 6 present three case studies in which the method is applied for each of three following test objects:

- Case study I: A 200 kVA 10.4/0.462 kV YNyn6 opened transformer (T_1)
- Case study II: A 2.5 MVA 22/0.4 kV Dyn5 sealed transformer (T_2)
- Case study III: A 6.5 MVA 47/27.2 kV YNd5 sealed transformer (T_3)

In each case study, electrical parameters of the transformers are determined in two different forms:

- Discrete values at low frequencies calculated directly from measurements for diagnostic purpose
- Frequency dependent functions in broad frequency range developed from measurement-based values and experimental formulae for a *physical* FRA interpretation

In addition, due to the fact that the transformer T_1 is open, several electrical and mechanical failures are performed in the transformer active part, from which the contribution of new approaches to the current diagnostic methods (conventional and FRA) is introduced.

Finally, in the last chapter, the capability and limitations of the new method in practical application will be concluded.

Introduction

Power transformers, static devices that transfer electrical power between isolated circuits, are important devices that interconnect components of the power system such as generators, transmission/distribution lines and loads for purpose of efficient power supply to users from remote sources. The main part of a power transformer consists of two or more electrical isolated windings wound around a magnetic core (core-type) that transfer electric power from one winding to another via magnetic-electric induction. Other part of the transformer includes components for operation (tap changer, regulator), insulation (pressboard, paper and liquid), cooling (radiator, fan, pump) and accessories (relay, temperature indication, oil level indicator, pressure relief device, over voltage protection device etc.). Figure 1 depicts main components of a typical power transformer, which can be easily observed from outside.

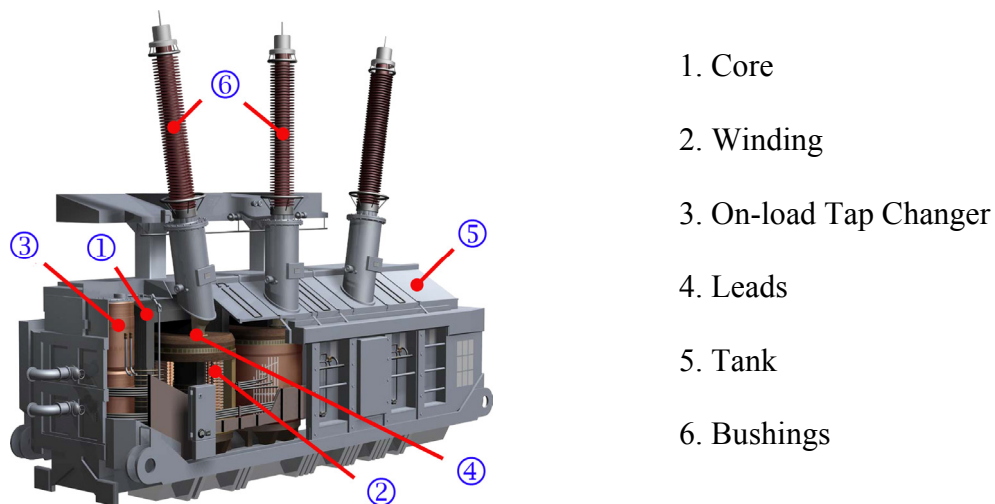


Figure 1: Main components of a power transformer [Omicron-12]

In order to maintain the reliability in operation and control of the power system, maintenance and failure diagnostics of transformers are of importance since a small change of transformer condition will lead to serious failures if it could not be detected timely. To have an overview of component's failures taking place in power transformers in reality, Figure 2 shows statistical data of transformer failures from two international surveys: a CIGRE report summarizes more than 1000 failures of large power transformers up to 20 years of age in the period of 1968 to 1978 in 13 countries from 3 continents [Bossi-83, Lapworth-06, Jagers-09a] and a survey on 112 major failures in a population of 2690 large power transformers from 20 utilities in Germany, Swiss, Austria and the Netherlands within the period of 2000 to 2011 [Tenbohlen-11, Tenbohlen-12]. According to the surveys, most major failures have roughly the same rates and take place in the tap changer (33.9 % - 40 %), winding (30 % - 32.1 %), bushings (11.6 % - 14 %) and the core (5 % - 7.1 %) as shown in Figure 2; lower failure rates associate with other components such as leads, tank, cooling unit etc. that are not identical between the two surveys. A conclusion drawn from the surveys is, the above mentioned transformer components whose failure rates are high should be in general paid attention for maintenance and diagnostics in order to reduce the failure rate of transformers for a reliable and safe operation versus time.

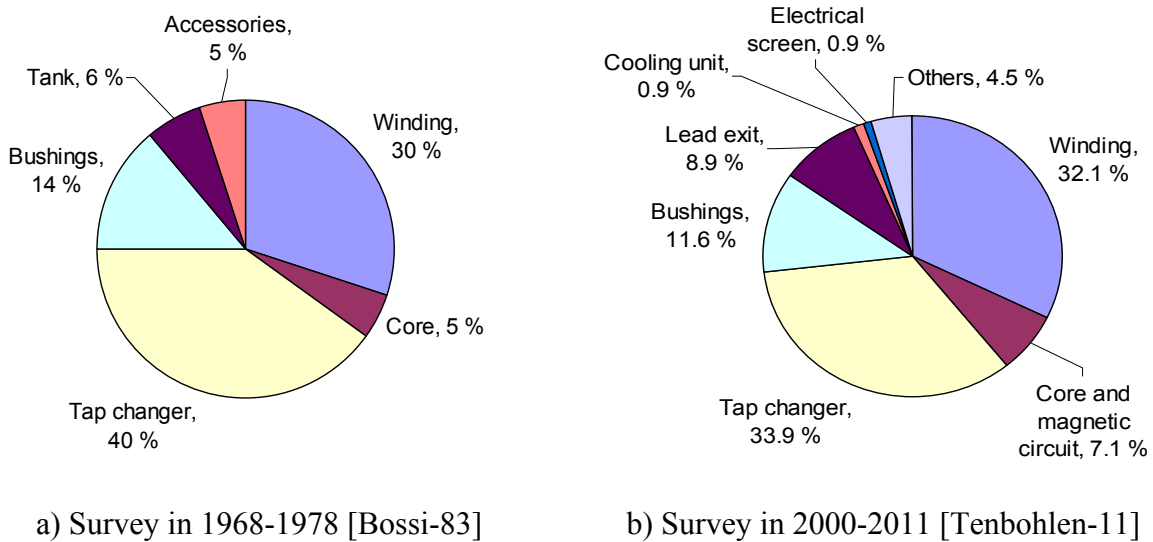


Figure 2: Percentage of failure locations in power transformers from international surveys

In classification of failure causes, there are several main failure modes associated with a certain component analyzed in the survey [Tenbohlen-11] shown in Figure 3a, from which majority of failure modes are electrical and dielectric (27.7 %), mechanical (17 %), thermal (15.2 %) and then physical chemistry (8.9 %). In Figure 3b, most of actions taken after the failures are repair in workshop (39.3 %), scrapping (35.7 %) and onsite repair (total 24.2 %) [Tenbohlen-11]. It is therefore concluded that premature detection of transformer failures plays a key role in prevention of the disconnection of the transformers from the power system for repairing or scrapping later on.

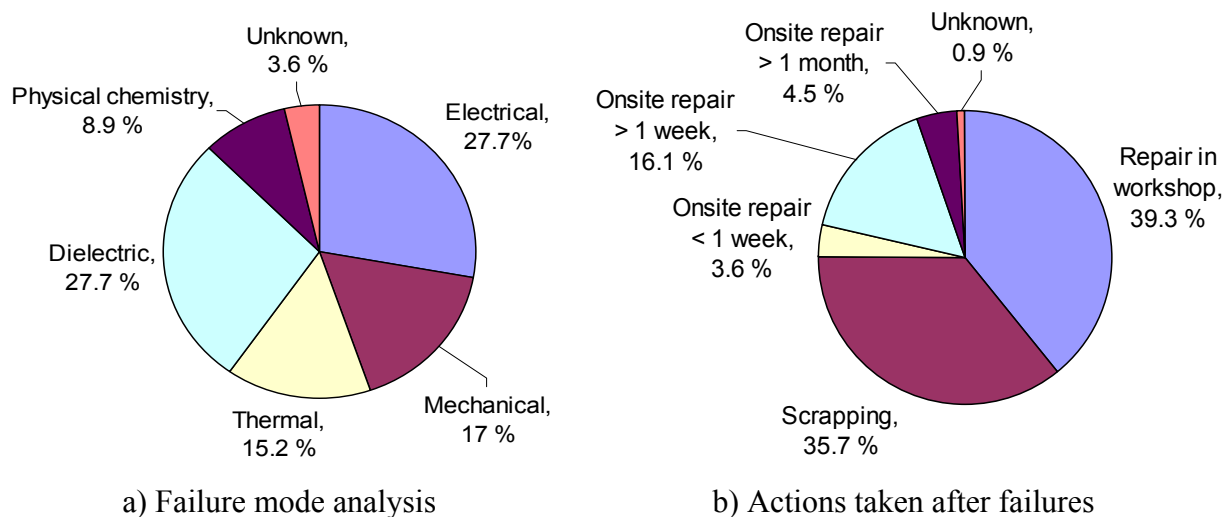


Figure 3: Failure modes and actions taken after 112 transformer failures [Tenbohlen-11]

In the viewpoint of measurement and diagnostics, a change of transformer condition, first indication of a failure mode, can be reflected via a change of relevant physical electrical parameters of the transformers; for example, if there is a mechanical failure appearing in the winding, the leakage inductance and/or winding capacitances would change. Therefore, determination of the parameters from measurements is of great importance in maintenance and diagnostics.

For a physical representation for diagnostic purpose, the electrical parameters of power transformers must consist of impedances of the core (legs and yokes), resistance and capacitances of and between windings as well as inductance of leakage and zero-sequence paths. Nevertheless, depending on application purpose, there are two different forms of the physical electrical parameters defined in the dissertation as follows:

1. Distributed/sectional form: the lumped electrical parameters of a *small section* of transformer components, e.g. self inductance of a small winding section or mutual inductance between two sections of one winding or two windings with/without appearance of the core. Normally the distributed form is suitable for theoretical investigation at high frequencies and the distributed parameters can only be calculated analytically based on *design data* [Bjerkar-05, Jayasinghe-06, Sofian-07, Abeywickara-07, Zhu-08, Hosseini-08, Shintemirov-09, Davari-09, Shintemirov-10a]. Actually there are several measurement-based approaches proposed to calculate the distributed electrical parameters, e.g. analysis based on the traveling wave theory [Akbari-02, Shintemirov-06], neutral network [Eldery-03], genetic algorithm [Rashtchi-05], ABC algorithm [Mukherjee-12] or particle swarm optimization algorithm [Rashtchi-08]; but the validation of these parameters at high frequencies is still in general unsolved and there is so far no evidence showing that the approach is applicable for windings in transformer bulk.
2. Lumped/equivalent form: the lumped electrical parameters of *whole* transformer components, e.g. leakage inductance between two windings or (total) inductance of a whole core section. The electrical parameters can be in general determinable through measurements at low and mid frequencies and therefore applicable for diagnostic purpose and advanced analysis, e.g. FRA or transients [Schellmanns-98, Schellmanns-00, Noda-02, Ang-08, Martinez-05a, Martinez-05b, Mork-07a, Mork-07b].

Figure 4 depicts two kinds of physical electrical parameters of one phase of a two-winding core-type transformer in corresponding circuits. Explanation of the inductive and capacitive parameters in Figure 4 is mentioned in Table 1. Details on how to establish the circuits and other resistive parameters will be mentioned in next chapters.

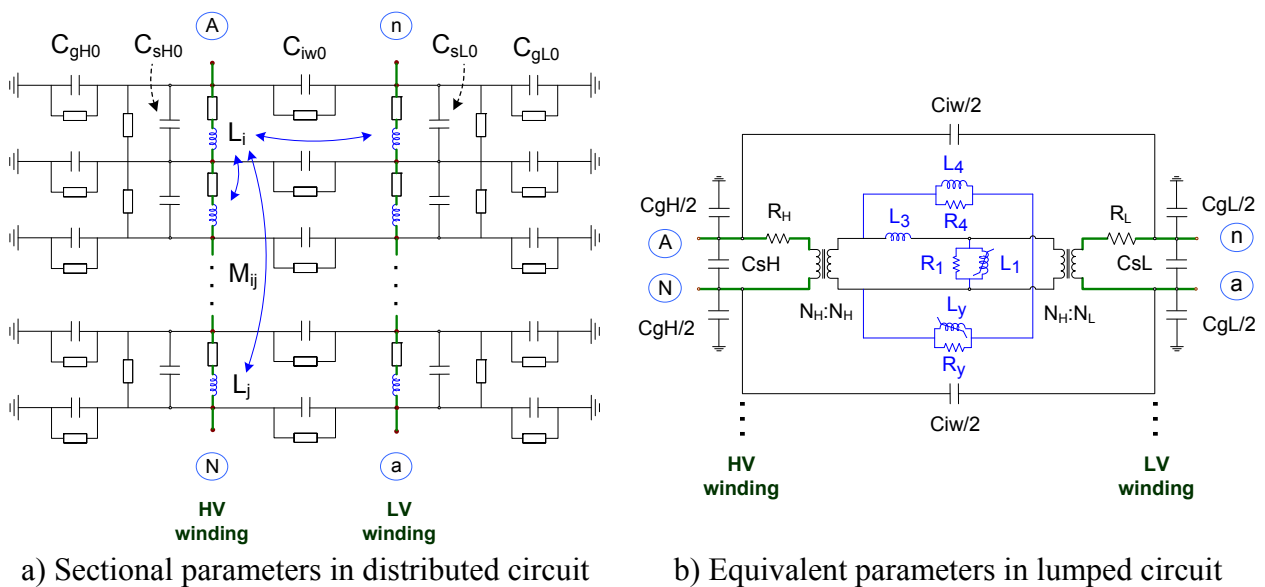


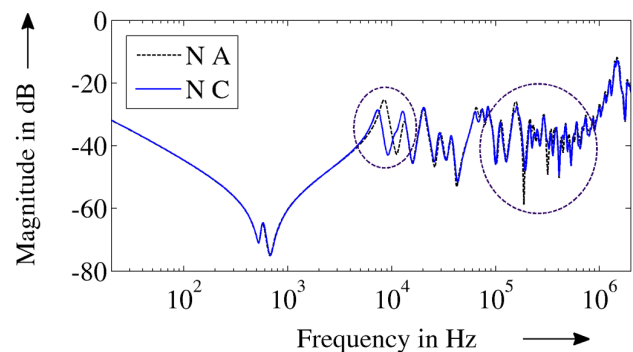
Figure 4: Physical equivalent circuits of a HV and LV phase winding of a transformer

Table 1: Parameter explanation

Parameter	Distributed circuit	Lumped (equivalent) circuit
Core inductance	L_i, L_j, M_{ij} (at low frequencies)	Core leg and yoke : L_L and L_Y
Leakage inductance	L_i, L_j, M_{ij} (at high frequencies)	L_3
Zero-sequence inductance	absent	L_4
Winding capacitances	Series C_{sH0}, C_{sL0} Ground C_{gH0}, C_{gL0} Inter-winding C_{iw0}	Series C_{sH}, C_{sL} Ground C_{gH}, C_{gL} Inter-winding C_{iw}

One of the limitations of current diagnostics of transformer failures is that several electrical parameters can not be in general determined from measurements, e.g. the core section inductance and the winding series capacitance. In fact, the core section inductance can only be calculated from measurements carried out on transformers at the star connected winding side; if the winding is in delta connection, it must be opened [Mork-07b, Martinez-05b]. Regarding the series capacitance of the windings, there is so far a measurement-based approach to determine the capacitance in transformer bulk [Aponte-12]; however the calculation accuracy depends strongly on the valid separation of leakage inductance into HV and LV side, which is not guaranteed from measurements at the moment. In addition, effect of inter-winding capacitances between phases is very important but not investigated, e.g. in the approach [Aponte-12] as the tested object is a small single-phase transformer and in another one [Ragavan-08] in which the single-phase equivalent circuit is based on. In winding bulk there is another approach based on initial distribution of voltage along the winding, but the approach is destructive and only applicable for windings that are isolated and brought out of the transformer [Pramanik-11]. Determination of core inductances and winding series capacitances, as well as other electrical parameters, based on non-destructive measurements on three-phase transformers regardless of how the winding is connected is of great importance since the parameters are used directly in detecting relevant failures.

Recently there has emerged a new technique that is considered efficient for detecting mechanical failures in transformer windings – the Frequency Response Analysis (FRA). The FRA is expected to provide special indicators relating to the failure, e.g. deviation of measured FRA traces in different transformer conditions at frequencies from several tens kHz to several hundreds kHz, which can not be revealed from other measurement methods. Nevertheless, more investigations on the ways to interpret the FRA traces and to analyze quantitatively the deviation are still requested since there is so far no formal international standard¹ which can help users to make reliable assessments for all cases in reality. For illustration, Figure 5 compares two measured end-to-end open-circuit FRA traces of two outer phase HV windings (between the HV neutral “N” and terminal “A” or “C” for phase A or C) of a 6.5 MVA 47/27.2 kV YNd5 large distribution transformer from which the current FRA assess-

**Figure 5:** Comparison of FRA traces measured on phases A and C at HV side

¹ There are so far only the Chinese standard [DL/T911-04] and several draft guides/standards from CIGRE, IEC, IEEE: [CIGRE-08], [IEC 60076_18-09], [IEEE PC57.14D9.1-12]

ment from the Chinese standard [DL/T911-04] reveals no failure. In such case, one would like to know what happens in the transformer or in other words, which parameters are changed associated with the deviations in Figure 5? Obviously, the current FRA assessment which is based on non-physical analyses is not fully efficient and should be accompanied with a physical interpretation via analysis of electrical parameters for a better diagnostic.

Objective of the work

In order to provide a better diagnostic of mainly electrical and mechanical failures on the active part of power transformers by solving above mentioned problems concerning the state-of-the-art diagnostics and FRA assessments, the dissertation proposes a new practical method consisting of new and adapted approaches for determination of all electrical parameters of power transformers, which are required suitably for both FRA and diagnostic purpose.

Since the transformer's electrical parameters in the dissertation are investigated ultimately for the diagnostic purpose, the equivalent form of the parameters in a lumped equivalent circuit will be researched in the approaches in detail. The advantage of using the equivalent form is that the electrical parameters could be identified through measurements but in other words, the corresponding equivalent circuit is only appropriate for analysis at low and mid frequencies since the distributed electrical parameters are the preferred ones for investigations at mid and high frequencies. Due to the fact that transformer design data are requested for characterization of the distributed parameters, which is normally not guaranteed in reality, especially for old transformers, it is expected that the equivalent electrical parameters obtained from the new method can be used instead, since the both parameter forms are relative. If it is the case, then the analysis of transformer frequency responses at mid and high frequencies becomes possible without the need of transformer design data. (It is true for winding capacitances but there are more challenges for inductances, i.e. converting leakage inductance between the whole HV and LV windings into self and mutual inductances of sections of and between the windings).

1 State-of-the-art of electrical measurement methods in diagnostics of electrical and mechanical failures in the active part of power transformers²

In this chapter, state-of-the-art of electrical measurement methods in context of diagnostics of mechanical and electrical failures in the active part of power transformers will be presented. Together with advantages, limitations and challenges of key measurement methods are also introduced as motivations for development of a new measurement-based method.

Mechanical and electrical failures in the active part of power transformers mentioned in the dissertation include failures that change electrical parameters of transformers such as failures in the core (lost of core ground, short of core laminations etc.) and failures in windings (open-circuited, shorted turns/discs, short-to-ground, axial and radial displacement, buckling, tilting etc.). It is important to mention that although the failures may change the condition of the insulation system, the dissertation does not focus on the topic of the transformer insulation, but on a change of relevant electrical parameters such as winding capacitances; therefore electrical measurement methods such as partial discharge detection, dissipation factor measurement, Frequency Domain Spectroscopy (FDS), Polarisation and Depolarisation Current (PDC) etc. will be not investigated.

1.1 Traditional measurement methods

Traditional measurement methods are defined as conventional methods that measure transformers at DC and power frequency (50 Hz or 60 Hz) such as: DC winding resistance, turn ratio, no-load (exciting) current/impedance, magnetic balance, short-circuit impedance, zero-sequence impedance, capacitances [BR-05, IEC 60076/1-00, IEEE C57.125-91, IEEE 62-95, Velasquez-10d, Velasquez-11, Krüger-08, Krüger-11, Omicron-12]. The purpose of these tests is to determine the electrical parameter or “condition” of components in the transformer active part at DC and power frequency for a comparison with those from reference data for relevant diagnostics.

1.1.1 Measurement methods to detect core problems

Currently there is no traditional method to determine impedances of core sections (legs, yokes) of power transformers, except an advanced method in [Mork-07b] which can be only applicable for transformers with star-connected windings. The method will be presented in the next chapter since it is based on equivalent transformer circuits that are the main content of the chapter. Therefore, instead of determination of core section impedances, which is not easy and feasible for diagnostic purpose, several following traditional measurement methods are referred to detect an abnormal condition of transformer core (and also of windings) [Velasquez-10d, Krüger-08, Krüger-11]:

- No-load exciting current/impedance
- Magnetic balance

It is required that the core insulation resistance and inadvertent core grounds should be checked in addition to assure that there is no influence from core insulation issue on the assessed condition. More information on the core insulation resistance and inadvertent ground tests can be found in [IEEE 62-95].

² Power transformers mentioned in the dissertation are two-winding three-legged core-type transformers, unless stated otherwise.

The above mentioned tests are normally performed on the HV winding of power transformers since application of test voltage at LV side may generate high open-circuit voltages at HV side, which is not recommended for safety reasons. To illustrate these tests, a YNyn6³ transformer whose active part sketched in Figure 1.1 is exploited; in this case, the quantities (current, voltage, impedance) after measurement are referred into the HV side. Because of the vector group, the polarity of the HV phase windings (W_1 , W_2 and W_3) is opposite with that of the LV phase windings (W_4 , W_5 and W_6). For easy observation, the HV and LV phase windings are separate although in reality they are coaxial windings, covering the whole core legs.

The principle of the tests is applying single-phase voltage on a HV phase winding while other phase windings are left floating, then measuring the associated current and induced voltages on other HV phase windings. By this way, the core condition can be examined by comparisons of exciting currents and induced voltages, which are derived from measurements on each of three phase windings. Table 1.1 summarizes procedures of the tests and assessments from relevant standards.

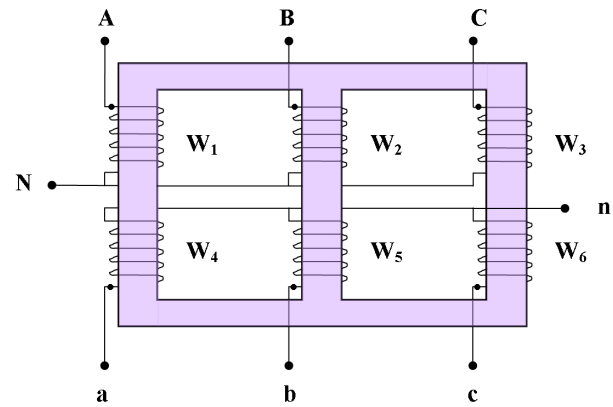


Figure 1.1: Main components of the active part of a YNyn6 transformer

Table 1.1: Traditional diagnostic tests of core condition of power transformers

Test	Applied voltage	Measurement	Assessment
No-load exciting current	V_{AN} V_{BN} V_{CN} see (i)	I_{AN} I_{BN} I_{CN}	Compare the results with that of the previous tests or comparison of results between phases Tolerance: 5 % to 30 %, see (ii) and (iii)
Magnetic balance see (iv)	V_{AN} V_{BN} V_{CN}	V_{BN}, V_{CN} V_{AN}, V_{CN} V_{AN}, V_{BN}	Compare the applied voltage and the sum of induced voltages, see (v)

- i. The test should be performed at highest possible voltage that does not exceed the voltage rating of the excited winding [IEEE 62-95].
- ii. The pattern for most of cases is, two similar high current readings on outer phases and one lower reading on the middle phase. [IEEE 62-95] suggested a tolerance of 10% between currents of outer phases; however, smaller tolerance may be indicative of core problem. [CIGRE-10] recommended tolerances of 5 % between outer phase currents and 30% between an outer and a middle phase current.
- iii. A change of current reading due to core remanence can be significant. In such case, reliable demagnetization methods should be applied to exclude residual magnetism in the core [IEEE 62-95].
- iv. The test is not mentioned in relevant standards. A low applied voltage is recommended.
- v. The equality between the applied voltage and the sum of induced voltages reveals the magnetic balance between phases. In normal condition, when an outer phase winding is excited, the induced voltage on the

³ Transformers with other vector groups, i.e. Yd, Dy, Dd, can be tested in the same manner.

middle phase winding is about 85-90 % of the applied voltage while the middle phase winding is excited, voltages induced on outer phase windings are about 40-60 % [Velasquez-11].

The tests are then applied to detect whether there is a problem in the core such as lost of core clamping, core movement during transportation or shorted core laminations. However, since core failures are rarely a problem in reality, it may be concluded that the tests are sufficient for diagnostic of the transformer core condition. Anyway, it would be appreciate if electrical parameters of core sections, i.e. legs and yokes, could be determined for a better assessment since in general, a significant difference of core section impedances at different conditions can reveal where the problem is, i.e. in legs or yokes. In addition, the exciting current and magnetic balance test results can be recovered from the core circuit with pre-determined core section impedances whereas the inverse direction is impossible. Obviously, determination of *electrical parameters* of transformer core and windings, together with the above mentioned tests, is the best solution for the diagnostics.

1.1.2 Measurement methods to identify winding electrical parameters

Unlike the core, electrical parameters associated with windings for detection of electrical and mechanical failures can be determined directly through measurements. The electrical parameters consist of those from windings itself, e.g. resistances and capacitances, and dual magnetic-electric parameters outside or between windings such as zero-sequence and leakage inductances. In context of traditional diagnostic tests, the following parameters associated with transformer windings can be measured:

- DC resistance ($R_{W\ DC}$)
- Per-phase equivalent resistance from total stray losses ($R_{AC\ stray\ losses}$)
- Per-phase leakage inductance ($L_{leakage}$)
- Zero-sequence inductance (L_0)
- Ground and inter-winding HV-LV capacitances (C_{gH} , C_{gL} and C_{HL} respectively)

Table 1.2 summarizes relevant traditional tests with assessments for the diagnostic purpose. It is also noted that other condition-reflected tests such as ratio, exciting current or dissipation factor can be carried out in addition to specify the failure [BR-05, Omicron-12, Velasquez-10d, Velasquez-11].

Table 1.2: Traditional diagnostic tests for measurements of winding-associated parameters of power transformers (at DC or power frequency) [BR-05]

Parameter	Measurement procedure	Tolerance	Diagnostic application
$R_{W\ DC}$	DC test → apply DC voltage on each phase winding and measure the corresponding current (other phase winding left opened)	5 %	loose connections on bushings or tap-changers, broken strands and high-contact resistance in tap-changers
$R_{AC\ stray\ losses}$	Per-phase short-circuit test → apply sinusoidal voltage on a HV phase winding while the corresponding LV phase winding is shorted	–	shorted parallel strand
$L_{leakage}$		3 %	mechanical failures

Parameter	Measurement procedure	Tolerance	Application
L_0	Zero-sequence test → apply sinusoidal voltage between three connected (HV) terminals and the neutral, the winding at other side is left open	–	problems associated with phase windings and zero-sequence path (between windings and the core)
C_{gH}, C_{gL}	Capacitance tests → multi-tests to measure capacitances between HV and LV winding, between HV and the tank (ground), between LV winding and the tank.	–	mechanical winding failures, insulation deterioration, structural problems (displaced wedging, winding support)
C_{HL}			

It is realized in Table 1.2 that the parameters which can be used to detect electrical and mechanical failures in windings are the ones derived from DC winding resistance, short-circuit and capacitance tests, i.e. DC winding resistance, leakage inductance and winding capacitances. Since the DC resistance and short-circuit test are quite straightforward and already introduced, the capacitance multi-tests are now explained in detail.

According to [IEEE 62-95], a capacitance model of two-winding transformers, which consists of three phase capacitances:

- C_{HG} : ground capacitance of three connected HV phase windings
- C_{LG} : ground capacitance of three connected LV phase windings
- C_{HL} : inter-winding HV-LV capacitance between HV and LV phase windings

is required and thus introduced in Figure 1.2.

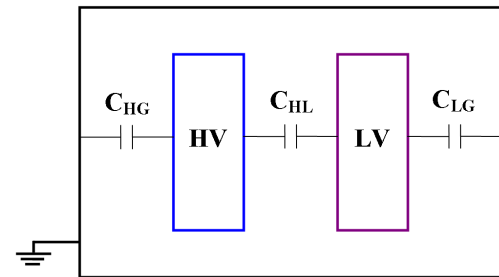


Figure 1.2: Equivalent capacitances of a two-winding transformer

Due to the fact that there are two different kinds of capacitances to be measured, i.e. capacitance to ground and capacitance between two ungrounded points, three different test modes are necessary:

- Ungrounded specimen test (UST): applicable for measuring capacitance between two terminals that are ungrounded or can be removed from ground. As shown in Figure 1.3, C_A is the ground capacitance from terminal ① and C_B is the capacitance between the terminals ① and ② which needs to be measured. Thanks to the connection in the UST mode only current flowing through the C_B is measured and thus the C_B is determined. If one replaces terminals ① and ② in Figure 1.3 by HV, LV terminals in Figure 1.2 respectively, the C_{HL} will be measured.

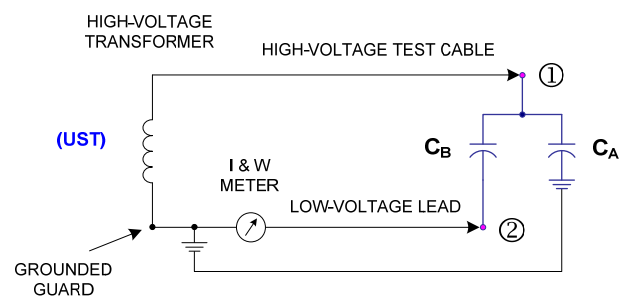


Figure 1.3: UST mode – Measure C_B only [IEEE 62-95]

- Grounded specimen test (GST): applicable for measurement of total ground capacitance from an ungrounded to grounded terminal(s). Figure 1.4 depicts the measurement mode in which both capacitances C_A and C_B are measured (terminal ② is grounded). If the terminals ①, ② are HV, LV terminals respectively, the $C_{HL} + C_{HG}$ will be measured if the LV terminals are grounded.

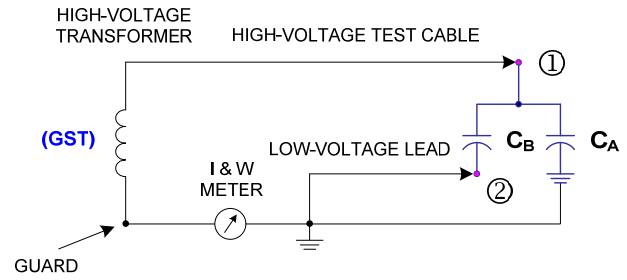


Figure 1.4: GST mode – Measure C_A and C_B [IEEE 62-95]

- Grounded specimen test with guard (GSTg): applicable for measurement of ground capacitance from an ungrounded terminal. As illustrated in Figure 1.5, ground capacitance from terminal ① C_A is measured whereas capacitance between two ungrounded terminals C_B is not measured. This mode is appropriate for measuring the C_{HG} or C_{LG} in Figure 1.2.

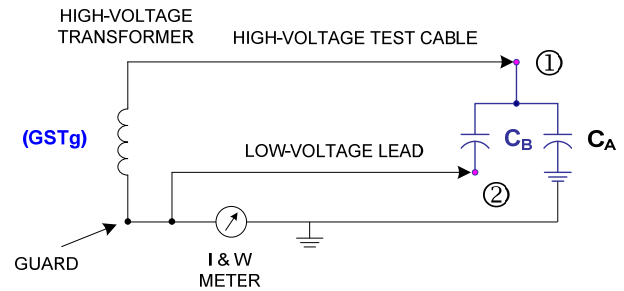


Figure 1.5: GSTg mode – Measure C_A only [IEEE 62-95]

Table 1.3 summarizes multi-tests for measuring capacitances of two-winding transformers. For three-winding transformers, the procedure is nearly the same and described in [IEEE 62-95].

Table 1.3: Capacitance tests for two-winding power transformers ($V_{\text{test max}} = 1.2 V_{\text{rated}}$)

Test	Test mode	Energize	Ground	Guard	UST	Measure
1	GSTg	HV	–	LV	–	C_{HG}
2	GSTg	LV	–	HV	–	C_{LG}
3	UST	HV	–	–	LV	C_{HL}
4	UST	LV	–	–	HV	C_{HL} (i)
5	GST	HV	LV	–	–	$C_{HG} + C_{HL}$ (ii)

- Test number 4 is an alternative of the test number 3 in measuring C_{HL} .
- Test number 5 is to check the first and third tests

Thanks to the guard technique different capacitances and corresponding dissipation factors of power transformers can be measured. The only point which is not very appropriate for very aged insulation systems is that the applied voltage should be high enough (maximum 1.2 times of rated voltage) due to high capacitive reactance at power frequency and it may damage the insulation⁴. In addition, the winding series capacitance, which is very important for diagnostic of different mechanical failures in transformer windings [Velasquez-11] and for other investigations

⁴ It is true for testing one of the test transformers in the dissertation: the opened transformer T_1 has very aged insulation system and no oil, which is a good object to perform electrical and mechanical failures on the active part.

such as analysis of transients or surge phenomena, can not be measured through the capacitance tests. That is the motivation for a new method which will be introduced in next chapters.

1.2 Advanced measurement methods

Advanced measurement methods as defined in the dissertation, and also in [Velasquez-10d, Velasquez-11] are methods that measure electrical parameters or condition of power transformers at other frequencies than power frequency. The aim of these methods is to explore the frequency dependent performance of the transformer parameters/condition. Currently there are two different advanced measurement methods classified with regard to frequency range:

- Measurements in low frequency range: open- and short-circuit, zero-sequence, capacitance and dissipation factor etc.
- Measurements in broad frequency range, e.g. tens of Hz to several MHz: frequency responses of voltage ratios and input impedance/admittance.

Since the main content of the work is to explore the possibility of extraction of electrical parameters of power transformers for relevant diagnostics, the topic of insulation is not investigated. Therefore, only measurement methods involving electrical parameters or condition of power transformers such as:

- Open-circuit tests, including exciting current and magnetic balance (core condition)
- Short-circuit test (stray losses and leakage inductance)
- Zero-sequence test (zero-sequence inductance)
- Capacitance test (winding capacitances)
- FRA tests (core impedance, leakage, zero-sequence inductance, winding capacitances)

are considered. Since the advanced open- and short-circuit, zero-sequence and capacitance test are nearly the same with the corresponding traditional ones (the difference is only frequency), they will not be mentioned. Thus, this section is devoted for FRA tests.

1.2.1 What is FRA and applications of the FRA method

FRA is the abbreviation of Frequency Response Analysis. The term FRA applicable for power transformers means analysis of frequency responses measured at transformer terminals for the purpose of diagnostic. The FRA method is considered as one of new techniques efficient for diagnostic of mechanical failures in power transformers.

According to the newest draft standard [IEEE PC57.149/D9.1-12], the FRA test can be used to detect mechanical failure or damage in transformers in several typical scenarios as follows:

- Factory short-circuit testing
- Installation or relocation
- After a significant through-fault event
- As part of routine diagnostic measurement protocol
- After a transformer alarm, e.g. gas detector, Buchholz etc.
- After a major change in on-line diagnostic condition
- After a change in electrical test conditions
- Modeling purposes

The main interest of FRA method is to detect mechanical deformations of transformer windings that may be consequence due to very large electromagnetic forces resulting from over-current faults and to check electrical integrity of transformers that may be changed after transportation or installation, which can not be detected through other diagnostic methods [CIGRE-08, IEEE PC57.149/D9.1-12]. Major mechanical failure modes in windings include:

- Buckling
- Tilting
- Bending
- Telescoping
- Spiral tightening under twisting forces
- Movement of winding leads, tap leads

In addition, the FRA method is useful in detection of other electrical failures that can be also diagnosed through other electrical measurement methods (magnetic balance, ratio, exciting current, short-circuit, capacitance test) such as [Velasquez-10d]:

- Short-circuited winding turns/strands
- Short-circuit to ground
- Short-circuited core laminations
- Lost of core ground
- Open-circuit failure

1.2.2 How the FRA measurement is conducted

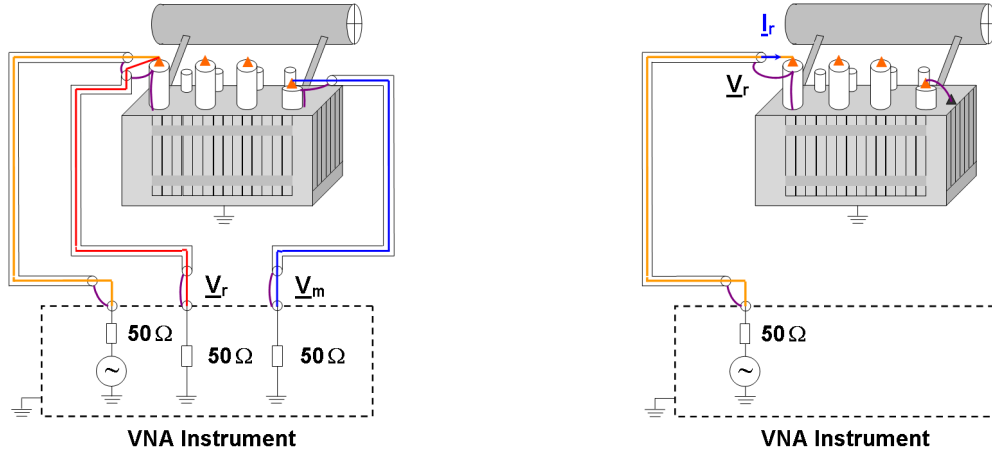
The measurement was first formally introduced in [Lech-66, Dick-78] with aim to analyze frequency responses measured at transformer terminals, which were used to detect mechanical winding deformation. According to the publications, there are two kinds of frequency responses that can be used for the diagnostic:

- Voltage ratio (mentioned currently in draft standards → named as standard frequency response)
- Input impedance (not yet standardized → called as non-standard⁵ frequency response)

The principle of the standard measurement method is the application of either impulse or sinusoidal voltage signal whose frequency is changeable from a low value, e.g. 20 Hz, to a high value, e.g. several MHz, to a terminal of a test transformer, being measured and named as reference voltage to ground \underline{V}_r , and the measurement of response voltage at another terminal, named as \underline{V}_m , so that the frequency response of voltage ratio in such frequency range can be obtained. For the non-standard measurement, the current associated with the applied voltage is measured for determination of input impedance or admittance of the transformer at the injected phase winding. Figure 1.6 illustrates the standard and non-standard frequency response measurement on a two-winding transformer by means of a scattering-parameter Vector Network Analyzer (VNA) whose measurement mechanism is based on traveling wave calculation, i.e. determination of incident and reflected signal from transmitted signal at the reference plane. Of course one can measure frequency responses by means of other devices such as the network analyzer (with current probe for measuring currents), or any z- or y-parameter devices, but the s-parameter

⁵ There are also other frequency responses such as current ratio, input admittance, transfer impedance/admittance but they are not appropriate for parameter determination and thus will not be investigated in the dissertation

network analyzer is recommended since the responses should be measured over a broad frequency range [Martinez-09].



a) A standard FRA measurement

b) A non-standard FRA measurement

Figure 1.6: FRA measurement method by means of a s-parameter VNA

Then the frequency responses can be determined based on measured quantities:

- For standard frequency responses

$$\text{FRA magnitude: } \text{Mag} = 20 \cdot \log_{10} \left(\left| \frac{V_m}{V_r} \right| \right) \quad (1.1)$$

$$\text{FRA phase angle: } \text{Pha} = \varphi_{V_m} - \varphi_{V_r} \quad (1.2)$$

- For non-standard frequency responses:

$$\text{Input impedance magnitude: } |Z_{in}| = \left| \frac{V_r}{I_r} \right| \quad (1.3)$$

$$\text{Input impedance phase angle: } \varphi_{Z_{in}} = \varphi_{V_r} - \varphi_{I_r} \quad (1.4)$$

Depending on measurement configuration, there are different types of voltage ratios as well as input impedances to be measured. Concerning standard frequency responses, guides and draft standards [DT/L911-04, CIGRE-08, IEC 60076/18-09, IEEE PC57.14D9.1-12] define four following main FRA test types shown in Figure 1.7:

- End-to-end open-circuit (EEOC): source can be injected at phase or neutral terminal
- End-to-end short-circuit (EESC): short-circuit can be made on single or three phases
- Capacitive inter-winding (CAP)
- Inductive inter-winding (IND)

Note that there are more measurement configurations with respect to terminal connection proposed for the purpose of identification of frequency responses which are sensitive to fault detection, i.e. having as many natural frequencies as possible [Satish-05, Satish-08]; however, the measurement configurations in Figure 1.7 are only referred since assessments of only standard frequency responses are necessary to be compared with results derived from analysis of input impedances in the next chapters.

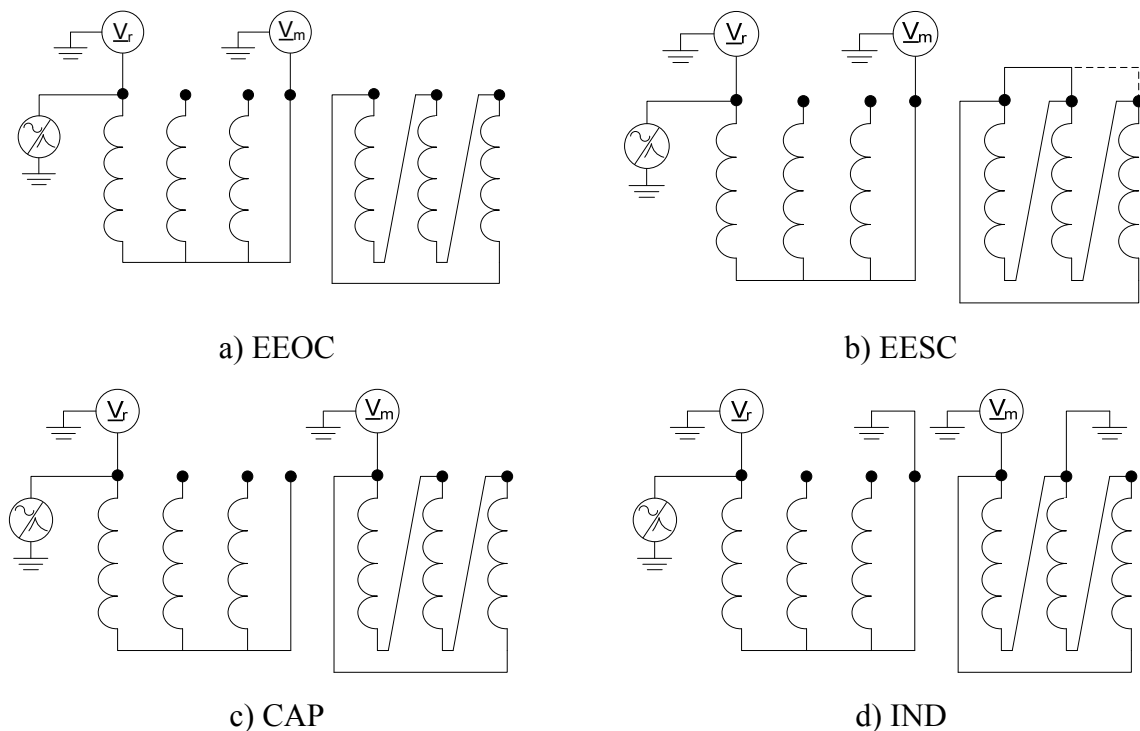


Figure 1.7: Four main standard FRA tests on a YNd transformer

1.2.3 Assessment of FRA results according to current standards

According to current draft guides and standards, the FRA method is a comparative method. That means the measured frequency responses corresponding to each kind of measurement types, i.e. EEOC, EESC, CAP or IND, will be compared to detect deviations which are considered as indicators of failures. To achieve reliable diagnostics with the FRA method, first of all the reproducibility of the measurement needs to be guaranteed; afterwards, depending on reference data, *quantitative* comparative modes and/or *qualitative* experience-based judgment are performed.

Reproducibility security: All FRA tests should be conducted in the same and recommended procedure in terms of instrument (applied voltage, dynamic range, frequency range), measurement setting (frequency points, noise suppression level, receive bandwidth, sweep mode), measurement accessories (cables, grounding braids), calibration, environment (grounding, isolation), test object preparation (test lead connection, bushings, tap-changers) etc. More information on how to conduct good FRA measurements can be found in [CIGRE-08, IEEE PC57.14 D9.1-12].

Quantitative comparative modes: there are three possible modes for diagnostic:

- Time-based comparison (TBC): comparison of measured responses at different points of time (test type and measurement connection are the same)
- Construction-based comparison (CBC): comparison of measured responses on identical/twin transformers (test type and measurement connection are the same)
- Phase-based comparison (PBC): comparison of measured responses on (outer) phases of the test transformer.

It is noted that for comparisons, only the magnitude of frequency responses is referred; the phase angle may be used for modeling purposes, not for the diagnostic assessment. Figure 1.8 shows an example in which a comparison of standard frequency responses of a HV phase winding of a distribution transformer in TBC mode from 10 kHz to 1 MHz after an axial displacement is performed. It is observed from the figure that the failure causes certain deviations in four main FRA test types. However, the way to assess quantitatively these deviations, in particular, and the deviations in other cases, in general, is still not widely approved in any formal international standard.

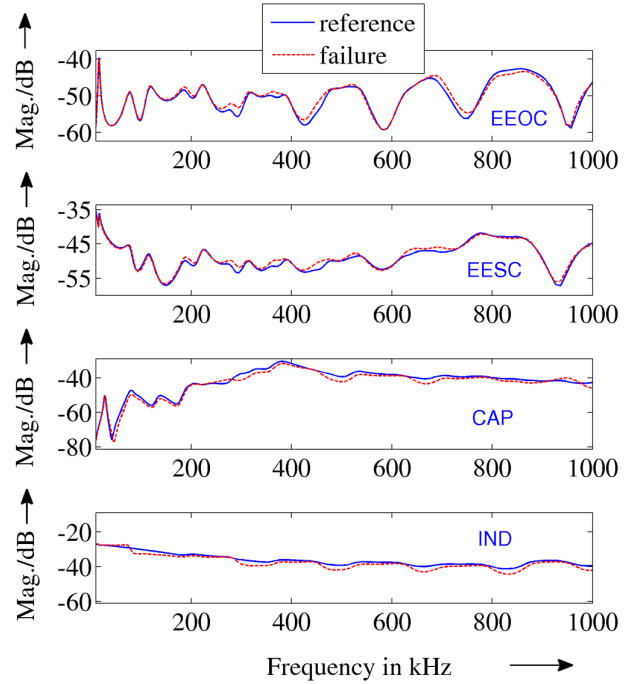


Figure 1.8: Illustration of FRA results for a case of mechanical winding failure

The standard [DL/T911-04] is currently the only national one⁶ that can provide quantitative assessments shown in Table 1.4 from the deviations between measured frequency responses. Interpretation of assessments for the FRA test types in Figure 1.8 according to the standard is introduced in Table 1.5.

Table 1.4: Quantitative assessment of FRA deviation according to the [DL/T911-04]

Assessment rule	Assessment result	Application scope
$R_{LF} \geq 2$ AND $R_{MF} \geq 1$ AND $R_{HF} \geq 0.6$	Normal winding	suitable for 6 kV and above voltage power transformers and other transformers for special uses ⁷
$2 > R_{LF} \geq 1$ OR $0.6 < R_{MF} \leq 1$	Slight deformation	
$1 > R_{LF} \geq 0.6$ OR $R_{MF} < 0.6$	Obvious deformation	
$R_{LF} < 0.6$	Severe deformation	

where: R_{LF} , R_{MF} and R_{HF} are correlation coefficients⁸ calculated from the deviations of frequency responses within range of 1 to 100 kHz, 100 to 600 kHz and 600 kHz to 1MHz respectively

Table 1.5: FRA assessment on the comparisons in Figure 1.8

FRA test type	Assessment result
EEOC	Normal winding
EESC	Normal winding
CAP	Slight deformation
IND	Obvious deformation

From Table 1.5 there emerge several questions which should be clarified for the final conclusion:

- What is the real failure in the winding concluded from the assessments?
- How serious is the failure?

Since the questions can not be answered based on the assessments, it is suggested that the

⁶ There is another one called NCEPRI, named after North China Electric Power Research Institute, available at www.ncepri.com

⁷ It is also recommended for application on transformers with power higher than 1 MVA [FRAnalyzer-09]

⁸ Calculation of the correlation coefficient is presented in detail in the [DL/T911-04]

standard-based assessments shall be considered as additional information rather than the final decision since it is only clear that there is a (mechanical) problem in the winding.

Qualitative experience-based judgment: the deviations between measured FRA waveforms can be assessed in a qualitative manner to detect specific failures [CIGRE-08, PC57.14 D9.1-12, IEC 60076/18-09]. Therefore success of the method depends greatly on experience of experts. For illustration, Table 1.6 and Figure 1.9 shows rules of experience for detection of the radial winding deformation from FRA measurements according to the [PC57.14 D9.1-12] (there is no rule for detection of the axial displacement failure in current standards).

Table 1.6: Qualitative FRA assessment of the radial winding deformation [PC57.14 D9.1-12]

Frequency range	Radial deformation (no other failure mode exist)
20 Hz – 10 kHz	EEOC: unaffected by radial winding deformation. EESC: generally exhibits slight attenuation within the inductive roll-off portion.
5 kHz – 100 kHz	EEOC and EESC: shift or produce new resonance peaks and valleys depending of the severity of the deformation. However, this change is minimal and difficult to identify.
50 kHz – 1 MHz	EEOC and EESC: Radial winding deformation is most obvious in this range. It can shift or produce new resonance peaks and valleys depending of the severity of the deformation.
> 1 MHz	EEOC and EESC: generally unaffected. However, severe deformation can extend into this range.

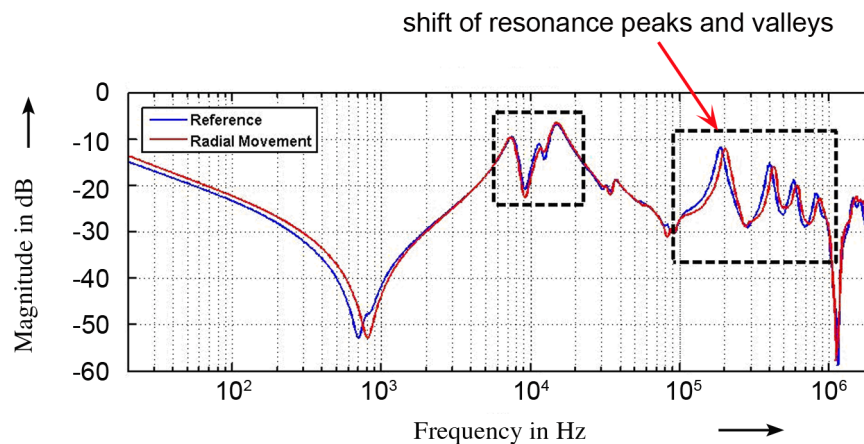


Figure 1.9: Waveform identification from EEOC-FRA tests on a LV winding for detecting the radial winding deformation [PC57.14 D9.1-12]

It is concluded that the quantitative and qualitative assessments based on current standards [DL/T911-04, PC57.14 D9.1-12] can not afford to give the expected answer in the case of axial displacement failure and perhaps in many other cases. Because although the standard is formed based on investigations on a large number of power transformers having mechanical failures on their windings, there is still a certain uncertainty in the assessment since:

- The standard did not cover all of transformer types and design. In fact it is impossible to investigate the mechanical failure in a variety of transformers with different structures (normal/auto, core/shell-type, single/multiple-phase), and design (power, voltage, winding number and type (disc, layer, helical, foil), winding connection (star, delta)).
- The failure nature (single/multiple, type, position and level) has great influence on the measured frequency responses and hence the deviations. In fact under different scenarios

of a mechanical failure in a transformer winding in terms of position and level, the measured frequency responses and thus deviations may look differently.

- Reproducibility of the measurement is in general not secured [Velasquez-10a, Velasquez-10b] even there are instructions for conducting good measurements [Wimmer-06, CIGRE-08, Velasquez-10c, IEEE PC57.149/D9.1-12]. Influencing factors such as different users or instruments can affect the FRA results measured on a test transformer.

1.2.4 Assessment of FRA results according to worldwide researches

There is a large amount of worldwide publications concerning FRA assessment for diagnostics of power transformers and therefore there are various viewpoints in classification of FRA assessment methods, e.g. in [Sofian-07, Velasquez-11]. Figure 1.10 summarizes FRA assessment methods with regard to non-physical and physical analysis since the motivation of the dissertation is the introduction of a physical way in assessment of terminal frequency responses, which can be combined with other conventional diagnostic testing methods to improve the diagnostic quality applicable to power transformers. Note that only off-line FRA measurements are investigated since there exist more problems, and hence more assessment rules, for on-line measurements when the transformer is energized and connected to the network [Setayeshmehr-06, Gonzalez-07, Bagheri-11].

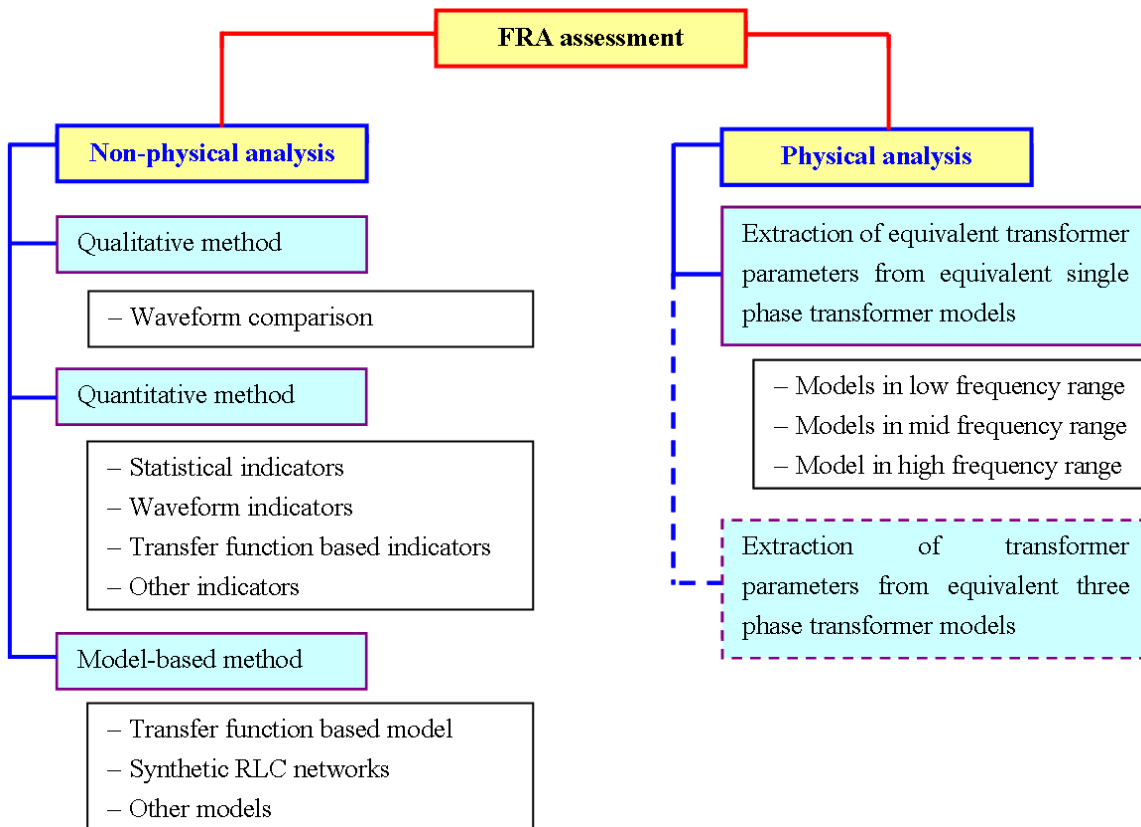


Figure 1.10: Classification of assessment methods for FRA measurement results

Most of the assessments in Figure 1.10 is devoted for non-physical analysis that considers measured frequency responses as signals of discrete values. Afterwards, information from each signal, e.g. resonance frequencies, magnitudes at those frequencies, quality factors etc. and/or quantitative indicators calculated from comparison between two signals, e.g. error function,

expectation function, standard deviation, R-factor, tolerance bands etc. [Leibfried-99, Ryder-03, Gui-03, Rahman-06, Wimmer-07, Firoozi-09, Velasquez-10e] or failure reflected coefficients such as transfer function discrimination, deformation coefficient etc. [Florkowski-07, Joshi-08] are calculated and interpreted. Figure 1.11 shows an example in capturing resonance peaks/valleys with corresponding frequencies and magnitudes for a quantitative assessment.

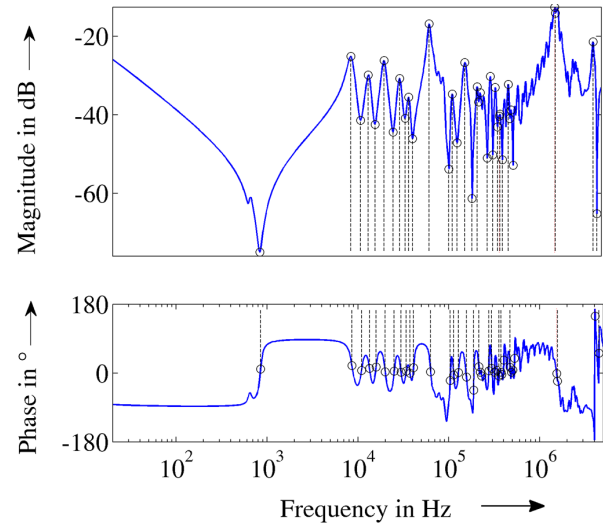


Figure 1.11: Quantitative indicators calculated from waveform of a FRA trace

Another kind of non physical analysis is the model-based method that convert the measurement results into approximation-based indicators, e.g. pole-zero representation, or kind of synthetic model, e.g. black-box model or RLC network whose components have no connection with those of transformers [Gustavsen-04a, Gustavsen-04b, Zambrano-06, Sofian-07, Joginadham-08, Heindl-09, Purnomoadi-09, Gustavsen-10, Pordanjani-11]. Figure 1.12 depicts a RLC network derived from a rational approximation of a measured frequency response, where each component in the circuit is derived as equivalence of corresponding terms in the approximation equation [Gustavsen-02]:

$$y(s) = \sum_{m=1}^N \frac{c_m}{s - a_m} + d + s \cdot e \quad (1.5)$$

where

- $y(s)$ rational function in s-domain
- N number of poles
- c_m m^{th} residual
- a_m m^{th} pole
- d and e constants

Then the synthetic circuit can be derived with its components as:

- $C_0 = e$, $R_0 = 1/d$
- Each real pole forms a RL branch:
 $R_1 = -a_m/c_m$, $L_1 = 1/c_m$
- Each complex conjugate pair forms a RLC branch with R , L , C , G . Their formulas can be found in [Gustavsen-02] and will not presented here due to complex expansion.

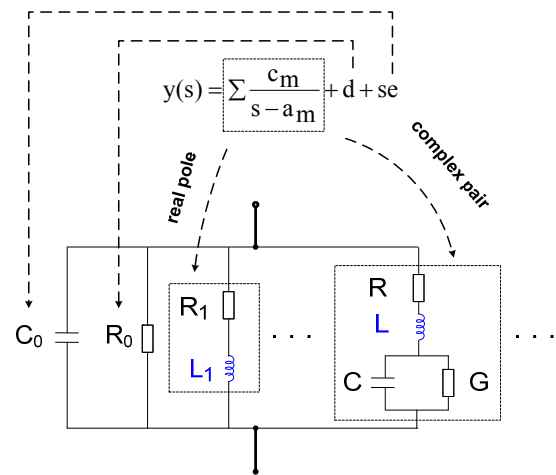


Figure 1.12: A non physical synthetic circuit from rational approximation of a measured frequency response [Gustavsen-02, Pordanjani-11]

The challenge of all non-physical analysis based methods is to set limits for the indicators so that abnormal and normal condition of transformers can be distinguishable, but it has been not successful in general so far. It may happen that good diagnostics can be achieved with several methods if the real failures are close to what investigated before in the methods; but this is not

always obtained in reality. It is due to the non physical meaning of the methods, the uncertainty of the measurement caused by reproducibility issue and the nature of the failures. A big disadvantage of the non-physical analysis based methods is, the calculated indicators from a method can not be further exploited in combination with those from other methods, especially physical indicators as electrical parameters measured through diagnostic testing methods, for a better diagnosis since they have no physical meaning.

As a result, investigations on how to assess the measured frequency responses in a physical way are suggested in last recent years [Heindl-10, Heindl-11, Velasquez-11]. The common procedure is to extract electrical parameters of transformers from the FRA traces and then make the diagnostic based on these parameters. The advantage of physical methods is that, the extracted parameters are good indicators for the diagnostic and can be verified with those obtained from other measurement methods.

To extract electrical parameters of power transformers from the FRA measurements, several simple models such as equivalent single phase circuits in different frequency ranges have been proposed so that the components in such models, i.e. equivalent transformer parameters, can be calculated from measured frequency responses [Islam-97, Gonzalez-06, Heindl-10, Velasquez-11]. However, the parameters are not very useful in application since they are not sensitive enough to the failure detection. It is therefore required that better transformer models, e.g. three-phase transformer circuits, should be based to analyze the circuit parameters. Topics of physical transformer circuits and the way to extract the electrical parameters from FRA measurements for a physical assessment will be solved in detail in next chapters.

2 Physical electrical transformer models

Physical electrical models of power transformers are defined as electrical circuits derived from convertibility of real magnetic-electric phenomena in the transformers so that the models can be used to investigate transformer performance under specific conditions of excitation and terminal connection. In context of the dissertation, physical electrical transformer models appropriate for analysis of terminal frequency responses at low applied AC field and in broad frequency range are researched for two main applications: the determination of transformer's electrical parameters, including several key indeterminable parameters at the moment for diagnostics of electrical and mechanical failures such as core section impedances and winding series capacitance, and the way to assess and interpret the FRA measurement results physically based on these parameters.

The chapter introduces first the classification of physical transformer models for different purposes: an equivalent single phase circuit for a general analysis at power frequency, lumped single phase circuits in different frequency ranges, lumped three-phase circuit for transient analysis in low and mid frequency range, and distributed three-phase circuit for FRA at high frequencies. Afterwards, the most appropriate circuit for purposes of diagnostic and FRA interpretation is then proposed so that measurement strategies can be developed to determine the electrical parameters.

2.1 Classification of physical electrical models for power transformers

Power transformers are normally designed and used to transfer electric power at rated applied high voltage and power frequency, (50 Hz or 60 Hz). In reality, transformers have one-phase and multi-phase design (three-phase in most of cases) but in theoretical analysis, only equivalent single phase circuits are preferred to analyze transformer's working condition since in normal situations, the parameters in each of three phases are nearly the same for three-phase transformers [Kulkarni-04]. Therefore multiple-phase circuits are not necessary.

However, during operation time, power transformers suffer dangerous agents from inside, e.g. inrush current, internal faults or from outside, e.g. over-voltage transients (lightning strikes, switching in the power system), or some extreme faults such as asymmetrical external high-current short circuits or phase-to-ground faults. As a result, transformers should be tested at maintenance times and after a suspect fault via routine and diagnostic tests. A complete investigation on transformers requires different equivalent circuits which can be frequency dependent for the conclusion that transformers are then ready for operation or removed for repair. Following sub sections will recall different transformer circuits for the aim of selection of the most appropriate one for the diagnostic and FRA purpose.

2.1.1 Single phase transformer circuit at power frequency

To represent a power transformer under operation condition at power frequency, an equivalent single phase circuit is enough shown in Figure 2.1. In the circuit, two phase windings, namely primary and secondary, are isolated by an ideal transformer $N_p:N_s$ that provides the turn ratio. The electrical parameters of the transformer include:

- Magnetizing resistance R_m represents equivalent core loss (no-load loss)

- Leakage inductances of the phase windings, L_p and L_s respectively, indicate short-circuit impedance (load loss)

Windings' resistances R_p and R_s and magnetizing inductance L_m at power frequency are not so important compared with the R_m and L_p , L_s respectively in the viewpoint of main losses in power transformers in no-load and load operation. Other parameters such as capacitances can be neglected since their reactances are very high at the frequency.

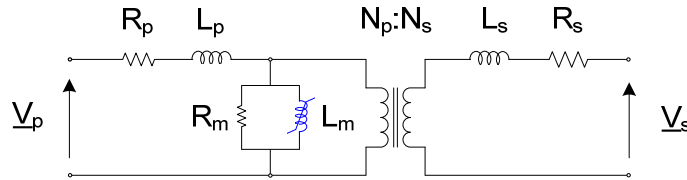


Figure 2.1: Equivalent single phase transformer circuit at power frequency [Kulkarni-04]

The equivalent circuit in Figure 2.1 can be also used to analyze transformer performance at other frequencies than power frequency; in such case, the frequency dependence of parameters should be taken into account, and also capacitances, if the frequency is high or capacitances are large. In principle, the circuit is only suitable for analysis of each of three phases in balanced operation condition. In case the balanced condition is not guaranteed, e.g. during a single phase fault, the three sequence circuits, i.e. positive, negative and zero-sequence, should be based on. However, the circuit is not very appropriate for mid or high frequency analysis of three-phase power transformers since the interaction between phase windings are not accounted for.

2.1.2 Single phase transformer circuits in different frequency ranges

There are various single phase circuits established based on distinct terminal behaviours at different frequency ranges such as [Islam-97, Schellmanns-98, Islam-00, Gonzalez-06, Siada-07, Rahimpour-09, Heindl-10]:

- Inductive property from core inductance at low frequencies
- Interaction between (core/leakage) inductances and winding capacitances at mid frequencies
- Capacitive behaviour at high frequencies

To show simplest examples, Figures 2.2, 2.3 and 2.4 present equivalent circuits of two power transformers (30 MVA and 390 MVA) in low, mid and high frequency range respectively [Islam-97]. The circuits consist of specific components which can be considered as physical electrical parameters applied for diagnostic. The procedure for parameter extraction is then based on the agreement of transfer function of voltages on the windings (V_s/V_p) between calculation and measurement. At low frequencies up to 2 kHz,

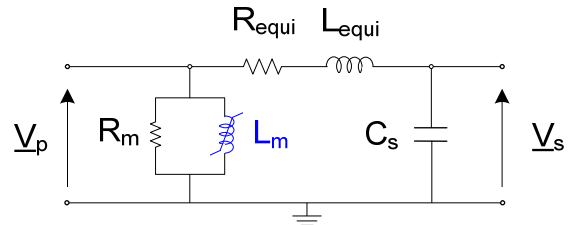


Figure 2.2: Low frequency transformer circuit [Islam-97]

the circuit in Figure 2.2 whose components are equivalent electrical parameters such as:

- Core equivalent resistance (R_m) and inductance (L_m)
- Total windings' resistance (R_{equi}) and leakage inductance (L_{equi})

- Secondary ground capacitance referred into primary side (C_s) can be used to analyze terminal transformer performance at such frequencies.

In Figure 2.3, both ground capacitances in primary and secondary side (C_p and C_s) appear which provides the clear interaction between leakage inductance and the capacitances whereas the core impedance is recommended to be retained, but referred into secondary side (R'_m and L'_m). The frequency range suggested for analysis is from 2 kHz to 80 kHz.

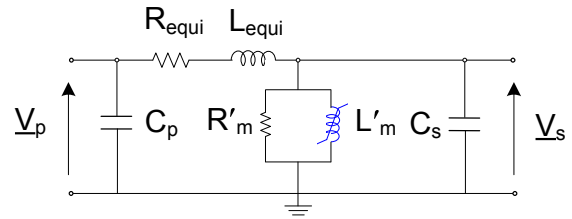


Figure 2.3: Mid frequency transformer circuit [Islam-97]

In Figure 2.4, pure capacitive behaviour is observed from 80 kHz up to 1 MHz and therefore, only capacitances appear. The inter-winding capacitance between primary and secondary side C_{ps} is added, replacing the R_{equi} and L_{equi} .

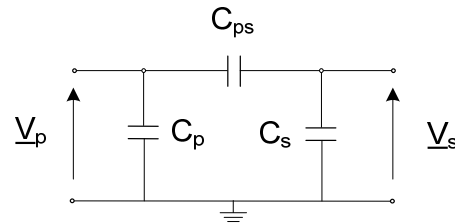


Figure 2.4: High frequency transformer circuit [Islam-97]

Although the parameters calculated from the three transformer circuits can be used to diagnose mechanical winding faults for several transformers such as a 30 MVA 132/66/11 kV YyN0d1 and a 390 MVA 23/350 kV Ynd1 transformer, there are still some limitations concerning failure diagnostic and FRA interpretation as follows:

- The parameters calculated from the method are not real physical ones. In fact, they are equivalent parameters observed at the measured terminals. They can be used to distinguish the failures between phases, but the frequency responses recovered from the circuits are not good, compared with the measured ones.
- The circuits are only appropriate to the tested transformers, but may be not suitable for other transformers in terms of frequency range and circuit component's appearance. For instance, there are several transformers whose inter-winding capacitance C_{ps} is much higher than ground capacitances of windings in primary and secondary side. Therefore, the circuit in Figure 2.3 is in general not fully valid at mid frequencies, it is suggested that the C_{ps} should be added.
- The winding series capacitance that is very important for mechanical failure diagnostic and FRA interpretation in certain cases can not be determined through the method.
- The single phase circuits do not take into account the inter-phase interaction (core connection, winding capacitances, winding connection). It is recommended that three-phase transformer circuit should be used instead.

2.1.3 Three-phase transformer circuits for purpose of transient analysis

There are several equivalent three-phase transformer circuits exploited for purpose of analysis of transients in transformers:

- Geometry based equivalent circuit [Andrieu-99]
- Magnetic analysis based equivalent circuit [Meredith-08, Colla-10]
- Duality principle based equivalent circuit [Cho-02, Chiesa-05, Martinez-05a, Martinez-05b, Mork-07a, Mork-07b, Hoidalén-08, Chiesa-10a, Chiesa-10b]

The similarity between the above mentioned circuits is, they are valid in low and mid frequency range and are developed as complete models for use in transient analysis software such as EMTP (Electromagnetic Transient Program) or ATP (Alternative Transient Program). Of those circuits, the duality principle based one is popular and most used because it takes into account the dual magnetic-electric property in transformers at low frequencies. Thus, the procedure of circuit development is here recalled since later on the circuit will be adapted and used in the dissertation.

The development procedure starts with the core topology of a two-winding three-legged core-type transformer with magnetic fluxes at three-phase excitation depicted in Figure 2.5. On each phase of the transformer there are several main magnetic fluxes as follows:

- Φ_1 flux in core legs
- Φ_y flux in core yokes
- Φ_2 flux between core legs and inner windings
- Φ_3 flux between inner and outer windings (leakage)
- Φ_4 flux outside outer windings (zero-sequence)

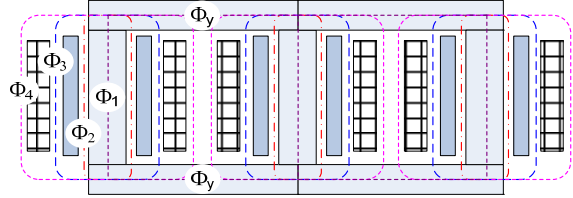


Figure 2.5: Core topology with fluxes

The equivalent magnetic circuit of the transformer is then obtained and shown in Figure 2.6 when the fluxes Φ are represented by corresponding reluctances \mathfrak{R} and electrical sources are replaced by magnetomotive forces F . Note that reluctances of the core sections (legs and yokes) are non-linear since they represent magnetic materials.

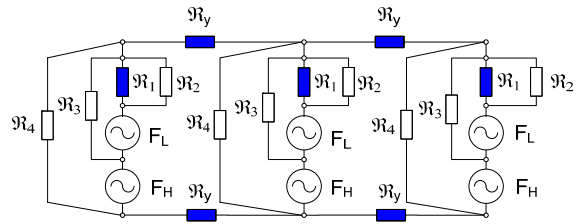


Figure 2.6: Magnetic circuit

The duality principle [Cherry-49, Dixon-94] shown in Table 2.1 is then necessary to convert the magnetic circuit into the dual electrical one. Before applying the duality principle, the magnetic circuit should be marked with nodes and meshes so that the transformations can be conducted. Figure 2.7 shows the magnetic circuit with nodes and meshes where a node is defined as a point in a certain space area, e.g. outside or in a closed circuit, and meshes are defined as lines connecting nodes and intersecting a circuit component (a reluctance or a MMF).

Then the dual electrical circuit is derived after following transformations: magnetomotive forces, linear reluctances of leakage, zero-sequence paths and non-linear saturable reluctances of core sections in the magnetic circuit are replaced as voltage sources, linear and non-linear

Table 2.1: Duality transformation

Magnetic circuit	Dual electric circuit
MMF $F = N I$, in A.turn	Voltage, in V
Flux ϕ , in Wb	Current I , in A
Reluctance \mathfrak{R} , in H^{-1}	Inductance L , in H
Meshes	Nodes
Nodes	Meshes

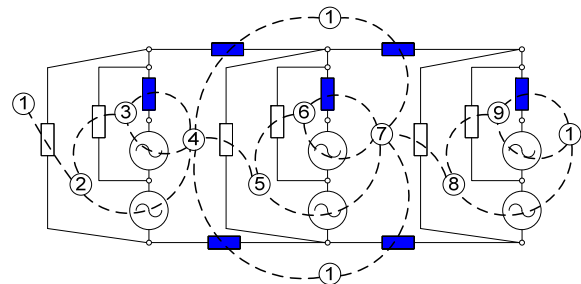


Figure 2.7: Magnetic circuit with nodes and meshes

inductances/impedances respectively. Meshes and nodes are also interchanged; consequently series/parallel magnetic circuits are converted into parallel/series dual electrical ones. Figure 2.8 plots the dual electrical circuit of the magnetic circuit in Figure 2.6 where the reluctance \mathcal{R}_2 and its dual inductance L_2 are neglected since the L_2 is small and not measurable whereas L_y represents both upper and lower yokes.

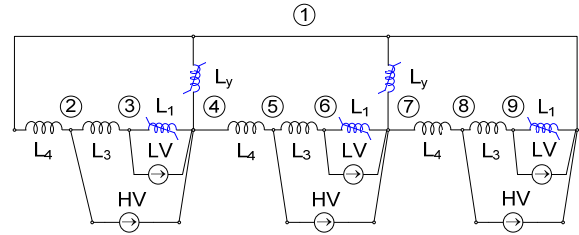


Figure 2.8: Dual electrical circuit with nodes

Ideal transformers are afterwards added since they provide primary-to-secondary and electric-magnetic isolations and turn ratio [Martinez-05a]. Winding resistances appear at both sides accounting for their real losses. Figure 2.9 shows the lumped duality based equivalent circuit in low frequency range, i.e. without capacitances, of the transformer under balanced excitation. In Figure 2.9, $Z_1 = R_1/L_1$, $Z_y = R_y/L_y$ are non-linear core leg and yoke impedances respectively; L_3 are per-phase leakage inductances; $Z_4 = R_4/L_4$ are per-phase zero-sequence impedances; R_H and R_L are resistances of HV and LV windings. All of them are frequency dependent. Note that the circuit can be universally applied to transformers with star, delta, or auto winding connection [Mork-07a].

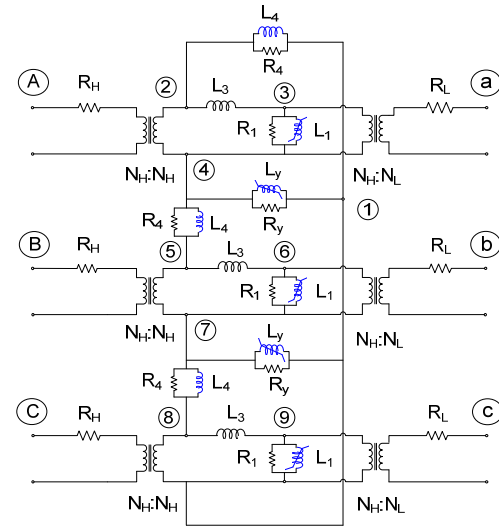


Figure 2.9: Duality principle based equivalent circuit under three-phase excitation

For final representation, winding connection and vector group should be taken into account. Furthermore, winding capacitances should be added to extend the valid frequency range of the circuit. Figure 2.10 shows a complete duality principle based transformer circuit of a YNyn6 transformer referred into HV side in which only ground capacitances of HV and LV phase windings (C_{gH} , C_{gL}) and inter-winding HV-LV capacitances (C_{iw}) appear; they are divided into two identical parts connected to ends of the windings. The inter-winding HV-HV capacitances can be ignored since their influence is insignificant compared with that of other capacitances and can not be determined. The winding series capacitance, which is very important in some certain cases, is not considered since there is so far no method to determine this capacitance in transformer bulk⁹. In such cases, without winding series

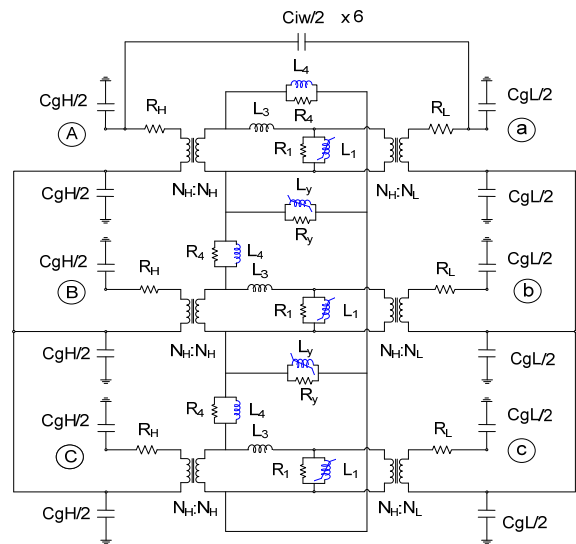


Figure 2.10: Duality principle based equivalent circuit of a Yy0 transformer

⁹ Determination of winding series capacitance is possible if the winding is isolated, i.e. brought out of transformers, and ready for measurements or when the design data are available [Pramanik-11, Chowdhuri-87, Bigdeli-12]

capacitance, any investigation on transformers with regard to frequency, e.g. transient or frequency response analysis, is not fully meaningful. Therefore, the determination of the winding series capacitances in transformer bulk is one of the goals of the dissertation.

2.1.4 Three-phase transformer circuits for purpose of FRA

Until now, simulation-based investigations on FRA for power transformers have been based on *transformer design data*. In such cases, electrical parameters can be calculated when the transformer is in either healthy or faulty condition, which enables the simulation for analysis of parameter influence or failure type on terminal frequency responses. Transformer circuits used for FRA simulation can be categorized into two main groups as follows:

- Lumped equivalent circuit in low and mid frequency range
- Distributed equivalent circuit in mid and high frequency range

The lumped equivalent circuit for FRA purpose is also obtained based on the duality principle [Ang-08] or magnetic and capacitance modeling [Pleite-06, Shintemirov-10b, Andrieu-99, Colla-10]. Figure 2.11 depicts a duality based equivalent circuit of a Yy0 transformer derived from the method presented in [Ang-08] in order to compare with the one in Figure 2.10¹⁰. One can observe that in the Figure 2.11, resistive components are not considered since the main goal of the paper is to investigate the tendency and location of resonances mainly caused by the interaction between inductances and capacitances; without resistances, damping of frequency responses' magnitude at resonances does not take place. Furthermore, zero-sequence inductances do not appear in the circuit, which means the simulation of the circuit may not be valid at a mid frequency where the influence of the zero-sequence inductances takes place in several cases. In addition, the fact that the circuit is found fully balanced between three phases, due to appearance of three per-phase leakage inductances, might not be fully correct since the FRA measurement is performed on single phases, and consequently, the circuit should be developed under single phase excitation; for instance, the leakage inductance is only found in the phase where the FRA measurement is conducted. Lastly, introduction of winding series capacitances in the circuit validates the simulation in some certain cases, which is not found in the circuit in Figure 2.10.

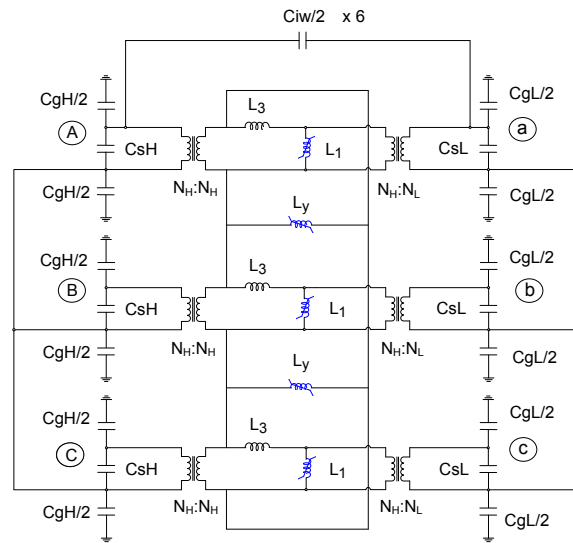


Figure 2.11: Duality based equivalent circuit of a YNyn0 transformer

In contrast with the lumped equivalent circuit in which each component represents the per-phase equivalent parameter, e.g. L_3 is the per-phase total leakage inductance, the distributed one focuses on the division of the equivalent parameters into a number of sectional parameters. Figure 2.12 shows a per-phase distributed circuit of a HV and a LV phase winding from which the total distributed circuit of the whole transformer is derived by combination of three of them [Jayasinghe-06, Sofian-07, Abeywickara-07].

¹⁰ The real circuit in [Ang-08] developed based on the duality principle is for a three-winding autotransformer

In Figure 2.12, C_{gH0} , C_{sH0} and C_{gL0} , C_{sL0} are ground and series capacitances of a section of the HV and LV phase winding respectively; C_{iw0} is the inter-winding capacitance between sections of HV and LV winding. Since the HV and LV windings are divided into small sections, the concept of leakage inductance is no longer appropriate; only self and mutual inductance assigned as L_i (L_j) and M_{ij} respectively. Rectangles in Figure 2.12 represent resistances of winding sections and conductances of capacitances.

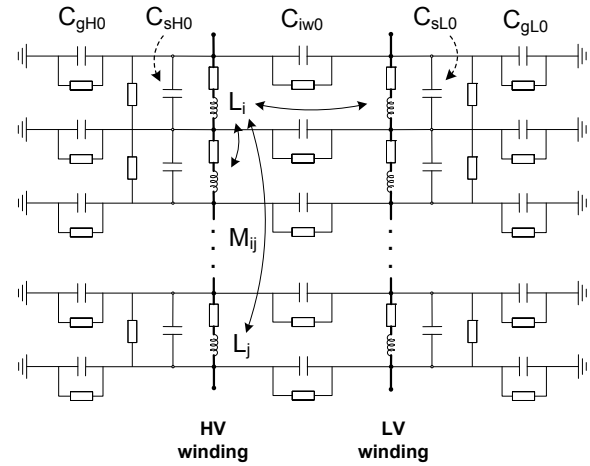


Figure 2.12: Per-phase distributed circuit of a transformer

The advantage of the distributed circuit is that, it allows the direct coupling between sectional parameters, e.g. self, mutual inductances and winding capacitances, which should be considered at high frequencies. Consequently, the distributed circuit provides a better FRA interpretation in mid and high frequency range which is not achieved with the lumped circuit in Figure 2.11 or Figure 2.10.

2.2 Summary of state-of-the-art transformer circuits for diagnostic and FRA purpose

It is clear that the three-phase equivalent circuits should be used for investigations of transformers for FRA purpose since influence of non-tested phase windings on the winding-under-test is confirmed [Ang-08, Wang-09a, Sofian-10]. Of the three-phase equivalent circuits, the duality based equivalent circuit is found the best for parameter-based diagnostic since its components, the electrical parameters, can be determined through measurements whereas the distributed one is the preferred selection when transformer design data are available and analytical investigations at high frequencies are required such as determination of which FRA test is sensitive to a certain failure mode [Rahimpour-03, Jayasinghe-06, Abeywickara-07] or how the frequency responses change with regard to changes of electrical parameters and transformer winding connection [Wang-09a, Sofian-10]. Since the availability of transformer design data is not guaranteed in most of cases, the lumped equivalent circuits are the only choice for investigations of power transformers in reality. Table 2.2 summarizes characteristics of the three-phase lumped equivalent circuits with aim to identify and develop the most appropriate transformer circuit for diagnostic and FRA purpose.

Table 2.2: Overview of lumped circuits for investigations in frequency domain

Characteristic	Lumped circuits for transient analysis	Lumped circuits for frequency response analysis
How to determine parameters	From measurements	From design data
Limitations	Lack of winding series capacitances	Lack of zero-sequence impedances
	Core impedances cannot be determined if the test winding is connected in delta	Resistive components are missing
	Single phase excitation is not accounted for	Single phase excitation is not accounted for

As a result, a new lumped equivalent circuit which overcomes the limitations shown in Table 2.2 is requested. In addition, all of the parameters in the new circuit could be determinable from measurements so that they can be applied to diagnose failures as well as to give a parameter-based FRA interpretation in low and mid frequency range.

2.3 Adapted duality based equivalent circuits for FRA purpose

A combination of the circuits in Figures 2.10 and 2.11 provides the best one for the desired purposes; that means the new circuit should be based on the duality principle and includes zero-sequence inductances (if the test winding is the star one), winding series capacitances as well as resistive components. In addition, the circuit should be adapted to be compatible with single phase excitation FRA measurements so that it can be used to simulate frequency responses for the comparison with those from measurements. Lastly, all of components in the new circuit, i.e. electrical parameters of transformers, must be determinable for the feasibility of complete investigations.

Below are several points dealt with for the development of the new circuit shown in Figure 2.13 for a YNyn6¹¹ transformer [Pham-12b]. Note that the circuit is developed for investigations on the HV winding; in case analyses at the LV side are necessary, another circuit should be built since the parameters such as zero-sequence inductance/impedances and core impedances referred into both sides are in general different:

- The core will not be saturable at low applied field in FRA measurements. Thus, the saturation of the core does not need to be taken into account. However, the core may have remanence that can influence the calculation of core parameters. To remove effect of core remanence, it is suggested that the core should be demagnetized prior to FRA measurements.
- (Per-phase) leakage inductance (L_3): It appears on the excited phase of transformers with star winding (since there is no leakage flux in other phases) or all phases of transformers with delta winding.
- (Per-phase) zero-sequence inductance: Appearance of all three per-phase zero-sequence impedances is uncertain under single phase excitation; even in balanced excitation condition in transient analysis, they can be reduced into two placed at outer phases or concentrated into one positioned at the center phase [Martinez-05a]. For a general consideration, three per-phase zero-sequence impedances will be taken into account, unless otherwise stated in some special cases, e.g. when the transformer has no tank, the zero-sequence inductance of the star winding is appreciably higher than that of the same transformer which has a tank [Kulkarni-04] and therefore should be accounted for. For the sealed transformer with excited delta winding, the zero-sequence impedance can be neglected since they have insignificant contribution and can not be measured at the delta side.

¹¹ A certain vector group requires certain winding connection and terminal markings [IEC 60076-1-00, IEEE C57.12.70-00]

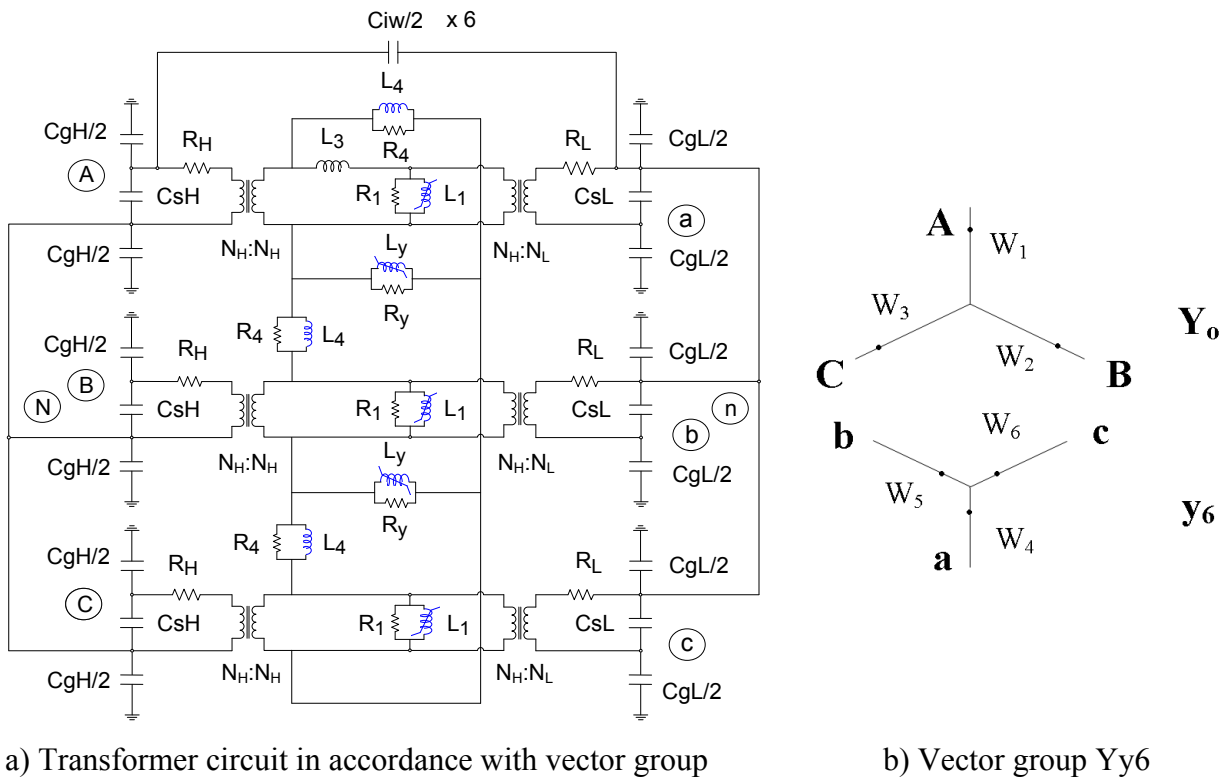


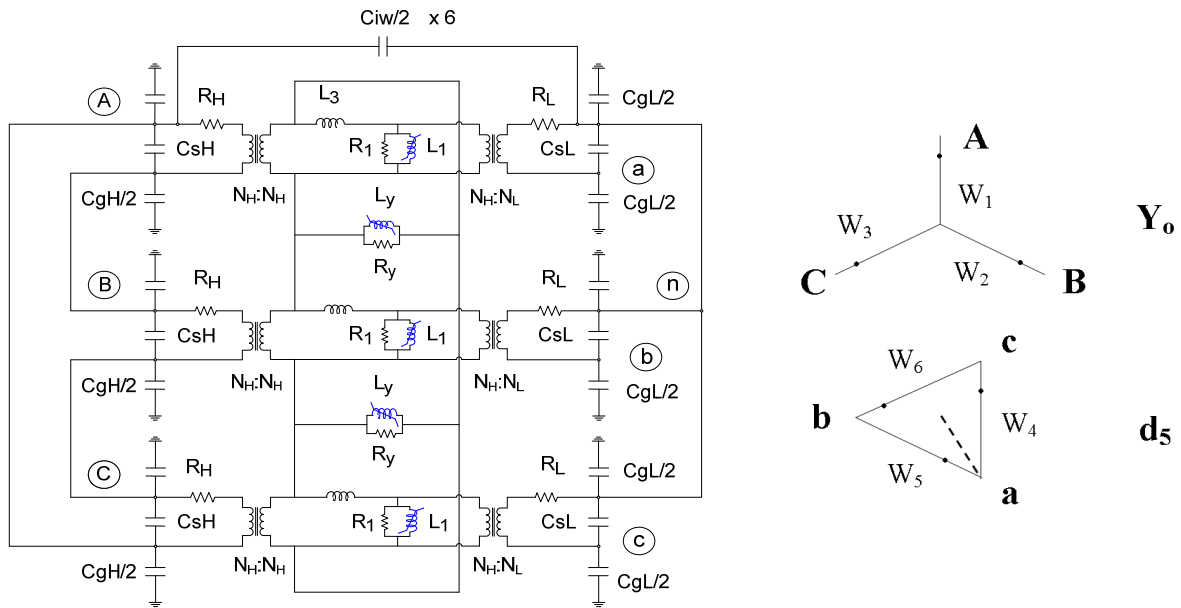
Figure 2.13: Duality based equivalent circuit of a YNyn6 transformer (for tests on phase A)

In Figure 2.13a the terminal markings should be in accordance with the vector group illustration in Figure 2.13b. It can be explained as follows. Assign the windings at HV and LV side are W_1, W_2, W_3 and W_4, W_5, W_6 for phases A, B and C respectively. Since the dots in Figure 2.13b indicate the “vector” direction of the windings, the HV terminals (A, B and C) and the LV neutral should have the same “polarity”. Therefore the LV terminals (a, b and c) are in opposite position compared with the HV ones as depicted in Figure 2.13a [IEEE C57.12.80-02].

It is important to note that the equivalent circuit in Figure 2.13 is considered only valid for analyses at HV side since appearance of leakage, zero-sequence inductance and ideal transformers are dependent and referred into the HV side (hence the electrical parameters, excluding resistance of the LV winding and all capacitances, calculated based on analysis of the equivalent circuit are also referred into the HV side). In case analysis at LV side is required, the circuit should be adapted in terms of the dependent components, i.e. leakage, zero-sequence and ideal transformers.

In case transformers with other vector groups are considered, the connections between phase windings and the terminal markings should be adapted accordingly whereas the magnetic-electric circuit part is hold likely unchanged, except zero-sequence impedances¹² since they are independent on winding connections. Figure 2.14 and 2.15 show adapted equivalent circuits for the Dyn5 and YNd5 transformer that will be investigated in next chapters together with the YNyn6 one. The three test objects are necessary for the development and verification of the new method since their vector groups are different.

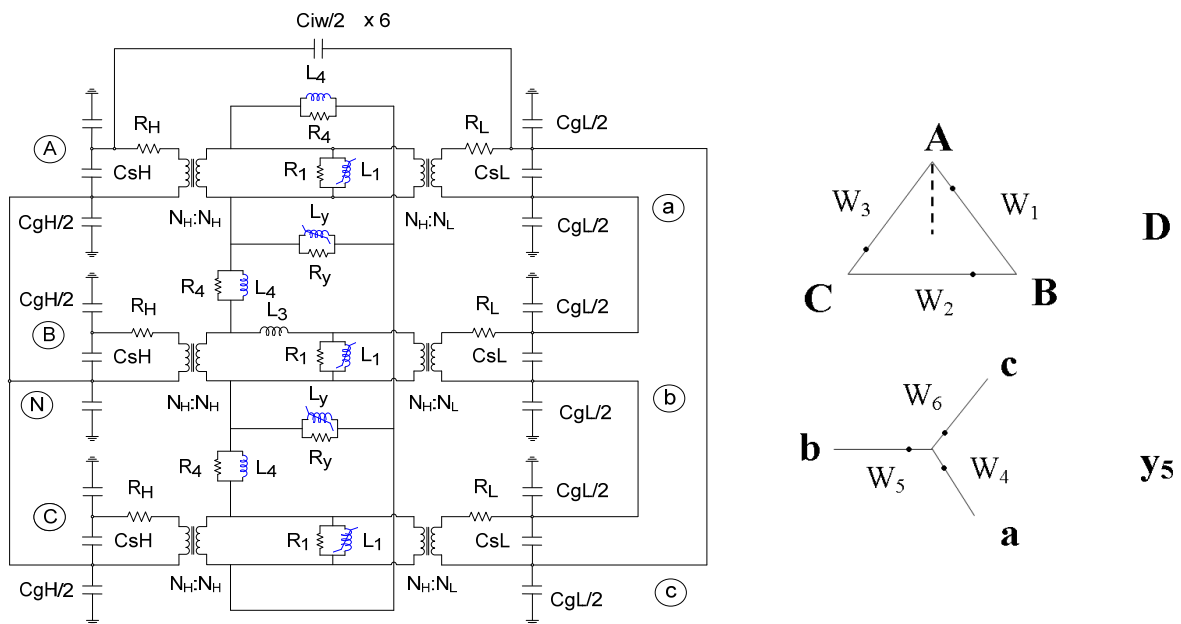
¹² The zero-sequence fluxes in Figure 2.5 and corresponding impedances in Figures 2.6 to 2.11 are fully valid for analyses in which (balanced) excitation is on the HV winding of transformers with star-star vector group



a) Transformer circuit in accordance with vector group

b) Vector group Dy5

Figure 2.14: Duality based equivalent circuit of a Dyn5 transformer (for tests at HV side)



a) Transformer circuit in accordance with vector group

b) Vector group Yd5

Figure 2.15: Duality based equivalent circuit of a YNd5 transformer (for tests on phase B)

After the physical electrical transformer models are obtained, different measurement-based approaches will be carried out to determine components of the models, i.e. electrical parameters of the transformers, appropriate for FRA interpretation and failure diagnostic purpose. Since the circuits are then exploited to simulate the frequency responses measured at transformer terminals for a physical interpretation, the electrical parameters must be available in broad frequency range, which suggests that the measurements for parameter determination should be compatible with. Starting from this viewpoint, the next chapter will describe a new method combining these approaches in determination of the electrical parameters based on the measurements of frequency responses of terminal input impedances of transformers performed by means of a VNA.

3 A new method for FRA interpretation and failure diagnostics

Due to limitations from state-of-the-art diagnostic methods in measuring transformer's electrical parameters mentioned in chapter 1, there is a demand to develop new measurement-based methods which can be used to provide a physical FRA interpretation and also a comprehensive diagnostic in terms of key electrical parameters such as core impedances, leakage and zero-sequence inductance, and *all* winding capacitances.

To fulfill the demand, a new method that combines different adapted and new approaches in determination of electrical parameters in broad frequency range is introduced in this chapter. The new method is based on measurements of non-standard¹³ frequency responses, the input impedances, by means of the VNA and relevant analyses with regard to the adapted transformer circuits presented in chapter 2. Thanks to the calculated electrical parameters obtained from the new method, a parameter-based FRA interpretation/assessment at low and mid frequencies by circuit simulation and a comprehensive diagnostic of electrical and mechanical failures of power transformers are feasible as summarized in Figure 3.1 and Table 3.1.

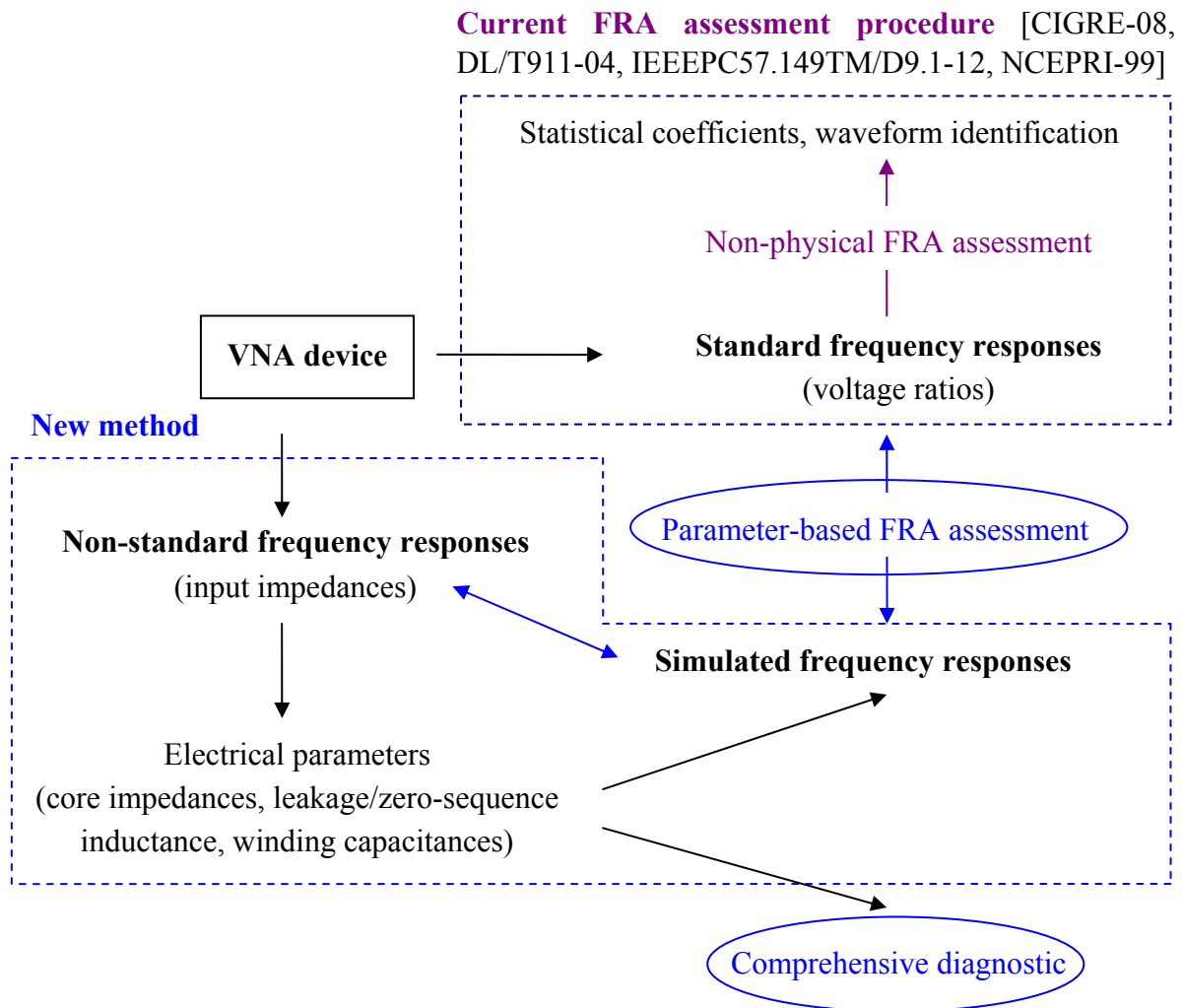


Figure 3.1: Overview of the new method and its application

¹³ Analysis of transformer's electrical parameters based on standard frequency responses, transfer functions of voltage ratio, is not straightforward [Pham-12a]

Table 3.1: Overview of electrical parameters and relevant approaches in the new method

Electrical parameter	Measurement/Analytical/Simulation-based approach	Classification
Total resistance for stray losses and winding resistance Leakage inductance	<ul style="list-style-type: none"> – Per-phase short-circuit input impedance tests (analyzed at low frequencies) – Analytical formulae (at high frequencies) 	Adapted approach from conventional diagnostic one
Zero-sequence impedance	<ul style="list-style-type: none"> – Zero-sequence input impedance test (analyzed at low frequencies) – Analytical formulae (at high frequencies) 	Adapted approach from conventional diagnostic one
Core section impedances (yoke/leg)	<ul style="list-style-type: none"> – Open-circuit input impedance test (analyzed at low frequencies) – Analytical formulae (at high frequencies) 	First new approach
Ground and inter-winding capacitance	<ul style="list-style-type: none"> – Capacitive input impedance tests 	Second new approach
Winding series capacitance	<ul style="list-style-type: none"> – Simulation-based approach 	Third new approach

According to Table 3.1, five following steps are implemented in succession to determine electrical parameters for the desired purposes:

- Build an appropriate lumped equivalent circuit of the test transformer
- Calculate frequency dependency of winding resistances and leakage inductances from per-phase *short-circuit* input impedance tests at low frequencies and relevant analytical formulae at high frequencies
- Calculate frequency dependency of zero-sequence resistance and inductance from the *open-circuit zero-sequence* input impedance test performed on star winding with accessible neutral at low frequencies and relevant analytical formulae at high frequencies
- Determine ground and inter-winding HV-LV capacitance from *capacitive* input impedance tests
- Identify the winding series capacitance based on simulation

3.1 Equivalent transformer circuit

Development of an appropriate equivalent circuit is the first and important step since the type of circuit and its components decide the research goal. For the desired tasks of the dissertation, the duality based lumped equivalent circuit of power transformers appropriate for low and mid frequency analysis is necessary since it will be exploited to analyze measurements carried out on the test transformers.

For the three test transformers investigated in the dissertation:

- Transformer T₁: 200 kVA 10.4/0.462 kV YNyn6 opened transformer
- Transformer T₂: 2.5 MVA 22/0.4 kV Dyn5 sealed transformer
- Transformer T₃: 6.5 MVA 47/22 kV YNd5 sealed transformer

the adapted duality based equivalent circuits introduced in chapter 2 are the appropriate ones. The circuits have two parts: the middle area represents the dual magnetic-electric transformation which does not depend on winding connections and the outer areas are devoted for HV and LV windings: resistance, capacitances and connection between phase windings in accordance with transformer vector group.

Figure 3.2 depicts a basic duality based equivalent circuit for a two-winding three-legged transformer where the dual magnetic-electric circuit is nearly unchanged and isolated from winding areas by ideal transformers; the winding areas are then adapted in accordance with the transformer vector group, e.g. YNd5¹⁴ in this case. If the vector group is changed, only the winding terminals and their connections need to be adapted. It is important to mention that the circuit is only appropriate for investigations at one transformer side, i.e. the star winding at HV side; in cases analysis at delta winding side is required, another circuit should be developed since electrical parameters in the circuit, e.g. zero-sequence/leakage inductances or core section impedances, calculated based on measurements at star winding side are not fully valid for simulations at the delta side.

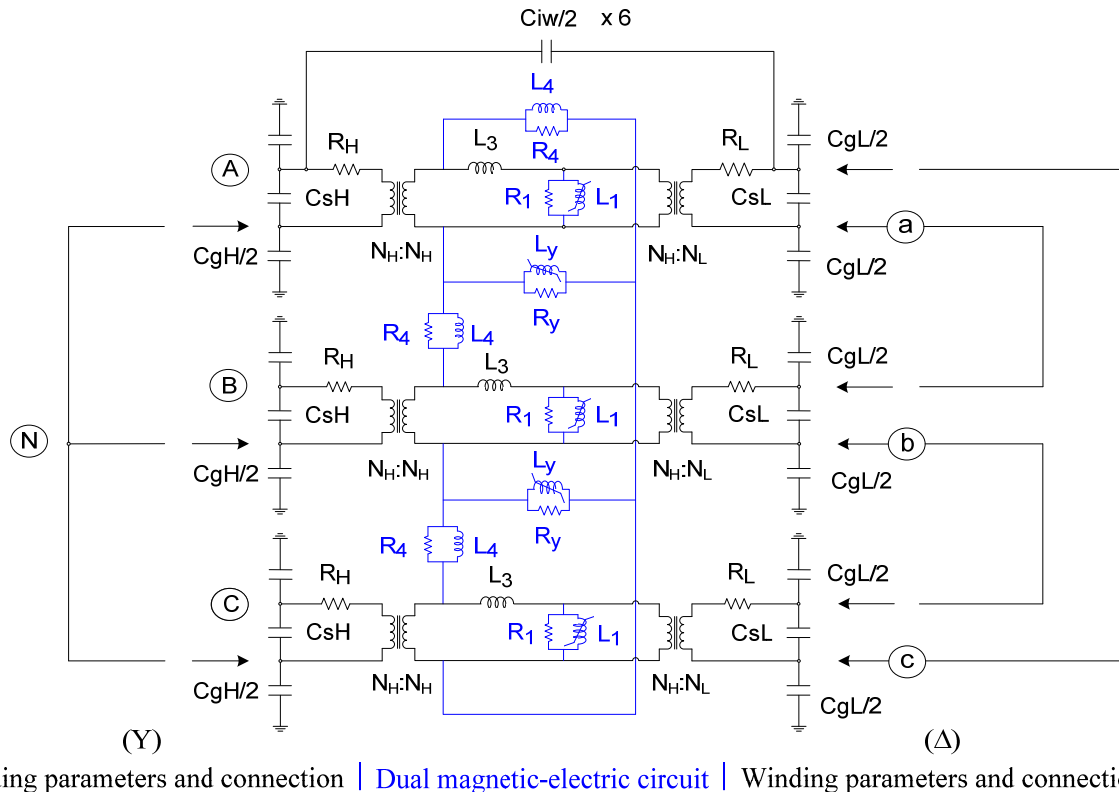


Figure 3.2: A duality based equivalent circuit of a two-winding YNd5 transformer

After the equivalent transformer circuit is obtained, measurements shown in Table 3.1 are then performed and analyzed based on the circuit to determine relevant electrical parameters. The measurements of input impedances are recommended to be performed by means of the VNA with settings selected appropriate for the purpose of FRA, i.e. low open-circuit voltage and broad frequency range. In the dissertation, different input impedances are measured by means of the “FRAnalyzer” device of Omicron with settings:

- Open-circuit source voltage 1 V (~ 7.05 dBm source power)
- Frequency range 20 Hz to 2 MHz¹⁵ with 801 points in logarithm scale
- Receive bandwidth 30 Hz for efficient denoising effect

These settings are similar with those used for measuring standard frequency responses (transfer functions of voltage ratios) so that the electrical parameters determined from non-standard frequency response measurements can be used to interpret or assess the standard ones. Detail in-

¹⁴ The transformer vector group YNd5 is selected as example since analyses on star and delta winding are possible

¹⁵ The term “broad frequency range” in the dissertation is defined from 20 Hz to 2 MHz, unless otherwise stated

formation of the device in term of measurement procedure can be found in [FRAnalyzer-09, Bode100-10].

3.2 Per-phase short-circuit input impedance tests and relevant electrical parameters

In the second step of the method, the per-phase short-circuit input impedance tests are first conducted and analyzed to determine the so-called total resistance from stray losses ($R_{\text{stray_losses}}$), AC winding resistances (R_H and R_L) and leakage inductances (L_3) of each of three phases since these tests are independent of each others and of other test types. AC winding resistances and leakage inductances of three phases derived after analysis of measurements have values from a low frequency, e.g. 20 Hz, till a low frequency where the purest inductive behaviour is observed in the measured impedances. The frequency can be from several kHz to several tens of kHz depending on transformer capacitances; over this frequency the capacitive behaviour takes place in measured impedances and therefore, the winding resistances and leakage inductances are only determined from measurements within a certain limited frequency range.

For the purpose of diagnostic the calculated resistances of winding (or stray losses) and leakage inductances within the limited frequency range can be used. However, for purpose of parameter-based interpretation of frequency responses via simulation in broad frequency range, frequency dependency of the parameters should be reached. Thus, this section will also introduce the way to develop the frequency dependent functions based on the combination between measured values at low frequencies and analytical values from relevant experimental formulae at high frequencies.

The whole procedure including measurements, parameter analysis from measurements at low frequencies as well as the development of frequency dependency of the parameters at high frequencies is named as the first adapted approach. The term “adapted” is due to the fact that the author introduces a new procedure for development of the electrical parameters in broad frequency range based on the existing traditional measurement method and analytical formulae.

3.2.1 Per-phase short-circuit input impedance tests and measurement based parameters (winding resistance, leakage inductance) at low frequencies

The per-phase short-circuit input impedance test is performed similarly to the conventional short-circuit diagnostic test, i.e. a single phase winding at the analyzed side (normally at HV) is excited whereas the corresponding single phase winding at another side is shorted. However, there are two small differences between the two methods: firstly due to the fact that the VNA measures input impedances using one cable connected to a winding terminal [Bode100-10], the other winding terminal should be grounded; secondly the conventional diagnostic short-circuit test is often performed at HV side at rated current level (LV winding is shorted) by default for safety reason, especially for transformers with high turn ratios whilst the short-circuit input impedance test can be made at both side due to very low applied voltage – this enables advanced analysis of parameters referred into LV side, which is considered as an improvement compared with normal analysis of conventional measurement methods.

Figure 3.3 and 3.4 depicts the whole measuring circuits in context of a short-circuit input impedance test performed on a HV and LV winding of the YNd5 transformer respectively at low frequencies for easy observation (i.e. without capacitances). It is recommended that all connections

such as short-circuit between terminals or grounding should be made by means of coaxial cables to reduce interference since the measurements are conducted in broad frequency range.

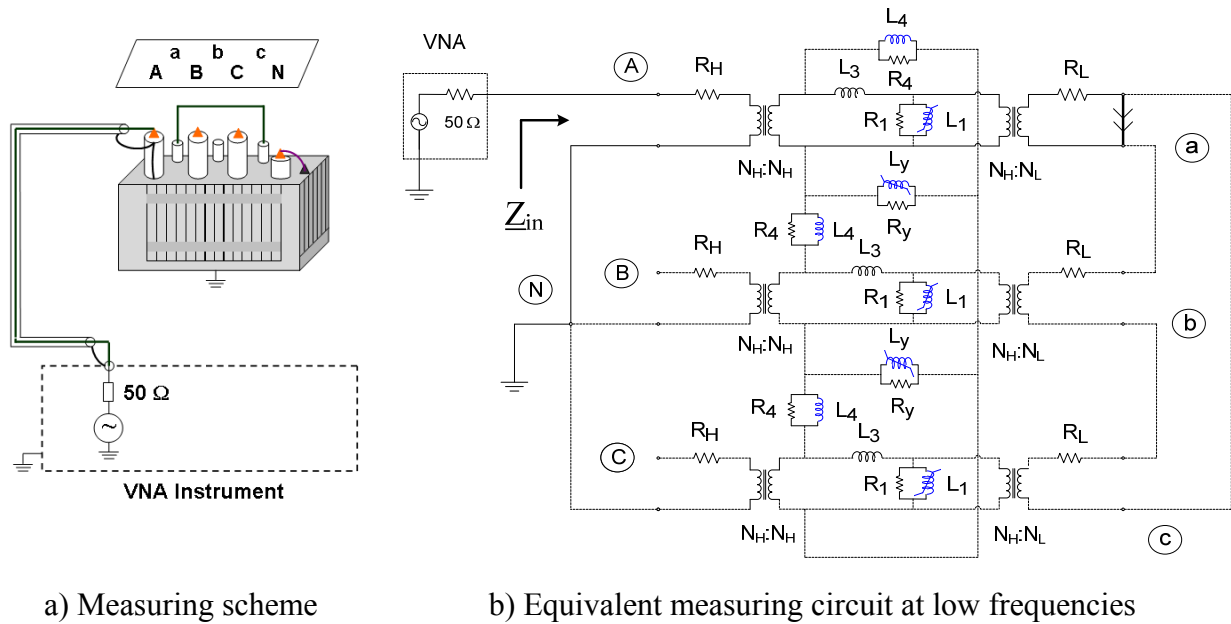


Figure 3.3: Short-circuit input impedance test on the star winding of the YNd5 transformer

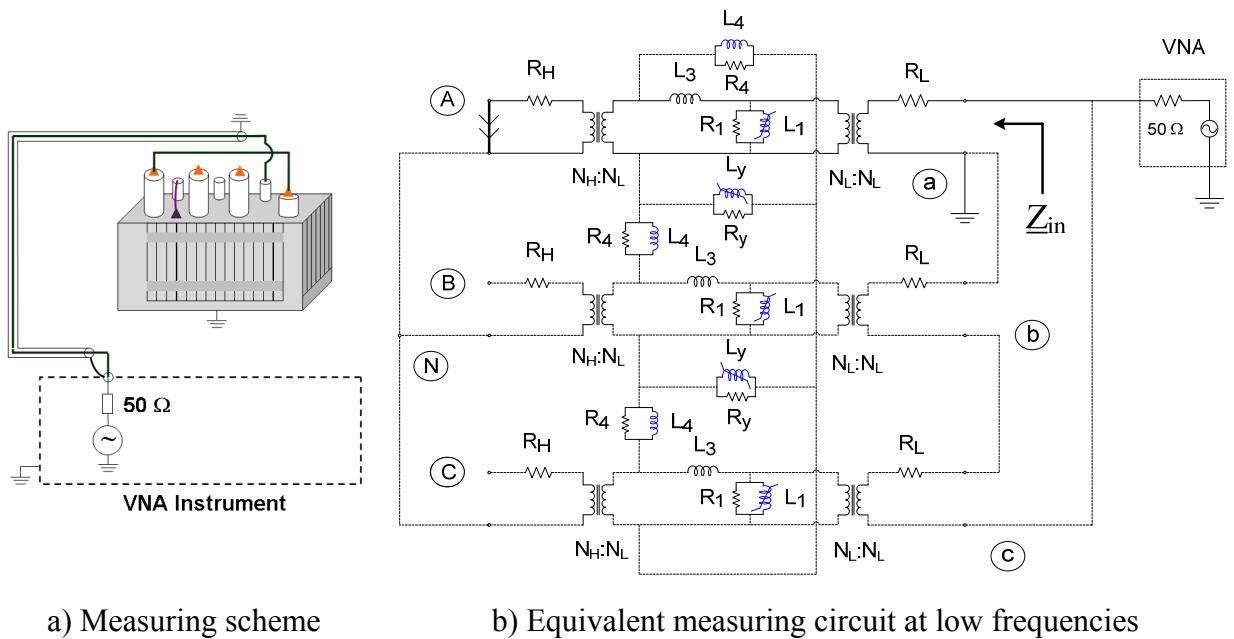


Figure 3.4: Short-circuit input impedance test on the delta winding of the YNd5 transformer

From Figures 3.3b and 3.4b, it is seen that the short-circuit input impedance test can be performed in the same manner regardless of the fact that the winding is connected in star or delta. The resultant impedance in two cases is mainly from the measured phase winding. To be correct for the circuit in Figure 3.4b, the zero-sequence impedances should be removed by short circuits since they could not be measured at the delta winding side; and the ideal transformers should be changed also because the parameters calculated at the star winding side cannot be applied for investigations at the delta winding side, which will be explained more detailed in next sub sections.

Regarding the measured impedance in broad frequency range, it is realized from Figure 3.3 that the circuit's active part associated with the test is on the tested phase whereas the remaining part from other phases is not involved. Therefore, the short-circuit input impedances can be independently calculated from corresponding tests to determine resistances from stray losses and of windings as well as leakage inductances of three phases at low frequencies. To illustrate how the measured impedance in broad frequency range looks like for the analysis, Figure 3.5 introduces a typical measurement result obtained from the short-circuit input impedance test in Figure 3.3.

In Figure 3.5, the inductive behaviour constituted from equivalent resistance representing stray losses and leakage inductance is observed within 20 Hz to several kHz. However, the resistance and inductance can only be determined clearly from 20 Hz to a higher frequency, e.g. around 400 Hz in this case, where the phase angle reaches nearest 90° since beyond that frequency influence of capacitance starts taking place. Now it is possible to determine total resistance from stray losses, winding resistances and leakage inductances from the measured input impedances.

The measured input impedances obtained from the short-circuit tests on each of three phases within the frequency range from 20 Hz to 400 Hz consist of two components referred into the measurement side: a resistance representing total losses ($R_{\text{stray losses}}$) in real part and a leakage inductance (L_3) representing corresponding leakage flux between the HV and LV winding in imaginary part. Now the point is to calculate winding resistances R_H and R_L from $R_{\text{stray losses}}$ since they are required for analysis.

In general, the total losses consist of several components: winding eddy loss (skin effect), circulating current loss in windings (proximity effect) and other losses from other transformer parts due to leakage flux such as flitch plate, core edge, frame and tank [Kulkarni-00, Kulkarni-04, ABB-07, Mork-07a]:

- Winding eddy loss is due to leakage flux generated by the current flowing in the winding; the leakage flux creates another current called eddy current in winding conductors, resulting in an unevenly distribution of the total current in the cross section of the conductor, i.e. most current distributes near the conductor surface, which in turn increases the losses when frequency rises (see Figure 3.6a)
- Proximity effect is mainly caused by interaction between circulating currents in parallel nearby strands/conductors (see Figure 3.6b and 3.6c)
- Other losses are caused by stray fluxes circulating in metallic structures and the tank (see Figure 3.7)

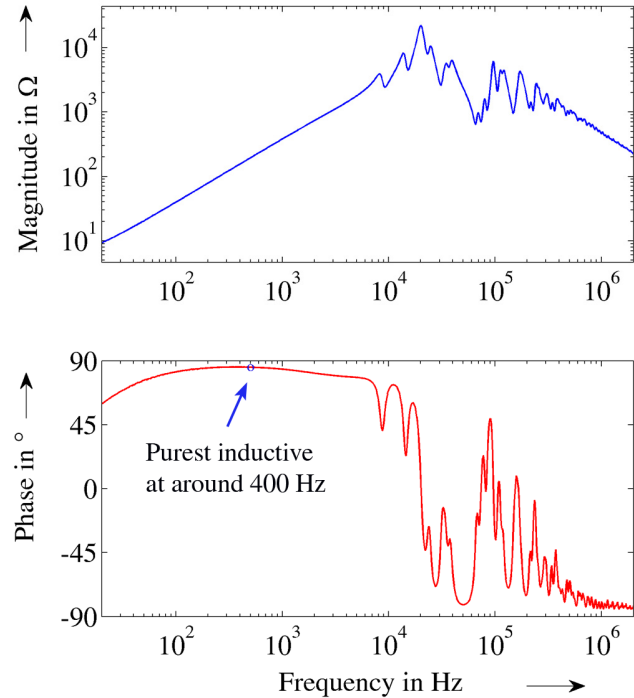
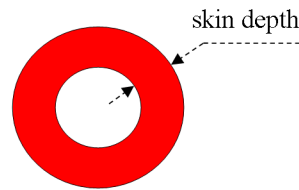
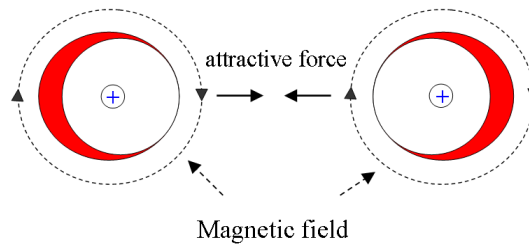


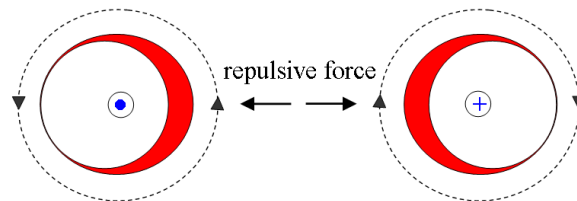
Figure 3.5: Frequency response of input impedance in the short-circuit test in Figure 3.3



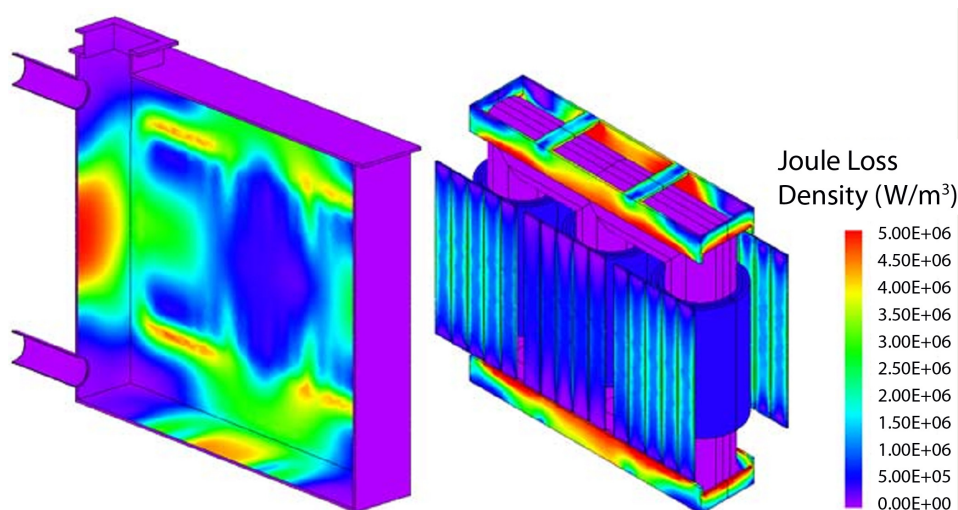
a) Current distribution due to skin effect in conductor



b) Proximity effect of two nearby conductors when the currents are in the same direction



c) Proximity effect of two nearby conductors when the currents are in opposite direction

Figure 3.6: Skin and proximity effect in circular winding conductors [Agrawal-01]**Figure 3.7:** Stray loss analysis of the tank and its interior for a transformer [JMAG-13]

For a separation of the total losses into individual components in order to determine winding resistances, there is so far no efficient measurement method since only very accurate Finite-Element-Method (FEM) based simulations with available transformer design data can calculate frequency dependent resistances of each winding. In addition, the fact that all resistive components in the equivalent circuit in Figure 3.2, including winding resistances, contribute only to the

damping of frequency responses at resonance frequencies [Ang-08], the winding resistances can be considered maximum as half of that from the stray losses, i.e. $R_{Hmax} = R_{Lmax}/(N_H:N_L)^2 = 0.5 \times R_{stray_losses}$ (in this case, other losses are ignored under low applied field). It is realized though simulation later on that any selection of factors for winding resistances from R_{stray_losses} is acceptable because only the winding resistances at analyzed side, e.g. HV side, are taken into account in analysis of open-circuit input impedances but they do not influence much the frequency responses from which interactions between inductances and capacitances are of importance and interest (LV winding resistances have no contribution on open-circuit frequency responses at HV side in general). For the purpose of FRA interpretation, the accurate separation of windings' resistances from R_{stray_losses} is not so important than how to develop them at high frequencies since they cannot be calculated from measurements at those frequencies and the losses are much higher than those at low frequencies.

3.2.2 Winding resistances and leakage inductance at high frequencies

There exist several experimental formulae and graphs that can be used to represent frequency dependence of winding resistances. In general, the winding resistances must take into account at least effect of the eddy current loss, as suggested in [Martinez-05b, Fuchs-00] (other losses and temperature effect are only considered if possible). Figure 3.8 shows the frequency dependency of a winding resistance R of a power transformer via a function of X/R where X is leakage reactance in comparison with the corresponding ratio derived from a series R-L model. It is clear from Figure 3.8 that the series R-L model cannot represent the frequency dependency of the winding resistance at frequencies higher than 100 Hz, hence other models such as the second-order series Foster circuit¹⁶ should be used for acceptable representation. Since the dissertation focuses on development of frequency dependent functions, instead of combination of circuit elements RLC, for component representation, i.e. the functions are used directly to characterize circuit components in the equivalent circuit, analysis on how to represent winding resistance from such Foster circuit is no longer important and thus will not be investigated in detail.

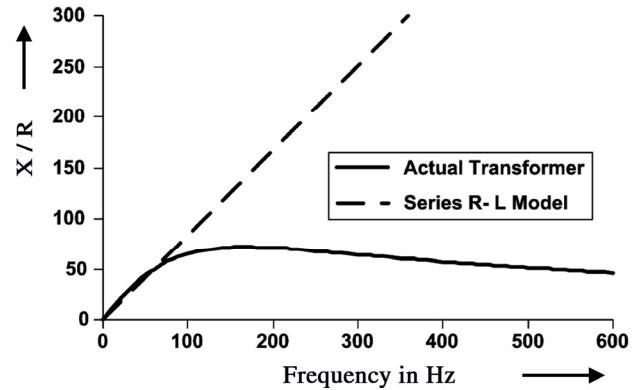


Figure 3.8: Frequency dependency of the factor X/R [Martinez-05b]

For a general analysis, the two-term power function which accounts for skin effect and is equivalent to the second-order Foster circuit can be used to represent AC winding resistance of power transformers [Martinez-05b, Fuchs-00]:

$$R_{AC} = R_{DC} + \Delta R_{AC} \cdot \left(\frac{f}{f_0} \right)^m \quad (3.1)$$

where R_{AC} : AC frequency dependent winding resistance
 R_{DC} : DC winding resistance
 f and f_0 : calculated and power frequency respectively

¹⁶ The second-order series Foster circuit includes three blocks R_0 , $(R_1 // L_1)$, $(R_2 // L_2)$ in series

ΔR_{AC} : factor represents eddy current loss
 m : factor between 1.2 and 2

Unlike winding resistance, leakage inductance can be considered fairly constant through ranges of frequencies since it represents the non-magnetic path between windings [Mork-07a]. Hence, any function which expresses the constant tendency against frequency can be used to represent leakage inductance at high frequencies.

3.2.3 Frequency dependencies of winding resistances and leakage inductances in broad frequency range (20 Hz to 2 MHz)

For the feasibility of simulation of frequency responses measured at transformer terminals for the purpose of FRA interpretation, frequency dependencies of circuit components must be available in broad frequency range. Therefore measurement-based values of winding resistances and leakage inductances at low frequencies should be converted into corresponding frequency dependent functions so that they will be combined with those at high frequencies. For a simple and convenient application of those functions for circuit simulation, following requirements should be taken into account:

- Functions which fit measurement-based values at low frequencies should be as simple as possible. Thus available fitting functions in [MATLAB-CFT] shown in Table 3.2 should be referred.
- The number of functions for representing each circuit component, e.g. winding resistance or leakage inductance, should be as minimal as possible. Normally two functions, one for low-frequency fitted values and another one for high-frequency formula, are the preferred choice. However, it is realized that only one function representing both low- and high-frequency values for winding resistance/leakage inductance is feasible. That reduces the complexity of the simulation later on.

Table 3.2: Available simple fitting functions for use in [MATLAB-CFT], with a, b, c, d ... are constants

Fitting function	Form	Formula
Power	one-term	$a \cdot f^b$
	two-term	$a \cdot f^b + c$
Exponential	one-term	$a \cdot \exp^{(b/f)}$
	two-term	$a \cdot \exp^{(b/f)} + c \cdot \exp^{(d/f)}$
Polynomial	linear	$a \cdot f$
	quadratic	$a \cdot f^2 + b \cdot f + c$
	cubic	$a \cdot f^3 + b \cdot f^2 + c \cdot f + d$
	n^{th} polynomial	$a \cdot f^n + b \cdot f^{(n-1)} + c \cdot f^{(n-2)} + \dots$
Rational	numerator and denominator are polynomials	polynomial/polynomial

To the three test transformers, it is seen that the two-term power and linear/linear rational function are the best choices for representing total resistance from stray losses (winding resistance) and leakage inductance respectively. The two-term power function that is recommended for consideration of skin effect at high frequencies in (3.1) is found also suitably in fitting low-frequency measurement-based winding resistance whereas the rational function introducing a constant tendency at high frequencies is appropriate in fitting measurement-based leakage induc-

tance at low frequencies. Detailed information concerning fitting as well as combination of fitted functions and experimental formulae for each test transformer will be presented in next chapters.

3.3 Zero-sequence input impedance test on star winding and zero-sequence impedances

In the third step of the method, the zero-sequence input impedance test is implemented and analyzed to determine the zero-sequence resistance (R_4) and inductance (L_4) of the star winding. Similarly to the approach based on the short-circuit impedance tests, the zero-sequence parameters obtained from this approach are also calculated from the measurement in low frequency range and from analytical formulae at higher frequencies.

For diagnostic purpose the zero-sequence inductance calculated in the low frequency range can be referred whereas for simulation, frequency dependency of zero-sequence resistance and inductance are generally required. Thus, the second adapted approach introduced in this section is devoted for analysis of the parameters in broad range of frequencies.

3.3.1 Overview of the zero-sequence impedance in power transformers

The zero-sequence impedance of power transformers is the inductive impedance associated with fluxes created by zero-sequence applied voltage; that means the inductance represents the non-magnetic zero-sequence path like leakage inductance whereas the resistive component represents relevant active losses. For power transformers, unlike the positive-sequence leakage inductance which is important in most of cases, the zero-sequence impedance is only considered important for analyses of transformers in asymmetrical operation condition, e.g. under single phase measurements¹⁷ or faults. In addition, since the zero-sequence impedance, or reactance/inductance, may differ significantly from the positive-sequence leakage reactance/inductance depending on magnetic circuit type, tank condition and winding connections, it is worth to introduce briefly general knowledge about the zero-sequence impedance in terms of winding connections and tank influence because the three test transformers although have the same magnetic circuit (three-phase three-legged core-type) but different vector groups (YNyn6, Dyn5, YNd5) and tank appearances (opened/sealed transformers).

With regard to change of zero-sequence inductance in terms of winding connections and tank appearance of two-winding three-limb core-type transformers¹⁸, there are several following scenarios:

- *For transformers without delta connected winding:* since fluxes created by per-phase zero-sequence currents in three limbs have the same magnitude and direction, they must circulate through paths outside the core. The transformer tank in this case influences the zero-sequence inductance in the following manner. In one side, it provides a low reluctance path compared to air or dielectric materials to the zero-sequence flux, which increases the inductance; on the other hand, it acts as a short-circuited delta winding confining the flux which in turn reduces the inductance. The latter effect is more dominant and thus in case the transformer has no tank the zero-sequence inductance of a winding is significantly more than that covered by the tank.

¹⁷ Most FRA measurements are under single-phase excitation

¹⁸ Scenarios for other transformers such as three-phase five-limb or single-phase three-limb ones can be referred in [Kulkarni-00]

For illustration, Figures 3.9 and 3.10 depict respectively FEM simulations of zero-sequence flux and magnetic energy produced by zero-sequence currents flowing through the star connected HV winding of the opened YNyn6 transformer (T_1) at 1 V and 50 Hz while the LV winding is left floating.

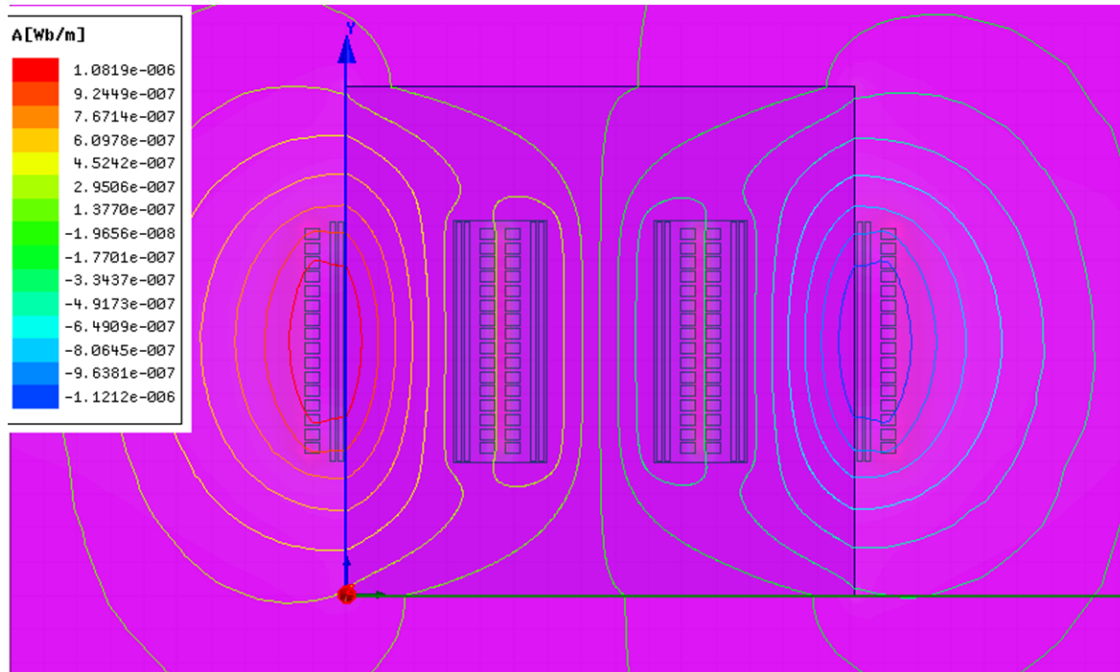


Figure 3.9: FEM simulation of zero-sequence flux of the open YNyn6 transformer at HV side at 50 Hz and 1 V supplied

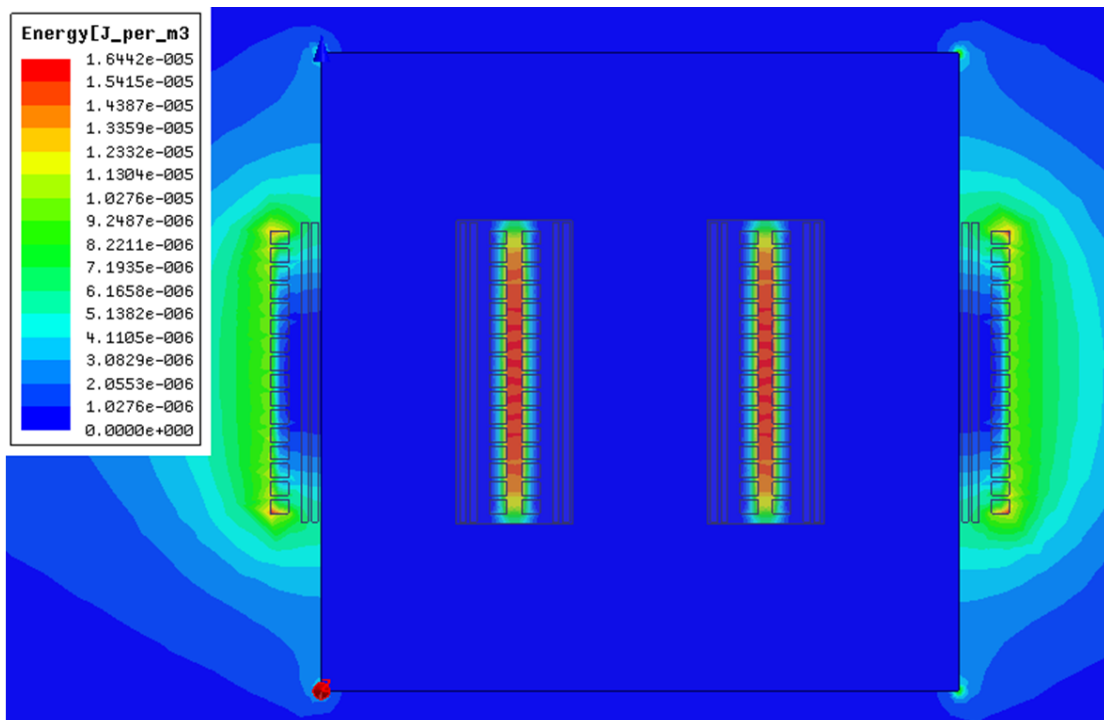


Figure 3.10: FEM simulation of stored energy density (W_{m0} in J/m^3) associated with zero-sequence flux in Figure 3.9

It can be easily seen that the flux reaches space outside the transformer, increasing the total magnetic energy and hence the inductance since they are proportional to each other [Kulkarni-04]:

$$L = \frac{2W_m}{I^2} \quad (3.2)$$

where L : inductance calculated through energy-based method, in H
 W_m : total energy of the magnetic field produced by a current I , in J
 I : current flowing in closed path, in A_{RMS}

The total energy in (3.2) and Figure 3.10 is calculated from the simulation software “Maxwell” as:

$$W_m = \frac{1}{2} \int_{\text{volume}} \mathbf{A} \cdot \mathbf{J} \cdot dv \quad (3.3)$$

where \mathbf{A} : magnetic vector potential in volume unit (dv), in Wb/m
 \mathbf{J} : current density vector, in A/m^2
 dv : volume unit/element of the geometry, in m^3

- *For transformers with one delta connected winding:* when zero-sequence voltage is supplied to the star winding, there are currents flow in the delta winding and also the tank which can be considered as another delta winding. Depending on the position of the delta winding, i.e. inner or outer, there are two different cases for the zero-sequence inductance of the star winding¹⁹:
 - If the delta winding is the outer one: in this case the outer delta winding acts as a shield which confines the zero-sequence flux within the space between the two windings, that means the zero-sequence inductance is nearly equal the (positive-sequence) leakage inductance.
 - If the delta winding is the inner one: the zero-sequence inductance is calculated approximately equal the (positive-sequence) leakage inductance multiplying with the ratio of the area between the star winding and tank to the area between the delta winding and tank due to effects of the currents flowing through the delta winding and the tank. Since the delta winding is the inner one, the ratio is less than one indicating that the zero-sequence inductance is always less than the (positive-sequence) leakage inductance.

It is therefore concluded that the zero-sequence inductance of the star winding in transformer bulk should be considered in case the transformer has no tank and actually it is true for the test transformer T_1 . Furthermore, due to the change of zero-sequence inductance depending on the position of the analyzed winding and the other winding, i.e. inner or outer, it is recommended that one equivalent circuit is only appropriate for analysis at one side; that means in cases both HV and LV side of a transformer need to be investigated, two equivalent circuits should be developed independently in order to calculate transformer parameters referred into each side.

¹⁹ Detailed calculations can be found in [Kulkarni-00]

3.3.2 Determination of zero-sequence impedance

The zero-sequence input impedance test is performed in a same way as the conventional zero-sequence test, i.e. the source is supplied between the three connected phase terminals and the neutral at the same side, i.e. HV or LV, of transformers; hence the zero-sequence test is only feasible at star winding side with accessible neutral, e.g. for the YNd5 transformer the zero-sequence test is possible at HV side. Due to use of only one cable for measurements of zero-sequence input impedance by means of the VNA, the neutral should be grounded so that the source voltage is applied between the phase terminals and the neutral. The zero-sequence impedance is defined as per-phase quantity and therefore calculated as three times of the total impedance derived directly from the ratio between applied voltage and measured total current.

Basically there are two kinds of zero-sequence impedance for a winding in transformer bulk [Kulkarni-04]:

- Open-circuit magnetizing impedance: terminals of all other windings are left floating
- Short circuit leakage impedance: terminals of the other winding are short-circuited

For FRA interpretation, the open-circuit zero-sequence impedance is requested since most frequency responses are measured at one side when the winding at other side are left open. Thus the zero-sequence impedance mentioned hereafter will be referred to the open-circuit one.

In order to determine open-circuit zero-sequence impedance of the star winding from measurements, Figure 3.11 depicts a measuring circuit in context of the zero-sequence input impedance test carried out on the HV winding of the YNd5 transformer as an example.

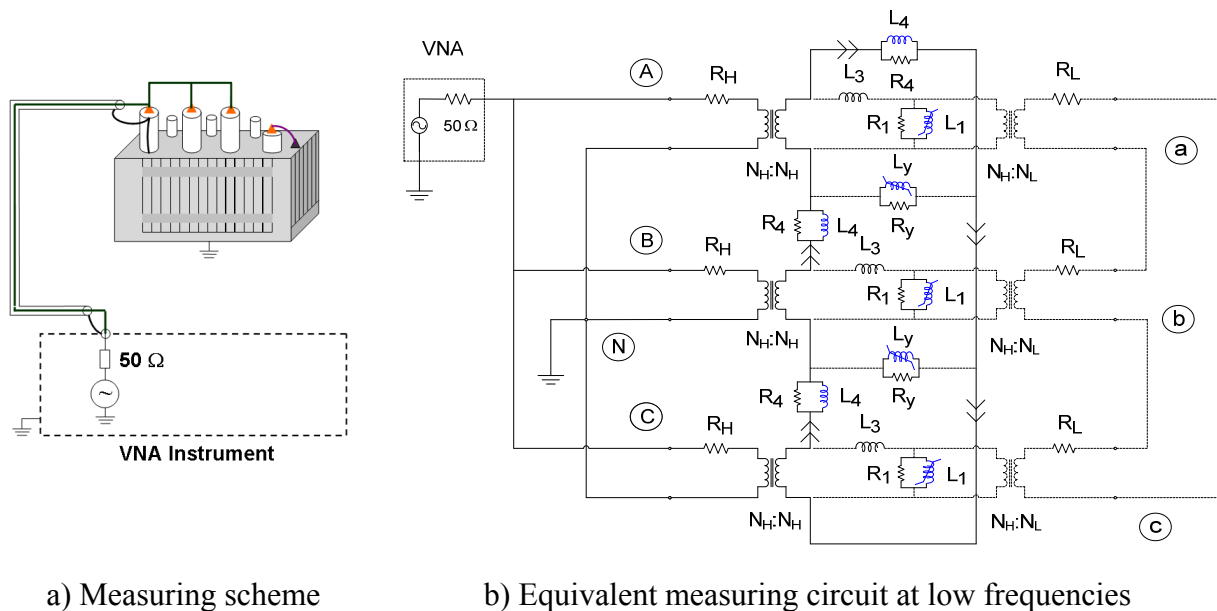


Figure 3.11: Open-circuit zero-sequence input impedance test at HV side of the YNd5 transformer

In Figure 3.11, it is observed from the excited active part of the circuit that the zero-sequence currents flow only through three (per-phase) zero-sequence impedances $\underline{Z}_4 = R_4/L_4$ and three winding resistances R_H since the core impedances ($\underline{Z}_1 = R_1/L_1$ and $\underline{Z}_y = R_y/L_y$) are significantly higher than zero-sequence ones, i.e. no magnetizing currents through core impedances. Therefore the zero-sequence impedance can be determined in general as:

$$\underline{Z}_4 = 3 \cdot \underline{Z}_{\text{mea}} - R_H \quad (3.4)$$

where $\underline{Z}_{\text{mea}}$: input impedance measured by means of the VNA
 R_H : HV winding resistance

Equation (3.4) and Figure 3.11b are fully valid in cases the LV winding is the inner winding, connected in star and left open since then there is no influence from the LV side to the HV zero-sequence currents or fluxes (i.e. transformer vector group YNyn). In fact, since the inner LV winding of the YNd5 transformer is connected in delta, there are short circuit zero-sequence currents flowing in the delta winding (not shown in Figure 3.11b) and the tank. The current in the delta winding with opposite direction with those in HV winding “induces” another current to flow back through the leakage inductances L_3 in the magnetic-electric circuit, affecting the main zero-sequence current. Thus the zero-sequence impedance/inductance in this case should involve the L_3 and \underline{Z}_4 according to the circuit in Figure 3.11b.

For more accurate analysis, the duality based equivalent circuit of power transformers is not fully appropriate for this case since the zero-sequence impedance/inductance derived from the duality principle is associated with flux outside the windings (see Figure 2.5). This assumption is only valid for transformers with star-star winding and the outer winding is excited. However, it is obvious that for the YNd5 transformer, the zero-sequence flux exists both outside and *between* the windings, i.e. involving the \underline{Z}_4 and L_3 in the equivalent circuit respectively. So the general solution in determination of open-circuit zero-sequence impedance of the star winding for power transformers is to ignore influence of the secondary winding, i.e. the circuit with active part is the one in Figure 3.11b regardless of which connection the secondary winding has. Results in chapter 6 later on confirm that the zero-sequence inductance calculated based on this assumption is reasonable.

For analysis of the zero-sequence parameters, Figure 3.12 shows frequency response of the input impedance measured at HV side of the YNd5 transformer. It is observed that, similarly to the measured input impedance in the short circuit test, an inductive impedance is recognized at low frequencies whereas at higher frequencies interaction between the inductance and total capacitance is obvious. Hence the zero-sequence impedance can be calculated in the same manner like for winding resistance and leakage inductance, i.e. from measurements at low frequencies as well as from experimental formulae at high frequencies.

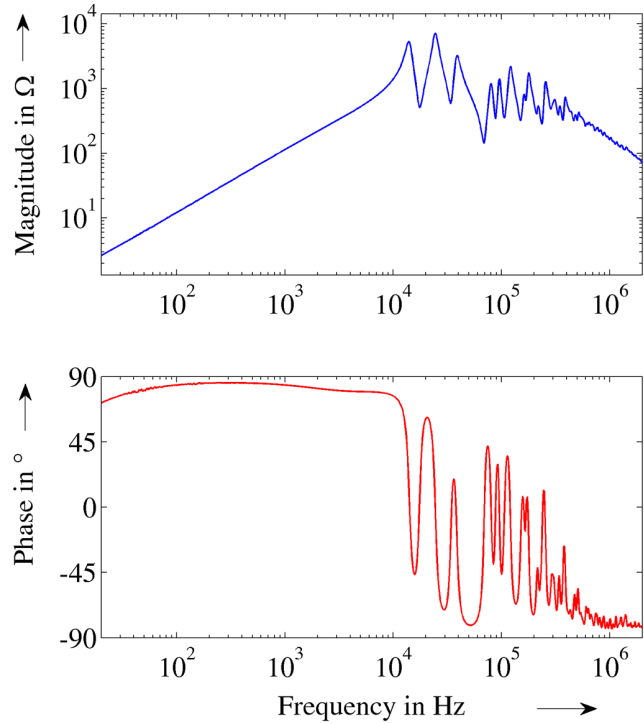


Figure 3.12: Frequency response of input impedance in the zero-sequence input impedance test in Figure 3.11

Hence the zero-sequence impedance can be calculated in the same manner like for winding resistance and leakage inductance, i.e. from measurements at low frequencies as well as from experimental formulae at high frequencies.

In Figure 3.12, the inductive behaviour constituted from a resistance and an inductance representing active loss in transformer parts and non-magnetic path induction respectively from zero-sequence flux is observed within 20 Hz to ~ 10 kHz. Nevertheless, the zero-sequence resistance and inductance could only be determined in a low frequency range, i.e. from 20 Hz to around 400 Hz (where the phase angle reaches nearest 90°) for an accurate analysis. Knowing R_H of three phases, the Z_4 and afterwards, R_4 and L_4 , can be easily determined in this low frequency range. Note that the low frequency range varies from transformer to transformer but it has no influence to the diagnostic and FRA interpretation since a few values at low frequencies are sufficient for the diagnostic and development of parameter's frequency dependency.

To develop frequency dependency of zero-sequence resistance and inductance at high frequencies, the fitted functions in Table 3.2 can be applied thanks to measurement-based values at low frequencies:

- For zero-sequence resistance: since the relevant loss is out of the windings, and there are many scenarios for zero-sequence flux to circulate depending on position and connection of the windings, any function in Table 3.2 can be applied if it shows the same tendency like that for winding resistance, i.e. increase with increasing frequency. A detailed and accurate fit at high frequencies for zero-sequence resistance is not necessary and also not feasible.
- For zero-sequence inductance: the function used for representing leakage inductance can be applied to derive the frequency dependency of the zero-sequence inductance since both of them represent the non-magnetic path induction between and outside the windings.

It is seen after analyzing the three test transformers that for characterizing zero-sequence resistance and inductance in broad frequency range, only one function in Table 3.2 is sufficient, which is convenient for application since it reduces the complexity of the circuit simulation procedure. Detailed calculation and results for the three test transformers will be presented in corresponding next chapters.

3.4 Open-circuit input impedance tests and core section impedances

To determine core section impedances (yokes, legs) in the duality based equivalent circuit, there is so far an advanced measurement method in [Mork-07a, Mork-07b] which can be only applicable for transformers with star windings. In case there is a delta winding in the transformer, the winding should be opened up; and that is not realistic in reality! Therefore a new and non-destructive measurement-based approach in determining core section impedances in general for power transformers with star/delta winding is required and will be presented in this section. To be able to do so, the open-circuit input impedances should be measured and analyzed. Of course the core section impedances can only be calculated from measurements only in a low frequency range since their inductive effect is dominant in measured terminal impedances at those frequencies.

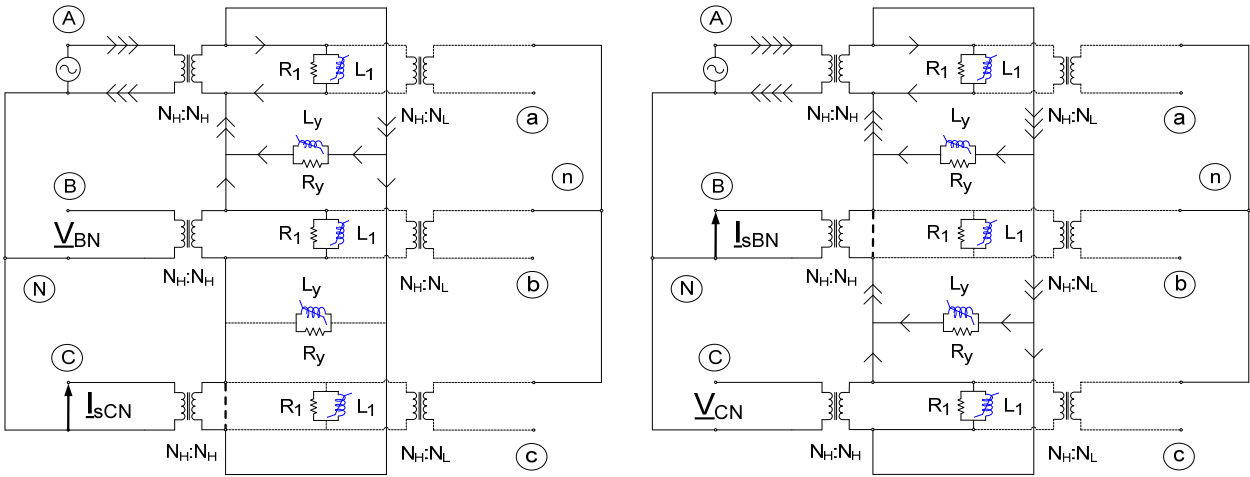
In addition, the frequency dependency of core impedances at high frequencies is also required since otherwise, the circuit simulation solution is not possible in broad frequency range. As a result, the core section impedances at high frequencies then will be determined based on experimental formulae, which requires a few magnetic and transformer design data. Of the tested transformers, the T_1 is opened implying that the analytical calculation of its core electrical parameters

is feasible since the required data can be approximately achieved. For practical application, the analysis of core electrical parameters of any transformer at high frequencies is necessary and will be presented in appropriate sections.

3.4.1 Measurement-based approach to calculate core impedances at low frequencies

3.4.1.1 Core (section) impedances referred into the star winding side

The idea for introduction of the new approach originates from the advanced measurement-based method in [Mork-07b] by considering two measurement configurations in determination of core impedances referred into the HV side of the YNyn6 transformer in Figure 3.13a and 3.13b. In Figure 3.13, single phase source voltage is supplied to the winding of phase A, whereas centre and outer phase winding is in succession shorted to measure short-circuit currents through the shorted windings and open-circuit voltages on the other phase winding. The purpose is to calculate core impedances of the legs ($\underline{Z}_l = R_l // L_l$) and yokes ($\underline{Z}_y = R_y // L_y$) based on measured quantities without influence from LV winding side (since the star LV winding is left floating).



a) Measuring circuit with the other outer phase winding short-circuited at low frequencies

b) Measuring circuit with the center phase winding short-circuited at low frequencies

Figure 3.13: a) Core leg (\underline{Z}_l) determination from \underline{V}_{BN} and \underline{I}_{sCN}

b) Core yoke (\underline{Z}_y) determination from \underline{V}_{CN} , \underline{I}_{sBN} and \underline{Z}_l

In Figure 3.13a, the short circuit current \underline{I}_{sCN} flowing through the shorted winding C-N implies the short circuit of the corresponding part (dashed line) in the magnetic-electric core circuit in the middle; thus the core leg and yoke of phase C are shorted. Hence the short circuit current \underline{I}_{sCN} flowing through the core leg of phase B resulting in an open-circuit voltage \underline{V}_{BN} . From that the core leg impedance can be determined as:

$$\underline{Z}_l = \underline{V}_{BN} / \underline{I}_{sCN} \quad (3.5)$$

In Figure 3.13b, the short circuit current \underline{I}_{sBN} flowing through $\underline{Z}_l // \underline{Z}_y$ of phase C (the winding of phase B is shorted) causing the open-circuit voltage \underline{V}_{CN} on phase C. Hence the core yoke impedance \underline{Z}_y is then determined based on \underline{V}_{CN} , \underline{I}_{sBN} and \underline{Z}_l :

$$\underline{Z}_l // \underline{Z}_y = \underline{V}_{CN} / \underline{I}_{sBN} \equiv \underline{Z}_{ly} \quad (3.6)$$

$$\underline{Z}_y = \underline{Z}_l \cdot \underline{Z}_{ly} / (\underline{Z}_l - \underline{Z}_{ly}) \quad (3.7)$$

The advanced measurement method has limited application since it is only applied for transformers with star windings. In addition, several following disadvantages were realized when the method was applied to characterize core impedances of the test transformer:

- Inconsistence of calculated core impedances when the applied voltage is on other outer phase, e.g. phase C. It is understandable since measured quantities are not identical between the cases in which voltage is applied on phase A and C. It is therefore required that the core impedances should be calculated based on measurements with voltage application on three phases, not single phase.
- The measurements are performed at several frequencies to calculate the frequency dependency of core impedances. This introduces more problems when frequency increases since influence of other accessories such as wire/cable, measuring devices should be taken into account. In addition, denoising of measured quantities is also an issue when measuring with high-accuracy devices such as digital storage oscilloscope (DSO) at low applied voltage for compatibility with FRA interpretation purpose.

Figures 3.14 depicts measured voltages $V_{sCN}(t)$ on a $15\text{-}\Omega$ resistance measured by means of a 12-bit resolution DSO “Accura” to determine short circuit current I_{sCN} when the applied voltage V_{AN} is 1 V^{20} at 20 Hz and 400 Hz to illustrate difficulties in signal processing when frequency rises.

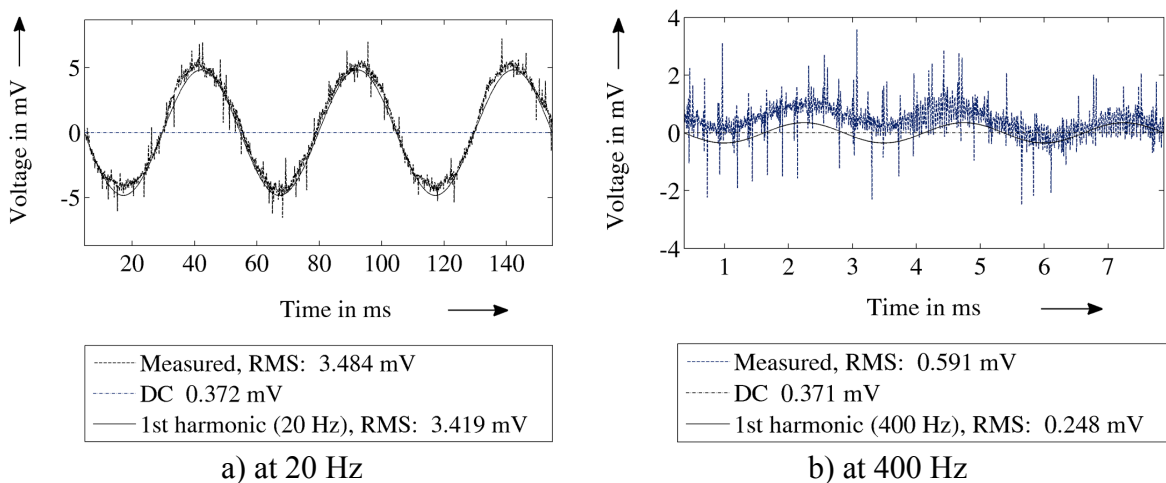


Figure 3.14: Voltage $V_{sCN}(t)$ and its fundamental harmonic on a $15\text{-}\Omega$ resistance

Figure 3.15 shows comparisons between applied voltage $V_{AN}(t)$ and short-circuit voltage $V_{sCN}(t)$ to calculate phase shift between them for determination of complex core impedances at 20 Hz and 400 Hz. It is observed that the analysis procedure is not simple at 400 Hz, which suggests a new way by using the VNA as main instrument to overcome difficulties taking place due to use of traditional instruments for measurements.

²⁰ The low voltage (1 V) is best applied in the measurements since the calculated parameters then will be used appropriately to interpret standard frequency responses measured also at the same voltage by means of the VNA. Note that another higher voltage can also be applied but the highest voltage of commercial broad-frequency range generators is only a few Volts, e.g. the HAMEG 8150 generator has maximum open circuit voltage of 20 V_{p-p} for sinusoidal waves in frequency range of 10 mHz to 12.5 MHz [HM8150-07].

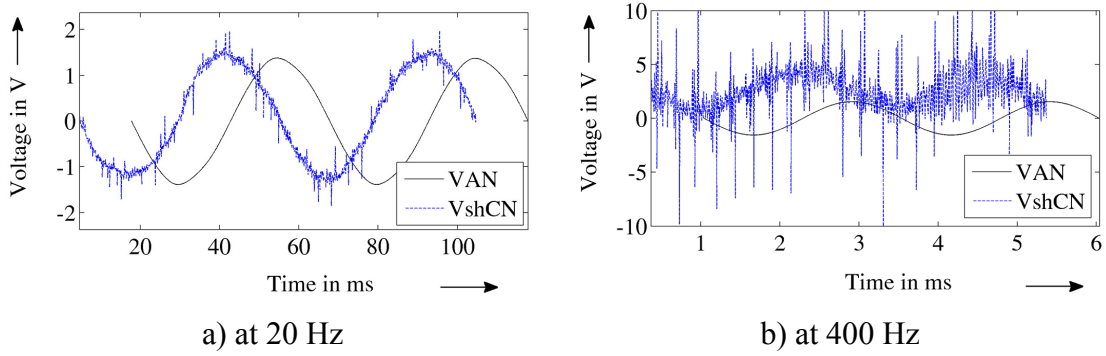


Figure 3.15: Comparison of $V_{AN}(t)$ and $V_{sCN}(t)$ to calculate phase shift

The advantage of the scattering-parameter VNA compared with traditional instruments in the measurements is that when frequency increases, the noise is no longer a problem. In addition, other advantages of use of the VNA in the new approach can be listed as follows:

- The number of frequency points measured by the VNA is not limited and can be adjusted. Therefore, it is convenient and much faster to conduct measurements.
- No other accessories, e.g. connection wire/cable and measured devices, are required. There is only one measuring cable connected from the VNA to a transformer terminal, but the influence of this cable is removed by calibration.
- Measured impedances are obtained directly after measurements with acceptable accuracy if they are within measuring range of the instrument; thus, it is much comfortable.
- Since only open-circuit impedances will be measured at one side, the floated winding at other side has no influence to the measured impedances regardless it is connected in star or delta. Thus, the new approach can be applied for any transformer with delta winding.

However, due to the fact that measured terminal impedances consist of different combinations of core section impedances at low frequencies, the way to analyze measured impedances is much complicated. That is the only disadvantage but can be solvable. The solution for such problem is the main content of the new approach, which will be introduced step-by-step below.

a) Determination of the low frequency range for analysis of core impedances from open-circuit input impedances

It is first required that a low frequency range where the core effect is dominant should be identified in order to calculate core impedances from measurements. Figures 3.16a and 3.16b show the whole measurement circuit and corresponding open-circuit input impedance between the terminals A and N carried out by means of the VNA for illustration.

Similarly to measured impedances in short-circuit and zero-sequence tests, a pure inductive impedance is observed in region ② in Figure 3.16b at low frequencies till 1 kHz in this case. However, for an accurate identification of core impedances from measured impedances, only a narrow frequency range in which only effect of the core is realized, i.e. within region ① in Figure 3.16b from 20 Hz to 400 Hz, is considered since at higher frequencies the capacitances start to influence. The value of 400 Hz in this case is the upper limit of the low frequency range to be analyzed to calculate core impedances from measurements; in general the upper limit of the low frequency range *varies* from transformer to transformer, e.g. from several tens Hz to several kHz, but it is always identified from measurement results for the analysis.

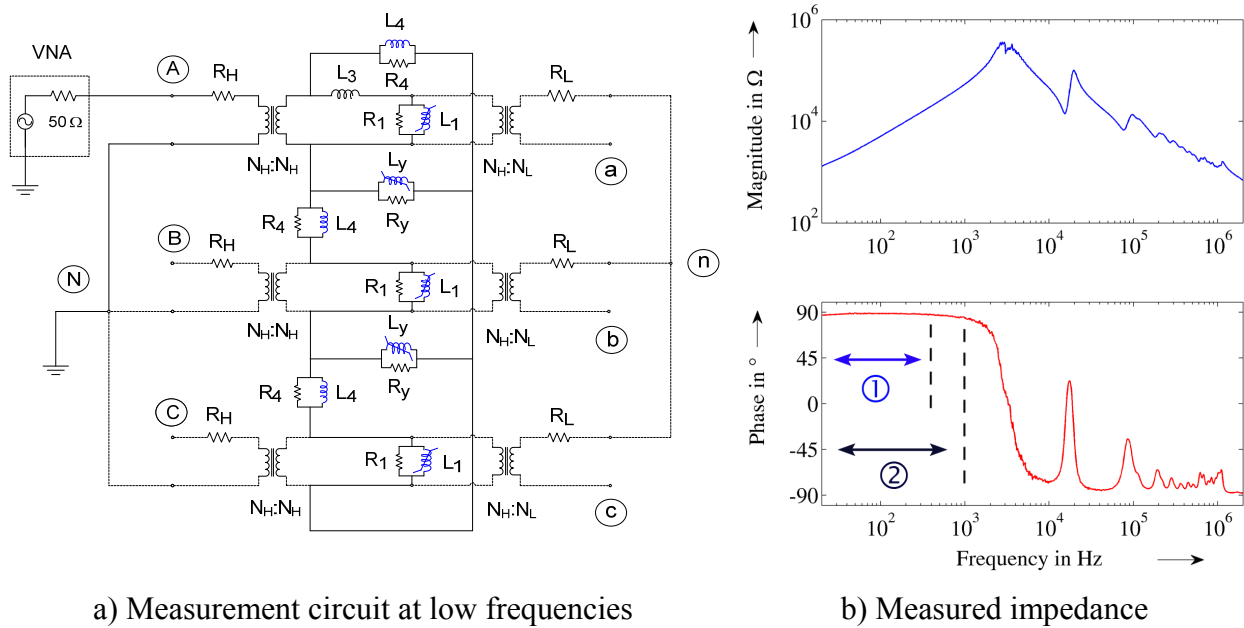


Figure 3.16: Measurement circuit and measured input impedance observed at phase A

b) Measurement configurations of input impedances required for the analysis

It can be assumed without loss of generality that other parameters than core impedances (Z_1, Z_y) such as winding resistance (R_H, R_L), leakage inductance (L_3) and zero-sequence impedance (Z_4) will not have significant influence on measured input impedances at low frequencies and thus will not be taken into account. This assumption is always valid unless the transformer has no tank, i.e. zero-sequence inductance is higher appreciably than leakage inductance, which may have small but certain influence on the calculated core impedances. But first of all, the circuit with only core impedances will be analyzed due to its simplification.

There are in total nine measurement configurations of open-circuit input impedance that can be measured by means of the VNA. Based on the equivalent circuit in Figure 3.13a, different measurement configurations are then analyzed shown in Table 3.3.

Table 3.3: Measurement configurations and calculated equivalent impedances for star windings at low frequencies (secondary winding has no influence)

Index	Configuration	Calculated equivalent impedance
1	A-N excited (in Figure 3.16a)	$(Z_1 // Z_y + Z_1) // (Z_1 // Z_y)$
2	A-N excited, B-N shorted	$(Z_1 // Z_y) // (Z_1 // Z_y)$
3	A-N excited, C-N shorted	$Z_1 // (Z_1 // Z_y)$
4	B-N excited	$(Z_1 // Z_y + Z_1 // Z_y) // Z_1$
5	B-N excited, C-N shorted	$(Z_1 // Z_y) // Z_1$
6	B-N excited, A-N shorted	$(Z_1 // Z_y) // Z_1$
7	C-N excited	$(Z_1 // Z_y + Z_1) // (Z_1 // Z_y)$
8	C-N excited, B-N shorted	$(Z_1 // Z_y) // (Z_1 // Z_y)$
9	C-N excited, A-N shorted	$Z_1 // (Z_1 // Z_y)$

For explanation of a typical configuration, the first one in Table 3.3, the circuit which is active is shown by solid lines in Figure 3.16a. Since leakage inductance L_3 and zero-sequence parameters R_4, L_4 are not considered, i.e. being short-circuited, it is seen that the equivalent core impedance of phase C (Z_{1C}/Z_{yC}) is in series with the core impedance of phase B (Z_{1B}) as observed from the excited winding, i.e. phase A. Finally the impedance combination between phases B and C is found in parallel with the core impedance of phase A (Z_{1A}/Z_{yA}). The final calculation is expressed in Table 3.3 with the fact that impedances of legs (and yokes) are identical, i.e. $Z_{1A} = Z_{1B} = Z_{1C} = Z_1$, and $Z_{yA} = Z_{yC} = Z_y$.

c) Solution identification

Now one has to solve a mathematic problem with two non-linear variables (Z_1 and Z_y) based on measurement configurations in Table 3.3 at each low frequency. The principle is to identify the mathematic problem as an optimization one in terms of types of optimization, objective function and constrain; afterwards appropriate solver and algorithm are then selected to solve the problem.

There are several tables which are designed to help selecting a best solution for an optimization problem [MATLAB-OPT, MATLAB-GLOPT]. The first group of tables is designed to help selecting appropriate solver and algorithm for a local solution and therefore is called as “local-searching” table group in which several following options are introduced:

- Type of optimization
 - Single-objective
 - Multi-objective
 - Equation solving
 - Data-fitting
- Type of objective function
 - Linear
 - Quadratic
 - Least squares
 - Smooth nonlinear
 - Non-smooth
- Type of constraints
 - Unconstrained
 - Bound
 - Linear (including bound)
 - General smooth
 - Discrete

A suitable solver/algorithm selected from the “local-searching” table group can only provide a local solution for an optimization problem. That means when a minimization, for example, needs to be solved, a local minimum may be derived. Consequently, a second table group for selecting a global optimization solver is necessary. To deal with the problem, there are several optimizers which can be applied as:

- Global-Search
- Multi-Start
- Pattern-Search

- Genetic-Algorithm
- Simulated Annealing

However, “global-searching” optimizers can not guarantee a global solution since they are all stochastic. The advantage of using them is to extend searching range with hope to reach a global solution.

d) Data fitting procedure

Solution for solving the problem of determination of core impedances based on measurement configurations in Table 3.3 is then identified as follows. It is type of single-objective (data-fitting) optimization since only minimization of errors between measured and calculated equivalent terminal impedances is required. The corresponding objective function type is least squares with bounds as constraints since core impedances are inductive. From that, the non-linear least squares solver with the “trust-region-reflective” algorithm is selected.

Determination of core impedances from measured terminal impedances is now possible thanks to different configurations in Table 3.3. Depending on selection of measurements on a single phase or combination of different phases as inputs for the solver, one will have possibilities of unbalanced or balanced analysis respectively. For illustration, the unbalanced analysis on phase A, i.e. three first configurations in Table 3.3 is now explained with details as follows.

Determination of core impedances in unbalanced analysis (single phase input mode)

In the first stage, i.e. local minimum determination, the objective functions are then established as:

- Norm of real and imaginary impedance errors:

$$\|f_1\|_2^2 = \sum_{i=1}^n \left(\left| \operatorname{Re} \left\{ \underline{Z}_i^m(\omega_j) - \underline{Z}_i^c(\omega_j) \right\} \right|^2 + \left| \operatorname{Im} \left\{ \underline{Z}_i^m(\omega_j) - \underline{Z}_i^c(\omega_j) \right\} \right|^2 \right) \quad (3.8)$$

or

- Norm of absolute and phase angle impedance errors:

$$\|f_2\|_2^2 = \sum_{i=1}^n \left(\left| \underline{Z}_i^m(\omega_j) - \underline{Z}_i^c(\omega_j) \right|^2 + \left| \angle \underline{Z}_i^m(\omega_j) - \angle \underline{Z}_i^c(\omega_j) \right|^2 \right) \quad (3.9)$$

where $\underline{Z}_i^m(\omega_j)$, $\underline{Z}_i^c(\omega_j)$ are measured and calculated equivalent impedances at frequency ω_j of i^{th} configuration; $i = 1, \dots, n$ where $n = 3$ is the total number of measurement configurations supplied to the solver.

A comparison between (3.8) and (3.9) as objective function shows that optimization in terms of real and imaginary parts of impedance errors gives better results with lower errors between measured and calculated terminal impedances. That is understandable since it is realized that the phase angle components in (3.9) do not play an important role in solving problem. Hence, the function expressed in (3.8) is chosen as the objective function hereafter for analysis.

The parameter determination procedure starts with a set of initial values of variables, i.e. complex impedances \underline{Z}_1 and \underline{Z}_y , which are selected identically as minimum of the boundary between $1 + j \Omega$ and $10 + j10 \text{ M}\Omega$ to cover all cases of inductive impedances. Then the algorithm evaluates and minimizes the $\|f_1\|_2^2$ with regard to variable values in iterations at each frequency based on approximated Jacobian (gradient) of single components, i.e. real or imaginary impedance errors, inside the objective function (3.8). The procedure terminates whenever one of stopping criteria shown in Table 3.4 is reached. Since the procedure must be repeated from frequency to frequency, different options of stopping criteria with regard to running time and accuracy are designed. They include fast, normal and detailed modes. Due to the fact that the procedure is off-line, the detailed mode is selected for slowest execution but best performance.

Table 3.4: Different modes for stopping criteria

Item	Mode		
	Fast	Normal	Detailed
Max iterations	10^3	10^4	10^6
Max function evaluations	10^5	10^6	10^6
Impedance error tolerance, in Ω	10^{-5}	10^{-6}	10^{-9}
Objective function tolerance	10^{-5}	10^{-6}	10^{-9}

In order to evaluate the efficiency of solvers/algorithms, there are two sets of indicators. The first indicator set based on outputs directly from the solver consists of:

- Norm of accumulate residuals ($\|f_1\|_2^2$): It can be used to compare performances between good and bad solvers/algorithms. However, between comparable solvers, the so-called “individual residuals” mentioned below are much helpful.
- Individual residuals: They are lowest values of single components in (3.8) after iterations stop. For instance, in case three measurement configurations of phase A are supplied as inputs to the solver, there are consequently six individual residuals from real and imaginary parts of impedance errors in (3.8):

$$|\text{Re}\{\Delta Z_i\}| = \left| \text{Re}\{Z_i^m(\omega_j) - Z_i^e(\omega_j)\} \right|, i = 1 \div 3 \quad (3.10)$$

$$|\text{Im}\{\Delta Z_i\}| = \left| \text{Im}\{Z_i^m(\omega_j) - Z_i^e(\omega_j)\} \right|, i = 1 \div 3 \quad (3.11)$$

Table 3.5 presents the individual residuals $|\text{Re}\{\Delta Z_i\}|$ and $|\text{Im}\{\Delta Z_i\}|$ ($i = 1 \div 3$) (in Ω) after iterations finish. However, ohmic values do not reveal the solver performance since higher values of imaginary residuals compared with those of the real ones do not mean an unbalanced achievement. Thus, Table 3.6 shows a better overview of the solver performance via percentage values calculated by dividing values in Table 3.5 by real or imaginary part of relevant measured impedances $Z_i^m(\omega_j)$. These values are listed at several frequencies for illustration.

Table 3.5: Individual residuals at several frequencies (in Ω)

Frequency in Hz	$ \text{Re}\{\Delta Z_i\} $ in Ω			$ \text{Im}\{\Delta Z_i\} $ in Ω		
	i = 1	i = 2	i = 3	i = 1	i = 2	i = 3
20.0	5.6	4.1	3.2	35.3	25.2	20.8
50.2	4.7	3.4	2.8	51.3	37.7	29.4
100.2	5.1	3.5	3.1	102.9	76.4	58.4
200.0	0.5	1.2	0.3	192.3	143.0	109.1
299.3	10.6	6.5	7.0	274.0	203.3	155.8
399.1	7.8	7.5	3.2	367.8	271.8	209.9

Table 3.6: Individual residuals at several frequencies (in %)

Frequency in Hz	$ \text{Re}\{\Delta Z_i\} $ in %			$ \text{Im}\{\Delta Z_i\} $ in %		
	i = 1	i = 2	i = 3	i = 1	i = 2	i = 3
20.0	8.5	8.4	4.6	2.7	2.8	1.7
50.2	9.1	8.0	5.4	1.9	2.0	1.2
100.2	4.6	4.1	3.1	2.0	2.2	1.2
200.0	0.2	0.6	0.1	1.9	2.1	1.2
299.3	2.1	1.7	1.6	1.8	2.0	1.1
399.1	1.0	1.3	0.5	1.9	2.0	1.1

It can be observed from Table 3.6 that most percentage individual residuals decrease with increasing frequency. The fact that low errors derived (maximum 2.1 %) when frequency is higher than 200 Hz shows that the solver and algorithm are reasonable selected. Highest errors (9.1 %) at frequency lower than 100 Hz appearing only on the real parts do not mean that the solver has bad performance. Observation in Table 3.5 reveals that the relevant ohmic error is relative small (4.7 Ω). Note that in such frequencies, core inductances are dominant and the lower errors (maximum 2.8 %) in imaginary parts are much more important.

Table 3.7: Maximum errors between measured and calculated impedances – single phase input mode

Configuration	Magnitude error		Phase angle error in degree
	in Ω	in %	
A-N excited (in Figure 3.13a)	422.8	2.1	0.8
A-N excited, B-N shorted	259.2	2.0	0.4
A-N excited, C-N shorted	255.8	1.5	0.4
B-N excited	187.2	10.3	0.9
B-N excited, C-N shorted	893.4	4.8	0.6
B-N excited, A-N shorted	885.6	4.8	0.6
C-N excited	141.0	0.7	0.7
C-N excited, B-N shorted	484.8	3.5	0.6
C-N excited, A-N shorted	440.0	2.4	1.0

The second indicator set which could be used to evaluate the efficiency of solvers/algorithms is based on the maximum error shown in Table 3.7 of the equivalent terminal impedances (see Ta-

ble 3.3) between measurement and calculation after the solver (after Z_l and Z_y are derived). Since the impedance changes with frequency, the maximum equivalent impedance error of each measurement configuration in Table 3.7 can appear at any frequency from 20 Hz to 400 Hz. Note that due to the fact that measured impedances increase when frequency increases, a small ohmic error at a low frequency may correspond to a high percentage value and vice versa.

From Table 3.7, it is realized that whereas the maximum phase angle errors are insignificant, maximum magnitude errors of non-analyzed configurations, for example, from phases B are much higher than those from the analyzed phase (highest 10.3 % at 21.8 Hz). It is concluded that the balanced analysis with all input mode should be performed for better performance.

The second stage with attempts to search the global optimization after the first stage is then conducted. The purpose is to check whether a better solution can be reached under the same conditions of inputs, stopping criteria, algorithm settings etc. There are two differences from the second stage compared with the first one. First, instead of starting with one set of initial variable values, the optimizer can run with different randomly or specifically sets of initial variable values. Use of different initial value sets might be efficient in some cases in which a global minimum exists but the algorithm only converges into a local minimum because this solution is near the initial values. Second, in case a computer core has multiple processors, the running time can be reduced significantly since the time-consuming analysis procedure with multiple initial value sets can be in parallel processed.

According to the selected algorithm for the parameter determination procedure in the first stage, the “MultiStart” optimizer is identified as the best in the second stage. The number of sets of initial variable values is selected as 50. Initial variable values should be set uniformly in logarithmic scale so that they cover all values appropriately from lower to upper bounds which are chosen as $1 + j \Omega$ and $10 + j10 \text{ M}\Omega$ respectively. However, results show that there is no better solution found and therefore, it can be said that the local minimum derived from the first stage is the optimal solution. It is therefore concluded that the selected solver and algorithm are good enough and can be exploited hereafter in solving such problem.

Determination of core impedances in balanced analysis (full input mode)

The balanced analysis is then conducted with aim to search better results since there are large errors in the measurement configurations of non-analyzed phases, especially phase B in Table 3.7. In the full input mode there are maximum nine measurement configurations from three phases supplied as inputs to the solver. As a result, there are eighteen individual residuals in the objective function (3.8). Observation on results indicates that most ohmic and percentage individual residuals are little higher compared with the ones from the single phase input mode since there are much more objects for the solver to minimize; however, there is a uniform distribution of percentage values. Table 3.8 confirms this fact via a flat distribution of maximum errors between measured and calculated equivalent impedances in the balanced analysis.

It is clear that the balanced input mode provides a better solution with reasonable uniform errors. It is logical because results of measurements on three phases are taken into account since although in symmetrical measurement configurations, e.g. “A-N excited” and “C-N excited”, measured impedances are not exactly the same whereas calculated equivalent impedances are the same (see Table 3.3). This contributes to the fact that transformer core parameters derived from

the method in [Mork-07b] is not fully appropriate since they are determined in the single phase input mode.

Table 3.8: Maximum errors between measured and calculated impedances - full input mode

Configuration	Magnitude error		Phase angle error in degree
	in Ω	in %	
A-N excited (in Figure 3.16a)	696.8	3.5	0.7
A-N excited, B-N shorted	99.8	0.8	0.5
A-N excited, C-N shorted	107.3	0.7	0.7
B-N excited	386.4	1.5	0.7
B-N excited, C-N shorted	649.5	3.5	0.4
B-N excited, A-N shorted	641.8	3.5	0.3
C-N excited	400.5	2.1	0.5
C-N excited, B-N shorted	310.6	2.6	0.4
C-N excited, A-N shorted	196.1	1.1	0.7

e) Influence of zero-sequence impedance

In some special cases in which zero-sequence impedance is significantly higher than the leakage inductance, for instance when transformers have star windings and no tank, the zero-sequence impedance should be taken into account when analyzing equivalent impedances in accordance with measured input impedances. In such cases the calculated equivalent impedances are much complicated than those in Table 3.3.

For illustration, the first case in Table 3.3 is then explained, i.e. the measurement configuration “A-N excited” whose equivalent circuit is shown in Figure 3.13 with appearance of all components. Since the HV winding of phase C is left open, total impedance of this phase seen from the excited winding, i.e. on phase A, will be $(\underline{Z}_1 + \underline{Z}_4) // \underline{Z}_y$. Then the winding of phase B is still opened, resulting in the core-leg impedance \underline{Z}_1 in series with \underline{Z}_4 on this phase. Therefore, total impedance of the two phases B and C seen from phase A will be $\underline{Z}_{BC} = (\underline{Z}_1 + \underline{Z}_4) // \underline{Z}_y + \underline{Z}_1 + \underline{Z}_4$. The \underline{Z}_{BC} is then parallel with the \underline{Z}_y of the core yoke of phase A forming $\underline{Z}_{BCy} = \underline{Z}_{BC} // \underline{Z}_y$. Next, the total impedance of the whole core seen from phase A is $\underline{Z}_{coreA} = (\underline{Z}_1 + j\omega L_3) // (\underline{Z}_{BCy} + \underline{Z}_4)$. Finally, the equivalent impedance in this case will be $\underline{Z}_{equi} = R_H + \underline{Z}_{coreA}$ (R_H and L_3 can be neglected due to insignificant influence).

It is seen from the analyses of the three test transformers that winding resistance, leakage inductance and zero-sequence impedance can be neglected when analyzing core impedances in all cases whereas the zero-sequence impedance may only be considered in special cases when the transformer is opened. The contribution of the zero-sequence impedance to the core impedance analysis will be shown in the next chapter which is devoted for investigations on the opened transformer T_1 .

f) Conclusion

It is important to mention that the above-mentioned analysis is not only valid for the star winding at HV side of the YNyn6 transformer (T_1) but also appropriate for the star winding side of other test transformers, e.g. the HV winding side of the YNd5 one (T_3) when the LV delta winding is left floating. Thus, the rule of thumb for successful analysis of core impedance from the measurements on the star winding can be stated as follows:

- Build an appropriate equivalent circuit accounting for the vector group
- Only core section impedances (\underline{Z}_1 and \underline{Z}_y) are considered in the circuit to calculate equivalent impedances with regard to measured open-circuit input impedances (other components are neglected)
- Full input mode should be analyzed
- Data fitting procedure is based on (3.8)

3.4.1.2 Core (section) impedances referred into the delta winding side

Analysis of open-circuit input impedances measured on delta winding in terms of core section impedances in the duality based equivalent circuit is not an easy task since there are interconnections between the core impedances. Therefore the equivalent circuit should be reduced in such a way that the analysis can be easier executed [Pham-13a].

To illustrate the way to reduce the duality based equivalent circuit for analysis of a delta winding, the equivalent circuit of the Dyn5 transformer (T_2) in context of an open-circuit input impedance carried out at the delta winding side at low frequencies is selected as a typical case to be analyzed as shown in Figure 3.17a. Due to the delta connection of the HV winding, the magnetizing currents are on three phases; hence the three ideal transformer $N_H:N_H$ are all active, connecting the HV winding circuit to the core circuit. As a result, the $\underline{Z}_1 // \underline{Z}_y$ of phase A is the total impedance between terminals A and B, the $\underline{Z}_1 // \underline{Z}_y$ of phase C is between terminals A and C, and the \underline{Z}_1 of center leg is between terminals B and C (other components rather than core impedances \underline{Z}_1 and \underline{Z}_y are removed). The reduced circuit is therefore derived and depicted in Figure 3.17b.

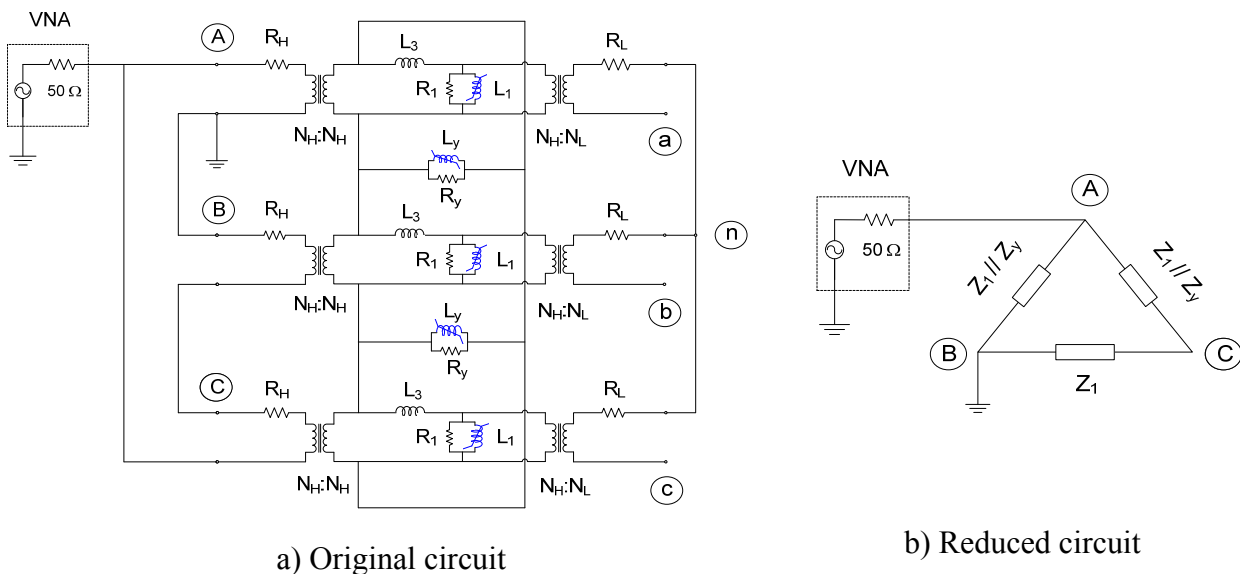


Figure 3.17: Equivalent and reduced measuring circuit in context of an open-circuit input impedance measured at the delta winding side of the Dyn5 transformer

After the reduced circuit is obtained, it is easy to calculate equivalent terminal impedances in accordance with measurement configuration. Similarly to analysis of measurements on the star winding, there are also nine measurement configurations conducted on the delta winding, but the calculated equivalent impedances are quite different shown in Table 3.9.

Table 3.9: Measurement configurations and corresponding calculated equivalent impedances for delta windings at low frequencies (secondary winding has no influence)

Index	Configuration	Calculated equivalent impedance
1	A-B excited (in Figure 3.17b)	$(\underline{Z}_1 // \underline{Z}_y) // (\underline{Z}_1 // \underline{Z}_y + \underline{Z}_1)$
2	A-C excited	$(\underline{Z}_1 // \underline{Z}_y) // (\underline{Z}_1 // \underline{Z}_y + \underline{Z}_1)$
3	A-B excited, B-C shorted	$(\underline{Z}_1 // \underline{Z}_y) // (\underline{Z}_1 // \underline{Z}_y)$
4	B-C excited	$(\underline{Z}_1 // \underline{Z}_y + \underline{Z}_1 // \underline{Z}_y) // \underline{Z}_1$
5	B-A excited	$(\underline{Z}_1 // \underline{Z}_y) // (\underline{Z}_1 // \underline{Z}_y + \underline{Z}_1)$
6	B-C excited, C-A shorted	$\underline{Z}_1 // \underline{Z}_y // \underline{Z}_1$
7	C-A excited	$(\underline{Z}_1 // \underline{Z}_y) // (\underline{Z}_1 // \underline{Z}_y + \underline{Z}_1)$
8	C-B excited	$(\underline{Z}_1 // \underline{Z}_y + \underline{Z}_1 // \underline{Z}_y) // \underline{Z}_1$
9	C-A excited, A-B shorted	$\underline{Z}_1 // \underline{Z}_y // \underline{Z}_1$

The solver/algorithm in data fitting procedure for the star winding can be applied for measurement configurations in Table 3.9 since the only difference in analyses of the two winding types is the change of calculated equivalent impedances. In Table 3.9, there are four different calculated equivalent impedances, which suggest three following analysis modes to determine core impedances:

- Single phase mode - Mode #1 (number of analyzed configurations $n = 3$): only measurements excited at one phase terminal, e.g. three first configurations in Table 3.9, by the instrument are used as inputs for the solver.
- Distinguishable input mode: Mode #2 ($n = 4$): it includes four configurations whose corresponding equivalent impedances in Table 3.9, e.g. the 1st, 3rd, 4th and 9th index, are different.
- Full input mode - Mode #3 ($n = 9$): this mode consists of all measurement configurations. It is generally considered as the best one since it takes into account the differences of measured impedances between configurations whose calculated equivalent impedances are identical.

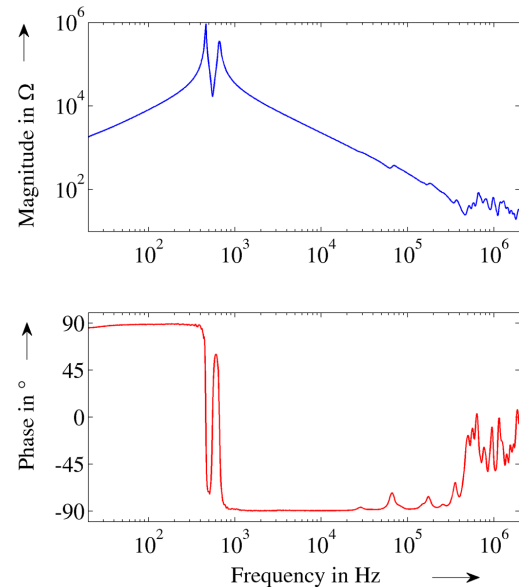


Figure 3.18: Frequency response of open-circuit input impedance of the first configuration in Table 3.9

Depending on which mode is selected, core impedances (\underline{Z}_1 and \underline{Z}_y) at low frequencies from 20 Hz to a frequency where inductive effect is best found, around 60 Hz in this case, are then calculated. In Figure 3.18 the purest inductive

impedance is within 100 Hz to 200 Hz, but due to influence of large capacitance, the value of 60 Hz is selected for analysis. Table 3.10 presents the magnitude errors for comparison.

Table 3.10: Percentage impedance magnitude error for three analyzed modes

Index	Configuration	Magnitude error, in %		
		Mode #1	Mode #2	Mode #3
1	A-B excited (in Figure 3.17b)	1.2	1.0	1.4
2	A-C excited	1.4	1.7	1.2
3	A-B excited, B-C shorted	0.2	3.3	2.5
4	B-C excited	8.3	1.5	2.8
5	B-A excited	0.9	0.6	1.0
6	B-C excited, C-A shorted	4.0	5.8	5.8
7	C-A excited	1.9	2.2	1.8
8	C-B excited	6.3	1.6	1.9
9	C-A excited, A-B shorted	1.3	4.4	3.8

A quick conclusion can be drawn from Table 3.10 is that due to lower impedance errors as compared with Mode #1, both Mode #2 and #3 can be applied to determine the core impedances (Mode #2 and #3 have highest errors of 5.8 %, compared with 8.3 % in Mode #1). However, the Mode #3 is selected as the best as mentioned since the corresponding impedance errors have a more uniform distribution.

Conclusion

The rule of thumb for successful analysis of core impedance from the measurements on the delta winding will be:

- Build the reduced circuit from the original equivalent one with appearance of only core impedances
- Analyze the full input mode
- Use (3.8) to fit data

It is noted that the rule of thumb is also appropriate for analysis of core impedances referred into the delta winding side of other transformers, e.g. the LV side of the YNd5 transformer (T_3). Furthermore, due to the fact that the rules for analysis at the star and delta winding side are actually identical whenever the equivalent circuit is achieved, it can be concluded that a general solution for determination of core impedances referred into star or delta winding side based on non-destructive measurements is now identified.

3.4.2 Formula-based approach to determine core impedances at high frequencies

To calculate core impedances at high frequencies, only analytical formulae will be based since the core effect cannot be recognized from any measurement at such frequencies. In addition, several magnetic and design parameters of transformers should be also available so that the formula-based calculation is possible. Among the test transformers, the T_1 one is opened, thus the

required parameters can be approximately derived²¹. As a result, the core leg impedances \underline{Z}_l of the transformer T_1 at high frequencies could be calculated, which enables the determination of the core yoke impedances \underline{Z}_y of the transformer as well as core impedances of other test transformers (T_2 and T_3) via a new solution proposed in chapter 4.

Fundamental background for analysis of core impedances in high frequency range is the understanding of phenomena taking place in transformer core laminations under certain applied field. In the scope of this dissertation, low AC field is applied for the measurements in broad frequency range and therefore it is only worth to analyze phenomena in transformer core under such condition.

3.4.2.1 Phenomena in transformer core under low applied field

Transformer core consists of numerous elements called as laminations or sheets made from steel and electrically isolated and stacked by means of glue (for small transformers) or steel straps/epoxy-cured stocking (for large power transformer). Below are several specifications of materials which are often found in core steel [ABB-07]:

- Core steel has low carbon content ($< 0.1\%$) which relates to hysteresis losses and ageing properties.
- Core steel is alloyed with Silicon whose content is normally kept lower than 3% for reducing the eddy current losses. (Grain-oriented steel is preferred for manufacturing transformer core lamination today since the magnetic flux density is increased about 30% in the coil rolling direction compared with non-oriented steel)

There are three fundamental phenomena contributing to the losses in transformer core: skin effect due to eddy current in laminations, hysteresis and anomalous mechanisms. However, the losses, as well as the magnetic properties, are different depending on the amplitude of applied field since the core laminations have non-linear and saturation effects; thus the three phenomena are only explained in the direction of low applied field:

- Eddy current (skin effect): It is a main effect caused by low alternating magnetic field in conductors such as windings and core laminations in transformers. For core laminations, when such magnetic field generated by alternating source penetrates a ferromagnetic material, induced circulating current loops appear and are called as eddy currents whose density has a non-linear distribution depending on frequency of the magnetic field shown in Figure 3.19. As a result, a non-linear distribution of magnetic flux (towards the surface) is associated. This phenomenon results in the eddy current loss which brings a rise of effective resistance and a reduction of inductance when frequency increases [Abeywickrama-07, Lammeraner-66]. Eddy current loss is proportional to the square of lamination thickness, square of frequency and square of effective value of flux density [Kulkarni-04]:

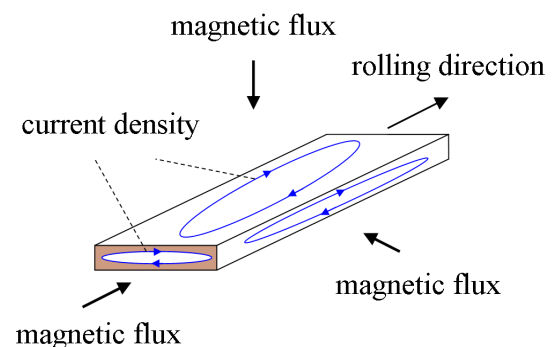


Figure 3.19: Skin effect in a core lamination

²¹ Design data of the transformer T_2 and T_3 were not available at the analysis time

$$P_e = k_1 f^2 t_0^2 B_{\text{rms}}^2 \quad (3.12)$$

where P_e : eddy current loss in the core
 k_1 : constant depending on material
 t_0 : thickness of individual lamination
 B_{rms} : flux density corresponding to the actual RMS sinusoidal voltage

- Hysteresis phenomenon:** It is a characteristic of a magnetic material to retain magnetization or to oppose a change in magnetization, which depends on applied magnetic field magnitude. When a low field is applied, there is reversible change in domain magnetic structures which causes the magnetization returns to its initial value on removal of the external magnetic field. As field strength is high enough for the so-called magnetic domain wall motion, both reversible and irreversible processes take place illustrated in Figure 3.20 so that the magnetization does not return to its original value on applied field removal [Littmann-70].

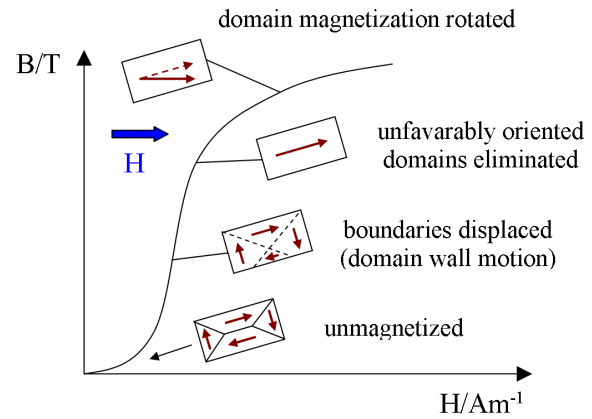


Figure 3.20: Changes of domain structure during magnetization at high field [Littmann-70]

- In case applied field is cyclic and its magnitude is high enough, there exists a hysteresis (B-H) loop. The relevant loss is proportional to the area of the B-H loop, i.e. to the magnetic material, frequency and exponential function of actual peak of flux density [Kulkarni-04]. However, under a low applied field for FRA measurements (~ 1 V), the corresponding hysteresis loop is a small elliptical loop whose area is very small depicted in Figure 3.21; therefore, hysteresis loss is considered insignificant compared with eddy current loss at high frequencies [Abeywickrama-07].

- Anomalous losses:** There exists another complicated phenomenon in the core which is called as diffusion effect in the crystal grid (domain structures) of the core material causing anomalous losses [ABB-07]. In short, this phenomenon contributes to an additional loss coming from skin effect when the reaction of eddy currents on the distribution of magnetic field (domain wall motion effects) is taken into account. That means the real magnetic flux density is not uniform over the cross-sectional area of core laminations as it would be assumed in calculating classical eddy current loss as plotted in Figure 3.22 [Zhu-93]. The losses are significant when transformers have load at power frequency [Brailford-64].

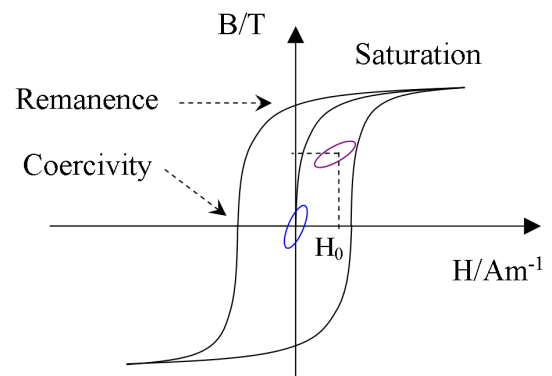


Figure 3.21: Changes of domain structure during magnetization at high field [Abeywickrama-07]

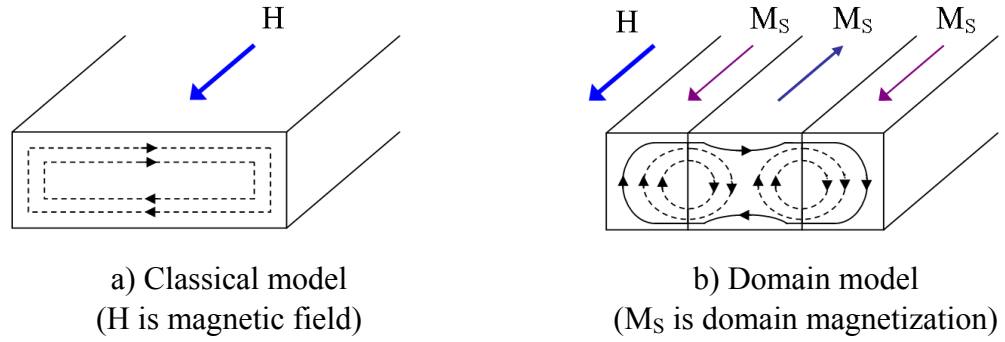


Figure 3.22: Eddy current in a core lamination in two cases [Zhu-93]

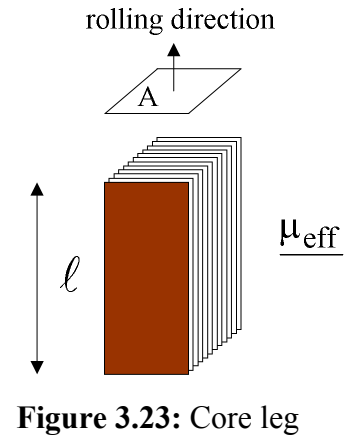
Conclusion: Under low field and no-load conditions, the (classical) skin effect has most influence whereas other phenomena can be neglected [Abeywickrama-07]. From that, core impedances are determined based on relevant experimental formulae.

3.4.2.2 Calculation of core impedances based on skin effect

a) *Magnetic reluctance:* Figure 3.23 shows a core leg section of the transformer T_1 for analysis at high frequencies due to availability of relevant magnetic and design data. First of all, the reluctance of the core section in the magnetic circuit representing a relation between the magnetomotive force F and corresponding flux Φ should be determined as [Cherry-49]:

$$\mathfrak{R} = \frac{F}{\Phi} = \frac{\ell}{\underline{\mu}_{\text{eff}} \mu_0 A_{\text{cr}}} \quad (3.13)$$

where ℓ : magnetic flux path length of the core section
 $\underline{\mu}_{\text{eff}}$: complex effective relative permeability of core lamination in rolling direction
 μ_0 : permeability constant of free space ($4\pi \times 10^{-7}$ H/m)
 A_{cr} : cross-sectional area of the core section



The complex effective relative permeability $\underline{\mu}_{\text{eff}}$ in the rolling direction of the magnetic flux, i.e. along the core section, is expressed as [Abeywickrama-07, Shintemirov-10b]:

$$\underline{\mu}_{\text{eff}} = \mu'_{\text{eff}} - j\mu''_{\text{eff}} = k_{\text{fe}} \mu_r \frac{\tanh\{(1+j)b_o/\delta\}}{(1+j)b_o/\delta} \quad (3.14)$$

where k_{fe} : stacking factor representing fraction of core steel in the total cross section
 μ_r : local relative permeability in the rolling direction
 b_o : half of a lamination thickness
 δ : skin depth or depth of penetration of eddy currents

The skin depth δ is frequency dependent and calculated as [Lammeraner-66]:

$$\delta = \sqrt{2/(\omega\sigma\mu_0\mu_r)} \quad (3.15)$$

where ω : angular frequency
 σ : electrical conductivity of the core lamination

b) *Dual electrical impedance*: The complex reluctance \mathfrak{R} accounting for skin effect has a dual electrical impedance \underline{Z} whose equivalent circuit consists of a resistance (R_s) in series with an inductance (L_s) [Cherry-49, Roger-06]:

$$\underline{Z} = j\omega N^2 \frac{1}{\underline{\mathfrak{R}}} \equiv R_s + j\omega L_s \quad (3.16)$$

where N : number of turns of the excited winding on the phase of the core section

From that, the resistance R_s (Ω) and inductance L_s (H) can be determined as:

$$R_s = -\omega N^2 \operatorname{Im}\{1/\underline{\mathfrak{R}}\} \quad (3.17)$$

$$L_s = N^2 \operatorname{Re}\{1/\underline{\mathfrak{R}}\} \quad (3.18)$$

Due to the fact that the equivalent electrical circuit of a core section includes only resistance and inductance in parallel, for instance \underline{Z}_1 consists of $R_1//L_1$, the R_s and L_s should be converted into R_p and L_p respectively for use.

3.4.2.3 Frequency dependency of core impedances in broad frequency range

The combination between measurement- and formula-based core components (resistances, inductances) in low and high frequency range respectively introduces the complete frequency dependency of core electrical parameters. Since the calculated core resistances and inductances are not available until now, part of the new approach in calculation of core electrical parameters of the transformer T_1 and also other transformers (T_2 , T_3) will be presented in the next chapter where results from measurements are shown in detail.

3.5 Capacitive input impedance tests and winding capacitances

There are in general three fundamental capacitances in power transformers in the view point of diagnostic and analysis at low and mid frequencies:

- Ground (or shunt) capacitance: the capacitance is defined between the windings and ground potential such as tank (to outer winding) and core (inner winding).
- Series winding capacitance: the “self” capacitance of the winding between turns and between discs (or layers). This capacitance depends only on the winding itself.
- Inter-winding capacitance: the capacitance between windings such as between HV and LV windings or between HV and HV windings (if the HV windings are outer ones).

Of those capacitances, only the *total* ground and inter-winding HV-LV capacitance can be measured by means of testing devices such as the CPC 100 of Omicron as mentioned in chapter 1. The concept of “total capacitance” means capacitances of three single phase windings are included since single phase winding capacitances can not be measured separately with enough accuracy. However, due to the fact that the universal testing device is not always available onsite for the measurements and more importantly, the capacitance measurement requires a high applied voltage (e.g. 10 kV), which is considered as a destructive measurement method for transformers having very aged insulation system since the high applied voltage can damage the insulation, real non-destructive alternative is requested for such case. That is the motivation for

introduction of a new approach in this section for determination of the total ground and inter-winding capacitance.

To illustrate the winding capacitances in transformer bulk under per-phase and total quantities for analysis, the duality based equivalent circuit of the YNyn6 transformer (T_1) at balanced excitation and its corresponding capacitance model are again depicted in Figures 3.24a and 3.24b respectively. One can easily observe that the total capacitances, e.g. C_{HG} , combine three corresponding per-phase quantities, i.e. C_{gH} , since the HV terminals (A, B, C, N) and LV terminals (a, b, c, n) are inter-phase connected. Note that the model in Figure 3.24b is always correct and does not depend on winding connection since all terminals of a three-phase winding are connected together.

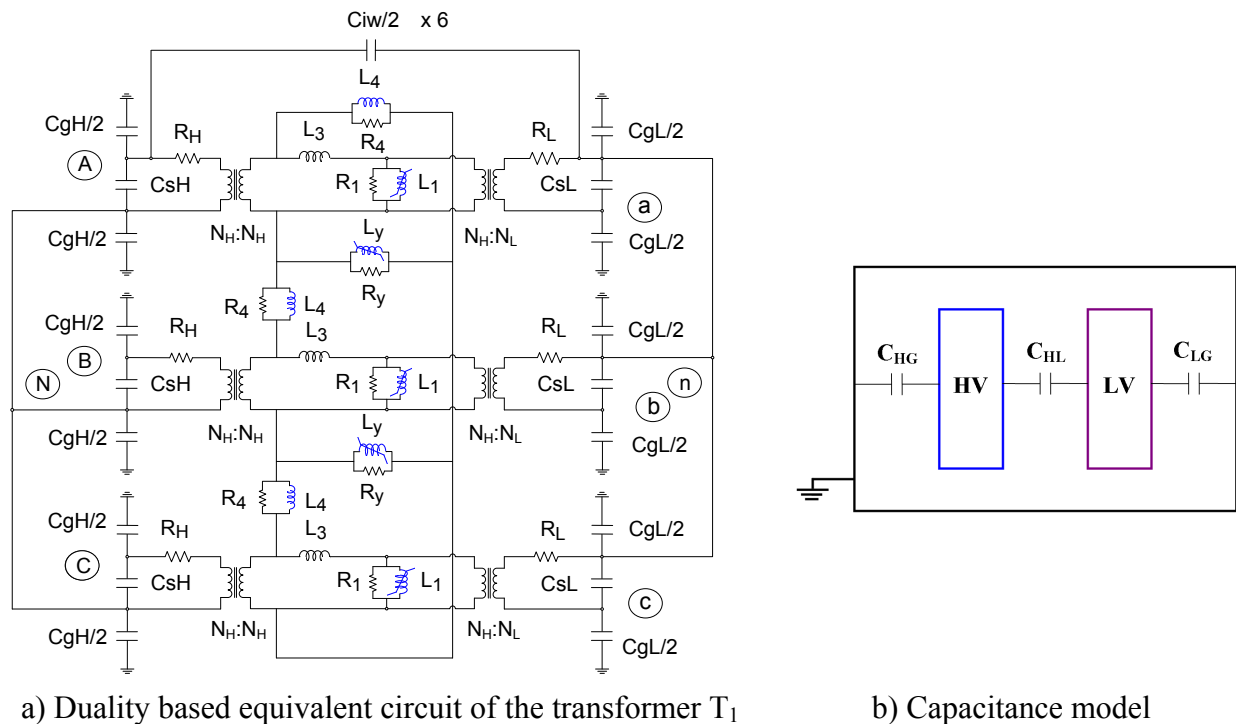


Figure 3.24: Equivalent and reduced measuring circuit in context of an open-circuit input impedance measured at the delta winding side of the Dyn5 transformer

The idea to calculate capacitances in Figure 3.24b is based on the fact that there are two ungrounded terminals “HV” and “LV”, and thus there are four different combinations of excitation in the measurement with the VNA. The four measurement configurations are shown in Table 3.11.

Table 3.11: Measurement configurations of capacitive input impedance

Index	Configuration	Equivalent capacitance
1	HV excited, LV shorted	$C_1 = C_{HG} // (C_{HL} \text{ series } C_{LG})$
2	HV excited, LV shorted and grounded	$C_2 = C_{HG} // C_{HL}$
3	HV shorted, LV excited	$C_3 = C_{LG} // (C_{HL} \text{ series } C_{HG})$
4	HV shorted and grounded, LV excited	$C_4 = C_{LG} // C_{HL}$

In order to find the capacitances C_{HG} , C_{LG} and C_{HL} , the equivalent capacitances C_1 , C_2 , C_3 , and C_4 in four measurement configurations in Table 3.11 should be identified in advance. In Figure 3.25a, observation of an impedance measured according to the second configuration in Table 3.11 shows that there is a short frequency range within which the pure capacitive character of the measured impedance is recognized in the direction of increase of frequency. By using the calculation illustrated in Figure 3.25b, the equivalent capacitance C is evaluated (ω_1 and ω_2 are boundaries of the frequency range).

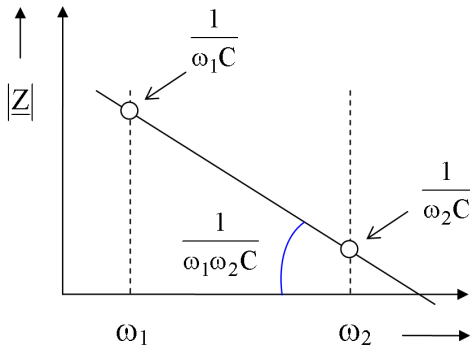


Figure 3.25b: Extract capacitance from a measured capacitive impedance in a frequency range

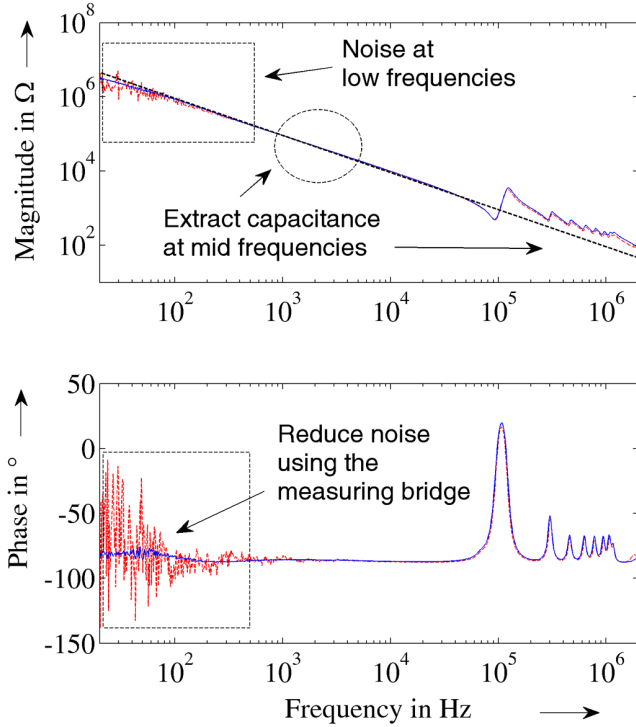


Figure 3.25a: A measured capacitive input impedance

It is important to mention that there might be more than one local frequency range where the pure capacitive character of the measured impedance is observed (see the phase angle of the measured impedance in Figure 3.25a); however, only the analysis in the first lowest range (before the first resonance takes place) is valid since the equivalent capacitances calculated in other ranges are lower than that calculated in the first frequency range. The differences between them are due to effect of total inductance as compensations.

Besides, the measurements on small transformers with low capacitances require the large dynamic range of the measuring device, e.g. a total capacitance of 1 nF requires approximately a dynamic range of:

$$Z \approx \frac{1}{2\pi \cdot 50 \cdot 10^{-9}} \approx 3.18 \text{ (M}\Omega\text{)} \quad (3.19)$$

at power frequency from the instrument to measure correctly, otherwise noise appears as shown in Figure 3.25a. Since the VNA used for investigation can measure impedances from 1 Ω till a few hundreds kΩ, a measurement bridge introduced in Figure 3.26 is used to extend the dynamic range of the instrument to several MΩ. Details on noise in measurements and how to improve

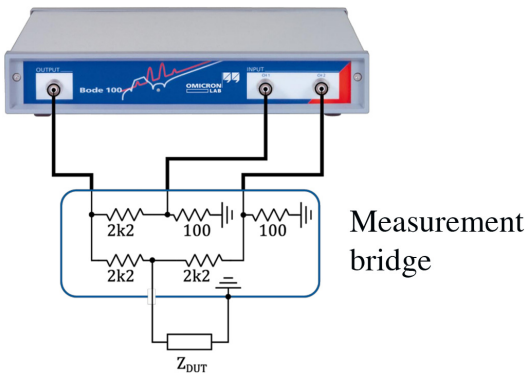


Figure 3.26: Measurement bridge to extend measuring range [Bode100-12]

the measurement accuracy in terms of noise, denoising and the measurement bridge are introduced in [Velasquez-09, Pham-11, Bode100-12].

Once the equivalent capacitances in Table 3.11 are calculated, the capacitances C_{HG} , C_{LG} and C_{HL} are easily to be determined based on following equations:

$$C_{HL} = \frac{C_{HL_1} + C_{HL_2}}{2} \equiv \frac{\sqrt{C_2(C_4 - C_3)} + \sqrt{C_4(C_2 - C_1)}}{2} \quad (3.20)$$

$$C_{HG} = C_2 - C_{HL} \quad (3.21)$$

$$C_{LG} = C_4 - C_{HL} \quad (3.22)$$

The C_{HL} calculated as average of the C_{HL_1} and C_{HL_2} is due to the fact that there are four equations but three variables in Table 3.11. The results are consistent if the C_{HL_1} and C_{HL_2} are near each other, which is often achieved in general when the selected frequency range is purest capacitive.

3.6 Circuit simulation for determining winding series capacitance and FRA interpretation

Now the duality based equivalent circuit with almost available components (i.e. frequency dependences of inductive impedances in broad frequency range and constant capacitances), except the winding series capacitances, can be used to simulate different standard and non-standard frequency responses by means of a commercial circuit simulation software for two purposes:

- To check whether the winding series capacitances have significant contribution to the total capacitance at mid frequency range and if it is the case, the series capacitances should be identified for the diagnostic purpose.
- To interpret frequency responses in terms of individual parameters by simulation until mid frequency range (FRA interpretation). Recall that the simulation is only valid in general in low and mid frequency range due to the limitation of the equivalent circuit explained in chapter 2.

The winding series capacitance is considered very important for different research activities: transient analysis, FRA, failure diagnostic etc. In state-of-the-art transient analysis, the winding series capacitance is often to be ignored since it cannot be identified and therefore in some cases in which the series capacitance should be taken into account, e.g. for transformers with high winding series capacitance (i.e. the winding type of multi-layer or inter-leaved), the fact that the series capacitance is missing in the analysis leads to unacceptable results. In addition, it is expected that the series capacitance is of great importance in diagnosing mechanical failures in transformer windings since it is a measure of how the windings change mechanically which can not be easily detected by other parameters. Thus it could be stated that the solution in determination of the winding series capacitance in transformer bulk, which is the third new approach presented in the dissertation, contributes to a great improvement to the above-mentioned research activities.

The new approach that determines the winding series capacitance in transformer bulk is based on the difference between measured and simulated non-standard open-circuit frequency responses at mid frequencies where the total capacitance of the transformer windings is dominant. In cases

there is no difference between the frequency responses at such frequencies, the winding series capacitance is not significant compared to other capacitances (ground, inter-winding); therefore it is not necessary (and also not possible) to evaluate this low series capacitance: it is the case for transformers T_1 (at HV side) shown in Figure 3.27a and T_3 (at LV side). In other cases the difference is obviously recognized, transformer T_2 (at HV side) shown in Figure 3.27b and transformer T_3 (at HV side), an appropriate value of the winding series capacitance which compensates the difference is reached via simulation attempts.

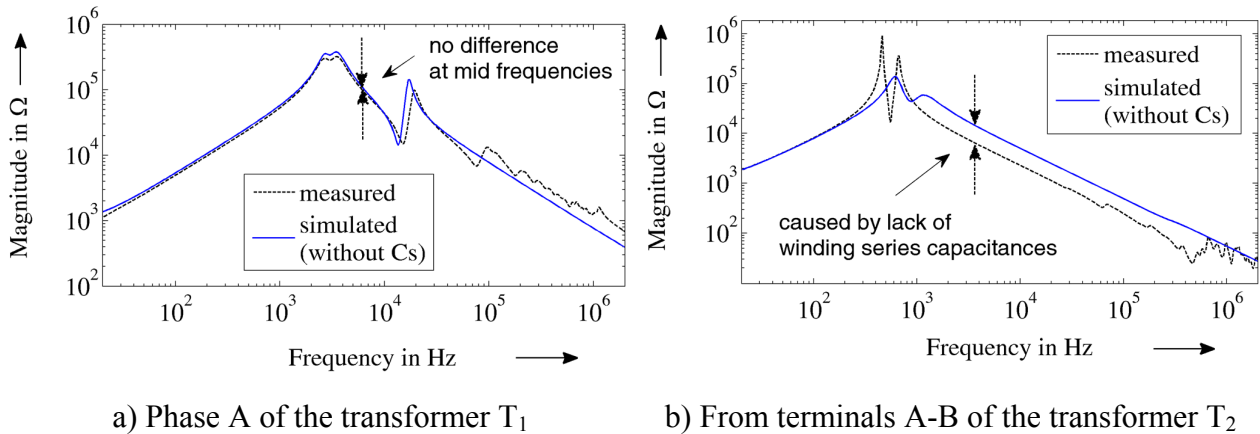


Figure 3.27: Measured and simulated open-circuit frequency responses in broad frequency range

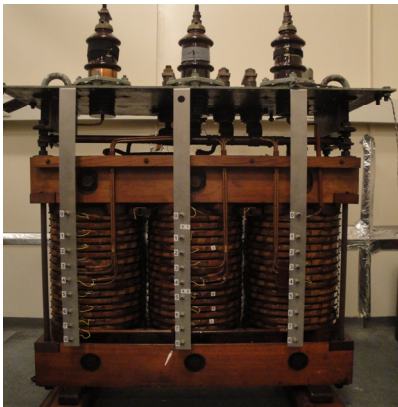
Details on the parameterization, circuit simulation and the way to identify the winding series capacitance will be presented in accordance with test transformers in next chapters since in this chapter, only the methodology is illustrated. Although the new method is applied on three small, medium and large distribution transformers, it is expected that the method is still valid for other larger power transformers since the fundamental background of the method, the duality based equivalent circuit, is confirmed efficient in FRA investigation of, for instance, large power auto transformers (1000 MVA 400/275 kV) in low frequency range [Ang-08].

4 Case study I: A 200 kA 10.4/0.462 kV YNyn6 transformer (T_1)

In this chapter, application of the new proposed method mentioned in chapter 3 on the transformer T_1 will be presented in detail. Since the transformer has no tank and is already opened, following key research activities are conducted:

- Calculation of frequency dependency of core leg impedances thanks to a few magnetic and transformer design data. More importantly, the frequency dependency of the core leg of the transformer T_1 then will be used to develop a solution from which frequency dependency of core section impedances of any transformer can be reached relatively at high frequencies. Recall that the development of frequency dependency of core impedances enables the simulation for FRA interpretation purpose in broad frequency range.
- Comparison of the conventional and proposed diagnostic method in diagnostic of several popular electrical failures in transformer windings, (e.g. shorted turns, short-to-ground, open-circuited) and the core (ungrounded core).
- Comparison of the conventional and proposed diagnostic method in diagnostic of several mechanical failures in transformer windings such as axial and radial deformations.

The transformer T_1 shown in Figure 4.1 was originally a Yz5 three-winding transformer, which was not an appropriate object to conduct above-mentioned investigations. In order to facilitate the research activities, the original transformer should be adapted into the YNyn6 one since the two-winding transformer should be first investigated to check the possibility of overcoming the limitations of the current diagnostic methods mentioned in chapter 1 in diagnosing electrical/mechanical failures in the transformer active part. Therefore the first part of the chapter is devoted for introducing the transformer and how to adapt it into a suitable test object for investigations.



Parameter	Value		Unit
Rated power	200		kVA
Rated voltages	10.4/10/9.6	0.4	kV
Rated currents	11.5	289	A
Vector group	Yz5		
Frequency	50		Hz
Rated short-circuit voltage	3.8		%
Year	1955		

Figure 4.1: Appearance of the transformer T_1 and its name-plate data

4.1 Adaptation of the transformer T_1 for research compatibility

The original transformer T_1 is a small distribution Yz5 10.4/0.4 kV one fixed at the first tap changer level, which is found often in the distribution network in Germany. It has three windings: a star winding at HV side (W_1 , W_2 and W_3), zig (W_7 , W_8 and W_9) and zag (W_4 , W_5 and W_6) winding at LV side shown in Figure 4.2.

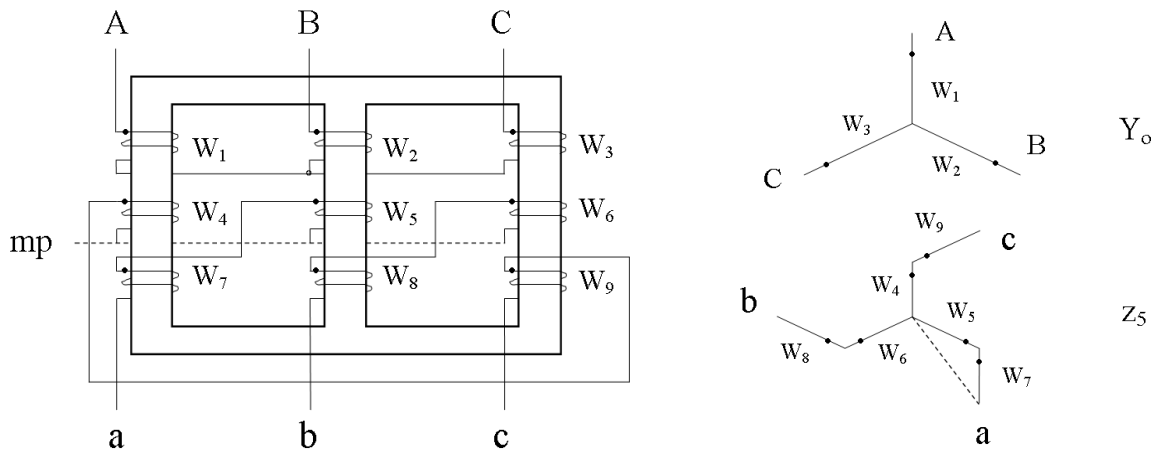


Figure 4.2: Winding connection of the original transformer T_1

There are several possibilities to convert the vector group of the original transformer by changing the connections between leads of the LV windings itself, i.e. the “zig” and “zag”, and from the LV winding to the bushings. For the simplest adaptation, the zigzag winding is changed into a single star or delta three-phase winding, i.e. the new vector groups are YNyn6 and YNd5 respectively. However, only the YNyn6 vector group depicted in Figure 4.3 is necessary for the research because of the availability of the YNd5 transformer T_3 as test object. The adapted transformer has an increase of rated voltage at LV side, 0.462 kV compared with 0.4 kV since there the zigzag winding has 15.47 % more turns compared to an ordinary winding at the same rated voltage; thus the factor for voltage modification is 1.1547 [Kulkarni-04].

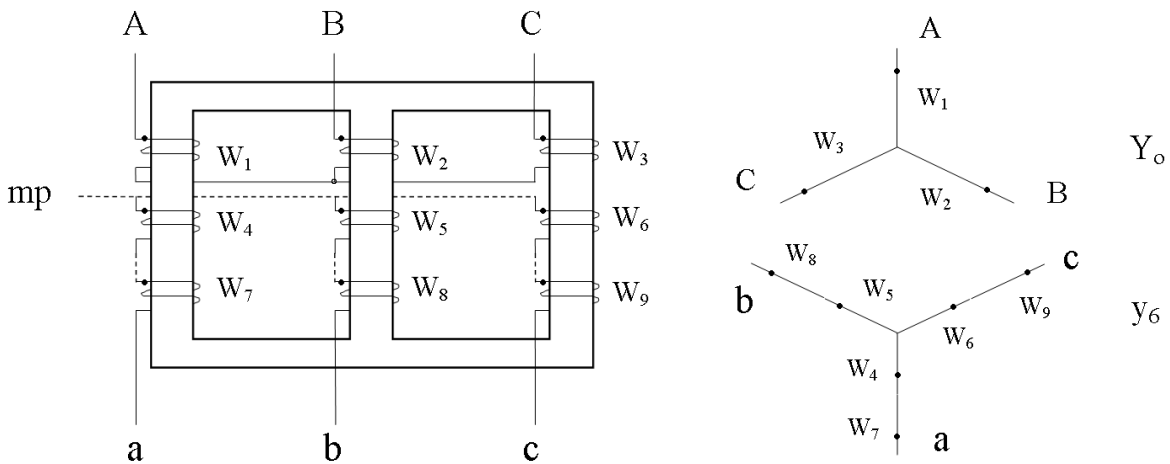


Figure 4.3: Winding connection of the adapted YNyn6 transformer

According to Figure 4.3, the duality based equivalent circuit of the YNyn6 transformer in accordance with its vector group for analysis of electrical parameters referred into the HV star winding with regard to different input impedance measurements is depicted in Figure 4.4.

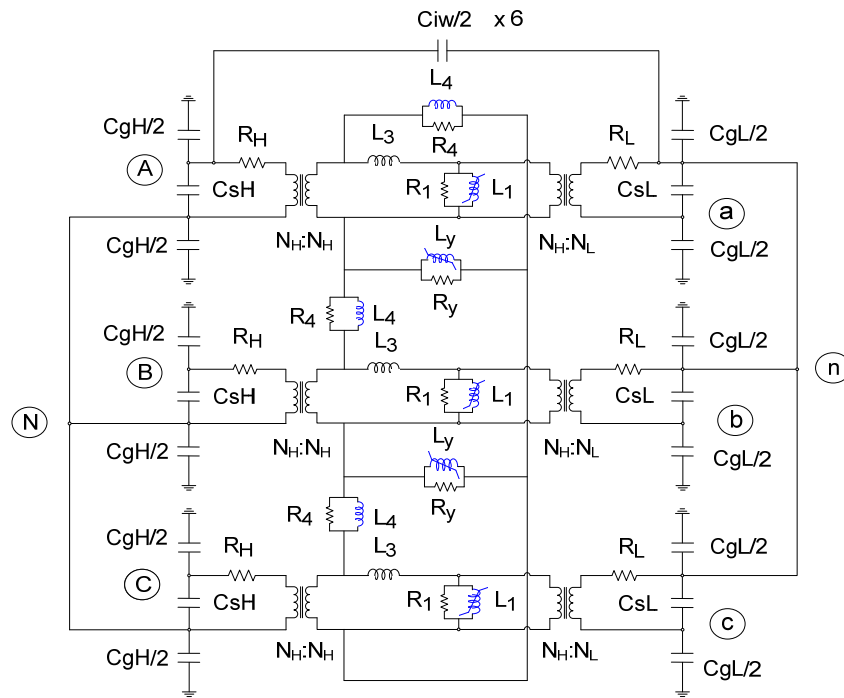


Figure 4.4: Duality based equivalent circuit of the transformer T_1 for balanced analysis at HV side

4.2 Application of the new method in determination of electrical parameters referred into the HV star winding

Overview of the electrical parameters of power transformers, together with corresponding measurements proposed in the new method in chapter 3, is here recalled since they are considered as fundamental background for the calculation in this chapter:

- Per-phase winding or total stray loss resistances and leakage inductances (from short-circuit input impedance test)
- Zero-sequence impedance (from zero-sequence input impedance test)
- Core section impedances (from open-circuit input impedance tests)
- Ground and inter-winding HV-LV capacitance (from capacitive input impedance tests)

Most of the above-mentioned inductive components (resistance, inductance) are frequency dependent. At low frequencies, they are only determined from the measurements and, together with ground and inter-winding winding capacitances, they will be applied directly for the diagnostic purpose; at high frequencies, they could be approximately calculated based on analytical formulae, which is meaningful for the simulation-based FRA interpretation in broad frequency range. The simulation approach is also useful in determining the contribution of the series winding capacitance to the total capacitance interacting with core inductance (at low frequencies) and zero-sequence/leakage inductance (at mid frequencies).

Now the electrical parameters of the transformer T_1 referred into the HV star winding will be calculated and presented in next sub sections. Note that only the HV side of the test transformer is analyzed since several input impedances at LV side cannot be measured correctly because they are lower than the measuring range of the VNA.

4.2.1 Per-phase winding resistances and leakage inductances

Figure 4.5 shows the input impedance measured on phase A at HV side of the test transformer as a typical measurement result for determining the low frequency range within it the electrical parameters can be reliably calculated. It is concluded from Figure 4.5 that the frequency range from 20 Hz to 10 kHz is the appropriate one for extracting the total resistance representing stray losses and leakage inductance from real and imaginary part of the measured impedance.

To achieve the frequency dependency of the stray loss represented resistance (or winding resistance), it is realized through the fitting procedure that the two-term power function is the best one since it not only represents the skin effect at high frequencies but also fits the measured values at low frequencies. The same achievement with the rational function for representing leakage inductance can be found in both low and high frequency range.

The fitting performances of the two-term power and rational function with regard to total resistance and leakage inductance respectively are shown in Figure 4.6.

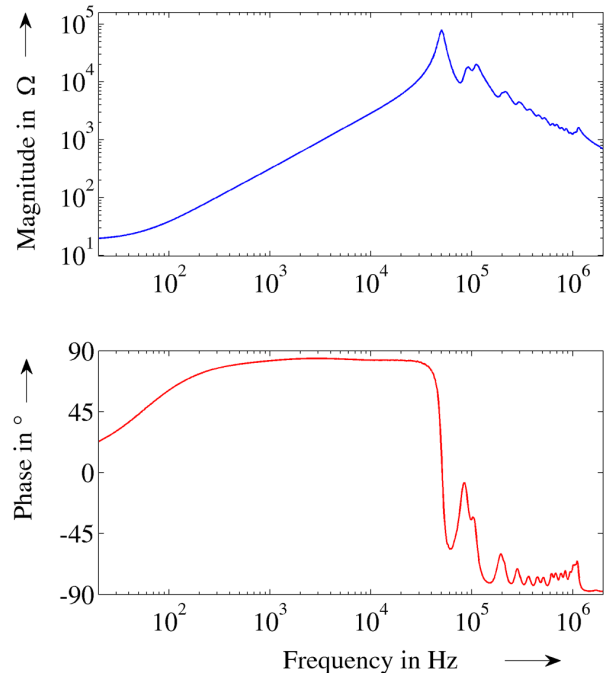
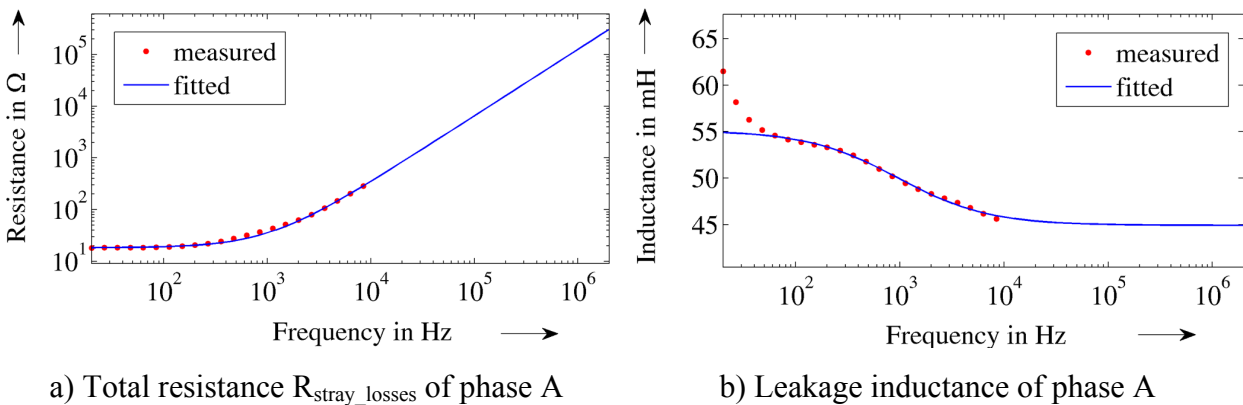


Figure 4.5: Frequency response of input impedance measured in the short-circuit test



a) Total resistance $R_{\text{stray_losses}}$ of phase A

b) Leakage inductance of phase A

Figure 4.6: Calculated values from measurement and fitted frequency dependencies

In Figure 4.6a, good agreement between measurement-calculated values and fitting functions at frequencies lower than 10 kHz shows that the two-term power function is efficient to represent the $R_{\text{stray_losses}}$, from which resistances of HV and LV windings can be calculated using rough factors. In Figure 4.6b, the fitting function of leakage inductance not only matches with calculated values at frequency range from 100 Hz to 10 kHz but also provides constant tendencies at other frequencies (lower than 100 Hz and higher than 10 kHz). The constant tendency at frequencies lower than 100 Hz is useful to adapt corresponding measured values in a correct way.

Table 4.1 compares leakage inductances of three phases between the conventional method measured by means of the CPC 100 device (named as CON) and the proposed method based on analysis of impedances (assigned as IMP) at low frequencies, from 20 Hz to 400 Hz. Low errors observed on three phases prove that the proposed method is efficient.

Table 4.1: Per-phase leakage inductance referred into HV side

Frequency in Hz	Leakage inductance, in mH								
	Phase A			Phase B			Phase C		
	CON	IMP	Error, in %	CON	IMP	Error, in %	CON	IMP	Error, in %
20	54.8	54.9	0.2	55.6	55.5	0.2	55.7	55.7	0
50	54.6	54.6	0	55.5	55.2	0.5	55.4	55.4	0
100	54.5	54.1	0.7	55.4	54.8	1.1	55.2	54.9	0.5
200	54.1	53.4	1.3	55.0	54.0	1.8	54.8	54.1	1.3
300	53.6	52.7	1.7	54.5	53.3	2.2	54.3	53.5	1.5
400	53.0	52.1	1.7	53.9	52.8	2.0	53.8	52.9	1.7

4.2.2 Zero-sequence inductance and resistance of the HV star winding

Figure 4.7 depicts the impedance measured from the open-circuit zero-sequence input impedance test at HV side of the test transformer. From Figure 4.7 the frequency range of 20 Hz to 3 kHz is selected to calculate the zero-sequence resistance and inductance from the measured impedance.

For zero-sequence resistances R_4 , the fitting function as a two-term power function of *logarithm scale* of frequency is chosen whereas for zero-sequence inductances L_4 , since it represents also the linear reluctance of non-magnetic material paths outside the windings, the fitting function for leakage inductances can be applied. Figure 4.8 plots fitted frequency dependent functions of zero-sequence components in wide frequency range, which yield good performances at low and high frequencies. Comparison of Figures 4.8b and 4.6b shows that the zero-sequence inductance is appreciably higher than the leakage one since the transformer has no tank which acts as shield to confine the zero-sequence flux paths.

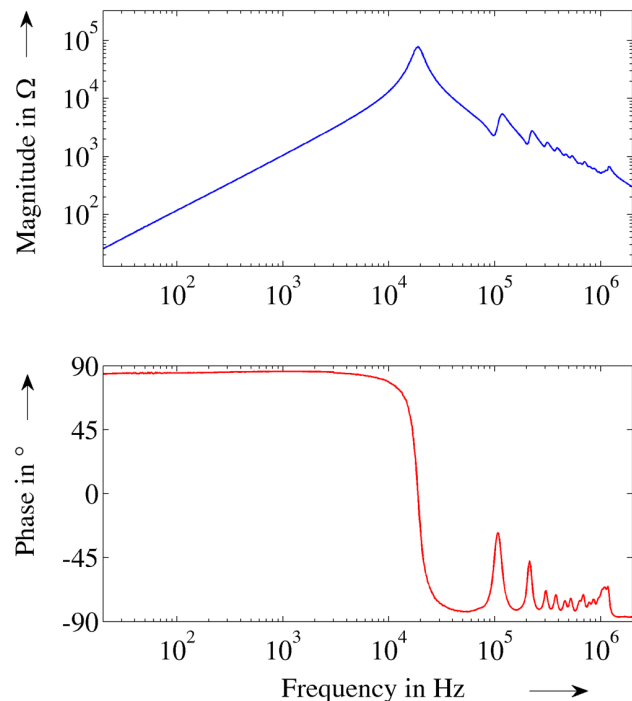


Figure 4.7: Frequency response of input impedance measured in the zero-sequence test

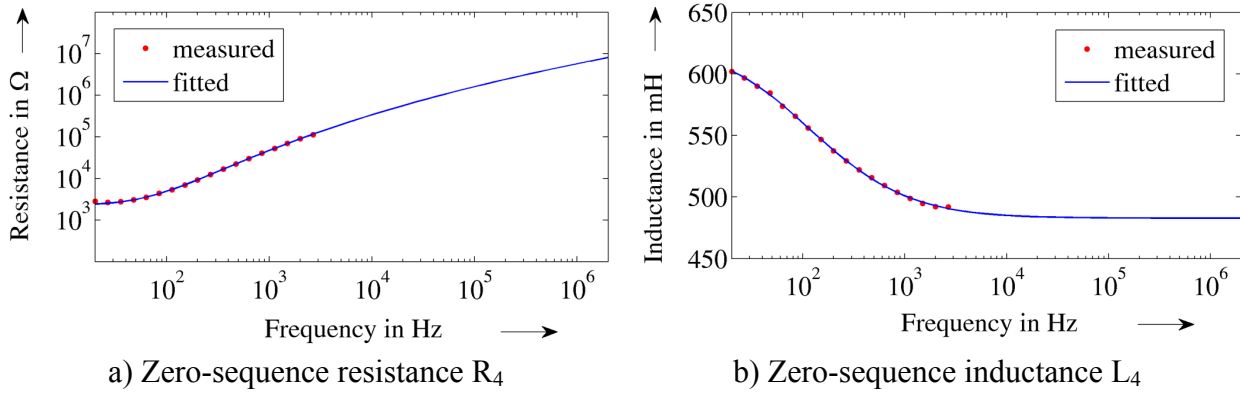


Figure 4.8: Calculated values from measurement and fitted frequency dependencies

Table 4.2 compares zero-sequence inductances measured from the conventional and proposed method at low frequencies from 20 Hz to 400 Hz. The average error is however higher than those calculated in the short-circuit tests, for instance 5.3 % (excluding the error of 11.4 % at 100 Hz) compared with 0.9 % calculated from leakage inductance errors of phase A, which means the proposed method is not so appropriate for determination of zero-sequence inductance/impedance in cases the transformer has *no* tank. It can be explained that in such cases the non-magnetic zero-sequence paths are between the windings and also in the space *outside* the transformer as depicted in Figures 3.9 and 3.10 in chapter 3, thus if the magnitude of the applied field in the measurements is too low, e.g. 1 V compared with tens or hundreds V in the conventional test, the distribution of flux, and therefore associated magnetic energy, in all zero-sequence paths is not fully proportional to those under high applied field. In case the transformer has a tank, the zero-sequence paths are limited within the transformer and the measurements under low applied field are quite reasonable. Concerning the largest error (11.4 %) between the two methods at 100 Hz, it is realized that the problem is from the conventional method whereas the results from the proposed method presents a good tendency of inductance versus frequency. Actually the measured inductance from the conventional method is abnormal but still acceptable since the non-magnetic dual electric-magnetic inductance is considered as constant with frequency. The abnormal value is recognized from the measurement report where the real current for the measurement (1.75 A) supplied automatically from the instrument CPC 100 is higher than the assigned one (1 A) at only this frequency.

Table 4.2: Open-circuit zero-sequence inductance of the star winding at HV side

Frequency in Hz	Zero-sequence inductance, in mH		
	CON	IMP	Error, in %
20	638.0	602.5	5.6
50	615.0	581.5	5.4
100	632.1	560.1	11.4
200	577.1	537.9	6.8
300	553.0	526.2	4.8
400	540.9	518.9	4.1

4.2.3 Core section inductances and resistances

4.2.3.1 From measurements at low frequencies (20 Hz to 400 Hz)

The core electrical parameters (\underline{Z}_1 , \underline{Z}_y) referred into the HV side of the transformer are determined based on analysis of the full input mode according to (3.8), taking into account the appearance of zero-sequence impedance, in the low frequency range from 20 Hz to 400 Hz.

Afterwards, the individual *parallel* components, i.e. resistances (R_1 , R_y) and inductances (L_1 , L_y) can be easily calculated from (4.1) and (4.2) and shown in Figure 4.9:

$$R = \frac{\left(\operatorname{Re}\{Z\}^2 + \operatorname{Im}\{Z\}^2\right)}{\operatorname{Re}\{Z\}} \quad (4.1)$$

$$L = \frac{\left(\operatorname{Re}\{Z\}^2 + \operatorname{Im}\{Z\}^2\right)}{\operatorname{Im}\{Z\}} \quad (4.2)$$

where R stands for R_1 (or R_y) and so on

The determined core electrical parameters R_1 , L_1 , R_y , L_y at low frequencies are then fitted to form frequency dependent functions, i.e. $R_1(f)$, $L_1(f)$, $R_y(f)$, $L_y(f)$, using fitting functions for circuit simulation application. Before the simulation is executed, the fitting functions are then checked analytically to see whether the functions are good enough to be exploited for the simulation. Figure 4.10 illustrates a comparison between the measurement result and the recovery from fits of the electrical parameters for an open-circuit input impedance calculated based on the analytical formulae in Table 3.3. Small errors from both magnitude and phase angle indicate the success of the analytical and fitting process which are required for the simulation later on.

4.2.3.2 From analytical formulae at high frequencies (400 Hz to 2 MHz)

Core electrical parameters can only be determined at high frequencies based on analytical formulae if several magnetic and design data are available. Since the transformer has no tank, the design data can be approximately measured whereas magnetic parameters of core lamination, which do not change much from transformer to transformer, in [Abeywickrama-07, Sintemirov-10] can be referred; these necessary parameters are

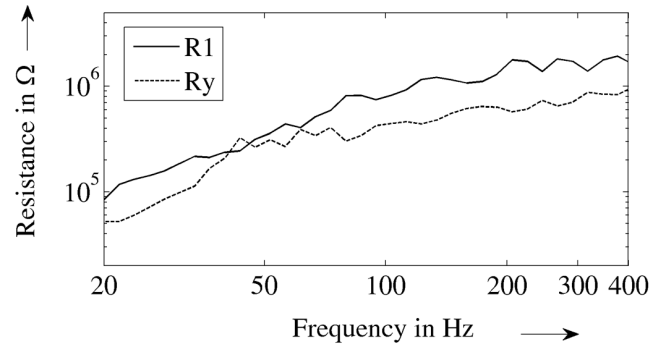


Figure 4.9a: Calculated core leg and yoke resistances

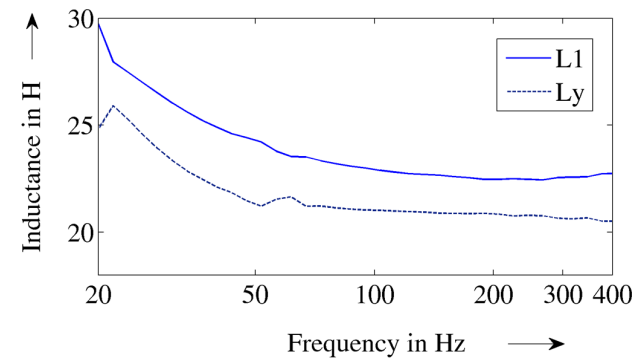


Figure 4.9b: Calculated core leg and yoke inductances

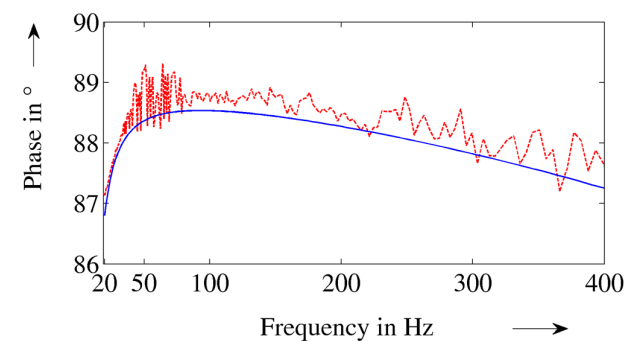
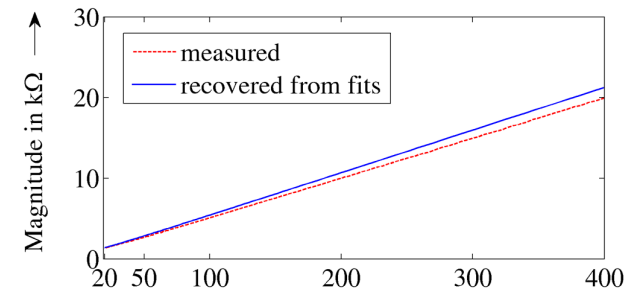


Figure 4.10: Measured and recovered frequency response of open-circuit input impedance observed at phase A at low frequencies

shown in Table 4.3. Afterwards, the core electrical parameters are derived from calculations in (3.14, 3.15) for R_S , L_S and then using (4.1, 4.2) to convert them into R_P , L_P respectively, see Figures 4.11 and 4.12.

Table 4.3: Necessary magnetic and design data for calculating core electrical parameters

Parameter	Description	Value
μ_0	permeability of free space	$4\pi \times 10^{-7}$ H/m
μ_r	relative permeability	500
σ	conductivity	5×10^6 S/m
t_0	lamination thickness	0.35×10^{-3} m
k_{fe}	stacking factor	0.92
ℓ	core section length	0.36 m
A	cross-sectional area of core section	25.6×10^{-3} m ²
N	number of turns	736 turns

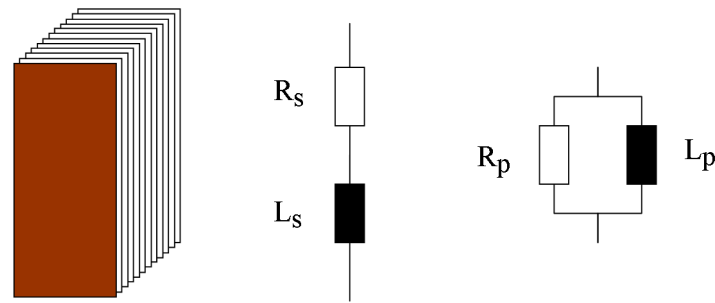


Figure 4.11: Core leg, its series and parallel model (from left to right respectively)

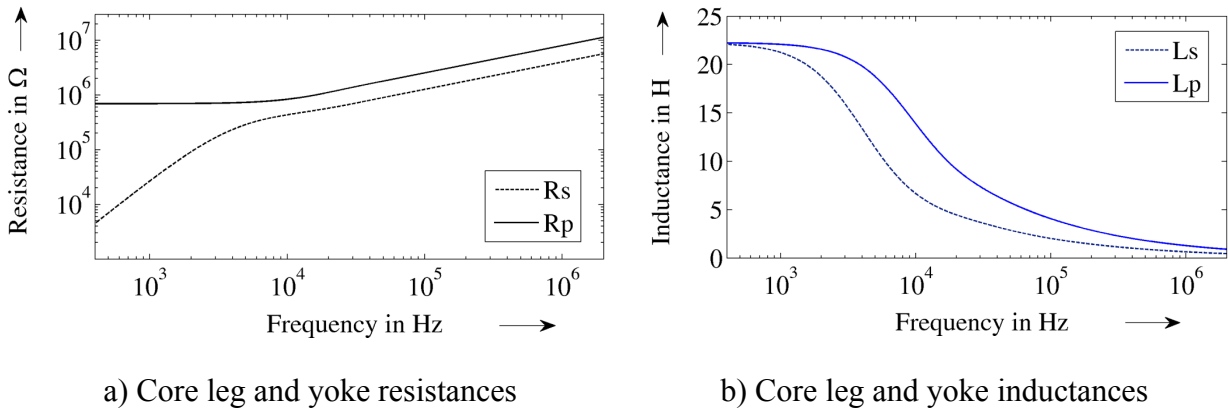


Figure 4.12: Frequency dependency of resistances and inductances of the core leg from 200 Hz to 2 MHz

From Figure 4.9b and 4.12b, a comparison between the measurement-based and formula-based components of the core leg at the *transition* frequency, i.e. 400 Hz in this case, shows that there is small error between L_1 and L_P , which indicates that the calculation of a core section based on skin effect is acceptable and therefore the results can be used at high frequencies. Error between R_1 and R_P at 400 Hz is much larger than that between the inductances but it has insignificant contribution to the terminal frequency responses since the resistances are too high (unit in $M\Omega$) and in parallel with the inductances in the circuit.

4.2.3.3 Frequency dependency of core electrical parameters in broad frequency range

By combining the frequency dependencies of the R_1 , L_1 (at low frequencies) and R_p , L_p (at high frequencies) at the transition frequency, frequency dependent functions of core leg resistance and inductance of the transformer T_1 are obtained. To be able to do so, the measurement-based values of the R_1 and L_1 at low frequencies should be available as frequency dependent functions since they are discrete values calculated from the open-circuit input impedance measurements. The fitting procedure is therefore necessary and has an advantage that the fitting functions will remove oscillations in the waveforms in Figure 4.9 (especially the curve R_1).

Figure 4.13 summaries Figures 4.9 and 4.12 in logarithm scale which yields the frequency dependencies of core parameters R_1 , L_1 (from measurements at low frequencies) and R_p , L_p (from analytical formulae at high frequencies) respectively in broad frequency range. Figure 4.13 also gives a valuable hint which helps to establish the calculation of frequency dependency of core section components of *any* transformer: “the value of core inductance calculated from the skin-based analytical formulae at the transition frequency (400 Hz²² in this case) is approximately equal the one calculated from the measurement at low frequencies”. Thus, for transformers whose design data are not available, the frequency dependent function of core electrical parameters at high frequencies can be calculated from their measurement-based values at the transition frequency and the *tendency* of parameter change at high frequencies. The tendency of parameter change can be obtained from the frequency dependent functions of the transformer T_1 by their normalization since the tendency which does not change much from transformer to transformer is more decidable, compared with design parameters, when frequency increases.

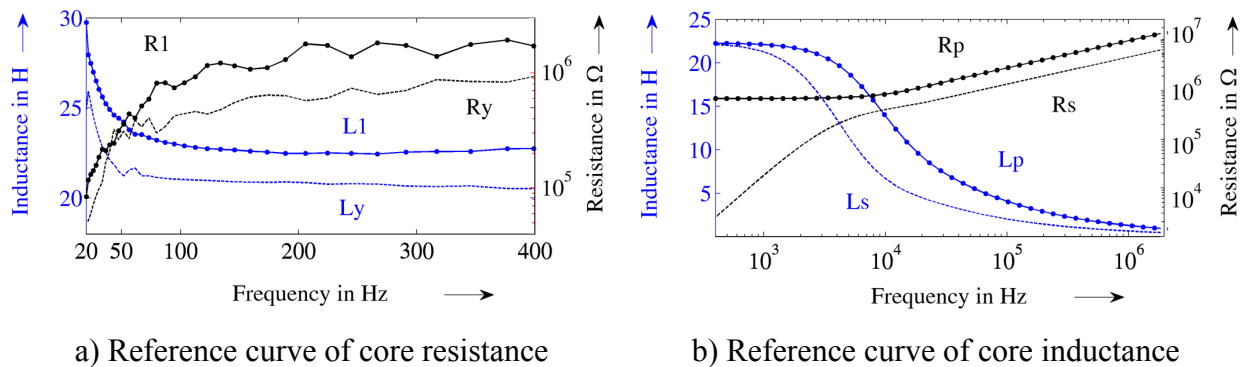


Figure 4.13: Tendencies of core electrical parameters at high frequencies

Figure 4.14 depicts the tendencies of core resistance and inductance of transformers derived after normalization, called as “reference curves”, which can be applied to calculate frequency dependencies of any transformer core section at high frequencies whenever the measurement values at the transition frequency are available. In Figure 4.14 the fitted functions of core resistance and inductance are also depicted since they will be exploited later on for application, not the calculated values. For application convenience, only one fitting function is required for each parameter and experience shows that the fitting function with regard to the *logarithmic scale* of frequency is the most appropriate one.

²² The transition frequency varies from transformer to transformer, depending on the interaction between core inductances and winding capacitances. It can be from several tens Hz to several kHz

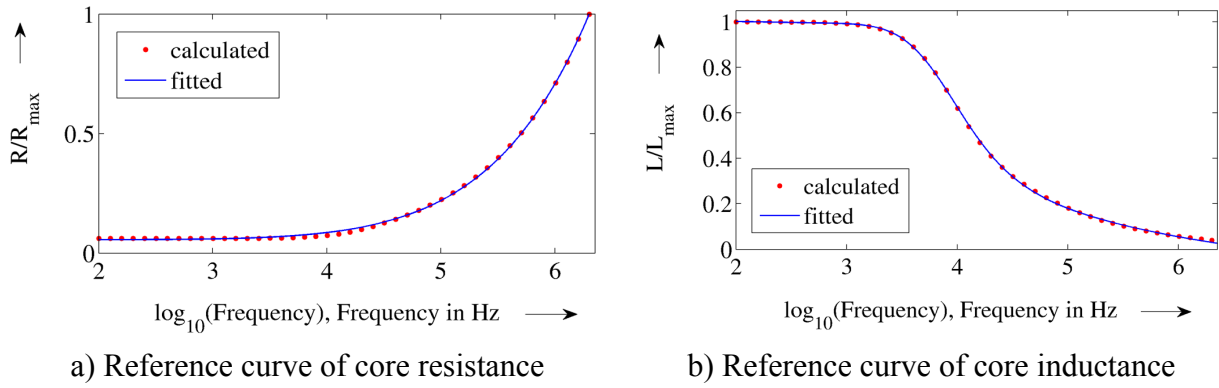


Figure 4.14: Analytical tendencies of core electrical parameters in wide range of frequencies

The normalization of the core leg resistance and inductance is necessary since it reduces the importance of the magnetic and design parameters as well as preserves the parameter changes in a scale of unit. Thus, it can provide reference curves for recovering parameters of core sections of any transformer at high frequencies. In fact, inductance and resistance of core yokes of the transformer can be obtained in such way since there is no winding in yokes, and therefore no number of turns, to calculate core yoke impedances from the analytical formulae (3.16); furthermore, the core yoke impedance in the equivalent circuit combines both upper and lower yoke sections as mentioned in chapter 2.

Then the frequency dependent functions of core resistance and inductance in general can be obtained by multiplying the “reference curves” with corresponding factors (k_R or k_L) determined as ratios of measurement-based values to corresponding formula-based values at the transition frequency (f_{trans}) as illustrated in Figure 4.15.

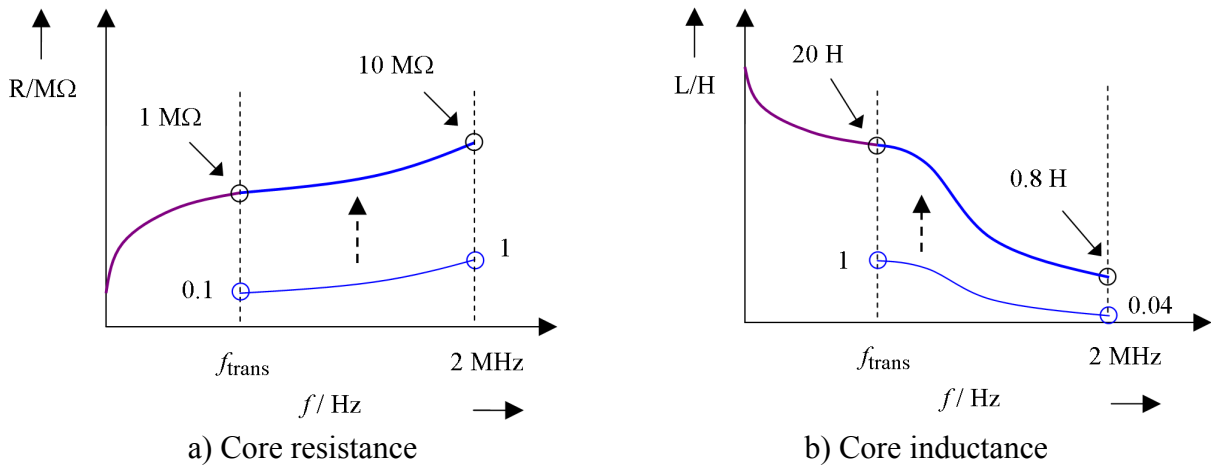


Figure 4.15: Example of recovery of core electrical parameters from reference curves and multiple factors at high frequencies ($k_R = 1 \text{ M}\Omega/0.1 = 10 \text{ M}\Omega$ and $k_L = 20 \text{ H}/1 = 20 \text{ H}$ at f_{trans})

In Figure 4.15, all values illustrated for the calculation of core resistance and inductance at the f_{trans} and 2 MHz are not correct compared with those in Figure 4.14; they are only mentioned as simple examples instead.

As a result, the core yoke resistance and inductance of the transformer T_1 (and also of other transformers) are determined thanks to the proposed calculation procedure. Figures 4.15a and 4.15b plot frequency dependencies of the core resistances and inductances of the test transformer

in the equivalent circuit in broad frequency range, which combine two frequency dependent functions in low and high frequency range for the simulation later. The transition frequency for core inductances is adjusted within range of 100 Hz to 400 Hz for a smooth representation since the measurement-based inductances at such frequencies are nearly constant.

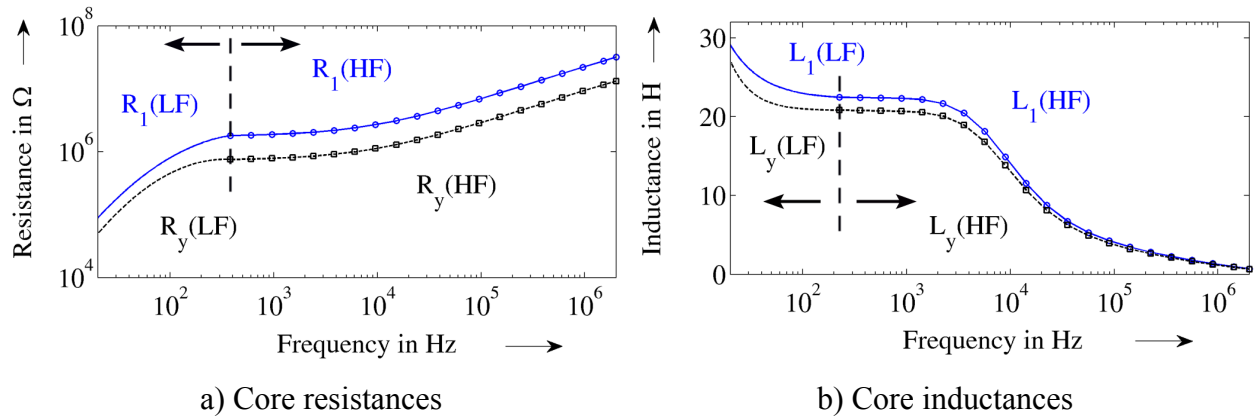


Figure 4.16: Plots of frequency dependency of core electrical parameters in broad frequency range

It is realized in Figure 4.16 that core resistances and inductances vary significantly at very low frequencies, e.g. from 20 Hz to 100 Hz. It is not clear whether the changes at such frequencies come from the transformer core itself or from the measurement system since the fitting process is guaranteed from the comparison between measured and calculated open-circuit input impedances. From the measurement system, the problem may be caused by the difference of characteristic impedances of the measuring cable (not 50Ω from 20 Hz to several tens kHz²³) and the instrument source (50Ω) since the measurement is performed by means of a scattering-parameter VNA. However, a good measurement with a known resistance in broad frequency range after calibration shows that the calibration removes the effect very well.

It is concluded that, for the purpose of simulation-based FRA interpretation, the frequency dependent functions plotted in Figure 4.15 can be used in whole frequency range whereas for the reliable diagnostic of transformer core, only constant values of core inductances at transition frequencies are used.

4.2.4 Ground and inter-winding HV-LV capacitance

Table 4.4 presents the ground and inter-winding HV-LV capacitances measured from the conventional and proposed method to compare the performance of the two methods. The conventional test is performed by means of the CPC 100 at power frequency at a voltage lower than the normal applied voltage (2 kV instead of 10 kV) since the transformer has no oil and the insulations are very aged (measured dissipation factors are higher than 20 %). The high losses in insulations influence much the accuracy of capacitances in the conventional test, especially the C_{LG} . If the applied voltage is increased, the conventional capacitance test may not be non-destructive for the very aged transformer since high applied voltage will damage the insulations. On the other hand, in the proposed method, equivalent capacitances are extracted from measured impedances at frequencies where very pure capacitive behaviours are found, which can not be

²³ The characteristic impedance of the cable used for the measurements has value of 54.5Ω at 30 kHz and approximate 50Ω at frequencies higher than several hundreds kHz

achieved with the conventional test at power frequency. Therefore, the results derived from the impedance tests are considered more accurate and will be used for further analysis.

Table 4.4: Capacitances measured through the two methods

Capacitance, in pF	CON (measured at 2 kV, 50 Hz)	IMP (measured at 1 V, ~ 1 kHz)
C_{HG}	290	316
C_{LG}	4118	3097
C_{HL}	1156	993

4.3 Parameter-based FRA interpretation and failure diagnostic

The above-mentioned electrical parameters of the test transformer are now applied for two purposes:

- Interpretation of FRA in broad frequency range via circuit simulation. By doing so, the contribution of the series winding capacitance to the bulk capacitance at mid frequencies will be identified and in case the contribution of the capacitance is significant, the capacitance will be determined based on the simulation solution.
- Comprehensive diagnostic of electrical/mechanical failures in the transformer active part.

4.3.1 Parameter-based FRA interpretation in broad frequency range

Since most electrical parameters of the transformer (core impedances, leakage/zero-sequence impedances, winding resistances and capacitances) are determined, the parameter-based FRA interpretation is now possible thanks to the simulation of the equivalent circuit in Figure 4.4 in accordance with real measurements. In this section, two open-circuit frequency responses are interpreted based on simulation: open-circuit input impedance (non-standard open-circuit frequency response) and end-to-end open-circuit (EEOC) voltage ratio (standard open-circuit frequency response). Interpretations of other standard frequency responses such as EESC, CAP and IND will not be presented due to their representations at low frequencies, leakage inductance, winding capacitance and core inductance respectively, are simple.

4.3.1.1 Interpretation of frequency responses of open-circuit input impedances

The circuit in Figure 4.4 without winding series capacitances is first simulated by means of a commercial circuit simulation software which is able to take into account the frequency dependencies of inductive components to see whether the series capacitances of windings has significant influence. To illustrate a typical case of interpretation of open-circuit impedances at HV side, Figure 4.17 shows comparisons between measured and simulated frequency responses of the open-circuit input impedance observed at phase A, i.e. source is sup-

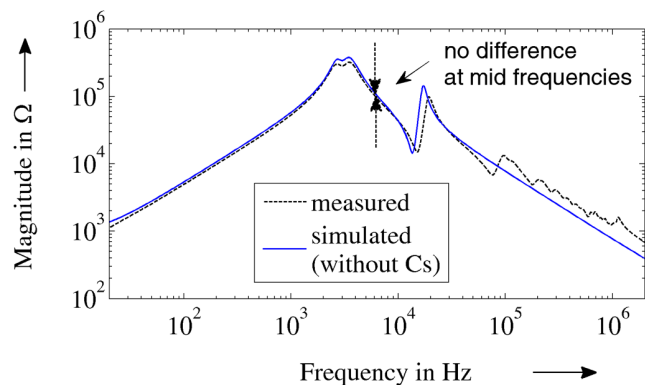


Figure 4.17: Measured and simulated frequency responses of open-circuit input impedance of phase A

plied between terminals A and N while other windings are left open. It is observed from Figure 4.17 that at mid frequencies where the total capacitance is dominant, there is no difference between measured and simulated frequency responses. That means the winding series capacitance has no significant contribution on the total capacitance.

It is then realized from Figure 4.17 that the validation of the simulation approach of the duality based equivalent circuit is in low and mid frequency range, i.e. from 20 Hz to 30 kHz. This is understandable since there is no direct coupling between leakage inductance and winding capacitances, or more correctly between self, mutual inductance and capacitances of winding sections, in the equivalent circuit, which is a “must” for acceptable agreement at high frequencies [Abeywickrama-07, Sofian-07]. In fact, they are isolated by the ideal transformers that are required for investigations at low and mid frequencies.

To check whether the direct coupling between leakage inductance and winding capacitances could give better performance, another equivalent circuit is then developed by moving the leakage inductance of phase A in the core circuit into the winding area and the ground capacitances $C_{gH}/2$ are terminated directly at two ends of the leakage inductance. Simulated results show that the adjusted equivalent circuit is able to capture the interaction between leakage inductance and winding capacitances in region ④ (around 100 kHz) as depicted in Figure 4.18.

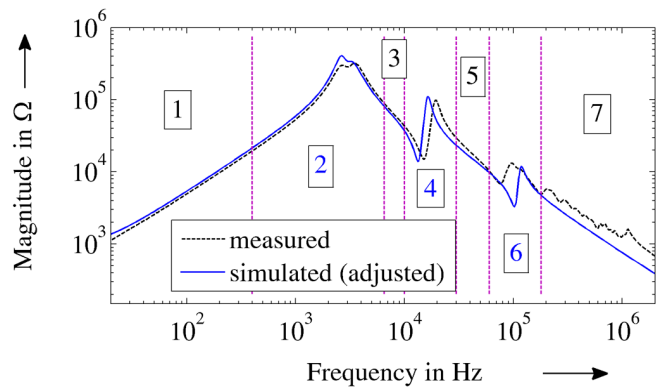


Figure 4.18: Measured and simulated frequency responses of open-circuit input impedance of phase A

From Figures 4.17 and 4.18, the interpretation of non-standard open-circuit frequency responses can be obtained as follows:

- Region ① (20 Hz to 400 Hz): dominant by inductive core influence.
- Region ② (400 Hz to around 6.5 kHz): interaction between core inductances and winding capacitances (from inductive into capacitive behaviour).
- Region ③ (6.5 kHz to around 10 kHz): dominant by winding capacitances. It is noted that the contribution of the winding series capacitances of HV and LV windings to the total capacitance is not significant since there is an agreement between measured and simulated frequency responses in this region²⁴. Therefore the HV winding series capacitance is small compared with other capacitances whereas the LV winding series capacitance can only be determined from analysis at LV side, which is not possible due to very low impedances measured at this side (out of measuring range of the device).
- Region ④ (10 kHz to 30 kHz): interaction between winding capacitances and total zero-sequence inductance.
- Regions ⑤ (30 kHz to 60 kHz): capacitive tendency from winding capacitances after compensating effect of total zero-sequence inductance.

²⁴ This is logical since the HV winding is the disc-type one with very low series capacitance [Kulkarni-04]

- Region ④ (60 kHz to ~100 kHz): interaction between capacitive effect from region ③ and leakage inductance.
- Regions ⑤ (~100 kHz to 2 MHz): interaction between winding capacitances and all inductances, including parasitic inductances from other components outside the transformer such as grounding braids, grounding network etc.

4.3.1.2 Interpretation of frequency responses of open-circuit voltage ratios (the standard EEOC-FRA tests)

The original duality based and adjusted circuits are then used to simulate the standard EEOC FRA test of phase A shown in Figure 4.19. At frequencies lower than 30 kHz, it is true that core impedances are validated and series capacitance of HV windings can be ignored since good agreements between measurements and simulations in sub frequency ranges like those in Figures 4.17 or 4.18 are still observed. At higher frequencies, large deviations however appear, meaning that the circuits are not very suitable for simulation of standard frequency responses. In comparison with the original circuit, the adjusted circuit is found better since the simulated result reflects interactions of winding capacitances and leakage inductance at the end of region ④ in Figure 4.19 (at around 42 kHz), in case the inductance is moved into the winding area. Nevertheless, a lot of peaks/valleys and maximum/minimum in region ⑤ in Figure 4.19 reveal that the duality-based transformer circuit is no longer valid and a distributed circuit should be developed for a better analysis. However, this may not be necessary for a general interpretation in the viewpoint of diagnostic since it is clear from Figure 4.17 or 4.18 that only interaction of leakage inductance and winding capacitances is expected within 30 kHz to at least 100 kHz.

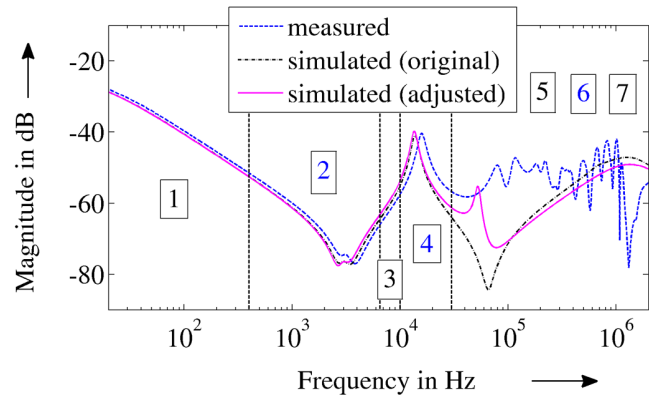


Figure 4.19: Measured and simulated standard open-circuit frequency responses of phase A

4.3.2 Parameter-based failure diagnostic

The parameter-based failure diagnostic is a preferred method used in reality since a significant change of one or more electrical parameters out of the safety tolerance reveals a change of transformer components which is often an indication of a failure. Compared with the conventional measurement methods, the proposed method has advantages in determination of *more* electrical parameters, which can be considered as a contribution to an improvement of the diagnostic as follows:

- Core inductance/impedance: since the conventional measurement method is able to determine the condition via exciting currents and magnetic balance (in chapter 1), the proposed method provides a direct indicator for core diagnostic via core leg/yoke inductance.
- Winding series capacitance: it is considered as a direct indicator for diagnostic of mechanical failures in transformer windings and can only be determined through the proposed method.

To illustrate the application ability of the proposed method, two kinds of feasible failures were performed on the active part of the test transformer T_1 :

- Electrical failures: open-circuit, short-circuit between discs, short-to-ground (in the HV winding) and loss of core ground [Pham-12c].
- Mechanical failures: axial and radial deformation of the HV winding [Pham-14].

for the parameter-based diagnostic presented in next sub sections as follows.

4.4 Application of the proposed method in diagnosis of electrical failures performed on the active part of the test transformer T_1

4.4.1 Overview of the electrical failures

The failures of open-circuit, short-circuit between discs and short-to-ground shown in Figure 4.20 were performed at or on the position of the 9th disc of each of three HV windings having in total 16 discs whereas the loss of core ground was conducted by removing the ground connection of the core. In reality, the failures of short-to-ground and open-circuit may happen to any “appropriate” position along winding while the short-circuit between turns for wound windings appears more frequently than the short-circuit between discs. However, the short-circuit through a disc is preferred since it is hard to distinguish from the short-to-ground as explained later in this section.

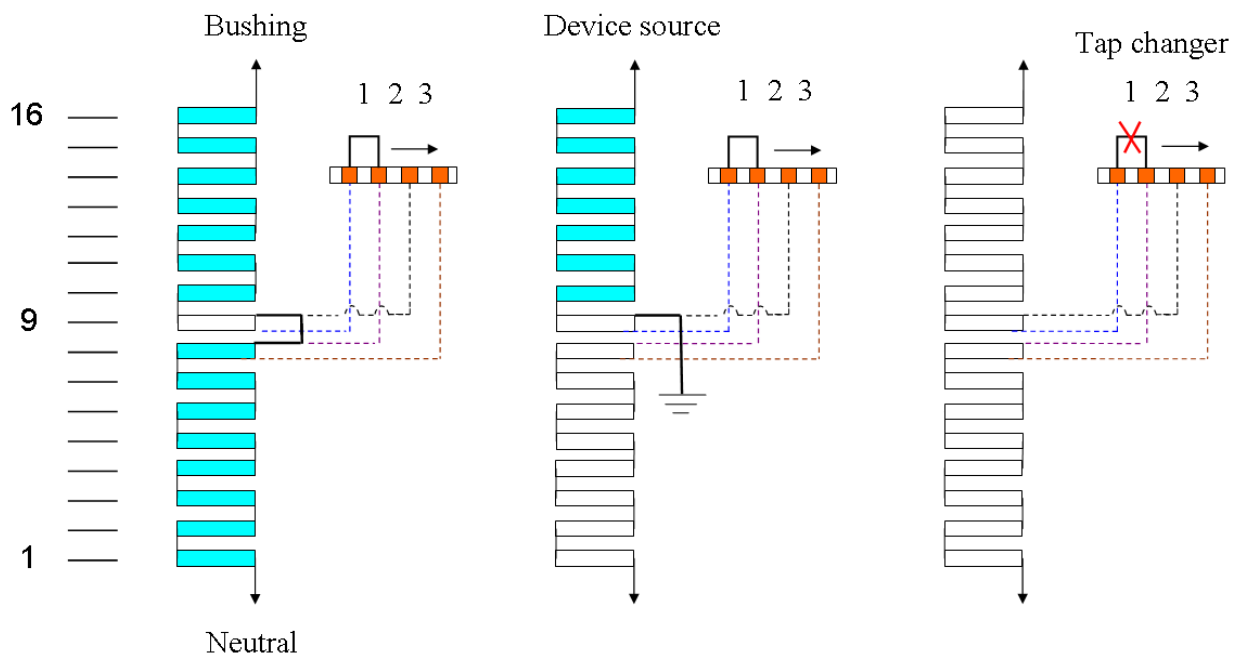


Figure 4.20: Short-circuit of a disc, short-to-ground and open-circuit failure on a HV winding (from left to right respectively)

4.4.2 Failure detection based on electrical parameters

4.4.2.1 Open-circuit failure on HV windings

From the short-circuit input impedance test analysis, negative “leakage inductances” are obtained for this failure mode. It is logical since capacitive currents flow in the faulty winding through the open-circuit position. Therefore, it is not necessary to analyze other test results since

the negative values are useful to detect an open-circuit failure on a winding. The failure is also easily to be detected by measuring the (DC) conventional winding resistance.

4.4.2.2 Short-to-ground and short-circuit-between-discs failures on HV windings

To detect the short-to-ground failure, the measurement of conventional DC winding resistance, insulation to ground of the windings, exciting current or dissipation factor etc. is sufficient whereas to detect the short-between-turns/discs failure, measurements of winding resistance, turn ratio, exciting current, magnetic balance etc. are helpful. However, depending on level of the failures, it can be easy or difficult to diagnose by using the conventional measurement method. Thus, the proposed method may be useful in supporting the diagnostic of such failures in real power transformers.

It is realized from the last chapter that the proposed method is efficient in determining electric-magnetic inductances and winding capacitances whilst resistive components are not reliable for diagnostic purpose because of low applied field in the measurements. To detect the short-to-ground and short-between-discs failures, the leakage inductance is helpful since its value changes in different conditions of the transformer, i.e. healthy/faulty. It can be explained that the failures reduce the magnetic energy in the leakage channel in terms of failure mode and hence the leakage inductances decrease [Kulkarni-04]. Figure 4.21 confirms a decrease of stored magnetic energy from 2D-FEM simulations of the short-circuit tests in different conditions.

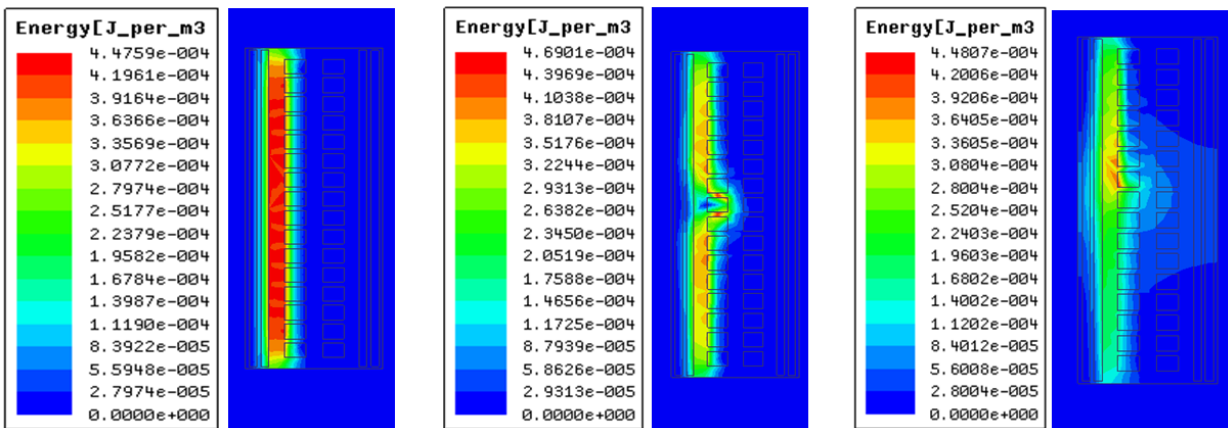


Figure 4.21: Magnetic energy distributions in the gap between HV and LV windings of phase A in healthy, shorted-disc and short-to-ground condition at 50 Hz (from left to right respectively)

Table 4.5 introduces a comparison of leakage inductances derived from the proposed method and from FEM simulations at 50 Hz and 1 kHz. A clear tendency of value change between all conditions is observed from FEM-based calculations whereas from the new method, the shorted-disc and short-to-ground failures can not be recognized exactly at 50 Hz; in fact they are only distinguished from the healthy condition and in such case, ground winding capacitance is a good indicator to discriminate them. However, a clear tendency of leakage inductance change obtained from the new method like that from the FEM calculation appears at higher frequencies, e.g. at more than 1 kHz since the measurement performance of the VNA at very low applied field is not reliable for the test transformer at frequencies around the power frequency (see Figure 4.6b).

Table 4.5: Change of leakage inductances in faulty condition compared with that in healthy condition, ΔL_3 in %

Failure mode	Proposed method (measured at 1 V)		FEM-based calculation (simulated at 1 V)	
	50 Hz	1 kHz	50 Hz	1 kHz
shorted-disc	- 16.5	- 16.4	- 15.1	- 16.2
short-to-ground	- 14.8	- 28.0	- 29.8	- 29.5

4.4.2.3 Loss of core ground

An electrical parameter which is reliable for detecting this failure mode is the ground capacitance of the LV windings since the LV windings are inner windings and the core ground is lost. Table 4.6 shows a comparison of the capacitance change in the failure mode derived from proposed method compared with that in healthy condition. As predicted, ground capacitance of the LV windings (C_{LG}) changes significantly in comparison with that of the inter-winding capacitance (C_{HL}) and ground capacitance of the HV windings (C_{HG}). As a result, it is the best indicator to detect this failure mode.

Table 4.6: Change of winding capacitances, in %, compared with that in healthy condition

Failure mode	ΔC_{HL}	ΔC_{HG}	ΔC_{LG}
Loss of core ground	8.2	- 21.8	- 90.7

4.5 Application of the proposed method in diagnosis of mechanical failures performed on the active part of the test transformer T_1

4.5.1 Overview of the mechanical failures

There are several typical types of mechanical failure appearing in transformer windings due to forces from high current short circuit faults [Sofian-07, Jayasinghe-06, Kulkarni-00]:

- Axial winding displacement due to axial forces
- Buckling of windings due to radial forces
- Bending, tilting of windings due to axial forces

Since the LV windings of the transformer are inner ones, only the HV windings are the main objects to be investigated. Of those above-mentioned failures, only the axial displacement is feasible; buckling and bending of the HV windings are not possible due to their small size and full insulation in gaps between HV and LV windings. Figure 4.22 plots the top and front view of a HV phase winding with an attempt to bend discs of the winding axially at even sequences of supporting spacers; it is however realized that a clear bending is difficult and not successful whereas a slight bending is not sufficient for the investigation.

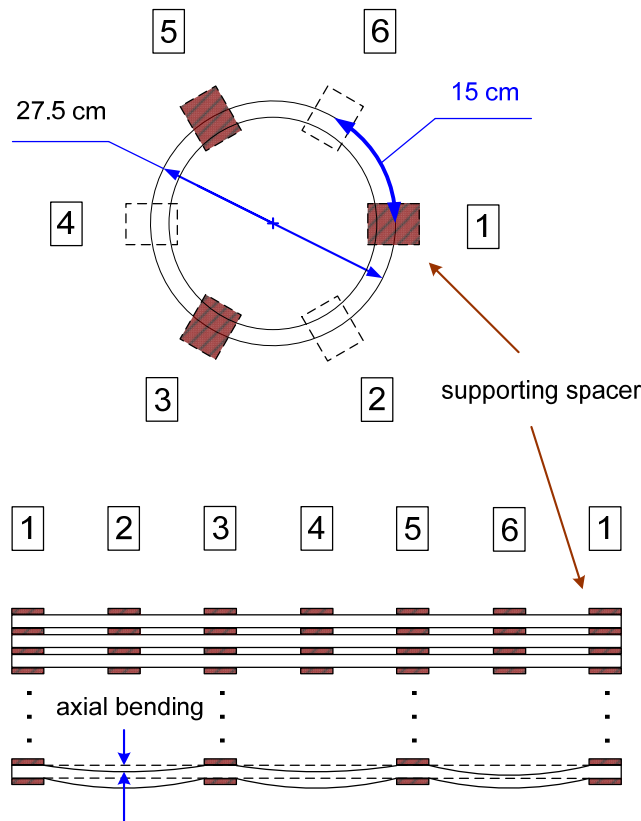


Figure 4.22: Top and front view of a phase HV winding consisting of 16 discs with 6 supporting spacers (A disc has approximately 46 turns with mean total height of 1.7 cm and mean total wide of 2.2 cm. Average gap distance between two consecutive discs is about 0.45 cm)

4.5.1.1 Axial displacement of the HV winding of phase C

Figures 4.23a and 4.23b depict phase C of the test transformer in healthy and faulty condition respectively. The axial displacement (Δh) is about 5.5 % of the height of the HV winding, which is considered large for such failure in power transformers.

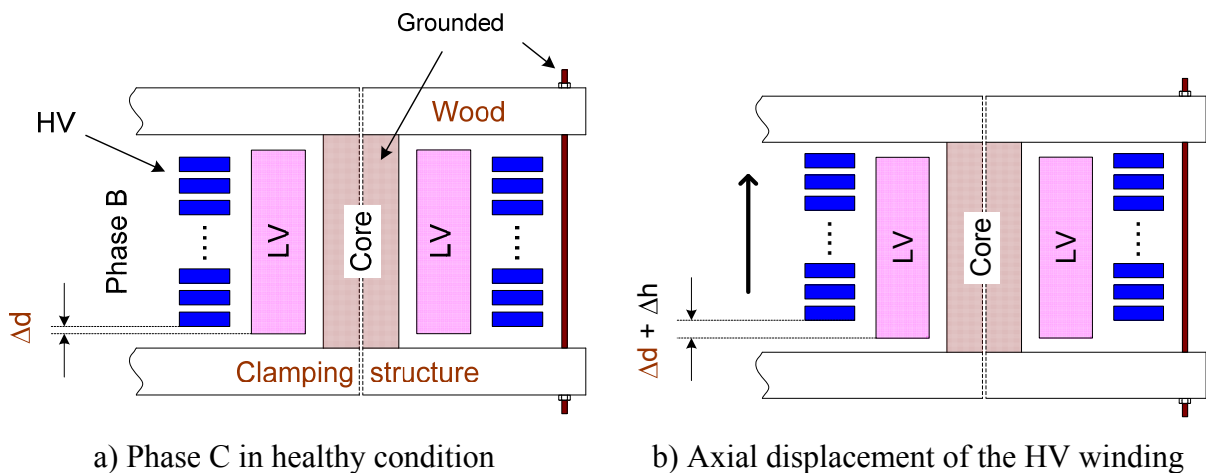


Figure 4.23: Phase C of the test transformer in different conditions (dimensions are not fully proportional with real values and insulation is not shown)

4.5.1.2 Radial displacement of the HV winding of phase C

The failure is executed at two levels to investigate the sensitivity of the standard FRA assessment and the change of electrical parameters: firstly the top 3 of 16 discs and secondly the top 7 of 16 discs are moved close to the HV winding of phase B as shown in Figure 4.24. In Figure 4.24b, n is the number of top discs of the HV winding being moved, and the displacement distance Δx is about 50 % of the gap between HV and LV winding.

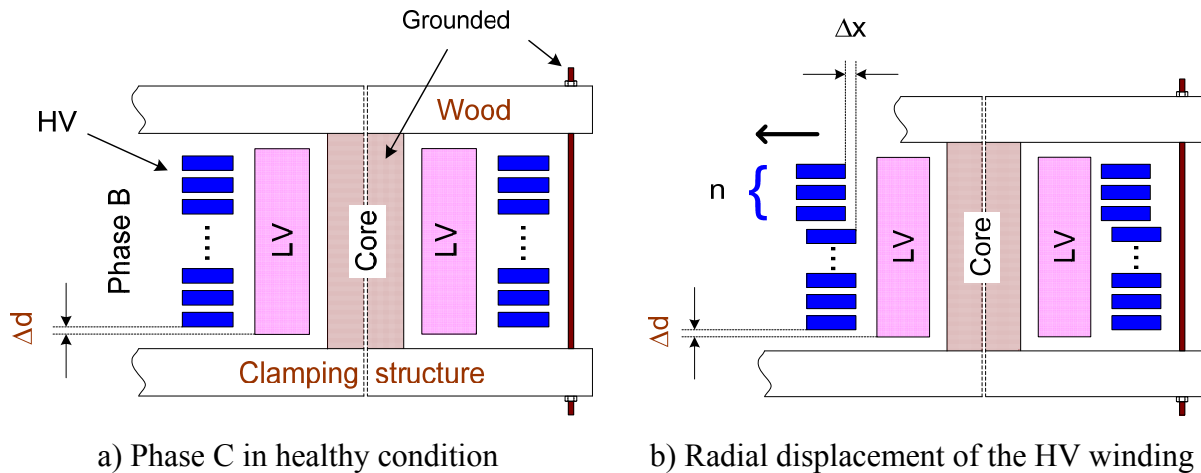


Figure 4.24: Phase C of the test transformer in different conditions (dimensions are not fully proportional with real values and insulation is not shown)

4.5.2 Failure detection based on FRA assessments and electrical parameters

4.5.2.1 Axial displacement of the HV winding of phase C

Figure 4.25 plots comparisons of four main standard FRA test types, the EEOC, EESC, CAP and IND from top down to bottom respectively, in the two conditions: healthy (reference) and faulty (failure) in frequency range from 10 kHz to 1 MHz. From the comparisons, the assessments shown in Table 4.7 conclude a clear failure from the CAP and IND comparison whereas the EEOC and EESC comparison reveal no failure, i.e. the winding is normal. In detail, the “slight deformation” in the CAP assessment is due to slight changes of the correlation coefficients in low frequency range (1 kHz to 100 kHz) and high frequency range (600 kHz to 1 MHz). The “obvious deformation” in the IND assessment is from the obvious change of the correlation coefficients in low frequency range (1 kHz to 100 kHz).

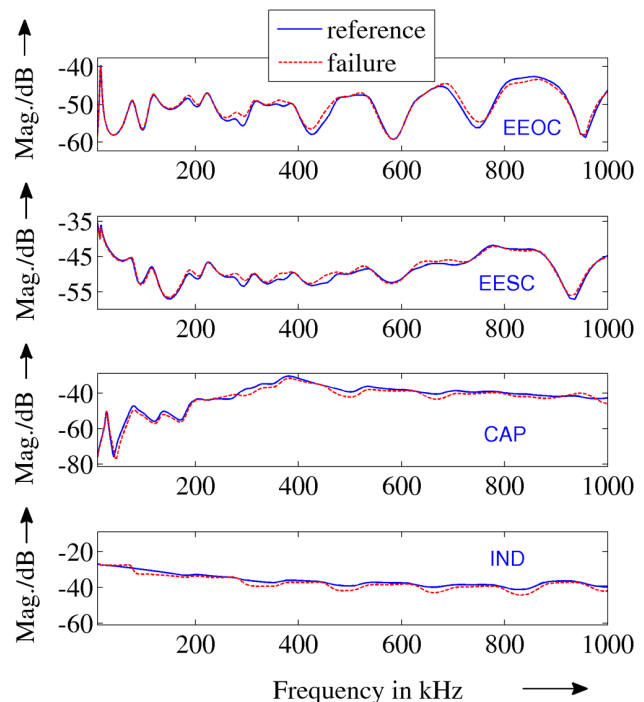


Figure 4.25: Comparisons of four standard FRA tests from 10 kHz to 1 MHz

Table 4.7: FRA assessment based on the DL/T911-2004

FRA test type	Assessment result
EEOC	Normal winding
EESC	Normal winding
CAP	Slight deformation
IND	Obvious deformation

Table 4.8: Deviations of electrical parameters between “healthy” and “faulty” condition

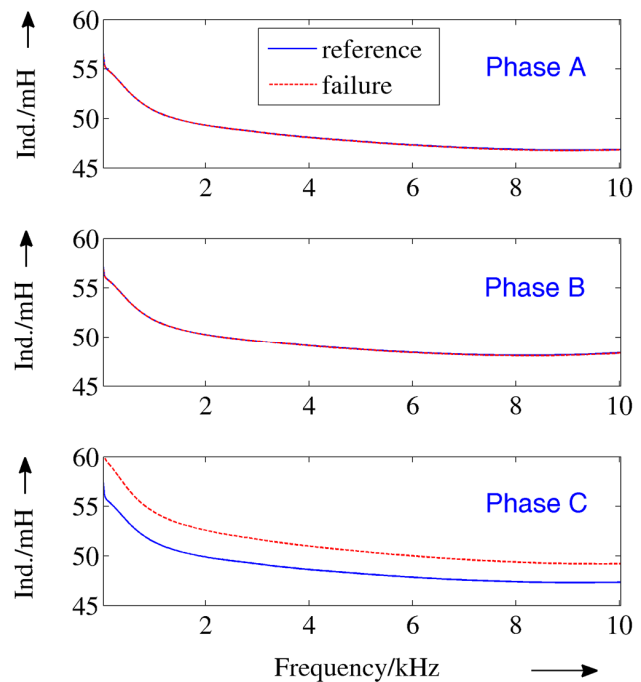
Electrical parameter	Deviation, in %
Leakage inductance of phase C (average from 20 Hz to 10 kHz)	+ 6.0
Ground capacitance C_{HG}	+ 0.9
Ground capacitance C_{LG}	- 1.1
Inter-winding capacitance C_{HL}	- 2.0

An obvious deviation from the IND comparison is actually only at frequencies from 50 kHz to 100 kHz, which is perhaps caused by the edge effect as the HV winding is upward moved. The agreement of the IND traces at frequencies lower than 50 kHz confirms that the core inductances are not changed and not involved in the failure detection.

The contribution of the impedance method in determining electrical parameters to the current FRA assessment is quite clear in this case: the significant change of leakage inductance and slight change of inter-winding HV-LV capacitances C_{HL} indicate there is problem in the gap between the HV and LV winding rather than in the windings, which can not be recognized via the standard FRA assessment. This conclusion is also in agreement with that in [Jayasinghe-06] which investigates the axial displacement of transformer windings based on simulation.

It is necessary to explain the physical cause of the deviations in Figure 4.25. The EEOC FRA tests reflect all electrical parameters of the transformer such as core inductance at very low frequencies, zero-sequence, leakage inductance and winding capacitances at mid and high frequencies. The EEOC assessment result shows that the changes of those parameters are not sufficient to cause a failure mode, which agrees with only the EESC assessment. The EESC assessment indicates that the leakage inductance changes within accepted tolerance, which is contrary with the real failure level. In fact, from the impedance method the per-phase leakage inductance changes significantly, about 6 %, as shown in Table 4.8 and Figure 4.26.

The CAP assessment reveals only slight changes of winding capacitances in ranges from 1 kHz to 100 kHz and from 600 kHz to 1 MHz. However, the helpful information that can be used to support the diagnostic is the change of inter-winding HV-LV capacitance, more than 2 %, presented in Table 4.8 obtained from the impedance method.

**Figure 4.26:** Deviations of leakage inductances of phases A, B and C after the axial displacement takes place in phase C

4.5.2.2 Radial displacement of the HV winding of phase C

For the two levels of the radial displacement of the HV winding, the assessments of all FRA test types conclude that there is no failure appearing in the winding since the deviations between the FRA traces, and consequently the changes of correlation coefficients (compared with healthy condition) are not significant. In those cases, the impedance method is helpful since it reveals the changes of parameters as sensitivities with regard to failure type and failure level. FRA comparisons of the case $n = 7$ and parameter changes in two cases are presented in Figure 4.27 and Table 4.9 respectively.

In Table 4.9, the decrease of ground capacitance of HV windings C_{HG} from radial displacement of 3 top discs to radial displacement of 7 top discs is expected since the distance from part of the HV winding to the grounded clamping bolt increases. Small but clear changes of leakage inductance (approximately 2 times) and ground capacitance C_{HG} (approximately 3 times) indicate the clear sensitivity of the impedance method with regard to failure level, which can not be achieved with the current FRA assessment.

4.5.3 Discussion

The section introduces a case study in which assessments of current FRA standards are applied to detect the level, i.e. slight or obvious degree, of two mechanical failures in a HV winding of a small distribution transformer. Although the current assessment is recommended to be applied for transformers with large rated power, e.g. more than 1 MVA [DLT911-04], the investigation shows that the only FRA method is not efficient to detect any detail of the failures, which is considered important for transformer failure diagnostics in reality.

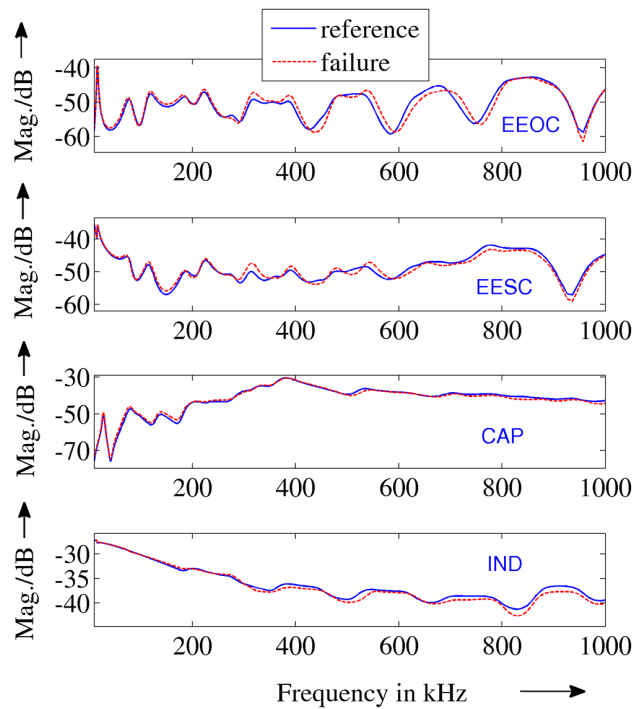


Figure 4.27: Comparisons of standard FRA tests between healthy condition and radial displacement of 7 top discs

Table 4.9: Deviations in % of changes of electrical parameters when n top discs are displaced radially

Electrical parameter	Deviation, in %	
	$n = 3$	$n = 7$
Leakage inductance of phase C (average from 20 Hz to 10 kHz)	-0.5	-1.0
Ground capacitance C_{HG}	-0.6	-1.8
Ground capacitance C_{LG}	-0.4	-0.6
Inter-winding capacitance C_{HL}	-0.8	-0.9

According to the impedance method, it is stated that winding mechanical failures are associated with changes of leakage inductance and different capacitances (ground, series and inter-winding HV-LV). Of those parameters, per-phase leakage inductances can be determined independently and reliably from measurements to detect failure type and failure level, which is illustrated in Figure 4.28 summarized from Tables 4.8 and 4.9.

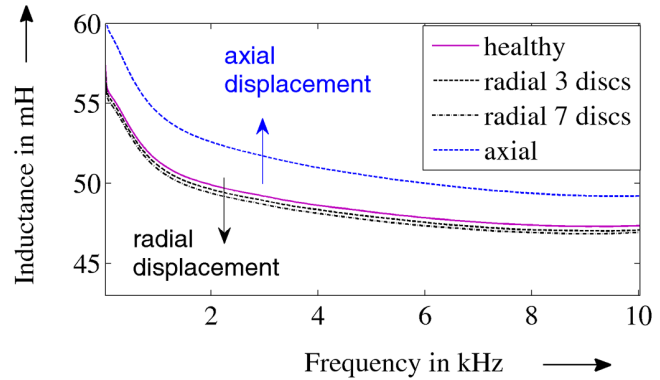


Figure 4.28: Change of leakage inductance with regard to failure type and level

Less important compared with leakage inductance, the capacitances C_{HG} , C_{HL} , C_{LG} should be also used in addition to identify the failures. However, due to the fact that the capacitances are from three corresponding parallel phase capacitances, the sensitivity associate with capacitances is not perfect. In fact, when a failure appears on a phase winding, the total capacitances are considered less sensitive compared with the per-phase capacitances that can not be determined separately. In addition, there are certain small tolerances in the determinations of equivalent capacitances from measured capacitive impedances and of three capacitances from four measurement configurations, which may influence the sensitivity of the diagnostic of slight failures.

4.6 Summary

The new method proposed in chapter 3 is applied to determine key electrical parameters of the test transformer T_1 for the purposes of FRA interpretation and failure diagnostic, which can also be measured through conventional and advanced measurement methods. Compared with existing methods, the application of the new method on the test transformer reveals several following advantages:

- The core's electrical parameters are now available for any relevant purpose, e.g. diagnostic of core failures based on calculated electrical parameters. In addition, thanks to the new method, the frequency dependency of core section parameters of any transformer in broad frequency range can be determined, which is considered useful in identification of the total capacitance from which the contribution of the winding series capacitance is found easily.
- Thanks to the core inductances, the total capacitance is determined which gives the conclusion that the series capacitance of the HV windings is very small to be neglected.
- The FRA interpretation based on transformer's electrical parameters and the duality based equivalent circuit is valid from 20 Hz to around 30 kHz. The valid frequency range extended with the adjusted equivalent circuit confirms that the distributed equivalent circuit should be used for high frequency analysis, which requires the availability of detailed transformer design data.
- For diagnostic of several electrical/mechanical failures in the transformer's active part, the method shows clearer contribution compared with the FRA assessment rules based on the Chinese standard [DL/T911-04]. It is thus suggested that the method should be combined with existing methods for getting a better diagnostic in reality.

5 Case study II: A 2.5 MVA 22/0.4 kV Dyn5 transformer (T_2)

In chapter 4, the proposed method has been successfully applied to analyze the electrical parameters referred into the star HV winding of the small distribution 0.2 MVA 10.4/0.462 kV transformer (T_1) for purposes of FRA interpretation and failure diagnostic. It is therefore required that electrical parameters referred into a delta winding of a larger power transformer should be investigated through the proposed method so that the method can be applied in reality in general. As a result, a medium distribution 2.5 MVA 22/0.4 kV sealed transformer (T_2) is absolutely an appropriate test object to test the proposed method.

Since the transformer T_2 is completely new and sealed as shown in Figure 5.1, only the electrical parameters referred into the HV delta winding of the test transformer when it is in healthy condition are searched for mainly the FRA interpretation. The electrical parameters are also “fingerprints” for a diagnostic in the future when there is any problem occurring in the transformer due to failures:

- Leakage inductances and winding resistances
- Core section impedances
- Ground and inter-winding HV-LV capacitance
- Winding series capacitance



Parameter	Value		Unit
Rated power	2500		kVA
Rated voltages	22/21.5/21/20.5/20	0.4	kV
Rated currents	72.17	3608.4	A
Vector group	Dyn5		
Frequency	50		Hz
Rated short-circuit voltage	5.64		%
Year	2011		

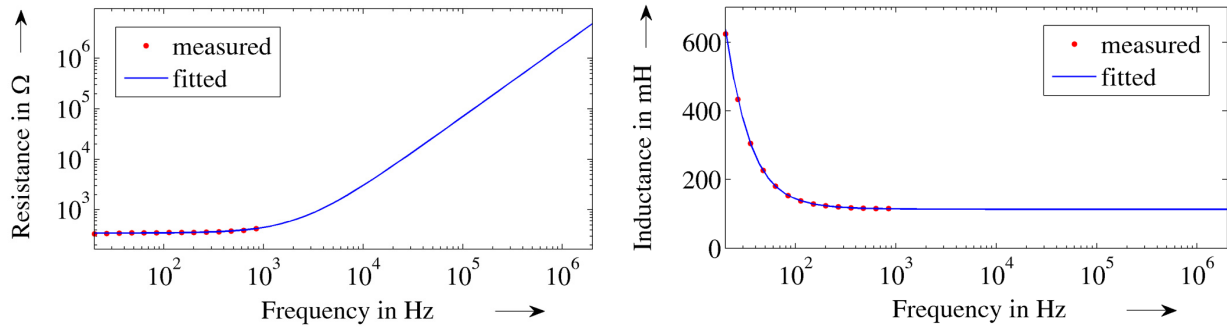
Figure 5.1: Appearance of the transformer T_2 and its name-plate data

5.1 Application of the new method in determination of electrical parameters referred into the HV delta winding

In this section, the electrical parameters of the test transformer T_2 referred into the HV delta winding will be analyzed through the proposed method presented in chapter 3 to check whether the new method is still appropriate for delta windings of larger power transformer, compared with star winding of the small distribution transformer T_1 .

The first difference in analyzing delta winding in transformer bulk compared with star winding is when a phase delta-connected winding is excited, other phase windings have also currents so the influence of other phase windings on the excited phase winding in short- or open-circuit tests is obvious. In addition, the zero-sequence impedance is neglected since it cannot be determined at the delta side and its influence on terminal frequency responses is insignificant. Figure 5.2

5.4b plot the measured and fitted frequency dependent functions of the electrical parameters referred into the HV side in wide frequency range for illustration.



a) Total resistance $R_{\text{stray_losses}}$ of phase A

b) Leakage inductance of phase A

Figure 5.4: Calculated values from measurement at low frequencies and fitting frequency dependencies in broad frequency range

In Figure 5.4b one can observe easily that the measurement results and thus the frequency dependency of the leakage inductance is not valid at low frequencies from 20 Hz to more than 200 Hz; it is due to the abnormal tendency of the phase angle at such frequencies. In contrary with the measured short-circuit impedances of the other transformers T_1 and T_3 , the impedance's phase angle in this case *decreases* with increasing frequency at those frequencies (see Figure 5.3), resulting in a significant decrease of the calculated leakage inductance starting at 20 Hz, which is probably due to influence of core inductance [Lachman-97]. This can be explained as follows: at an applied voltage lower than a minimum threshold associated with a limit point on the B-H curve, the flux density in the transformer core is extremely low; in such cases the transformer operates at a point lower than the limit point on the B-H curve, where “the magnetic permeability of the steel may be several orders of magnitude lower than in the operating region”, hence the core inductance decreases (compared with that at high applied field) and affect the measured impedance in the short-circuit tests. When frequency increases, the influence is less and thus the calculated per-phase leakage inductances become reasonable.

Then another question arises: why does the inaccuracy of calculated leakage inductances at very low frequencies appear only on the transformer T_2 whereas the same low voltage (~ 1 V) is applied in measurements for all tested transformers? The answer is simply the differences of the B-H curve between the transformers' cores and their limit point since only the transformer T_2 is new compared with other transformers (manufactured in 2011 with good material and modern technology). The inaccuracy of calculated leakage inductance at very low frequencies does not affect the simulation of open-circuit frequency responses since core impedances are dominant at those frequencies but for the diagnostic, the constant tendency at higher frequencies, e.g. starting from 300 Hz, should be used since it is comparable with the measured values obtained from the relevant conventional test carried out at higher applied field (supplied current 1 A).

For comparison of results between the conventional (CON) and input impedance (IMP) measurement-based approaches, Table 5.1 introduces per-phase leakage inductances derived from the two approaches and errors between them at several low frequencies.

Table 5.1: Per-phase leakage inductance referred into HV side

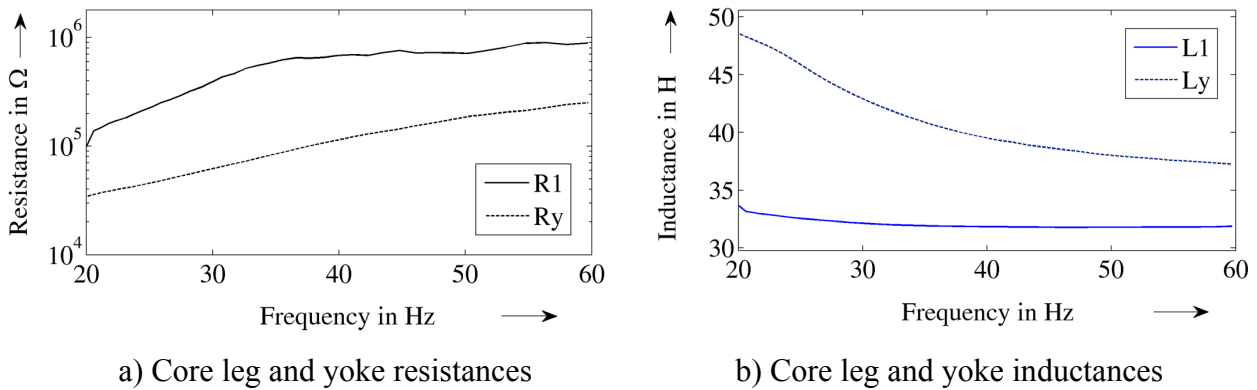
Fre- quency in Hz	Leakage inductance, in mH								
	Phase A			Phase B			Phase C		
	CON	IMP	Error, in %	CON	IMP	Error, in %	CON	IMP	Error, in %
20	123.1	638.5	419	125.6	545.6	334	129.2	726.8	463
50	117.6	215.9	83.6	119.6	199.1	66.5	122.9	242.3	97.2
100	116.3	143.7	23.6	118.2	141.2	19.5	121.3	155.1	27.9
200	115.3	123.5	7.1	117.2	125.1	6.7	120.7	131.0	8.5
300	114.2	119.1	4.3	116.1	121.5	4.7	119.2	125.8	5.5
400	113.8	117.3	3.1	115.7	120.1	3.8	118.6	123.7	4.3

5.1.2 Core section inductances and resistances

According to the method proposed in chapter 3, core section inductances and resistances referred into the delta winding of the transformer T₂ are determined from open-circuit input impedance measurements at low frequencies and the “reference curve” approach at high frequencies.

5.1.2.1 Measurement-based core electrical parameters at low frequencies (20 Hz to 60 Hz)

The core electrical parameters (Z_l , Z_y) referred into the HV side of the transformer are then determined based on analysis the full input mode according to (3.8) applied on the reduced equivalent circuit in low frequency range from 20 Hz to 60 Hz. Afterwards, they have to be converted into the relevant fundamental components (R_l , L_l , R_y , L_y) whose values in the low frequency range are depicted in Figure 5.5.

**Figure 5.5:** Calculated core electrical components from measurements

Due to the uncertainty of the transformer’s operating point on the B-H curve at low applied field mentioned in section 5.1.1, it is suggested that the core inductances calculated based on analysis of open-circuit input impedance measurements shown in Figure 5.5b are only suitable for interpretation of frequency responses measured also at the same applied voltage.

The calculated core electrical parameters R_1 , R_y , L_1 , L_y are then fitted into frequency dependent functions for application. To check the performance of the fitted functions $R_1(f)$, $L_1(f)$, $R_y(f)$, $L_y(f)$, Figure 5.6 depicts a comparison between the measurement result and its recovery from the fits of an open-circuit input impedance. Very small error of the magnitude and acceptable error of phase angle in the low frequency range in Figure 5.6 confirm the success of the analytical and fitting process proposed for analysis of core electrical parameters referred into the delta winding side.

5.1.2.2 Formula-based core electrical parameters at frequencies higher than 60 Hz

Since the transformer design data for calculation of core impedances at high frequencies are not available, the “reference curve” approach is then applied instead. According to the approach, values of core resistance and inductance at the transition frequency (60 Hz) are required; afterwards the “reference curves” are adapted using multiple factors to obtain the skin effect based core electrical parameters at high frequencies. The multiple factors are determined in detail at the transition frequency as shown in Table 5.2.

Table 5.2: Approximate calculation of the multiple factors for the adaptation

Electrical parameter of the core		Measurement-based value at 60 Hz (A)		Normalized value of the reference curve at 60 Hz (B)	Multiple factor (A/B)	
Resistance	legs	0.83	M Ω	0.056	14.81	M Ω
	yokes	0.24			4.32	
Inductance	legs	31.65	H	1	31.65	H
	yokes	35.34			35.34	

5.1.2.3 Frequency dependency of core electrical parameters in broad frequency range

Figure 5.7 plot frequency dependencies of core electrical parameters referred into the HV side of the transformer T_2 in broad frequency range. It is noted that the core yoke has higher inductance than the core leg, which is contrary to the tendency of the transformer T_1 . Explanation for such property will be given in the section of FRA interpretation since there is another phenomenon discovered when analyzing the contribution of core resistances to the frequency responses at resonances caused by the interaction between core inductances and winding capacitances.

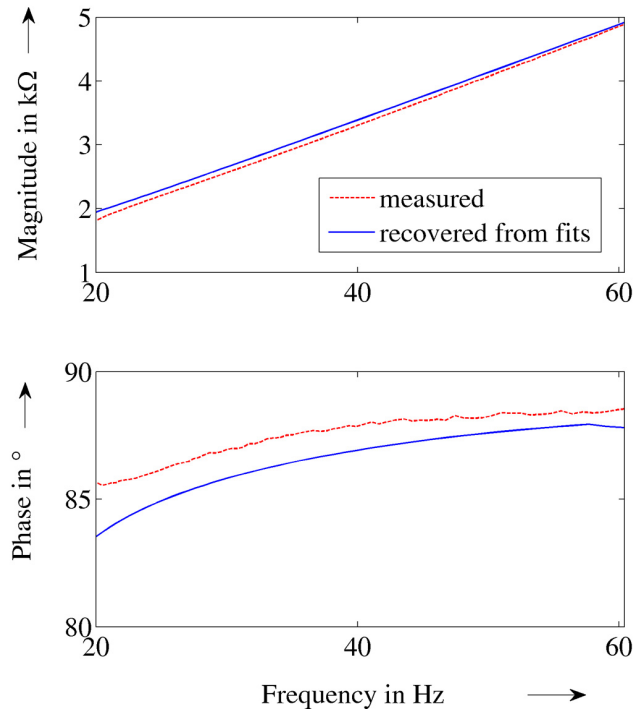


Figure 5.6: Measured and recovered frequency response of the open-circuit input impedance observed between terminals A-B at low frequencies

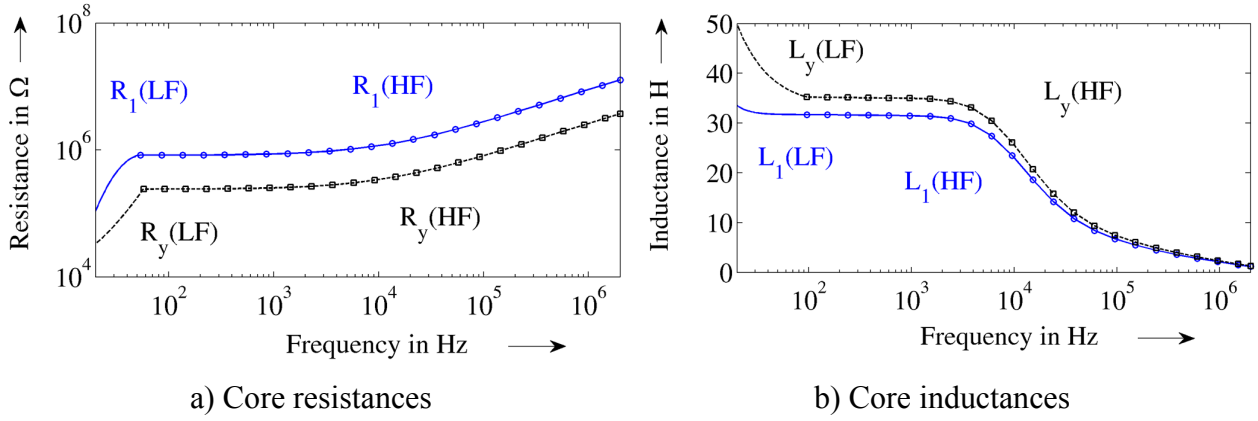


Figure 5.7: Plots of frequency dependencies of core section electrical parameters in broad frequency range

5.1.3 Ground and inter-winding HV-LV capacitance

Since the approach for calculation of ground and inter-winding capacitance from input impedance measurements does not depend on how the winding is connected, the capacitances can be determined thanks to the developed algorithms which are able to recognize automatically the low frequencies where pure capacitive characteristic reaches. Table 5.3 compares the capacitances derived through the two methods: the conventional (CON) and proposed (IMP) ones.

Table 5.3: Capacitances determined through the two methods

Capacitance, in pF	CON (measured at 10 kV, 50 Hz)	IMP (measured at 1 V, ~ 1 kHz)	Error, in %
C_{HG}	1732	1733	0.1
C_{LG}	16424	16029	2.4
C_{HL}	9135	9138	0.03

It is realized in Table 5.3 that the errors are small compared with that for the transformer T_1 , that means the proposed approach is successful tested. The reason is that the transformer T_2 and also its insulation system are new with corresponding measured dissipation factors of insulations between HV to ground, LV to ground, and HV to LV are lower than 1 % at frequencies from 50 Hz to 400 Hz.

5.2 Parameter-based FRA interpretation and failure diagnostic

From now it is possible to simulate frequency responses measured at transformer terminals for the purposes of determining whether the winding series capacitance has significant influence to the total capacitance and interpreting the frequency responses in terms of individual electrical parameters in the equivalent circuit.

Similarly to the transformer T_1 , only *open-circuit* frequency responses are investigated since the other ones, i.e. short-circuit, capacitive and inductive, are simple to interpret as they reflect relevant individual electrical parameters.

5.2.1 Parameter-based FRA interpretation in broad frequency range

5.2.1.1 Interpretation of frequency responses of open-circuit input impedances

The equivalent circuit in Figure 5.1 without appearance of the series capacitances of HV and LV windings (C_s) is used to simulate the measurement configuration of different open-circuit input impedances measured at the HV side of the transformer. To show a typical result of the simulation, Figure 5.8 compares measured and simulated frequency responses of the open-circuit input impedance observed between terminals A and B.

In Figure 5.8 it is clear that there is a certain deviation between the measured and simulated frequency response at mid and even high frequencies, which is caused by lack of the winding series capacitance. In this case the series capacitance has significant contribution to the total capacitance and thus cannot be neglected like in the first case study for the transformer T_1 .

Then the new approach in determining the winding series capacitance is applied thanks to simulation: various values of the capacitance are applied in the simulation in order to minimize the deviation between simulation and measurement at mid frequencies. Whenever the deviation disappears, it is said that the series capacitance is well identified. The approach is successful if core electrical parameters are appropriately determined in advance, since otherwise the simulated resonances between total core inductances and winding capacitances are different from the measured ones.

In fact there are two different series capacitances of the HV and LV windings, which contribute in general to the total capacitance in transformer bulk. However, the contribution of each of them is not identical depending on several factors, e.g. the ground and inter-winding capacitance and the winding connection. In principle, the two capacitances can only be determined based on analyses on two sides of transformers. Nevertheless, it is realized through simulation that the series capacitance of the LV winding in this case does not influence much the open-circuit frequency responses simulated at HV side; therefore it is easily to find the series capacitance of the HV windings (C_{sH} is identified approximately 2.3 nF) by simulation as shown in Figure 5.9.

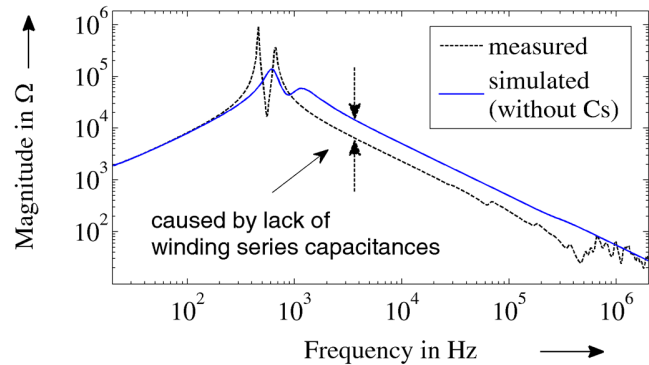


Figure 5.8: Measured and simulated frequency response of the open-circuit input impedance between terminals A-B

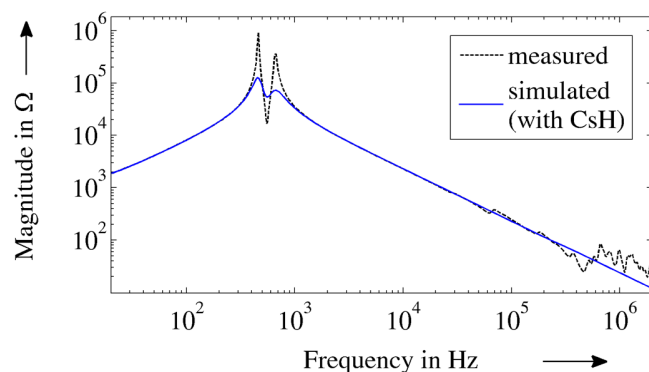


Figure 5.9: Measured and simulated frequency responses of the open-circuit input impedance between terminals A-B

(C_{sH} is identified approximately 2.3 nF) by simulation as shown in Figure 5.9.

When the winding series capacitance is taken into account in the simulation, the deviations between simulations and relevant measurements are eliminated, but there is still a disagreement at the resonances caused by interaction between core inductances and winding capacitances. According to analytical analysis, the disagreement is due to the resistive components in the circuit, the core resistances, since the capacitances have no accompanied conductances in the equivalent circuit.

A simple approach is then tested to confirm the problem caused by core resistances: part of the core resistances are then removed in the simulation to observe the tendency of new resonances. It is found that in case only the resistances of the two outer legs, i.e. R_{1A} and R_{1C} , appear in the circuit (other core resistances are removed), the simulated frequency responses match very well with the measured ones as illustrated in Figure 5.10. This fact, together with the abnormal tendency between core yoke and leg inductance in section 5.1.2.3, give a conclusion that the core resistances calculated based on

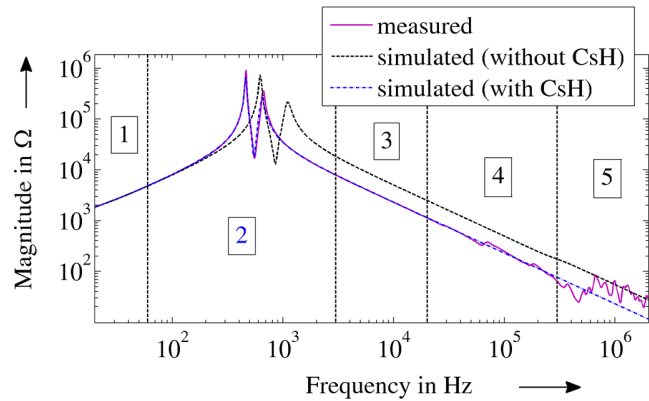


Figure 5.10: Measured and simulated frequency responses of open-circuit input impedance of phase A (with part of core resistances)

the “reference curve” solution is not so appropriate for *new* transformers. It can be explained based on the fact that the transformer T_2 is relatively new (manufactured in 2011) whereas the “reference” transformer T_1 is old (manufactured in 1955). The improvement in production of transformer core in terms of material and technology, e.g. grain-oriented steel and step-lap joint technique [ABB-07], is obviously more effective in reducing core losses; that means the core resistances are not high enough to limit the losses, which causes the disagreement at the parallel resonances between the core inductances and the winding capacitances.

From Figures 5.10, the interpretation of non-standard open-circuit frequency responses can be obtained thanks to the simulations where individual components are separately investigated as follows:

- Region ① (20 Hz to 60 Hz): dominant by inductive core influence.
- Region ② (60 Hz to around 3 kHz): interaction between core inductances and winding capacitances (from inductive into capacitive behaviour).
- Region ③ (3 kHz to around 20 kHz): defined as the mid frequency range where winding capacitances are dominant. The contribution of the winding series capacitance is significant, which is not the case in analysis of winding capacitances for the transformer T_1 .
- Region ④ (20 kHz to 300 kHz): it is thought that in this region there is the interaction between winding capacitances and leakage inductance in a capacitive tendency (effect of the leakage inductance can only be realized from the simulation when it is moved into the winding area to form the adjusted circuit like that of the transformer T_1)
- Regions ⑤ (300 kHz to 2 MHz): interaction between winding capacitances and all inductances, including parasitic inductances from other components outside the transformer.

5.2.1.2 Interpretation of frequency responses of open-circuit voltage ratios (the standard EEOC-FRA tests)

For the interpretation of the standard frequency responses, the equivalent circuit in Figure 5.2 is still exploited for simulation, but adapted based on measurement configurations for standard frequency responses. Figure 5.11 shows a typical comparison between a measured frequency response of voltage ratio between terminals C and A and its simulation result when the C_{sH} does not and does appear in the equivalent circuit. In case the C_{sH} is not in the circuit, deviations between measured and simulated frequency responses at mid (and also high) frequencies are still observed and larger than that in Figures 5.8 and 5.10, indicating that the effect of series capacitances is different in different measurement configurations. In addition, good congruity between measured and simulated (with C_{sH}) frequency response at low and mid frequencies obtained in Figure 5.11 when only part of the core resistances (R_{1A} and R_{1C}) appears in the circuit confirms the validation of the conclusion in applying the reference curve approach developed from an old transformer to a new transformer in the last sub section.

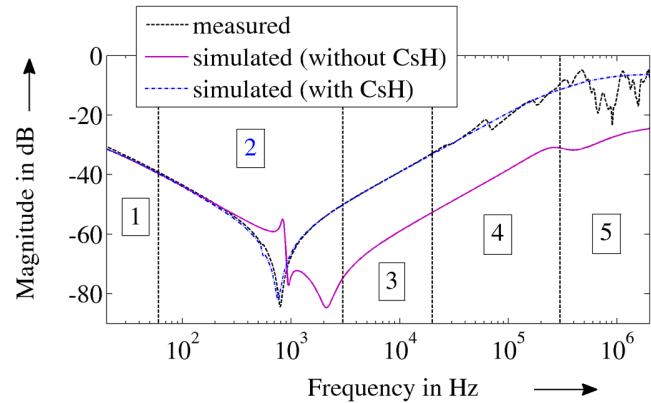


Figure 5.11: Measured and simulated typical standard frequency response (with/without C_{sH})

Figure 5.12 shows again the comparison of the measured and simulated standard frequency responses in Figure 5.11 but in term of appearance of core resistances (C_{sH} is considered in the simulations). It confirms that whenever good performances are achieved from the simulations of non-standard frequency responses, the same tendency will also be obtained for the simulations of the standard frequency responses. That means the FRA interpretation can be made from the simulations of either non-standard or standard frequency responses. It is also noted that the standard frequency responses can also be used to determine the winding series capacitance, but for the characterization of other electrical parameters, the non-standard frequency responses should be referred only.

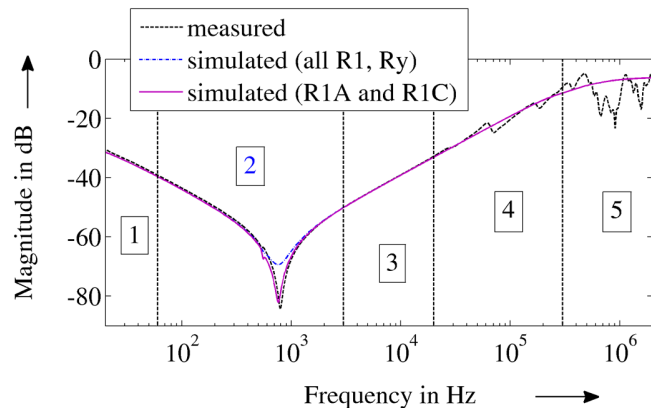


Figure 5.12: Measured and simulated typical standard frequency responses (fully/partly core resistances)

5.2.2 Parameter-based failure diagnostic

To diagnose mainly the electrical and mechanical failures in transformer active part, the electrical parameters determined through the proposed method at low frequencies, i.e. based on measurements, can be used as “fingerprint” for any comparison in the future; the high-frequency values calculated reasonably from analytical formulae are only appropriate for simulation-based interpretation of frequency responses.

Table 5.4 lists values of electrical parameters calculated from the proposed method for diagnostic purpose. Note that due to the significant change of core parameters at low frequencies, only constant values at the transition frequency (~ 60 Hz) are considered as reliable indicators to diagnose core failure. Furthermore, the HV windings of the transformer T_2 have high series capacitance (~ 2.3 nF) compared with their ground capacitance ($C_{gH} = C_{HG}/3 = 0.58$ nF), which is expected helpful in detecting mechanical failures in the windings later on. However, the resistive components such as core and winding resistances may not be reliable since their performance at very low applied voltage is not fully investigated and recommended for any diagnosis so far.

Table 5.4: Electrical parameters (referred into the HV side) of the transformer T_2 calculated from the proposed method

Electrical parameter		Value	Unit	at frequency, in Hz	Applicable for diagnostic
Core leg	R_1	0.83	$M\Omega$	~ 60	
	L_1	31.65	H	~ 60	✓
Core yoke	R_y	0.24	$M\Omega$	~ 60	
	L_y	35.34	H	~ 60	✓
Leakage inductance	L_{3A}	119.1	mH	300	✓
	L_{3B}	121.5	mH	300	✓
	L_{3C}	125.8	mH	300	✓
Ground capacitance	C_{HG}	1733	pF		✓
	C_{LG}	16029	pF		✓
Inter-winding capacitance	C_{HL}	9138	pF		✓
Series capacitance	C_{SH}	2.30	nF		✓
	C_{SL}	–	–		

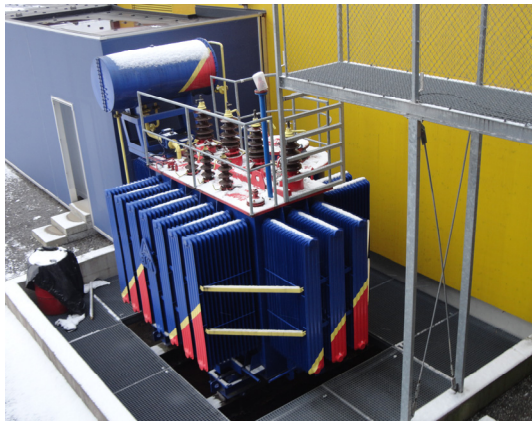
5.3 Summary

Application of the proposed method in chapter 3 on the transformer T_2 in determination of its electrical parameters for purposes of FRA interpretation and failure diagnostic is basically successfully implemented. The core, leakage inductances and different winding capacitances (ground, inter-winding and series) are reasonably calculated, which yields very good matches between measured and simulated frequency responses in broad frequency range. The fact that the winding series capacitance is identified via simulation approach confirms that the winding series capacitance in transformer bulk is now determinable, which is considered valuable for investigations on frequency dependent performances of power transformers such as FRA (in frequency domain) or transient analysis (in time domain). It is important to recall that currently the winding series capacitance is neglected in transient analysis in power transformers [Mork-07a, Mork-07b, Martinez-05b, Hoidalén-08, Chiesa-10b etc.], which might contribute to large errors in case the series capacitance is much higher than other capacitances, e.g. when the winding is multi-layer or interleaved one. The high total capacitance contributed from all capacitances of the transformer T_2 is the reason for the fact that the core's electrical parameters are only dominant in open-circuit frequency responses within a very limited low frequency range, from 20 Hz to 60 Hz, compared with the range from 20 Hz to 400 Hz for the T_1 transformer core.

6 Case study III: A 6.5 MVA 47/27.2 kV YNd5 transformer (T₃)

In chapters 4 and 5, the proposed method has been basically successful applied to analyze the electrical parameters referred into the star HV winding of the small distribution 0.2 MVA 10.4/0.462 kV transformer (T₁) and the delta HV winding of the medium distribution 2.5 MVA 22/0.4 kV transformer (T₂) for purposes of FRA interpretation and failure diagnostic. The common point between the investigations in the two chapters is analyses at the LV winding side are not executed since the input impedances observed at this side are too low to be measured correctly. Therefore a larger power transformer that enables analyses at both sides is therefore required to be investigated since large power transformers are the most important ones in the power system compared with small or medium power transformers.

Thanks to the cooperation between Schering-Institut and Omicron electronics concerning transformer parameter determination, the author had a chance to investigate the proposed method on a large distribution transformer at Klaus, Austria: a 6.5 MVA 47/22 kV YNd5 transformer (T₃) whose appearance and name-plate data are shown in Figure 6.1. The transformer T₃ not only meets the above-mentioned requirements but also has a very appropriate vector group (YNd5) with different winding connections, i.e. star-delta, so that it is considered as a perfect test object to test. Similarly to the transformer T₂, the transformer T₃ is sealed, that means the electrical parameters calculated from the proposed method are used for mainly FRA interpretation purpose and as “fingerprints” for any diagnostic in the future. In this chapter, results obtained from the new method will be compared with those derived from conventional measurement methods performed by Omicron for an objective conclusion for the application of the new method in reality [Pham-13b].



Parameter	Value		Unit
Rated power	6500 / 7800		kVA
Rated voltages	51.7/47/42.3	27.2	kV
Rated currents	79.8 / 95.7	138 / 166	A
Vector group	YNd5		
Frequency	50		Hz
Rated short-circuit voltage	6.26/5.95/5.68/7.51/7.14/6.81		%
Year	1962		

Figure 6.1: Appearance of the transformer T₃ and its name-plate data

6.1 Application of the new method in determination of electrical parameters referred into the HV star winding

The equivalent circuit for analysis at HV side at balanced excitation is introduced in Figure 6.2 which should be adapted for single phase measurements as mentioned in chapter 3. The adaptation is mainly on the appearance of zero-sequence impedances and leakage inductances that might not be very important since it is realized through simulation that there is no significant difference between simulated frequency responses when one, two or three zero-sequence impedances and/or leakage inductance are considered in the circuit. The most important thing is that

one circuit is only suitable for analysis at one side; for analysis at other side of the transformer, another circuit should be developed with regard to the changes of the ideal transformers and the values of resistive and inductive components. Thus the circuit in Figure 6.2 is only appropriate for analysis of the transformer electrical parameters referred into its HV side.

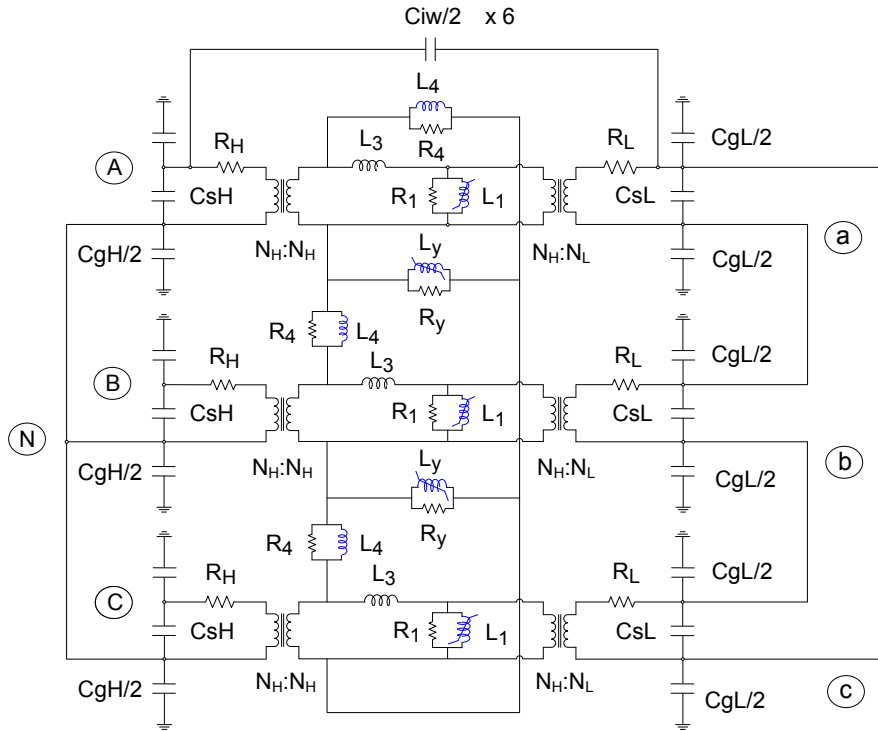


Figure 6.2: Duality based equivalent circuit for analysis of the transformer T_3 at the star winding side

6.1.1 Per-phase winding resistances and leakage inductances

The short-circuit input impedance test for determining per-phase winding resistances and leakage inductances of the transformer T_3 is shown in chapter 3 and will not be recalled here. To find the low frequency range for calculating the winding resistances and leakage inductances from measurements, Figure 6.3 plots the measured input impedance observed at phase A of the transformer from which the range of frequencies from 20 Hz to 400 Hz is selected to calculate the parameters thanks to the adapted approach in chapter 3. The calculated values from measurements at low frequencies and fitted frequency dependencies in broad frequency range for diagnostic and simulation purpose are then introduced in Figures 6.4a and 6.4b.

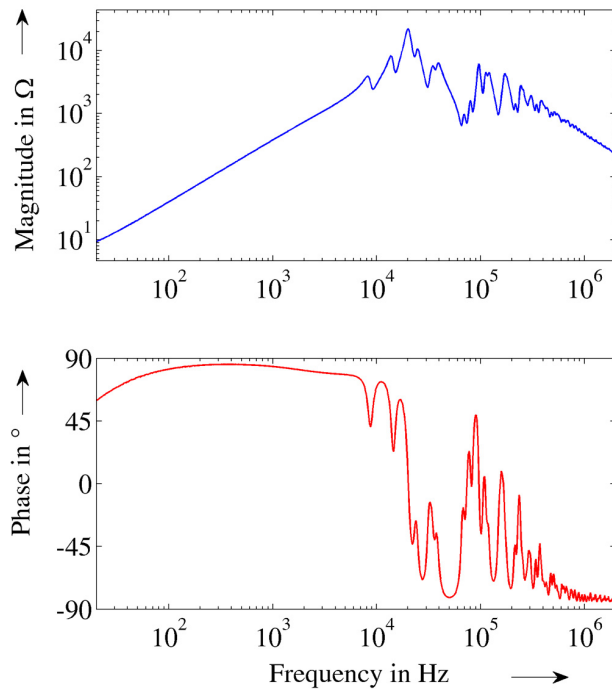


Figure 6.3: Measured frequency response of input impedance

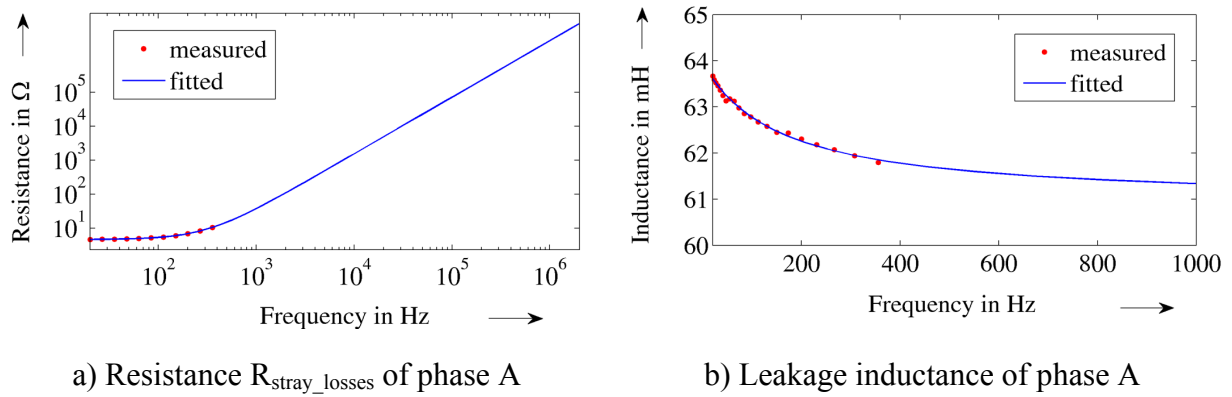


Figure 6.4: Calculated values from measurement at low frequencies and fitted frequency dependencies in broad frequency range

In Figure 6.4 it is observed that good results are derived from the calculation of the parameters at low frequencies, e.g. the calculated inductances at different frequencies are nearly constant and quite reasonable, which is not achieved with the transformers T₁ and T₂. Compared with those obtained from the conventional method (CON) conducted by Omicron, results obtained from either measurement extracted values or fitted frequency dependencies (IMP) are quite similar as observed from Figure 6.4 and Table 6.1. Note that the conventional measurements carried out by Omicron are only at power frequency, which is still considered sufficient for real diagnostics.

Table 6.1: Per-phase leakage inductance referred into HV side

Fre- quency in Hz	Leakage inductance, in mH								
	Phase A			Phase B			Phase C		
	CON	IMP	Error, in %	CON	IMP	Error, in %	CON	IMP	Error, in %
20	–	63.6		–	63.2		–	62.6	
50	62.7	63.2	0.8	62.3	62.9	1.0	61.6	62.2	1.0
100	–	62.8		–	62.5		–	61.7	
200	–	62.3		–	62.0		–	61.2	
300	–	62.0		–	61.8		–	60.9	
400	–	61.8		–	61.6		–	60.8	

6.1.2 Zero-sequence inductance and resistance of the HV star winding

The zero-sequence test of the star winding for transformers with Yd or Dy vector group is already introduced in chapter 3. For practical application, only analysis on the measured impedance obtained after this test is sufficient without any further consideration on the influence of the delta winding on the measured star winding. Therefore, only the measured impedance in Figure 6.5 is required for the analysis.

According to the adapted approach for determination of zero-sequence parameters, a low frequency range is first requested from analysis of the phase angle of the measured impedance (from 20 Hz to 400 Hz) so that the resultant zero-sequence inductance and resistance are then determined plotted in Figure 6.6. Recall that the zero-sequence parameters in this case are in accordance with the short-circuit condition since the LV winding is the delta one. However, it leads to no consequence since the calculated short-circuit zero-sequence parameters are part of the circuit used for the analysis of open-circuit frequency responses.

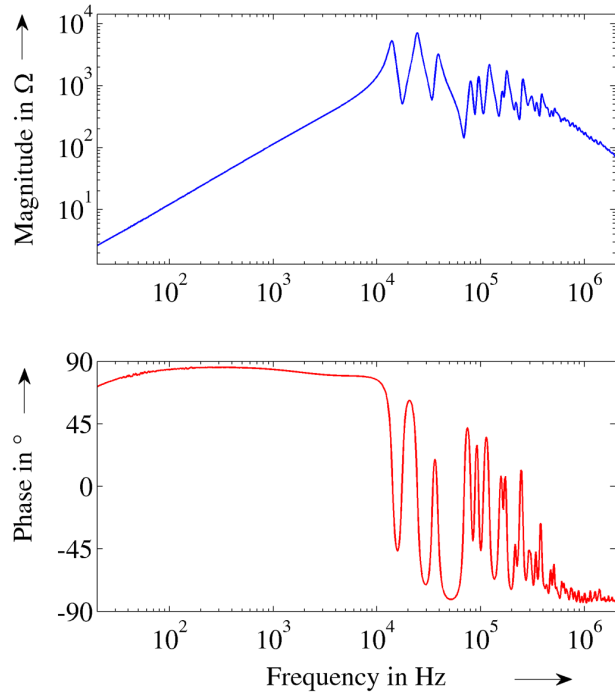


Figure 6.5: Measured frequency response of input impedance

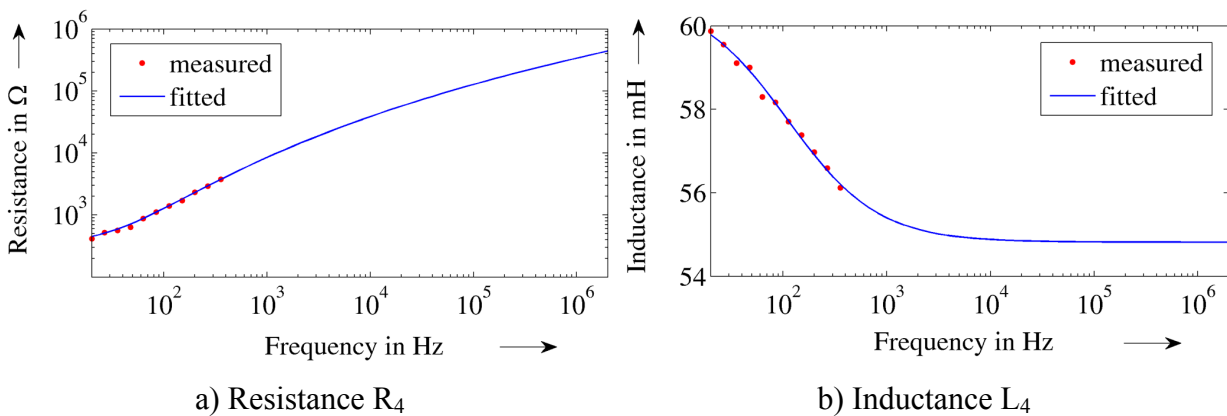


Figure 6.6: Calculated values from measurement at low frequencies and fitted frequency dependencies of zero-sequence parameters in broad frequency range

Table 6.2 lists the zero-sequence inductances of the star HV winding of the transformer T_3 calculated from the adapted approach at several frequencies from 20 Hz to 400 Hz and from the test report of Omicron at 50 Hz for comparison. Small error between the values at 50 Hz (0.8 %) indicates that the adapted approach is best used for large power transformers.

Table 6.2: Zero-sequence inductance referred into HV side

Frequency in Hz	Zero-sequence inductance, in mH		
	CON	IMP	Error, in %
20	–	59.8	
50	58.4	58.9	0.9
100	–	57.9	
200	–	56.9	
300	–	56.4	
400	–	56.1	

6.1.3 Core section inductances and resistances

6.1.3.1 Measurement-based core electrical parameters at low frequencies

According to the proposed approach for determination of core electrical parameters referred into the transformer's star winding in chapter 3, measurements of different open-circuit input impedances at the analyzed winding side are carried out whereas the other winding is left floating. Figure 6.7a illustrates the measurement circuit of a typical open-circuit input impedance at low frequencies for easy observation while Figure 6.7b depicts the measured impedance in wide frequency range for determination of the low frequency range for core parameter analysis. As a result, the range of frequencies from 20 Hz to around 100 Hz is selected for the analysis since within this range there is merely effect of core parameters in measured impedances.

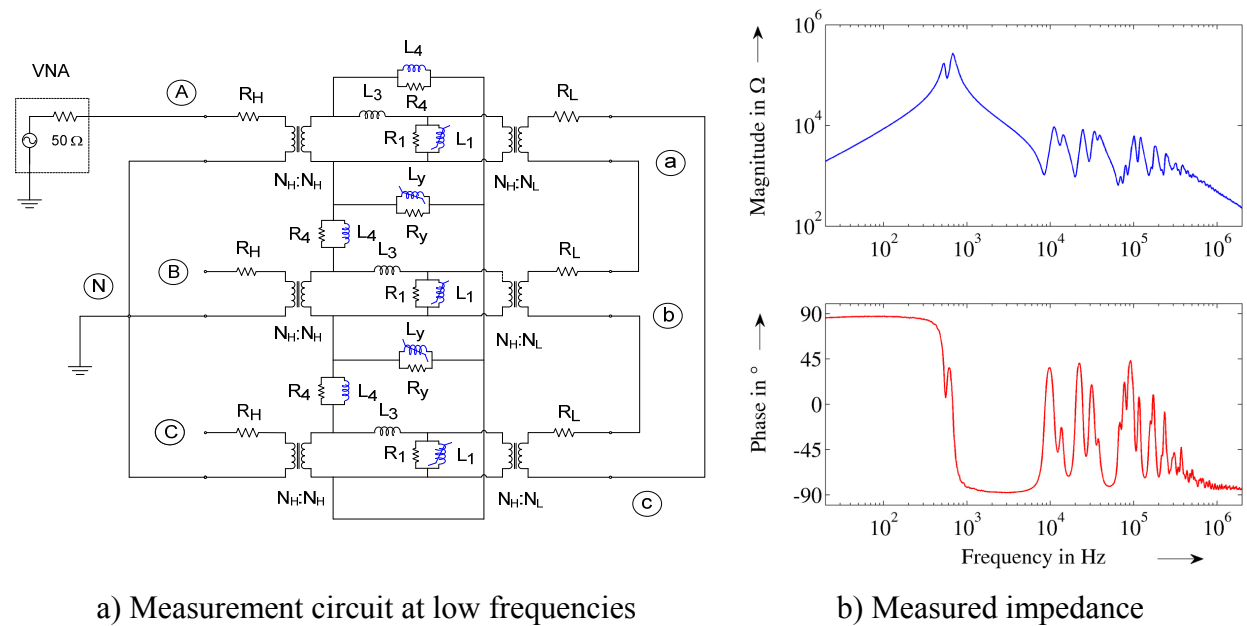


Figure 6.7: Measurement circuit and measured input impedance observed at phase A

Then the data fitting process based on (3.8) with full input mode is conducted to solve the variables Z_{l1} and Z_y at measured frequencies within 20 Hz to 100 Hz. With acceptable errors reported after the process (maximum 2.39 % for magnitude and 0.69° for phase angle from the nine measured configurations), the resultant Z_{l1} and Z_y are then converted into their fundamental components (R_1 , L_1 and R_y , L_y respectively) depicted in Figure 6.8.

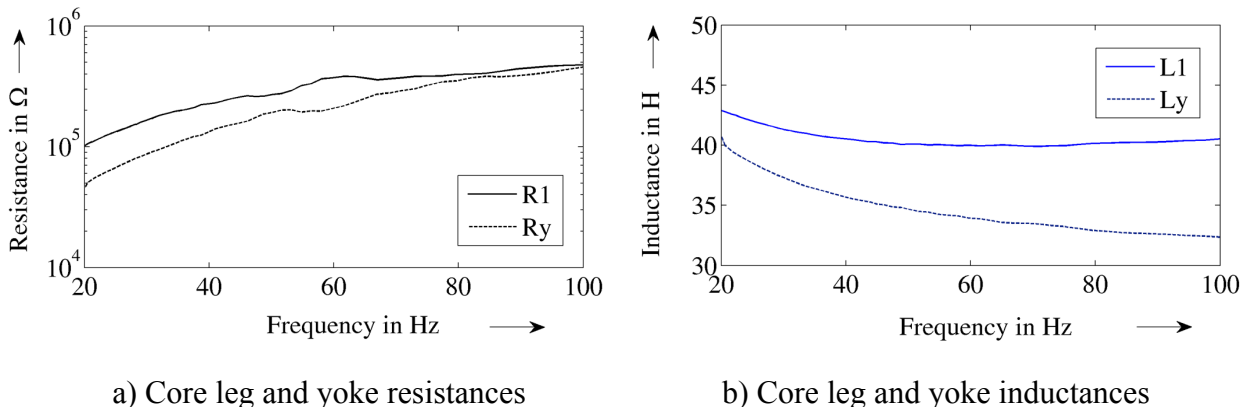


Figure 6.8: Calculated core electrical components from measurements

6.1.3.2 Formula-based core electrical parameters at frequencies higher than 100 Hz

At frequencies higher than 100 Hz (to 2 MHz), the “reference” curves developed from the transformer T₁ are multiplied with factors in Table 6.3 to obtain the analytical values corresponding to the measurement-based ones.

Table 6.3: Detailed calculation of the multiple factors for the adaptation

Electrical parameter of the core		Measurement-based value at ~100 Hz (A)		Value of the normalized reference curve at ~100 Hz (B)	Multiple factor (A/B)	
Resistance	legs	0.45	MΩ	0.056	8.04	MΩ
	yokes	0.43			7.68	
Inductance	legs	39.72	H	1	39.72	H
	yokes	31.50			31.50	

6.1.3.3 Frequency dependency of core electrical parameters in broad frequency range

Figure 6.9 plot frequency dependencies of core electrical parameters referred into the HV side of the transformer T₃ in broad frequency range by combining those in Figure 6.8 and the corresponding ones calculated from the reference curves with factors in Table 6.3. In Figure 6.9a, the core resistances are quite identical at high frequencies since the multiple factors are nearly equal due to the similarity of measurement based values at 100 Hz. More importantly, it is realized that the core inductances in Figure 6.9b have similar tendency, i.e. the relation between core leg and yoke, with that of the transformer T₁ since both transformers have the same age (the transformer T₃ was manufactured in 1962).

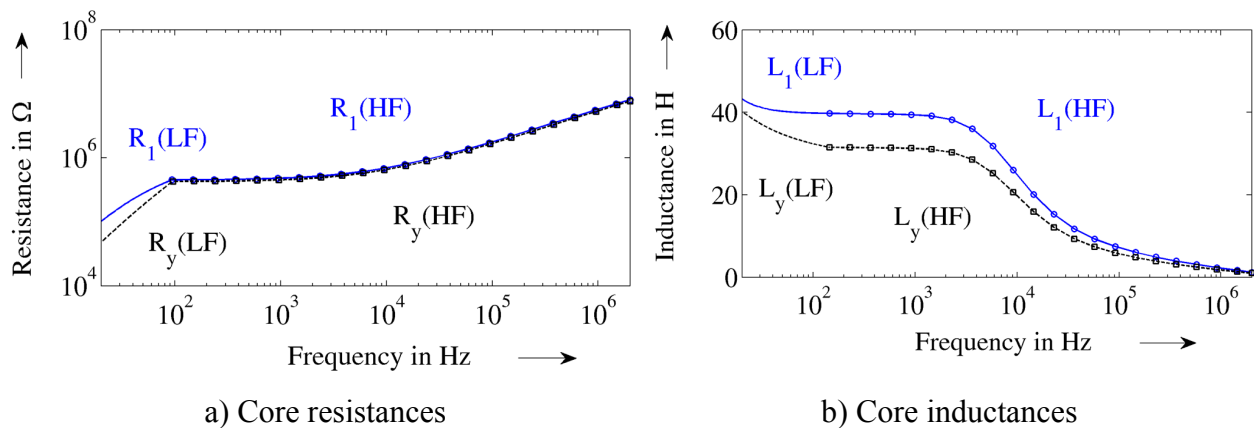


Figure 6.9: Plots of frequency dependencies of core section electrical parameters in broad frequency range

6.1.4 Ground and inter-winding HV-LV capacitance

The capacitive input impedances tests were performed with nearly the same procedure compared with that for the transformers T₁ and T₂. The only difference is that normal wires (without shield) were used to connect the measurement device to bushings and between bushings. Since the capacitances are extracted from the measurements at high frequencies, around 1 kHz compared with 50 Hz measured by the conventional method, large errors in Table 6.4 are obtained and

might be explained due to interference from metal construction outside the transformer (see Figure 6.1). Due to limitation of measurement time allowed by Omicron, measurements with coaxial cables were not performed to check whether the problem comes from the wires. However, it is possible to state that the proposed approach in determining ground and inter-winding capacitances of power transformers is quite reasonable.

Table 6.4: Capacitances determined through the two methods

Capacitance, in pF	CON (measured at 10 kV, 50 Hz)	IMP (measured at 1 V, ~ 1 kHz)	Error, in %
C_{HG}	1966	1886	4.1
C_{LG}	6620	6514	1.6
C_{HL}	8060	7591	5.8

6.1.5 Contribution of winding series capacitances

The equivalent circuit in Figure 6.2 without winding series capacitances is used to simulate configurations of different open-circuit input impedance tests measured at the HV side of the transformer to identify the contribution of the series capacitances of the windings. To show a typical result of the simulation at HV side, Figure 6.10 compares measured and simulated frequency response of the open-circuit input impedance observed at phase A with measuring circuit depicted in Figure 6.7.

In Figure 6.10 one can easily realize that there is a certain deviation between the measured and simulated frequency response at mid frequencies from 1 kHz to 4 kHz, where the winding capacitances dominate other electrical parameters in the open-circuit input impedances, which is totally caused by lack of the winding series capacitances (C_s).

It is realized through simulation that the series capacitance of both HV and LV windings has influence to the open-circuit frequency responses simulated at HV side. Therefore, the analysis of frequency responses at LV side is also required to figure out the win-ding series capacitances.

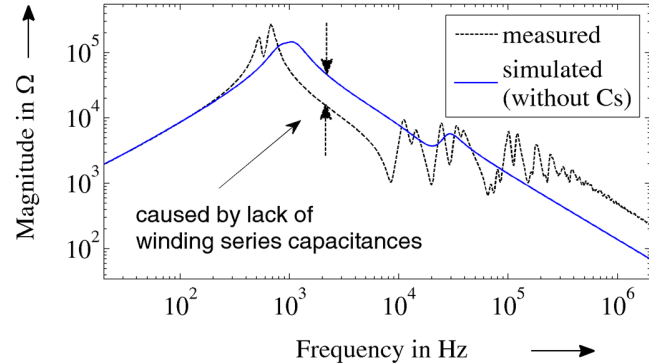


Figure 6.10: Measured and simulated frequency responses of open-circuit input impedance of phase A

6.2 Application of the proposed method in determination of electrical parameters referred into the LV delta winding

The equivalent circuit for analysis at HV side at balanced excitation is introduced in Figure 6.2; however, it cannot be used to simulate measurements conducted at LV side due to arguments introduced in chapter 3, e.g. the zero-sequence impedances are different if measurements are at different sides. Therefore, the equivalent for analysis at LV side shown in Figure 6.11 (source is applied on the right LV side) is necessary. Note that in the analysis, only the short- and open-

circuit tests are considered since the zero-sequence test does not exist for the delta winding whilst the capacitance test is already performed in 6.1.4.

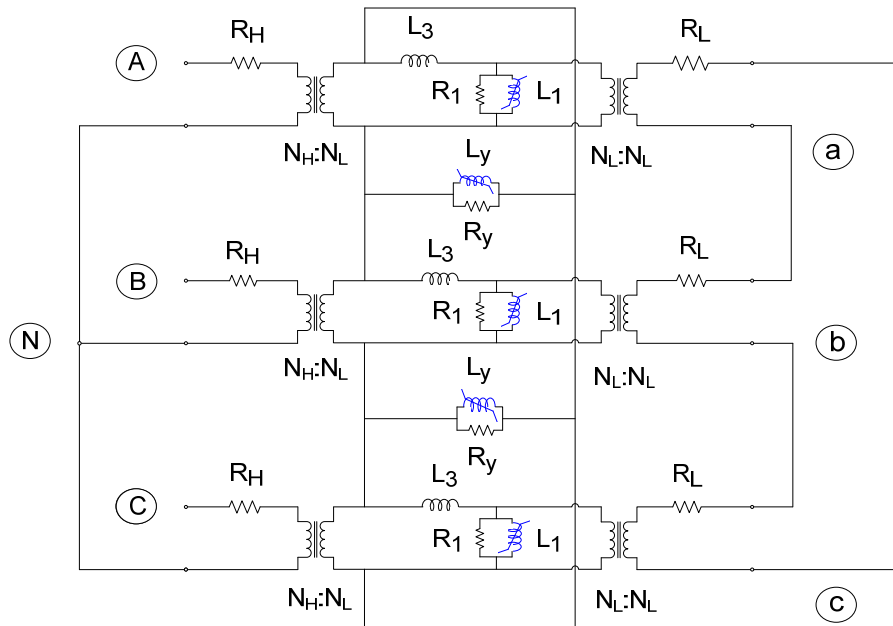


Figure 6.11: Duality based equivalent circuit for analysis of the transformer T_3 at the delta winding side at low frequencies

6.2.1 Per-phase winding resistances and leakage inductances

Similarly to the analysis at HV side, the same low frequency range for calculating winding resistances and leakage inductances from short-circuit input impedance measurements at LV side according to Figure 6.12 is obtained, from 20 Hz to 100 Hz. Afterwards the electrical parameters are determined and depicted in Figure 6.13. Small differences between the electrical parameters in Figures 6.13 (LV side) and 6.4 (HV side) are observed and explained due to the small ratio of the transformer (47/27.2 kV). Since there is no measurement result from the conventional method at LV side, the comparison between the two methods is not possible.

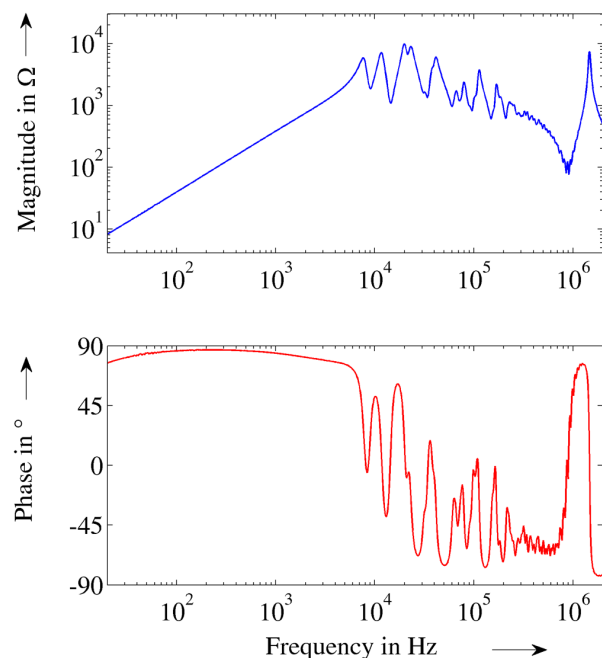


Figure 6.12: Measured frequency response of input impedance at LV side

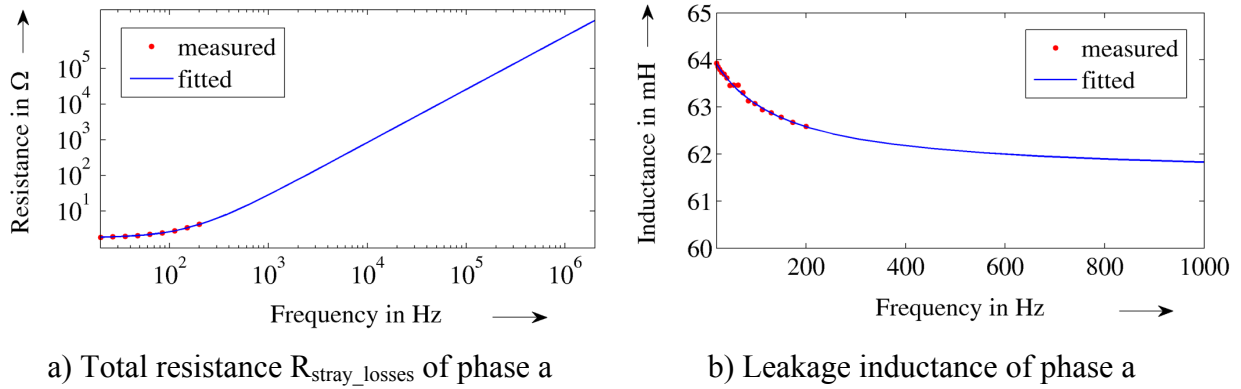


Figure 6.13: Calculated values from measurement at low frequencies and fitted frequency dependencies in broad frequency range

6.2.2 Core section inductances and resistances

6.2.2.1 Measurement-based core electrical parameters at low frequencies

For the analysis of the core electrical parameters referred into the LV side, Figures 6.14a and 6.14b present the measurement circuit of a configuration of an open-circuit LV input impedance and its result respectively. Compared with that in Figure 6.7b, the measured impedance in Figure 6.14b is quite similar with regard to magnitude and phase angle at low frequencies, from 20 Hz to 100 Hz; as a result, the core inductances referred into the LV side calculated after the fitting process are comparable with those referred into the HV side whereas there is large deviation observed with the core leg resistance R_1 . The large deviation of the resistive components is due to small difference between measured phase angles taken into account in the fitting process and has totally no significant influence to the circuit performance.

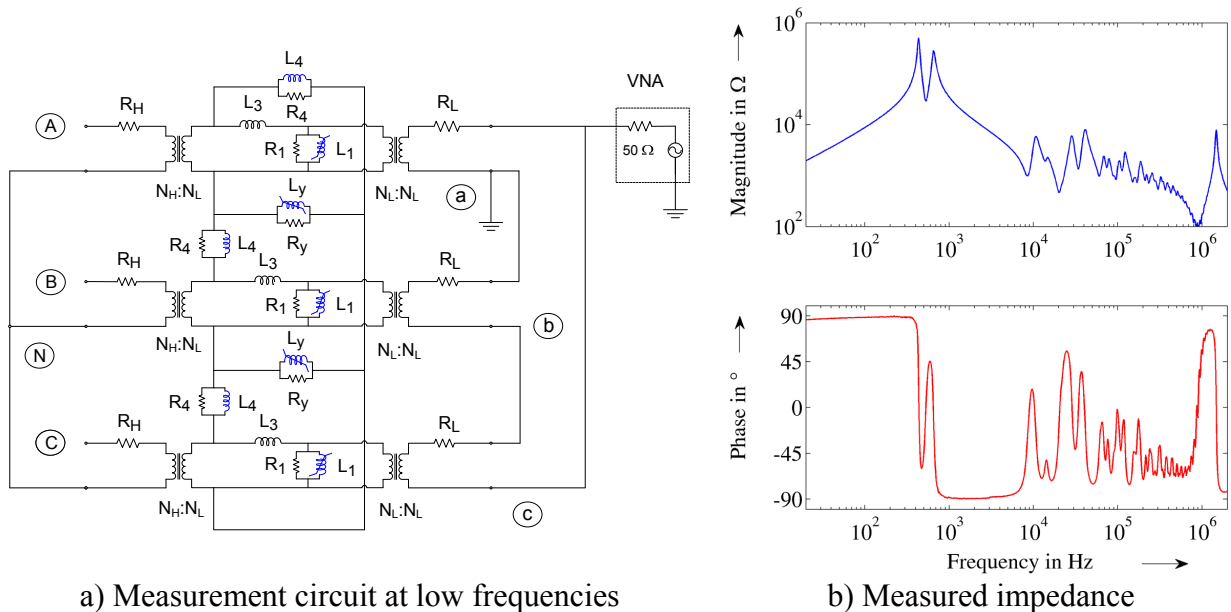


Figure 6.14: Measurement circuit and measured input impedance observed at phase A

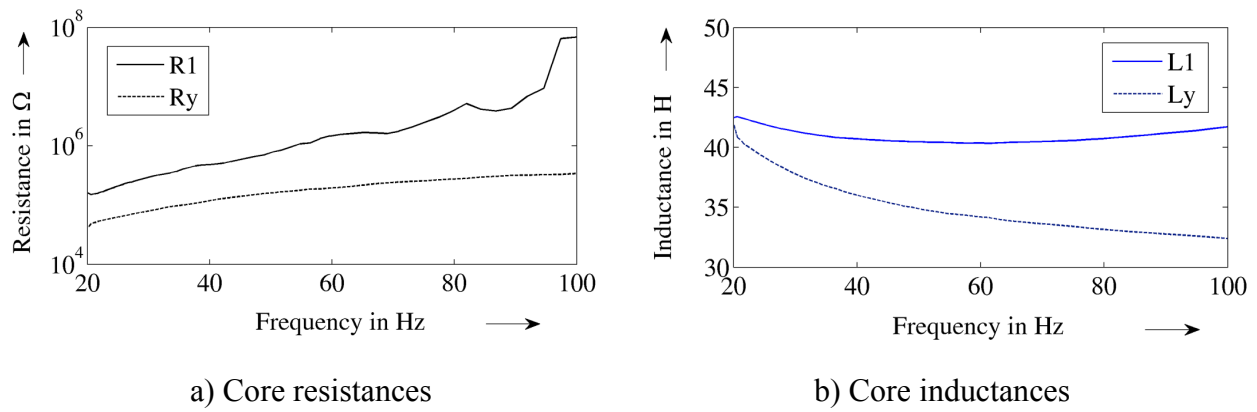


Figure 6.15: Calculated core electrical components from measurements

6.2.2.2 Formula-based core electrical parameters at frequencies higher than 100 Hz

Table 6.5 lists measurement based core values at the transition frequency (100 Hz) and the relevant multiple factors for getting the analytical values at frequencies higher than 100 Hz. A similarity between the multiple factors in Tables 6.5 (for LV side) and 6.3 (for HV side), except for core leg resistance, confirms that the parameters referred into both side are not significant different, which is due to the small ratio of the transformer.

Table 6.5: Approximate calculation of the multiple factors for the adaptation

Electrical parameter of the core		Measurement-based value at ~100 Hz (A)		Value of the normalized reference curve at ~100 Hz (B)	Multiple factor (A/B)	
Resistance	legs	5.34	MΩ	0.056	95.36	MΩ
	yokes	0.33			5.89	
Inductance	legs	40.35	H	1	40.35	H
	yokes	32.11			32.11	

6.2.2.3 Frequency dependency of core electrical parameters in broad frequency range

The calculated core parameters at low frequencies are then fitted and combined with those at high frequencies to form the final frequency dependencies of the core parameters. Figure 6.16 plots frequency dependencies of core electrical parameters referred into the LV side of the transformer T_3 in broad frequency range. It is noted that whereas the core inductances, the most important electrical parameters, are comparable with those referred into HV side, the core leg resistance at high frequencies (HF) is much higher than the core yoke resistance, which is not the case for analysis at HV side. The large difference indicates that the “reference curve” approach is only efficient when the values calculated from measurements are reasonable at the transition frequency. It is therefore suggested that the low frequency range should be carefully selected from the measurements in this case so that there is no significant change of phase angles of impedances inputted into the fitting process. Nevertheless, even in such cases, the core parameters are reasonable derived, which means the good performance of the approach is still reached and guarantees for the success in practical applications.

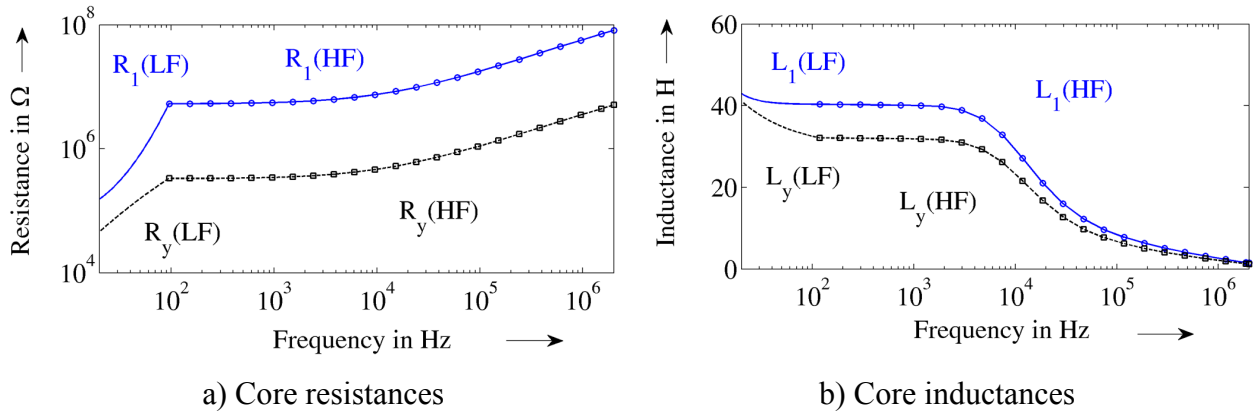


Figure 6.16: Plots of frequency dependencies of core section electrical parameters in broad frequency range

6.3 Determination of series capacitance of the HV and LV windings

Contribution of the winding series capacitances to the total capacitance can be recognized from observation of two typical open-circuit input impedances shown in Figures 6.17a and 6.17b measured and simulated (without series capacitances C_s) at HV and LV side respectively. It is realized from the figures that the contribution of the winding series capacitances is only significant for open-circuit frequency responses at HV side. It is understandable since the ground capacitance of the HV winding (~ 657 pF) is much lower compared with that of the LV winding (~ 2.53 nF). Consequently, the series capacitances of the windings which are necessary for investigations at HV side should be within a range of 657 pF to 2.53 nF.

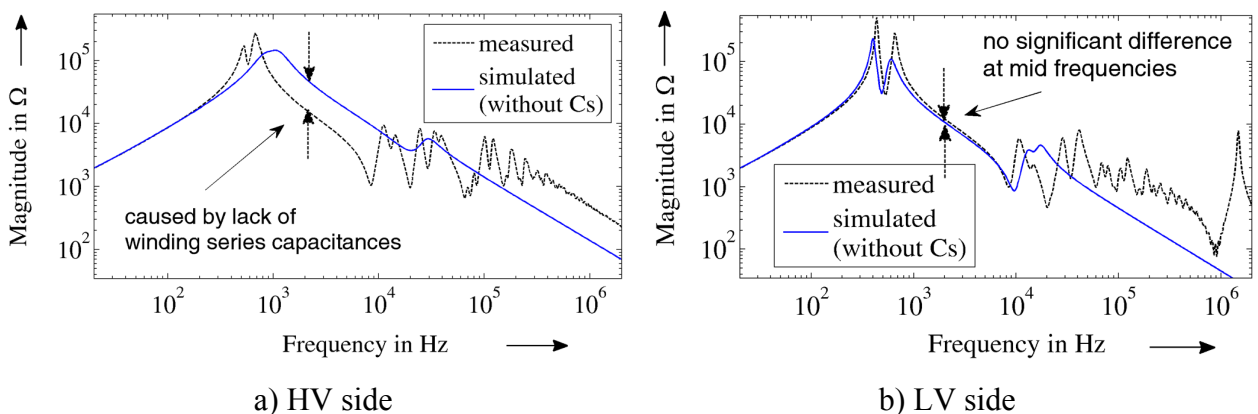


Figure 6.17: Typical open-circuit input impedances

Since the series capacitances of both HV and LV windings influence the open-circuit frequency responses, judgments of possibilities of series capacitances of HV and LV windings can be based on transformer type and rated voltages/currents because of unavailability of design data. It is well known that the series capacitance depends on only winding types and can be low (for continuous disc-type) or high (for interleaved disc-type). Since the transformer has rated parameters: 6.5 MVA, 47/27.2 kV and 79.8/138 A, it can be assumed that the transformer is a large distribution one with multi-layer windings (associated with medium series capacitance). Under this assumption, the LV winding should have higher series capacitance. Simulation result shown in Figure 6.18a in next section confirms this fact with approximate values of series capacitances of 1.3 nF for HV windings and 2.3 nF for LV windings. Although the series capacitances may not

be accurate, the approach provides a possibility to know how high the series capacitances are as compared with ground capacitances so that further investigations can be based on. It is valuable not for FRA application but also for transformer transient analysis which neglects the series capacitances due to their indeterminableness.

6.4 Parameter-based FRA interpretation and failure diagnostic

The proposed method was exploited to determine the electrical parameters that are considered important for purpose of a physical FRA interpretation and a comprehensive diagnostic of failure in the active part of power transformers. Each of the purposes then will be introduced in detail below.

6.4.1 Parameter-based FRA interpretation in broad frequency range

6.4.1.1 Interpretation of frequency responses of open-circuit input impedances

The principle of the physical FRA interpretation is based on the circuit simulation by investigation of the contribution of individual components in the equivalent circuit to the simulated frequency responses. For the transformer T_3 , interpretations of open-circuit input impedances at both sides based on Figures 6.18a and 6.18b are quite similar in most sub frequency ranges, except there is a difference at very high frequencies.

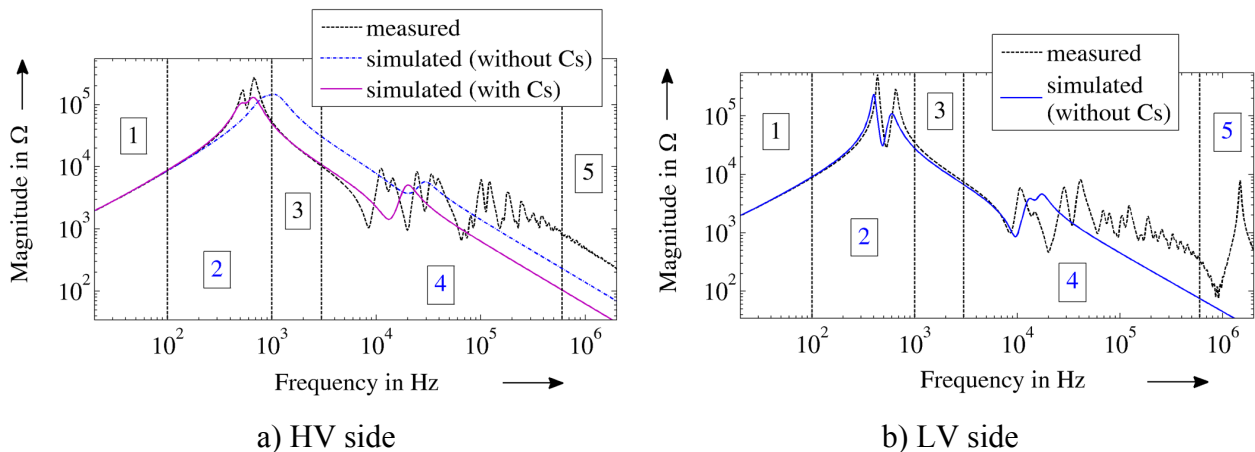


Figure 6.18: Open-circuit input impedances

From Figures 6.18, the interpretation of non-standard open-circuit frequency responses at both sides can be obtained as follows:

- Region ① (20 Hz to 100 Hz): dominant by inductive core influence.
- Region ② (100 Hz to around 1 kHz): interaction between core inductances and winding capacitances (from inductive into capacitive behaviour).
- Region ③ (1 kHz to around 3 kHz): dominant by winding capacitances. Contribution of winding series capacitances to open-circuit frequency responses is only significant at HV side.
- Region ④ (3 kHz to 600 kHz): interaction between winding capacitances and leakage inductance in a capacitive tendency. Only simulation of the distributed equivalent circuit could give reasonable agreements at such frequencies!

- Regions ⑤ (600 kHz to 2 MHz): interaction between winding capacitances and all inductances, including parasitic inductances from other components outside the transformer (capacitive tendency at HV side)

6.4.1.2 Interpretation of frequency responses of open-circuit voltage ratios (the standard EEOC-FRA tests)

It is noted that the interpretation for non standard frequency responses in the sub section 6.4.1.1 can be also applied for standard frequency responses in Figure 6.19 in terms of influence of individual electrical parameters in the circuit on the frequency responses in specific frequency ranges. The interpretation of both non-standard and standard frequency responses concludes that the duality based equivalent circuit for the transformer T₃ is valid in a very limited frequency range, from 20 Hz to 3 kHz, compared to the other test transformers. However, it is sufficient to determine the electrical parameters applicable for physical FRA interpretation and failure diagnostic.

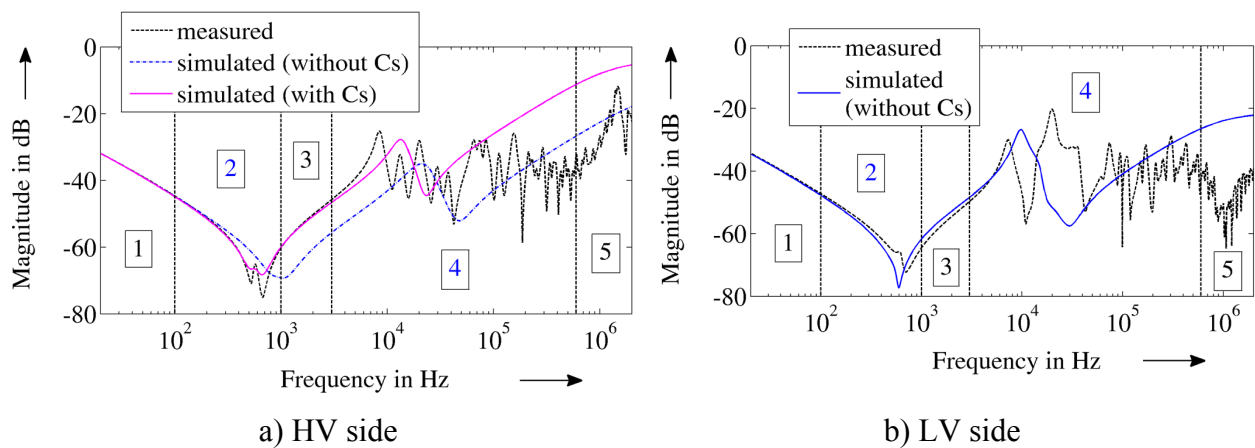


Figure 6.19: EEOC-FRA traces (simulation with appearance of winding series capacitances)

6.4.2 Parameter-based failure diagnostic

To diagnose mainly the electrical and mechanical failures in transformer active part, the electrical parameters determined directly from the measurements (core, leakage and zero-sequence inductances as well as ground and inter-winding capacitances) and from the simulation (winding series capacitances) through the proposed method can be used as “fingerprint” for the comparisons between phases (phase-based comparison mode) or between different time points (time-base comparison mode). Table 6.6 lists these parameters obtained from the proposed method for diagnostic purpose.

It is noticed in Table 6.6 that the winding series capacitances derived from simulation are in accordance with selected values of other electrical parameters determined from the proposed approaches. Thus these winding series capacitances may not be very accurate since there are certain errors of the ground and inter-winding capacitances compared with the conventional method depicted in Table 6.4. It is also important to state that the measured ground and inter-winding capacitances consist of other capacitive components inside transformers such as stray capacitances between winding leads and bushing capacitances. Nevertheless the proposed method is still useful in detection of the parameter change which makes sense for the diagnostic.

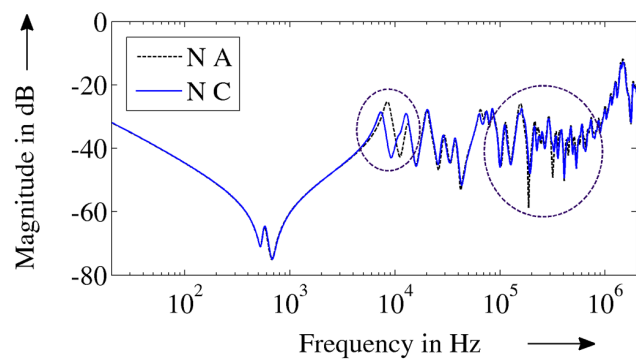
Table 6.6: Electrical parameters (referred into the HV side) of the transformer T_3 calculated from the proposed method

Electrical parameter		Value	Unit	at frequency, in Hz	Applicable for diagnostic
Core leg	R_1	0.45	$M\Omega$	~ 100	
	L_1	39.72	H	~ 100	✓
Core yoke	R_y	0.43	$M\Omega$	~ 100	
	L_y	31.50	H	~ 100	✓
Leakage inductance	L_{3A}	63.2	mH	50	✓
	L_{3B}	62.9	mH	50	✓
	L_{3C}	62.2	mH	50	✓
Zero-sequence inductance	L_4	58.9	mH	50	✓
Ground capacitance	C_{HG}	1886	pF		✓
	C_{LG}	7591	pF		✓
Inter-winding capacitance	C_{HL}	6514	pF		✓
Series capacitance	C_{SH}	1.3	nF		✓
	C_{SL}	2.3	nF		✓

6.5 Summary

The electrical parameters of the transformer T_3 are determined reasonably from the proposed method for the purposes of parameter-based FRA interpretation and failure diagnostic. Several conclusions about the electrical parameters can be drawn as follows:

- The resistive components in the equivalent circuit such as resistances of winding, zero-sequence path and core sections are only appropriate for the simulation since they are not consistent due to several factors: low applied voltage in measurements, uncertainty in analysis (small variation of phase angles leads to large change on core resistance) etc.
- The core inductances and capacitances determined from the proposed method can be applied for both FRA interpretation and relevant diagnostic whereas the zero-sequence/leakage inductance are only appropriate for the diagnostic since their influence on simulated frequency responses is not clear. An example for application of the proposed method in analysis of the transformer condition is a difference of 1.7 % between the leakage inductances of phases A and C in comparison with no information from the FRA assessment of the deviation between two standard frequency responses introduced in Figure 6.20 (or Figure 5 in the introduction part). Furthermore, the information of the series capacitances derived from the proposed method is considered valuable for diagnostic of mechanical winding failure, simulation-based interpretation at mid and high frequencies and transient analysis of the transformer.

**Figure 6.20:** Comparison of FRA traces measured on phases A and C at HV side

Conclusion

The dissertation is involved with two different issues in the field of diagnostics of electrical/mechanical failures in the active part of power transformers, whose state-of-the-art can be described as follows:

1. FRA interpretation and assessment to detect failures

Currently the FRA interpretation is mainly based on analysis of distributed transformer circuits in terms of sectional electrical parameters calculated from design data. It is however realized that the interpretation of terminal frequency responses at mid and high frequencies where effect of mechanical failures takes place has been not yet successful from investigations of windings in transformer bulk; in fact the investigations are only reasonable for analysis of windings when they are out of the transformers. Thus there is a question concerning the improvement of investigations of the distributed equivalent circuit for FRA purpose whereas the efficiency and effort are not proportional; in addition, the issue of design data is also problematic, at least for old transformers in operation.

On the other hand, assessments of frequency responses measured at transformer's terminals are mostly based on non-physical analysis, e.g. correlation coefficients between measured signals in different frequency ranges [DL/T911-04]. Due to the fact that the non-physical analysis reveals limited information with regard to failure type and level, it is therefore required that kind of *physical* analysis should be developed to support the diagnostic.

2. Determination of *necessary* electrical parameters of transformers for failure diagnostic

At the moment most electrical parameters of power transformers could be determined via conventional and advanced electrical testing methods, e.g. winding resistance, leakage and zero-sequence inductance, ground and inter-winding capacitances. However, the core section impedances and winding series capacitances are still in general indeterminable. For a comprehensive parameter-based diagnostic of failures in the transformer's active part, it is requested that the core electrical impedances and winding series capacitances should be identified.

In order to overcome these limitations for the purpose of getting a better failure diagnostic applicable to power transformers in terms of a physical FRA interpretation and the determination of key electrical parameters, the dissertation is promoted to find out a solution for solving both problems.

The solution investigated in the dissertation is a new and *non-destructive* method in determination of electrical parameters of power transformers, which is proposed based on following improvements/contributions from the author:

- Adaptation of the duality based equivalent circuit of power transformers, which is originally developed for transient analysis of power transformers in low and mid frequency range

- Selection of measurement of different input impedances carried out by means of the VNA at low applied voltage (~ 1 V) and broad frequency range (20 Hz to 2 MHz) as the main measurement since the measurement is required non-destructive and the determined parameters should be later on available in broad frequency range for further analysis
- Adaptation/development of several existing and new approaches in determination of relevant electrical parameters with regard to the measurements and corresponding analyses based on the adapted equivalent circuit

The proposed method has been applied on three test transformers with different rated powers, voltages and vector groups in order to check its performance for practical application. In summary, it can be stated that the proposed method is efficient for any two-winding transformer with regard to parameter determination since all necessary electrical parameters of the tested transformers could be determined conveniently by using only the VNA for the measurements. However, the effectiveness of the method for a better diagnostic of mechanical failures in comparison with the current FRA method was confirmed for only the opened transformer T_1 , since there was a chance to perform the failures in its active part; for the sealed transformer T_2 and T_3 , the method was only applied to determine their electrical parameters in healthy condition, which are considered as “fingerprints” for any comparison in the future for diagnostic purpose.

Regarding the physical FRA interpretation based on electrical parameters, it is concluded that the valid interpretation is limited from low to mid frequency range because of the lumped characteristic of the circuit and its components. Although the physical interpretation seems to be not helpful for the diagnostic of mechanical failures in transformer windings, since the interest frequencies associated with the failure is in mid and high frequency range, there are however three clear contributions which are considered important for further researches in the FRA and transient analysis field:

- The frequency dependency of electrical parameters of core legs and yokes is useful for improving the characteristic of the *distributed* transformer circuit in interpretation in *low* frequency range.
- The winding series capacitance in transformer bulk could be determined based on the assessment of measured open-circuit frequency responses and interpretation of simulated corresponding frequency responses at mid frequencies, where the total winding capacitance is dominant in open-circuit frequency responses.
- The (lumped) electrical parameters determined through the proposed method are considered as fundamental information for development of a distributed equivalent circuit for a better FRA interpretation at mid and high frequencies in cases transformer design data are not available. The challenge is only to calculate self/mutual inductance of winding sections from the leakage inductance since the sectional capacitances are easily found from the equivalent capacitances. Although the precise determination of the sectional inductances is hardly achieved, it is thought that reasonable calculation of the inductances is feasible since there is a relation between self and mutual inductances along and between the windings.

Below are separate conclusions obtained after applying approaches of the proposed method on the three tested transformers.

1. The duality based equivalent circuits

- The duality based equivalent transformer circuit is applied to analyze three different two-winding transformers in whole frequency range but is valid in low and mid frequency range. The mid frequency range is defined as the range where the influence of winding capacitances become dominant on the open-circuit frequency responses.
- The duality based equivalent circuit is ideally for detailed investigation of the interaction between core/zero-sequence inductances and winding capacitances. In fact interaction between winding capacitances and leakage inductance is not obvious since the leakage inductance belong to the electric-magnetic area in the circuit where the core and zero-sequence inductances appear.
- Although the duality based equivalent circuit is applied on three two-winding distribution transformers, it is expected that the circuit and the proposed method are still applicable to other transformers with different structures, e.g. auto-transformers, three-winding transformers etc. as confirmed through other researches.

2. First adapted approach in determining per-phase winding resistances and leakage inductances

In the first adapted approach, the traditional short-circuit test is performed by means of a VNA which is able to measure short-circuit input impedances in broad frequency range at both sides of transformers. The associated electrical parameters derived from the approach can be applied for both diagnostic purpose via measurement-extracted values at low frequencies and FRA interpretation purpose via frequency dependencies developed based on measured values at low frequencies and analytical formulae at high frequencies.

- Winding resistances determined from the method are not reliable for diagnostic purpose since they have different tendencies between phases of even new transformers (the T_2). That is caused by the low applied field produced by the instrument in the measurements which associates with the non-predictable distribution of stray losses in transformer structures. It is recommended that the winding resistances should be measured at DC and AC excitation mode at high applied field in addition for a consistent interpretation.
- In contrary with winding resistances, leakage inductances are reliably determined and useful for diagnostic and FRA purpose thanks to the magnetic linearity of non-magnetic materials, e.g. oil/air and winding insulations, in the leakage channel between windings. It is suggested that the applied voltage should be higher than 1 V to remove the effect of core inductance in the measurements (see chapter 5, section 5.1.1)

3. Second adapted approach in determining zero-sequence winding and inductance of the star winding

In the approach, the traditional zero-sequence test is performed by means of a VNA in broad frequency range. Similarly to the first adapted approach, the zero-sequence parameters derived from this approach can be applied for both diagnostic and FRA purpose.

- The zero-sequence resistance does not play an important role in failure diagnostic since it represents mainly the active losses associated with leakage paths outside the windings.

- The zero-sequence inductance can be interpreted together with the (positive-sequence) leakage inductances to find out whether there is any movement of the windings. In reality, the zero-sequence inductance depends much on position/connection of the windings and in some cases (explained in chapter 3), it is not useful for diagnostic since its value is less than the leakage inductances.
- The zero-sequence inductance is appreciably higher than the (positive-sequence) leakage inductances in case the transformers have no tank. In such cases the interaction between zero-sequence inductance and winding capacitances is prominent as introduced in chapter 4. In other cases the contribution of the zero-sequence inductance to the open-circuit frequency responses is not observable since its value is less than that of the leakage inductance.

4. First proposed approach in determining core section resistances and inductances

The first proposed approach is effective in calculation of core section electrical parameters from open-circuit input impedances measured at transformer terminals regardless of how the windings are connected, i.e. star or delta. Furthermore, application of the “reference” curves based on analysis of a test transformer (the T_1) in development of core electrical parameters of any transformer at high frequencies is in first time introduced. The core electrical parameters are then useful for both diagnostic of core failures (via its parameters) and the FRA interpretation in low frequency range.

- The proposed approach is considered very useful in calculation of core electrical parameters from measurements at low frequencies at low applied field for analysis of frequency dependent performance of power transformers. In fact it overcomes the problem of current measurement methods for transformer core parameter calculation that if the transformer has any delta winding, it should be opened up.
- The “reference” curve solution provides the feasibility for the simulation in broad frequency range by development of frequency dependencies of core electrical parameters at high frequencies, which cannot be achieved from any other solution. It is concluded from the investigations that the “reference” curve solution depends much on measurement based values at low frequencies and is applicable to determine best the core inductances at high frequencies in general.

5. Second proposed approach in measuring ground and inter-winding capacitance

The second proposed approach can be considered as an alternative of the conventional measurement method using the guard technique mentioned in chapter 1 in determining ground and inter-winding capacitance of power transformers, at least in research scale. Compared with the conventional method which requires measuring devices with high applied voltage, the measurement by means of a VNA at low applied field is more simple and safe. It is shown in chapter 5 that high accuracy of the measured capacitances can be achieved from the proposed approach.

6. Third proposed approach in identifying winding series capacitance in transformer bulk

The topic of winding series capacitance has been investigated for a long time since it is one of main electrical parameters for different transformer investigations. There is so far the only

possibility of determination of the capacitance based on destructive measurements of distributed voltages along the winding when it is brought out of the transformers. The third proposed approach is therefore considered as the first fundamental one for a lot of investigations later in the topic of determination of winding series capacitance in transformer bulk since it is shown that the winding series capacitance could be at first time determined completely in transformer bulk based on the combination of non-destructive measurements and simulation.

References

A

- [ABB-07] ABB: *Transformer handbook*, 3rd Ed., 2007
- [Abeywickara-07] N. Abeywickrama: *Effect of dielectric and magnetic material characteristics on frequency response of power transformers*, Doctoral dissertation, Chalmers University of Technology, Sweden, 2007
- [Agrawal-01] K.C. Agrawal: *Industrial power engineering handbook*, ISBN 978-0-7506-7351-8, Elsevier Inc., 2001
- [Andrieu-99] C. Andrieu, E. Dauphant, and D. Boss: *A frequency-dependant model for a MV/LV transformer*, Int. Conf. on Power Systems Transients IPST, pp. 468-473, Budapest Hungary, Jun. 1999
- [Ang-08] S. P. Ang, J. Li, Z. Wang, and P. Jarman: *FRA low frequency characteristic study using duality transformer core modeling*, Int. Conf. on Condition Monitoring and Diagnosis, Beijing, April 2008
- [Aponte-12] G. Aponte, H. Cadavid, J. C. Burgos, and E. Gomez: *A methodology for obtaining by measurements the transformer physical-circuitual model parameters*, Przegląd Elektrotechniczny (Elec. Review), ISSN 0033-2097, pp. 12-15, 2012

B

- [Bagheri-11] M. Bagheri, M.S. Naderi, T. Blackburn, and T. Phung: *Practical challenges in online transformer winding deformation diagnostics*, 2nd IEEE Int. Conf. on Electric Power and Energy Conversion Systems, UAE, Nov. 2011
- [Bigdeli-12] M. Bigdeli, M. Vakilian, E. Rahimpour and D. Azizian: *Theoretical and experimental investigation of transformer winding fault detection using comparison of transfer function coefficients*, ECTI Trans. on Elec. Eng., Electronics and Communications, vol. 10, no. 1, pp. 107-113, Feb. 2012
- [Bjerkan-05] E. Bjerkan: *High frequency modelling of power transformers – Stresses and Diagnostics*, Doctoral Thesis, Norwegian University of Science and Technology, 2005
- [Bode100-10] Omicron LAB: *Bode 100 User manual*, 2010
- [Bode100-12] Omicron LAB: *High impedance measurement - Extending the impedance measurement range of the Bode 100*, v1.1, 2012

- [Bossi-83] M. Bossi et. al.: *An international survey on failures in large power transformers in service*, Final Report of CIGRE Working Group 12.05: Reliability, Electra no. 88, pp. 20-48, May 1983
- [Brailford-64] F. Brailsford and R. Fogg: *Anomalous iron losses in cold-reduced grain-oriented transformer steel*, IEE Proceedings, vol. 111, no. 8, pp. 1463-1467, Aug. 1964
- ## C
- [Cherry-49] E Colin Cherry: *The duality between interlinked electric and magnetic circuits and the formation of transformer equivalent circuits*, Proceedings of the Physical Society, Section B, vol. 62, no. 2, pp. 101-111, 1949
- [Chiesa-05] N. Chiesa: *Power transformer modeling - advanced core model*, Master thesis, Politecnico di Milano, Jun. 2005
- [Chiesa-10a] N. Chiesa: *Power transformer modeling for inrush current calculation*, Doctoral Dissertation, Norwegian university of Science and Technology, Jun. 2010
- [Chiesa-10b] N. Chiesa, B.A. Mork, and H.K. Høidalen: *Transformer model for inrush current calculations: simulations, measurements and sensitivity analysis*, IEEE Trans. on Power Delivery, vol. 25, no. 4, pp. 2599-2607, Oct. 2010
- [Cho-02] S. D. Cho: *Parameter determination for transformer modeling*, Doctoral dissertation, Michigan technological university, Dec. 2002
- [Chowdhuri-87] P. Chowdhuri: *Calculation of series capacitance for transient analysis of windings*, IEEE Trans. on Power Delivery, vol. 2, no. 1, pp. 133-139, Jan. 1987
- [Colla-10] L. Colla, V. Iuliani, F. Palone, M. Rebolini and C. Taricone: *EHV/HV autotransformers modeling for electromagnetic transients simulation of power systems*, 19th Int. Conf. on Elec. Machines ICEM, Italy, 2010
- ## D
- [Davari-09] M. Davari, S.M. Aleemran, A.R. Mobarhani, H. Nafisi, I. Salabeigi, and G.B. Gharehpetian: *A novel approach to VFTO analysis of power transformers including FVL based on Detailed Model*, IEEE Int. Conf. on Industrial Technology, Feb. 2009
- [Dick-78] E.B. Dick and C.C. Erven: *Transformer diagnostic testing by frequency response analysis*, IEEE Trans. Power Apparatus and Systems, vol. PAS-97, no. 6, pp. 2144-2153, 1978

[Dixon-94] L. Dixon: *Deriving the equivalent electrical circuit from the magnetic device physical properties*, Texas Ins. Document, Oct. 1994 (available at <http://www.ti.com/lit/ml/slup198/slup198.pdf>)

E

[Eldery-03] M. A. Eldery, E. F. El-Saadany, and M.M.A Salama: *Parameters identification of sectional winding high frequency transformer model using neural network*, IEEE 46th Midwest Symp. on Circuits and Systems, vol. 2, pp. 974-977, 2003

F

[Florkowski-07] M. Florkowski, J. Furgal: *Transformer winding defects identification based on a high frequency method*, Meas. Sci. Technol., no. 18, pp. 2827-2835, 2007

[Firoozi-09] H. Firoozi, and M. Shishehchian: *Frequency Response Analysis - condition assessment of power transformers using mathematical and statistical criteria*, Proceedings of the 9th Int. Conf. on Properties and Applications of Dielectric Materials, pp. 253-256, 2009

[FRAnalyzer-09] Omicron brochure: *Sweep frequency response analyzer for power transformer winding diagnosis*, User Manual, 2009

[Fuchs-00] E.F. Fuchs, D. Yildirim and W.M. Grady: *Measurement of eddy-current loss coefficient P_{EC-R} , derating of single-phase transformers, and comparison with K-factor approach*, IEEE. Trans. on Power Delivery, vol. 15, no. 1, pp. 148-154, 2000

G

[Gonzalez-06] C. Gonzalez, J. Pleite, R.A. Salas, J. Vazquez: *Transformer diagnosis approach using Frequency Response Analysis method*, 32nd Annual Conf. on IEEE Industrial Electronics, pp. 2465-2470, 2006

[Gonzalez-07] C. Gonzalez, J. Pleite, V. Valdivia, and J. Sanz: *An overview of the On Line Application of Frequency Response Analysis (FRA)*, IEEE Int. Symp. on Industrial Electronics, pp. 1294-1299, 2007

[Gui-03] J. Gui, W. Gao, K. Tan, S. Gao: *Deformation analysis of transformer winding by structure parameter*, Proceedings of the 7th Int. Conf. on Properties and Applications of Dielectric Materials, Nagoya, pp. 487-490, 2003

[Gustavsen-02] B. Gustavsen: *Computer code for rational approximation of frequency dependent admittance matrices*, IEEE Trans. on Power Delivery, vol. 17, no. 4, pp. 1093-1098, Oct. 2002

- [Gustavsen-04a] B. Gustavsen: *Wide band modeling of power transformers*, IEEE Trans. on Power Delivery, vol. 19, no. 1, pp. 414-422, Jan. 2004
- [Gustavsen-04b] B. Gustavsen: *Frequency-dependent modeling of power transformers with ungrounded windings*, IEEE Trans. on Power Delivery, vol. 19, no. 3, pp. 1328-1334, Jul. 2004
- [Gustavsen-10] B. Gustavsen: *A hybrid measurement approach for wideband characterization and modeling of power transformers*, IEEE Trans. on Power Delivery, vol. 25, no. 3, pp. 1932-1939, Jul. 2010

H

- [Heindl-09] M. Heindl, S. Tenbohlen, A. Kraetge, M. Krüger, and J. L. Velásquez: *Algorithmic determination of pole-zero representations of power transformers' transfer functions for interpretation of FRA data*, Proceedings of the 16th Int. Symp. on High Voltage Eng. - ISH, South Africa, 2009
- [Heindl-10] M. Heindl, S. Tenbohlen, J. L. Velásquez, A. Kraetge, and R. Wimmer: *Transformer Modelling Based On Frequency Response Measurements For Winding Failure Detection*, Proceedings of the 2010 Int. Conf. on Condition Monitoring and Diagnosis, Japan, Sep. 2010
- [Heindl-11] M. Heindl, S. Tenbohlen, and R. Wimmer: *Transformer modeling based on standard frequency response measurements*, Proceedings of the 17th Int. Symp. on High Voltage Eng. - ISH, Hannover, Germany 2011
- [HM8150-07] HAMEG Instruments: *HAMEG 8150 Function generator - Manual*, 2007
- [Hoidalén-08] H.K. Hoidalén, B.A. Mork, F. Gonzalez, D. Ishchenko and N. Chiesa: *Implementation and verification of the hybrid transformer model in ATPDraw*, Electric Power Systems Research 79, pp. 454-459, Elsevier B.V., 2008
- [Hosseini-08] S.M.H. Hosseini, M. Vakilian, and G.B. Gharehpetian: *Comparison of Transformer Detailed Models for Fast and Very Fast Transient Studies*, IEEE Trans. on Power Delivery, vol. 23, no. 2, pp. 733-741, 2008

I

- [Islam-00] S.M. Islam: *Detection of shorted turns and winding movements in large power transformers using Frequency Response Analysis*, IEEE Power Eng. Society Winter Meeting, vol. 3, pp. 2233 - 2238, Jan. 2000

- [Islam-97] S.M. Islam, K.M. Coates, and G. Ledwich: *Identification of high frequency transformer equivalent circuit using MATLAB from frequency domain data*, Annual Meeting, Proceeding of IEEE Industry Applications Society, New Orleans, Louisiana, pp. 357-364, Oct. 1997

J

- [Jagers-09] J. Jagers, S. Tenbohlen.: *Differences approaches for the acquisition of reliability statistics*, Paper C-104, 6th Southern Africa, Regional Conf., Cigre 2009
- [Jayasinghe-06] J.A.S.B. Jayasinghe, Z.D. Wang, P.N. Jarman and A.W. Darwin: *Winding movement in power transformers: A comparison of FRA measurement connection methods*, IEEE Trans. on Dielectric and Elec. Ins., vol. 13, no. 6, pp. 1342-1349, Dec. 2006
- [JMAG-13] JMAG: *Newsletter of March issue*, Mar. 2013
<http://www.jmag-international.com/>
- [Joginadham-08] G. Joginadham, H. A. Mangalvedekar and A. Venkatasami: *Development of networks for SFRA data using circuit synthesis*, Int. Conf. on Condition Monitoring and Diagnosis, Beijing, China, Apr. 2008
- [Joshi-08] P.M. Joshi, S.V. Kulkarni: *Use of a Deformation Coefficient for Transformer Winding Diagnostics*, Int. Journal of Emerging Electric Power Systems, vol. 9, no. 3, 2008

K

- [Krüger-04] M. Krüger: *Application Guide: Capacitance and dissipation factor measurement with CPC 100 + CP TDI*, Omicron GmbH, Austria, 2004
- [Krüger-08] M. Krüger, M. Koch, A. Krätge and K. Rethmeier: *New tools for diagnostic measurements on power transformers*, Int. Conf. on Condition Monitoring and Diagnosis, Beijing, China, Apr. 2008
- [Krüger-11] M. Krüger, A. Krätge, K. Rethmeier and M. Koch: *New experience in the transformer diagnostic*, Transformer Life Management, Hannover, Germany, Jun. 2011
- [Kulkarni-00] S.V. Kulkarni and S.A. Khaparde: *Stray loss evaluation in power transformers-A review*, IEEE Power Eng. Society Winter Meeting, 2000
- [Kulkarni-04] S.V. Kulkarni and S.A. Khaparde: *Transformer engineering - design and practice*, Marcel Dekker Inc., 2004

L

- [Lachman-97] M.F. Lachman, and Y.N. Shafir: *Influence of single-phase excitation and magnetizing reactance on transformer leakage reactance measurement*, IEEE Trans. on Power Delivery, vol. 12, no. 4, pp. 1538-1546, 1997
- [Lammeraner-66] J. Lammeraner and M. Stafl: *Eddy currents*, Iliffe, 1966
- [Lapworth-06] J. A. Lapworth: *Transformer reliability surveys*, Paper A2-114, Cigre 2006
- [Lech-66] W. Lech, L. Tyminski: *Detecting transformer winding damage—the low voltage impulse method*, Electr. Rev. 179, pp. 768-772, 1966
- [Leibfried-99] T. Leibfried, K. Feser: *Monitoring of Power Transformers using the Transfer Function Method*, IEEE Trans. on Power Delivery, vol. 14, no. 4, pp. 1333-1341, 1999
- [Littmann-70] M.F. Littmann: *Iron and Silicon-Iron Alloys*, IEEE Trans. on Magnetics, vol. MAG-7, no. 1, pp. 48-60, Mar. 1971

M

- [Martinez-05a] J.A. Martinez and B.A. Mork: *Transformer modeling for low- and mid-frequency transients—A Review*, IEEE Trans. on Power Delivery, vol. 20, no. 2, pp. 1625-1632, April 2005
- [Martinez-05b] J. A. Martinez, R. Walling, B. A. Mork, J. Martin-Arnedo, and D. Durbak: *Parameter determination for modeling system transients-Part III: Transformers*, IEEE Trans. on Power Delivery, vol. 20, no. 3, pp. 2051-2062, Jul. 2005
- [Martinez-09] J.A. Martinez, and B. Gustavsen: *Parameter estimation from frequency response measurements*, IEEE Power and Energy Society General Meeting, pp. 1-7, 2009
- [MATLAB-CFT] Mathworks: *Curve Fitting Toolbox*, R2011
- [MATLAB-GOPT] Mathworks: *Global Optimization Toolbox*, R2011
- [MATLAB-OPT] Mathworks: *Optimization Toolbox*, R2011
- [Meredith-08] R.J. Meredith: *ATP modeling of core-form transformers by magnetic circuit analysis, including finite sectioning*, 2nd Ed., Jun. 2008
- [Mork-07a] B. A. Mork, Francisco Gonzalez, Dmitry Ishchenko, Don L. Stuehm, and Joydeep Mitra: *Hybrid transformer model for transient simulation – Part I: Development and Parameters*, IEEE Trans. on Power Delivery, vol. 22, no. 1, pp. 248-255, Jan. 2007

[Mork-07b] B. A. Mork, Francisco Gonzalez, Dmitry Ishchenko, Don L. Stuehm, and Joydeep Mitra: *Hybrid transformer model for transient simulation – Part II: Laboratory measurements and benchmarking*, IEEE Trans. on Power Delivery, vol. 22, no. 1, pp. 256-262, Jan. 2007

[Mukherjee-12] P. Mukherjee, and L. Satish: *Construction of equivalent circuit of a single and isolated transformer winding from fra data using the abc algorithm*, IEEE Trans. on Power Delivery, vol. 27, no. 2, pp. 963-970, Apr. 2012

N

[Noda-02] T. Noda, H. Nakamoto, and S. Yokoyama: *Accurate modeling of core-type distribution transformers for electromagnetic transient studies*, IEEE Trans. on Power Delivery, vol. 17, no. 4, pp. 969-976, Oct. 2002

O

[Omicron-12] Omicron brochure: *Diagnostic Testing Solutions for Power Transformers*, 2011

P

[Pham-11] D.A.K. Pham, J.L. Velásquez, T.M.T. Pham, V.N.C. Ho, H. Borsi, and E. Gockenbach: *Noise and denoising methods for measured frequency response signals of power transformers*, 17th Int. Symp. on High Voltage Eng., Hannover, Germany, Aug. 2011

[Pham-12a] D.A.K. Pham, T.M.T. Pham, M. H. Safari, V.N.C. Ho, H. Borsi, and E. Gockenbach: *FRA-based transformer parameters at low frequencies*, 2012 Int. Conf. on High Voltage Eng. and Application, pp. 605-608, Shanghai, China, Sep. 2012

[Pham-12b] D.A.K. Pham, T.M.T. Pham, V.N.C. Ho, H. Borsi, and E. Gockenbach: *Duality-based lumped transformer equivalent circuit at low frequencies under single-phase excitation*, 2012 Int. Conf. on High Voltage Eng. and Application, pp. 739-742, Shanghai, China, Sep. 2012

[Pham-12c] D.A.K. Pham, T.M.T. Pham, M. H. Safari, A. Kazemi, H. Borsi, and E. Gockenbach: *Transformer failure diagnosis based on parameter analysis*, Diagnostik Elektrischer Betriebsmittel, Fulda, Germany, 15-16.11.2012 (ISBN 978-3-8007-3465-8 VDE VERLAG GmbH Berlin Offenbach)

[Pham-13a] T.M.T. Pham, D.A.K. Pham, A. Kazemi, H. Borsi and E. Gockenbach: *Frequency response interpretation of a delta winding in transformer bulk in low- and mid- frequency range*, Proceeding of the 12th INSUCON Conference, pp. 133–138, Birmingham, UK, May 2013

- [Pham-13b] D.A.K. Pham, T.M.T. Pham, H. Borsi and E. Gockenbach: *A new method for purposes of failure diagnostics and FRA interpretation applicable to power transformers*, IEEE Trans. on Dielectrics and Elec. Ins., vol. 20, no. 6, pp. 2026-2034, Dec. 2013
- [Pham-14] D.A.K. Pham, T.M.T. Pham, H. Borsi and E. Gockenbach: *A new diagnostic method to support standard FRA assessments for diagnostics of transformer winding mechanical failures*, accepted to be published in the March/April issue of the IEEE Elec. Ins. Magazine, 2014
- [Pleite-06] J. Pleite, C. González, J. Vázquez, and A. Lázaro: *Power transformer core fault diagnosis using Frequency Response Analysis*, IEEE Mediterranean Electrotechnical Conf., pp. 1126-1129, 2006
- [Pordanjani-11] I. R. Pordanjani, C. Y. Chung, H. E. Mazin, and W. Xu: *A method to construct equivalent circuit model from frequency responses with guaranteed passivity*, IEEE Trans. on Power Delivery, vol. 26, no. 1, pp. 400-409, Jan. 2011
- [Pramanik-11] S. Pramanik and L. Satish: *Estimation of series capacitance of a transformer winding based on Frequency-Response data: An indirect measurement approach*, IEEE Trans. on Power Delivery, vol. 26, no. 4, pp. 2870-2878, Oct. 2011
- [Purnomoadi-09] A.P. Purnomoadi, and D.Fransisco: *Modeling and diagnostic transformer condition using Sweep Frequency Response Analysis*, Proceedings of the 9th Int. Conf. on Properties and Applications of Dielectric Materials, pp. 1059-1063, Harbin, China, 2009
- R**
- [Ragavan-08] K. Ragavan, and L. Satish: *Construction of physically realizable driving-point function from measured frequency response data on a model winding*, IEEE Trans. on Power Delivery, vol. 23, no. 2, pp. 760-767, Apr. 2008
- [Rahimpour-03] E. Rahimpour, J. Christian, K. Feser, and H. Mohseni: *Transfer function method to diagnose axial displacement and radial deformation of transformer windings*, IEEE Trans. on Power Delivery, vol. 18, no. 2, pp. 493-505, Apr. 2003
- [Rahimpour-09] E. Rahimpour, and M. Bigdeli: *Simplified transient model of transformer based on geometrical dimensions used in power network analysis and fault detection studies*, Int. Conf. on Power Engineering, Energy and Electrical Drives, pp. 375-380, 2009

- [Rahman-06] M.A.A. Rahman, P. Sankar Ghosh: *Diagnosis on mechanical movement in the winding of transformers using Frequency Response Analysis*, Int. Conf. on Condition Monitoring and Diagnosis, Changwon, Korea, 2006
- [Rashtchi-05] V. Rashtchi, E. Rahimpour, and E.M. Rezapour: *Using a genetic algorithm for parameter identification of transformer R-L-C-M model*, Elec. Eng. Journal, Springer Link, vol. 88, no. 5, pp. 417-422, Jun. 2005
- [Rashtchi-08] V. Rashtchi, H. Shayeghi, M. Mahdavi, A. Kimiyaghalam, and E. Rahimpour: *Using an improved PSO algorithm for parameter identification of transformer detailed model*, Int. Journal of Elec. Power and Energy Systems Eng., pp.138-144, 2008
- [Roger-06] D. Roger, E. Napieralska-Juszczak, and A. Henneon: *High frequency extension of non-linear models of laminated cores*, The Int. Journal for Computation and Mathematics in Elec. and Electronic Eng., vol. 25, no. 1, pp. 140-156, 2006
- [Ryder-03] S.A. Ryder: *Diagnosing Transformer Faults Using Frequency Response Analysis*, IEEE Elec. Ins. Magazine, vol. 19, no. 2, pp. 16-22, 2003
- S**
- [Satish-05] L. Satish, and S. K. Sahoo: *An effort to understand what factors affect the transfer function of a two-winding transformer*, IEEE Trans. on Power Delivery, vol. 20, no. 2, pp. 1430-1440, Apr. 2005
- [Satish-08] L. Satish, and A. Saravanakumar: *Identification of terminal connection and system function for sensitive frequency response measurement on transformers*, IEEE Trans. on Power Delivery, vol. 23, no. 2, pp. 742-750, Apr. 2008
- [Schellmanns-98] A. Schellmanns, K. Berrouche and J.P. Keradec: *Multiwinding transformers : a successive refinement method to characterize a general equivalent circuit*, IEEE Instrumentation and Measurement Technology Conf. St. Paul, pp. 717-722, USA, May 1997
- [Schellmanns-00] A. Schellmanns, J.P. Keradec, and J.L. Schanen: *Electrical equivalent circuit for frequency dependant impedance: minimum lumped elements for a given precision*, IEEE Industry Applications Conf., vol. 5, pp. 3105-3110, 2000

- [Setayeshmehr-06] A. Setayeshmehr, A. Akbari, H. Borsi and E. Gockenbach: *On-line monitoring of power transformer via measuring of transfer function*, ETG-Fachtagung "Diagnostik elektrischer Betriebsmittel," pp. 367-371, Kassel 2006.
- [Shintemirov-06] A. Shintemirov, and Q.H. Wu: *Transfer Function of Transformer Winding For Frequency Response Analysis Based on Traveling Wave Theory*, Proceeding of Int. Control Conf., 2006
- [Shintemirov-09] A. Shintemirov, W.H. Tang, and Q.H. Wu: *A hybrid winding model of disc-type power transformers for Frequency Response Analysis*, IEEE Trans. on Power Delivery, vol. 24, no. 2, pp. 730-739, Apr. 2009
- [Shintemirov-10a] A. Shintemirov, W.H. Tang, and Q.H. Wu: *Improved modelling of power transformer winding using bacterial swarming algorithm and frequency response analysis*, Journal of Electric Power Systems Research, vol. 80, no. 9, pp. 1111-1120, Sep. 2010
- [Shintemirov-10b] A. Shintemirov, W.H. Tang, and Q.H. Wu: *Transformer core parameter identification using Frequency Response Analysis*, IEEE Trans. on Magnetism, vol. 46, no. 1, pp. 141-149, Jan. 2010
- [Siada-07] A. A. Siada, and S. Islam: *High frequency transformer computer modeling*, Australasian Universities Power Engineering Conf., 2007
- [Sofian-07] D. M. Sofian: *Transformer FRA interpretation for detection of winding movement*, Doctoral dissertation, University of Manchester, 2007
- [Sofian-10] D. M. Sofian, Z. Wang, and J. Li: *Interpretation of transformer FRA responses—Part II: Influence of transformer structure*, IEEE Trans. on Power Delivery, vol. 25, no. 4, pp. 2582-2589, Oct. 2010

T

- [Tenbohlen-11] S. Tenbohlen, F. Vahidi, J. Gebauer, M. Krüger and P. Müller: *Assessment of power transformer reliability*, 17th Int. Symp. on high voltage Eng., Hannover, Germany, Aug. 2011
- [Tenbohlen-12] S. Tenbohlen, F. Vahidi, J. Gebauer, M. Krüger and P. Müller: *Zuverlässigkeitsbewertung von Leistungstransformatoren*, Stuttgarter Hochspannungssymp., Stuttgart, Germany, Mar. 2012

V

- [Velasquez-09] J.L. Velásquez, M. Krüger, S. Knütter, A. Kraetge, and S. Galceran: *Noise in FRA measurements: sources, effects and suppression methods*, Workshop "Diagnostic Measurements on Power Transformers", Omicron electronics GmbH, 2009

- [Velasquez-10a] J.L. Velásquez: *Frequency Response Analysis for condition assessment of power transformers: Basic and interpretation principles – Section 3. Factors effecting the repeatability of FRA results*, Supporting document for customers, Omicron Electronics GmbH, 2010
- [Velasquez-10b] J.L. Velásquez, M.A. Sanz-Bobi, W. Koltunowicz, A. Kraetge, and M. Heindl: *Pattern recognition of the factors affecting the reproducibility of FRA measurements in power transformers*, Proceeding of the CMD Conf., 2010
- [Velasquez-10c] J.L. Velásquez: *Frequency Response Analysis for condition assessment of power transformers: Basic and interpretation principles – Section 5. Guidelines for the right execution of FRA measurements*, Supporting document for customers, Omicron Electronics GmbH, 2010
- [Velasquez-10d] J. L. Velásquez, A. Hedgecock, M.A. Sanz-Bobi, and S.G. Arellanos: *Multiagent approach for integral condition assessment of power transformers using traditional and advanced diagnostic methods*, Advanced Research Workshop on Transformers - ARWtr2010, Santiago de Compostela, Spain, Oct. 2010
- [Velasquez-10e] J. L. Velásquez, A. Hedgecock, M.A. Sanz-Bobi, and S.G. Arellanos: *Reliable and automatic assessment of the frequency response analysis of power transformers: is it feasible?*, Advanced Research Workshop on Transformers - ARWtr2010, Santiago de Compostela, Spain, Oct. 2010
- [Velasquez-11] J. L. Velásquez: *Intelligent monitoring and diagnosis of power transformers in the context of an asset management model*, PhD dissertation, Polytechnic University of Catalonia, Spain, Jul. 2011

W

- [Wang-09a] Z. Wang, J. Li, and D. M. Sofian: *Interpretation of transformer FRA responses—Part I: Influence of winding structure*, IEEE Trans. on Power Delivery, vol. 24, no. 2, pp. 703-710 Apr. 2009
- [Wimmer-06] R. Wimmer, and M. Krüger: *Erhöhung der Reproduzierbarkeit von FRA-Messungen durch Standardisierung*, Stuttgarter Hochspannungssymposium, 2006
- [Wimmer-07] R. Wimmer, S. Tenbohlen, K. Feser, A. Kraetge, M. Krüger, and J. Christian: *Development of Algorithms to Assess the FRA*, 15th Int. Symp. on High Voltage Eng., University of Ljubljana, pp. 47-67, Slovenia, 2007

Z

- [Zambrano-06] G.M.V. Zambrano, A.C. Ferreira, L.P. Caloba: *Power transformer equivalent circuit identification by artificial neural network using Frequency Response Analysis*, IEEE Power Eng. Society General Meeting, 2006
- [Zhu-93] J.G. Zhu, S.Y.R. Hu and V.S. Ramsden: *Discrete modelling of magnetic cores including hysteresis eddy current and anomalous losses*, IEE Proceedings-A, vol. 140, no. 4, pp 317-322, Jul. 1993
- [Zhu-08] X. Zhu, H. Dong, G. Liang, and C. Ji: *A new hybrid model of transformer windings under very fast transient overvoltages*, Int. Conf. on Elec. machines and Systems, pp. 4296-4301, 2008

Guides and Standards

- [BR-05] US Bureau of Reclamation: *Transformers: Basics, Maintenance and Diagnostics*, Apr. 2005
- [CIGRE-08] CIGRE Report 342 W.G. A2.26: *Mechanical-condition assessment of transformer windings using FRA*, Apr. 2008
- [CIGRE-10] CIGRE WG A2.34: *Guide for transformer maintenance*, 2010
- [DL/T911-04] Chinese standard: *Frequency response analysis on winding deformation of power transformers*, Jun. 2005
- [IEC 60076/1-00] IEC 60076-1: *Power Transformer-Part 1: General*, Ed. 2.1, Apr. 2000
- [IEC 60076/18-09] IEC 60076-18: *Power transformers - Part 18: Measurement of frequency response*, Draft version, Nov. 2009
- [IEEE 62-95] IEEE Std 62: *IEEE Guide for diagnostic field testing of electric power apparatus-Part 1: Oil filled power transformers, regulators and reactors*, Mar. 1995
- [IEEE C57.12.80-02] IEEE C57.12.80: *IEEE standard terminology for power and distribution transformers*, May 2002
- [IEEE C57.125-91] IEEE C57.125: *IEEE Guide for failure investigation, documentation and analysis of power transformers and shunt reactors*, Jun. 1991
- [IEEE PC57.149TM/D9.1-12] IEEE PC57.149TM/D9.1: *Draft guide for the application and interpretation of frequency response analysis for oil immersed transformers*, Mar. 2012
- [NCEPRI-99] North China Electric Power Group Corp.: *Application Guideline for Transformer Winding Distortion Test Technology*, 1999

Curriculum vitae

Personal

Name Dinh Anh Khoi Pham
Birthday 23.10.1979
Birth place Ninh-Thuan, Vietnam
Family state married, two children

Education

1985 – 1990 Primary school, Ninh-Thuan, Vietnam
1990 – 1997 High school, Ninh-Thuan, Vietnam
1997 – 2002 Bachelor, Electrical and Electronics Engineering
Ho Chi Minh City University of Technology, Vietnam
2002 – 2004 Master, Power Systems and Networks
Ho Chi Minh City University of Technology, Vietnam
2008 – 2013 PhD, Electrical Engineering
Schering-Institut, Leibniz Universität Hannover, Germany

Professional career

since 2002 Lecturer,
Ho Chi Minh City University of Technology, Vietnam
04.2009 – 08.2012 Scientific assistant,
Schering-Institut, Leibniz Universität Hannover
09.2012 – 07.2013 Scientific employee,
Schering-Institut, Leibniz Universität Hannover

Publications

Conference – Author/co-author of 13 published national/international conference papers
Journal/Magazine – Co-author of 2 published national/international journal articles
– Author of an article accepted to be published on the IEEE Transaction on Dielectrics and Electrical Insulation, December 2013
– Author of an article accepted to be published on the IEEE Electrical Insulation Magazine on issue of March/April 2014

Hannover, 22.11.2013